DEPARTMENT OF THE INTERIOR
U.S. GEOLOGICAL SURVEY

NATIONAL EARTHQUAKE PREDICTION EVALUATION COUNCIL
SPECIAL REPORT I

Workshop on Special Study Areas in Southern California
San Diego, California
February 28-March 2, 1985

compiled by
Clement F. Shearer[1]

Open File Report 86-580

This report is preliminary and has not been edited or reviewed for conformity with U.S. Geological Survey publication standards and stratigraphic nomenclature.

[1]U.S. Geological Survey, 106 National Center
Reston, Virginia 22092

TABLE OF CONTENTS

PREFACE

The National Earthquake Prediction Evaluation Council (NEPEC) was established in 1979 pursuant to the Earthquake Hazards Reduction Act of 1977 to advise the Director of the U. S. Geological Survey (USGS) in issuing any formal predictions or other information pertinent to the potential for the occurrence of a significant earthquake. It is the Director of the USGS who is responsible for the decision whether and when to issue such a prediction or information.

NEPEC, also referred to in this document as the Council, according to its charter is comprised of a Chairman, Vice Chairman, and from 8 to 12 other members appointed by the Director of the USGS. The Chairman shall not be a USGS employee, and at least one-half of the membership shall be other than USGS employees.

The USGS began regular publication of the minutes of the Council in 1985 under its open-file services. To date, four proceedings volumes are available. This is the first special publication of the Council.

OVERVIEW OF WORKSHOP

INTRODUCTION

Earthquakes are a national problem with all or portions of 39 States lying in regions of moderate or major seismic risk. Catastrophic earthquakes in the United States are inevitable and hold the potential for causing great loss of life and widespread property damage. Such occurrences could have regional impact on public services and national impact on manufacturing, the economy, and national defense. Earthquake prediction is a significant and primary means of enhancing the effectiveness of preparedness activities and for mitigating the effects of great earthquakes.

The southern portion of the San Andreas fault in southern California is widely recognized by earth scientists as having a very high potential for producing a great earthquake within the next few decades. This high probability in conjunction with observations of crustal movements that are anomalous, but of uncertain significance, and a large population at risk indicate that this region is of greatest priority for development of an operational prediction capability.

Observations worldwide have demonstrated that many damaging earthquakes are preceded by patterns of anomalous phenomena that could be used for predictive purposes. Indeed, damaging earthquakes have been predicted in areas where instruments have been placed for these purposes in China, USSR, and Japan.

The goal of the workshop was to identify specific 30-km-long segments of the southern San Andreas and San Jacinto fault zones appropriate for detailed earthquake prediction studies.

There was considerable unanimity on the need to focus efforts in selected regions of southern California. While the Parkfield prediction experiment provides the best conceptual model for such focussed studies, there was a widespread sentiment that experiments had to be tailored to take account of the geological and geophysical characteristics of each region to be studied. For example, given a 150-km-long fault zone with high seismic potential, several years of intensified seismic and geodetic measurements throughout this zone would be needed to establish criteria for selecting a 30-km-long segment for detailed monitoring. Nonetheless, the necessity of addressing the high seismic risk of southern California with clustered monitoring efforts was clearly recognized, and there was wide, if perhaps not unanimous, agreement on where these studies should be located: the Anza slip gap on the northern San Jacinto fault, the southernmost end of the San Andreas fault near the Salton Sea, and the complex junction zone of the San Andreas and San Jacinto faults near Cajon Pass.

The papers, extended abstracts, and post-meeting comments are included here. In some cases papers were not presented, or are not available, and discussion instead focussed on photographic slides or handouts. Where available, copies of these materials are included in the document. As a result of the different methods of presentatation, this report loses some of the meetings's coherency, but we hope it nevertheless reflects the nature and content of the workshops's discussions, and provides some of the flavor of the informal proccedings and the range of opinions of the participants.

REVIEW OF PARKFIELD PREDICTION EXPERIMENT

OPTION PAPER

FOR

EARTHQUAKE PREDICTION STRATEGY

Prepared by the

U.S. GEOLOGICAL SURVEY

PURPOSE

This paper provides a basis for a decision on a strategy for earthquake prediction in the United States. The Secretary of the Interior has requested that the Director of the Geological Survey develop a plan for the implementation of a prototype operational earthquake prediction system in southern California. This request raises the question of not only how an operational earthquake prediction system might be established but, since other options exist, whether such a system should be pursued at this time. In the course of this paper the earthquake threat to southern California is discussed followed by a summary of the earthquake prediction problem. Programs in other countries are reviewed briefly. The status of the United States program is set down and, finally, options for how to proceed, including the development of a prototype operational system, are presented.

This paper specifically refrains from the use of technical terms and complex scientific arguments while it attempts to directly convey the current status of earthquake prediction, the problems to be faced, and programmatic options for the future.

The terms operational earthquake prediction system as used in this paper refer to proposed geophysical instruments and data analysis facilities that would be monitored and maintained 24 hours a day for the sole purose of earthquake prediction. Use of the term operational does not imply that the earthquake prediction problem is solved or reduced to a routine procedure.

ISSUE

Despite the lack of a definitive solution to the problem of reliable, short-term earthquake prediction and uncertainties over the social reaction to and economic benefits of such predictions, concern for public safety raises the issue: Given the high probability of a great earthquake along the southern San Andreas in the next 30 years and the possibility of smaller but still dangerous events from other faults in the region, should a more aggressive strategy be adopted to predict these events? Specifically, should the Federal Government, with State support, begin full or partial implementation of a prototype operational prediction system in southern California?

BACKGROUND

Earthquake Hazard: Ninety percent of the world's earthquakes occur in relatively narrow bands that mark the boundaries between large sections of the Earth's outer shell. These sections, called plates, are driven by the internal heat of the Earth and move slowly and inexorably with respect to each other. The boundary between the Pacific plate and the North American plate falls in California and forms the San Andreas fault system. Here the relative motion between the two plates is about 2 inches per year. Along most sections

of the fault the mechanics are such that the strain due to relative plate motion is not relieved continuously along the fault but through slow bending of the Earth's crust in the vicinity of the fault zone. Any mechanical system, when bent or strained without release, will eventually break and fail suddenly. This behavior gives rise to recurrent earthquakes of moderate to great significance. Along some sections of the fault, a moderate earthquake will occur every few tens of years while other sections remain quiet for a century or more before a major earthquake occurs. In each case, the strain begins to accumulate after an earthquake, and the cycle is repeated.

In historic times great earthquakes ruptured the main trace of the San Andreas in 1906 from San Juan Bautista to Cape Mendocino (400 km) and in 1857 from Cholame south to San Bernardino (350 km). Relative slip or displacement across the fault was measured in tens of feet in each case. These sections of the fault have accumulated significant strain that has not been released since these large events. Geological studies indicate that the southern section of the fault that broke in 1857 experiences a major displacement about every 140 years. Statistics applied to the geological evidence point to a 45 percent chance of another major earthquake along the southern (1857) section of the fault within the next 30 years. Estimates of damage from this earthquake range in the tens of billions of dollars and loss of life is estimated to be in the thousands.

In addition to its main trace, the San Andreas fault system consists of hundreds of ancillary or tributary faults. Although these lesser faults are

unlikely to give rise to large, devastating events, earthquakes along them can be dangerous and cause significant damage. The 1971 San Fernando and the 1983 Coalinga earthquakes occurred on faults of this type.

National Perspective: Earthquake prediction was formally introduced into the nation's scientific agenda with the passage of the National Earthquake Hazards Reduction Act of 1977. A stated objective of this legislation is to "introduce into all regions of the country subject to large and moderate earthquakes systems for predicting earthquakes and assessing earthquake risk.".

In the division of labor within the National Earthquake Hazards Reduction Program, the U.S. Geological Survey (USGS) of the Department of the Interior is charged with conducting earthquake prediction research. This is consistent with the responsibilities assigned to the Director of the Geological Survey under the Disaster Relief Act of 1974 to ". . . issue warnings to State and local officials of impending earthquakes, volcanic eruptions, landslides, and other geologic disasters.".

The scientific problem: Research supported by the Geological Survey on the problem of long-term earthquake prediction (earthquake potential) and estimates of strong ground shaking due to earthquakes has proceeded more rapidly than originally thought possible. Geologists at the USGS, the California Institute of Technology, and other institutions have, through detailed studies of fault zones, demonstrated that dates of large prehistoric earthquakes can be estimated from the geologic record. Scientists from Lamont-Doherty Geological Observatory, the University of California, and the

USGS have combined these results with seismological and other data to provide quantitative estimates of recurrence times of earthquakes in California, Nevada, and elsewhere. From estimates of recurrence times, or the length of the seismic cycle, and knowledge of the last large earthquake in a region, general or long-term predictions, accurate within a few years or decades, may be made. An effort is underway to systematically catalog active faults in the United States and estimate the earthquake potential of each.

Progress on the problem of short-term prediction, within a few hours or days of the event, has proven more difficult. For short-term prediction we must be able to identify and detect that portion of the seismic cycle just before a large earthquake occurs. This hinges on there being accelerated deformation in the rock at the fault hours or days before failure. Simply stated, the central notion behind short-term earthquake prediction is that most mechanical systems when subjected to deformation, such as a stick being bent or the Earth's crust being strained, will not fail catastrophically without premonitory indications, such as rapid yielding or minor brittle fracturing just before failure. In the case of earthquake prediction, the central questions are whether or not these indications will occur at a magnitude and time in order to form the basis of a timely and reliable warning of an impending earthquake.

Earthquake prediction research has resulted in an increase in our ability to measure and explain rapid deformation in the Earth's crust, in the sophistication of laboratory and theoretical models of eathquakes and crustal materials, and in our ability to process and analyze large volumes of seismic and other types of data and to interpret these data in terms of geologic and

earthquake processes. Nevertheless, since the beginning of the Federal program there has been no unequivocal case in which a significant earthquake in the United States was predicted in hours or days prior to its occurrence.

The social problem: In addition to the scientific and statutory aspects of earthquake prediction, consideration is given to the social preparations necessary to deal with an earthquake prediction effectively. It is generally agreed that official statements about an impending earthquake must be accompanied by explicit instructions on what measures should be taken. Progress has been made through the Southern California Earthquake Preparedness Project (SCEPP), an ongoing planning effort funded jointly by the Federal Emergency Management Agency and the State of California, in the preparation of guidelines for local officials in the event of an earthquake prediction. Similar planning efforts are underway in the San Francisco Bay area. However, no drills or exercises have been conducted to prepare the general public for rational reaction to a prediction. To assist officials with the responsibility to issue or assess earthquake predictions, the National Earthquake Prediction Evaluation Council (NEPEC) and the California Earthquake Prediction Evaluation Council (CEPEC) have been formed at the Federal and State levels, respectively. Although these councils have been asked to assess predictions by others, they have never recommended that an earthquake prediction be issued.

Successful prediction of a large earthquake for the southern San Andreas fault can result in significant benefits to society, both in reduction of casualties and in property loss. In modern, industrial society, for which it is hoped that the major loss of life can be averted through prudent land-use policies

and earthquake-resistant design and construction, it will be extremely difficult to eliminate all hazardous structures in seismically prone areas. In addition to alerting emergency response efforts, earthquake prediction can provide society a defense against the building that might collapse, the dam that might fail, and the vulnerable industrial practice. The safety benefits of a short-term earthquake warning in the Los Angeles area are reported to be approximately 4,400 deaths avoided. Although lives can be saved by a successful prediction, a prediction may entail costs in the form of losses in the regional economy. Losses due to a false prediction could be substantial. Thus net benefits of a prediction depend upon its reliability, how it is presented to the public, and how well the public is prepared to react to it.

PROGRAMS IN OTHER COUNTRIES

In addition to the United States, three other countries have established major national efforts to reduce earthquake hazards. Each of these efforts has a strong earthquake prediction component.

Soviet Union

The earthquake prediction program in the Soviet Union has continued for about 20 years under the leadership of the Institute of Physics of the Earth in Moscow. The centerpiece of the Russian program is a field facility at Garm east of Dushanbe near the Afganistan border. The purpose of this facility is to predict earthquakes in the surrounding region. The facility consists of about 20 buildings (including living quarters) and a staff of about 50

scientists and technicians who routinely analyze data from instruments in the region. The maximum dimension of this region is similar to that from San Diego to El Centro. Although several successful earthquake predictions have been reported from the Soviet Union, some of these appear to have been made after the event and none have been clearly documented.

China

In China, earthquake prediction has been given high national priority. The State Seismological Bureau in Beijing has been established as a separate ministry to give strong central direction to the Chinese program. The State Seismological Bureau maintains a field facility (about the same size of that at Garm) in western Yunnan province near the Burmese border. Through provincial governments the Chinese maintain prediction efforts in other parts of the country subject to destructive earthquakes. In 1975 a magnitude 7.3 earthquake near Haicheng, 300 miles northeast of Beijing, was successfully predicted 9 1/2 hours before the event. This event was preceded by precursors of many different types. However, in 1976 an earthquake near Tangshan killed over a quarter of a million people and was not predicted.

Japan

The Japanese earthquake prediction program began in 1965 and is now in its fifth 5-year cycle. The Japanese program is often used as a standard for comparison with the United States program. The annual budget for the Japanese program is reported to be about $30 million exclusive of salaries. The Large-

scale Earthquake Countermeasures Act of 1978 codified procedures for evaluating, issuing, and responding to an earthquake prediction.

The Japanese have designated the Tokai region, between Tokyo and Nagoya, as one of high seismic potential. (The distance from Tokyo to Nagoya is about the same as that from Santa Barbara to San Diego.) Because this region has high population and heavy industrial activity, prediction of the next great earthquake here is considered critical. A very dense network of instruments for monitoring various precursory phenomena has been established in the region and data are sent via telephone lines to a center in the Japan Meteorological Agency in Tokyo, which is staffed 24 hours a day and 7 days a week. When anomalous behavior is observed, an earthquake prediction council meets on several hours notice and evaluates the data. It conveys its findings to the director of the agency who in turn reports to the Prime Minister. A network of loudspeakers has been established in Tokai and radio and television announcements prepared to notify the public if a prediction is issued. Drills and exercises have been conducted so that individuals know how to respond in case of a prediction. In addition, other extensive measures are being taken to mitigate the effects of the earthquake whether it is predicted or not.

There are similar aspects to the approach taken to earthquake prediction in Japan, China, and the Soviet Union. Although the scale and details of the technical approach may differ, all three have established strong broad-based programs in fundamental research on earthquake processes, earthquake potential, and instrument development. Each has designated at least one area for intensive monitoring for earthquake prediction purposes. In Japan the area is densely populated and the prediction effort is directly linked to

public safety. The prediction study areas in the Soviet Union and China are less densely populated and linkage to local governments is not obvious.

STATUS OF THE UNITED STATES PROGRAM

The National Earthquake Hazards Reduction Program in the United States is comprised of activities in four separate agencies. Briefly stated, these agencies and their principle activities are:

Federal Emergency Management Agency is the lead agency for the national program and is responsible for emergency response planning and mitigation strategy development.

National Science Foundation supports basic research in the geological sciences and in earthquake engineering.

National Bureau of Standards supports the development of building codes and the design and testing of structures and materials.

The U.S. Geological Survey supports earthquake prediction research, studies of long-term earthquake potential, regional hazards assessments, engineering seismology, and the distribution of earthquake information.

Within the USGS program, geological and seismological studies are conducted to establish the long-term earthquake potential of a region. These studies have made significant advances over the past decade, and now earthquake potential can be expressed quantitatively for various regions of the San Andreas fault

(see Figure 1). These results form the foundation of work on more detailed hazard assessments and a basis for focussing earthquake prediction experiments.

There are three major elements to the current earthquake prediction program of the United States. The first of these is an effort to improve our understanding of the earthquake process through theoretical, laboratory, and field studies. Realistic theoretical and laboratory models have been constructed to study dynamic fault behavior using realistic geometries and fault properties and with realistic physical conditions. This element also includes field studies of fault properties and physical conditions at depths where earthquakes occur. These measurements are then used to make the laboratory and theoretical models and experiments more accurate and representative of actual Earth conditions.

The second major element of the program involves developing, deploying, and maintaining instrumentation to obtain geophysical, geochemical, and hydrological measurements in fault zones before large earthquakes. Rather than comprehensive studies of a specific region or fault segment, these efforts are aimed at testing the reliability of instruments under various conditions and determining the sensitivity of certain phenomena to expected premonitory variations. Data are collected in the Western United States, Alaska, and at certain foreign sites; in short, wherever conditions are favorable for extending our earthquake prediction data base most rapidly. In most cases, sites within a given region will measure only one type of data. The objective is to establish statistical relationships, if possible, between

proposed premonitory phenomena and large earthquakes including false-alarm and no-alarm occurrences.

The backbone of the field measurement program is the telemetered network of seismometers that monitor the entire length of the 1100 km long San Andreas fault system in California for the purpose of detecting and accurately locating all earthquakes of magnitude 1.5 and larger. Data from the network is used to map active faults in the subsurface, determine the nature of fault motion, and monitor variations in activity for indications of changing physical conditions in the fault system. The northern half of the California network consisting of about 300 seismometers is maintained by the USGS in Menlo Park, where data are recorded and analyzed. The southern half of the network of about 250 stations is maintained jointly by the California Institute of Technology and the USGS. The data are recorded and analyzed in Pasadena.

In addition to statewide coverage by the seismic network, the accumulation and release of strain is monitored by an extensive network of geodetic lines that are resurveyed on an annual basis using laser-ranging techniques. These measurements provide critical information on the rate of strain accumulation on specific faults and have provided evidence for regional scale variation in the crustal loading rate.

The final element of the prediction program involves concentrated studies of certain sections of the San Andreas fault in California. In central California, data from clusters of instruments near Parkfield and Mammoth Lakes and individual instruments elsewhere are transmitted to a data center at

Menlo Park where they are reviewed daily by scientists and monthly at formal data reviews. This is as close an approximation to an "operational system" as can be described for the current U.S. prediction program. Nevertheless, there are several shortfalls in this effort. Most of the instruments are deployed on the ground surface and research results on instrument reliability show them to be subject to spurious signals associated with daily and seasonal variations in temperature, rainfall, and other atmospheric phenomena. The density of the instrumentation and the reliability of the transmission lines are not optimal. Although some of the data channels are monitored by computer and connected to alarms, the people involved are scheduled to work 8-hour days; there is no 24-hour, 7 days a week surveillance of the data.

In southern California, instruments and measurement networks have been developed and are maintained by individual investigators at separate institutions. Individual instruments and survey sites are widely and sparsely distributed from Santa Barbara County south to the Mexican border. There is a dense concentration of crustal deformation sensors for instrument development and calibration at Pinon Flat, located 60 miles northeast of San Diego and operated by the University of California there. These instruments are located in the vicinity of a zone of high seismic potential on the San Jacinto fault near Anza; however many of them are impractical for wide deployment. Semi-annual meetings are held in which investigators present and discuss their data, but there is no central collection and analysis point at which all of the data can be reviewed promptly. An effort is being made to collect all of the data from southern California at Menlo Park through the use of satellite relays; however, it will be about 1 year before this is complete.

Table I (attached) summarizes the instrumentation currently being supported for earthquake prediction purposes in California. The instruments and related networks currently in use have evolved over the past 10 years and are of various vintages. The seismic networks are based chiefly on technology over 20 years old and are inadequate for recording the observable signals required for modern processing techniques. However, the volumetric strainmeters and the two-color laser strain measurement devices are "state-of-the-art" and represent the latest developments in continuous or near-continuous point strain measurement.

STRUCTURE FOR AN EARTHQUAKE PREDICTION STRATEGY

During the past several years, two important developments have strongly influenced the strategy by which research in short-term earthquake prediction is being pursued in California. First, continuing work between seismologists at the USGS in Menlo Park and at the University of California at Berkeley has strongly suggested that an M 6 earthquake will occur along a 20 km long segment of the central San Andreas fault near Parkfield in 1988 $\pm$ 4 years A.D. Second, because of the heightened risk of a great eathquake on the southern San Andreas fault north of Los Angeles (estimated as a 45 percent likelihood in the next 30 years) considerable thought has been given to the design of a second generation earthquake prediction network in this region. This system ultimately would replace existing instrumentation and the data obtained would be analyzed and monitored continuously. Research indicates that much of the 450 km long southern segment of the San Andreas fault is at risk, but the results also suggest that in specific subsections the risk is

greater (see Figure 1) and that several more localized regions may mark the sites where the expected large or great earthquakes will nucleate.

Both of these developments strongly indicate the necessity of intensified observations in identified regions of high seismic potential. At the same time, regional scale monitoring of crustal deformation (using geodetic methods) and seismicity (with a statewide seismographic net) must be maintained and improved in order to provide both a broad context for interpreting the local measurements and a firm basis for identifying new regions in which to focus intensified efforts in the near future.

The focus on selected localized regions as well as the need for a phased buildup in detailed monitoring efforts argue for the use of clusters of instruments that measure crustal deformation continuously or nearly so at points within a small region of approximately 20 km extent. It is now generally accepted that there is no single instrument, measurement, or physical phenomena that alone will hold the key to earthquake prediction. Measurements of various phenomena on various instruments and even duplicate instruments at the same site, are needed to provide the redundancy and thus the reliability needed for earthquake prediction. Since short-term prediction hinges on there being accelerated deformation near the fault in the hours or days before the earthquake, continuous direct or indirect measurement of strain (changes in volume or shape) at very minute levels are sought. The approach that has evolved requires different types of instruments sensitive to minute strain changes deployed in a region where prediction is being attempted, with data from these instruments analyzed in concert to avoid misinterpretation.

Each cluster would consist of a 2-color laser strain measurement device, several borehole strainmeters emplaced at 300 m depth or greater, one or more long baseline (500 m or more) strain or tiltmeters, and several fault slip detectors (creepmeters). Several prototype designs for borehole and long-baseline instrumentation have been field tested at Pinon Flat and are ready for deployment. At the same time, research will continue on new and improved designs with higher sensitity.

The data collection points at each cluster would serve as nodes in a network of modern digital seismographs with wide sensitivity and recording response. This network would be capable of detecting and providing data for analysis of all earthquakes of magnitude 1.5 or greater within 50 km of the fault segment being monitored by the strain measurement cluster. Approximately 10, 3-component seismometers would be associated with each cluster.

The strain instrumentation now at Parkfield represents the closest approximation to what we envisage a crustal deformation observatory cluster to be; however, at present the number and types of instruments is still not optimum and the outdated seismic instrumentation is inadequate.

OPTIONS FOR EARTHQUAKE PREDICTION PROGRAM

Within the context of this overall structure, the four options for a national earthquake prediction strategy are outlined below.

Option 1 - Continue Current Program: This option represents a linear

extension of our current activities in California and elsewhere. Individual research institutions supported by the Geological Survey will continue to collect data from instruments and networks they have deployed and maintained. Research based on the analysis of these data will be extended as will research to develop more sophisticated and reliable instrumentation. Efforts toward the consolidation of available data and a periodic reviewing of these data at regular meetings will be sustained. Earthquake prediction studies at Parkfield will continue with efforts to increase the density of instrumentation without seriously impairing regional coverage of seismicity and geodetic strain. Data from Parkfield will be transmitted electronically to the USGS center at Menlo Park for daily observation and monthly review under current procedures. Earthquake prediction research in the areas of laboratory experiments, determination of fault zone properties, and instrument development will continue along with collection of data from other (non-California) sites and certain foreign exchanges.

Option 2 - Prototype Prediction Clusters Deployed in Specific Study Areas: Under this option the basic program of earthquake prediction research outlined in option 1 above will continue. However, activities at Parkfield will be considerably expanded and intensified, and three to five regions of the southern San Andreas will be instrumented with clusters and be closely monitored.

Full advantage would be taken of the unique opportunity afforded by the imminent occurrence of the next Parkfield earthquake. A second cluster of strain monitoring instruments would be installed close to the expected epicenter of the event. In addition, several 1 km deep boreholes would be

drilled first to determine physical properties and state of stress and then to house sensitive strainmeters and seismometers in the low-noise conditions that prevail at such depths. A broad bandwidth, high-dynamic range 10-station seismic network would be installed to monitor the detailed source characteristics of the background microearthquake activity that occurs up until the M 6 main event takes place. A detailed seismic reflection-refraction survey would be carried out to determine three-dimensional seismic velocity structure and these results will both ensure better microearthquake locations and finer resolution of structural features at depth that may control rupture dynamics and precursory processes. Since the dynamic rupture characteristics and earthquake slip of the main shock may well be related to pre-earthquake seismicity and crustal deformation, these features must be very accurately determined. For these purposes a dense three-dimensional array of strong-motion accelerographs designed to complement the State instrumentation is needed to map recorded near-field motions back onto the mainshock fault plane. Finally, an augmented geodetic net is required to obtain the distribution of earthquake slip on the fault.

Areas for intensified study on the southern San Andreas system, in addition to Parkfield, will be chosen from among:

(1) The 40 km long segment of the San Andreas south of Cholame where slip in 1857 was only 3–4 m and long-term slip rate is about 35 mm/yr.

(2) Tejon Pass region near the complex junction of the Garlock and San Andreas faults where future great San Andreas earthquakes may nucleate.

(3) Cajon Pass region near the junction of the San Andreas and San Jacinto faults.

(4) San Gorgornio Pass in a complex structural area between the San Andreas and San Jacinto faults.

(5) Along the southern terminus of the San Andreas fault east of the Salton Sea and near the boundary between it and the Brawley seismic zone in the Imperial Valley to the south.

(6) The Anza region on the northern half of the San Jacinto fault. Adjacent regions have experienced a series of M=6-7 earthquakes early in this century while the Anza segment has not sustained significant seismic slip since at least 1890. (These regions 1-6 are identified by an index number on Figure 1.)

Option 3 - Deployment of a Prototype Operational Prediction System along the Southern San Andreas: Under this option, clusters of instruments would be located approximately every 20 km along all of the currently locked southern San Andreas fault in southern California. Sparser coverage would extend out to 30 km from the fault itself. All data collected would be monitored continuously in real or nearly real time and a sustained, dedicated effort would be made to provide short-term warning in advance of the next great earthquake to strike on the San Andreas in southern California.

This option would be best executed as an extension of the activities outlined under option 2. This is necessary in order to gain experience in the design

and operation of strain monitoring clusters and to ensure that areas of highest seismic potential are instrumented early on.

The prototype system for southern San Andreas would consist of 20-30 instrument clusters. The system would include a comprehensive modern seismograph network, a regional geodetic network based on conventional or satellite techniques and a data transmission, management, and analysis facility. Aspects of this system concept is elaborated more fully in a separate report (Dieterich, 1983) entitled "Assessment of a Prototype Earthquake Prediction Network for Southern California".

Option 4 - Full Deployment of a Prototype Operational Prediction System: This option is an extension of option 3 in that in addition to coverage along the San Andreas in southern California, instrument clusters be deployed in areas from Santa Barbara to San Diego west of the main fault. This comprehensive coverage would represent an attempt to predict damaging earthquakes not only on the main trace of the San Andreas but also on the active ancillary faults that underlie most of the heavily developed urban area to the west. Because the characteristics and even the location of many of these faults are poorly known, the chances of successful prediction of earthquakes on them are less than on the San Andreas. It is estimated that 50-60 clusters of instruments would be needed to provide comprehensive coverage.

In addition to wide coverage in southern California, this option should include deployment of clusters along the Hayward fault in the East Bay and in the San Juan Bautista-Hollister regions of central California.

Costs: Estimation of the costs required to purchase and install each cluster of instrumentation discussed above will be about $2 million. Annual operational costs for each cluster are estimated to be about $1/3 million. A detailed implementation plan based on the cluster concept and covering the options discussed above is being developed and will be completed in March 1985.

Conclusion: It cannot be guaranteed that any of the options discussed above will lead immediately to successful predictions of large earthquakes or that false alarms will not be issued. However, in areas where the described clusters of instruments have been deployed, high assurance can be given that a reasonable and strong effort has been made to provide an earthquake warning to the people living in that area.

DRAFT

TABLE I. CALIFORNIA PREDICTION INSTRUMENTATION AND SURVEYS

Earthquake Prediction Instrumentation in California

Type	Principal Scientist	Affiliation	No. Inst.	Area
Creepmeters				
	Sandra Schulz	U. S. Geological Survey	29	C CA
	Clarence Allen	Calif. Institute of Technology	7	So CA
	Peter Leary	Univ. Southern California	1	So CA
Dilatometers				
	Malcolm Johnston	U. S. Geological Survey	7	C & So CA
Geochemical Monitoring- Wells				
	Mark Shapiro	Calif. Institute of Technology	11	So CA
	Leon Teng	Univ. Southern California	9	So CA
	Yu Chia Chung	Scripps Inst. of Oceanography	9	So CA
	Chi Yu King	U. S. Geological Survey	4	C CA
Magnetometers- Permanent				
	Malcolm Johnston	U. S. Geological Survey	27	C & So CA
Seismometers				
	So CA Co-op Net	U. S. Geological Survey and	164	So CA
		Calif. Institute of Technology	27	So CA
	Leon Teng	Univ. of Southern California	28	So CA
	Rick Lester	U. S. Geological Survey	349	N & C Ca
	Rob Cockerham	U. S. Geological Survey	24	Mammoth
Strainmeters				
	Malcolm Johnston	U. S. Geological Survey	9	So CA
	Bruce Clark	Leighton and Associates	14	So CA
	Peter Leary	Univ. of Southern California	11	So CA

DRAFT

TABLE I. CALIFORNIA PREDICTION INSTRUMENTATION AND SURVEYS (continued)

Type	Principal Scientist	Affiliation	No. Inst.	Area
Tiltmeters				
	Carl Mortensen	U. S. Geological Survey	22	C CA & Mammoth
	Peter Leary	Univ. of Southern California	2	So CA
	Sean Morrissey	St. Louis University	8	So CA
Two-Color Laser				
	John Langbein	U. S. Geological Survey	2?	
Well Monitoring				
	Don Lamar	Lamar-Merifield, Geologists	30	So CA
	Chi Yu King	U. S. Geological Survey	6	C CA
	Tom Urban	U. S. Geological Survey	1	So CA
	Tom Henyey	Univ. of Southern California	11	So CA

DRAFT

TABLE I. CALIFORNIA PREDICTION INSTRUMENTATION AND SURVEYS (continued)

Earthquake Prediction Surveys in California

Type	Principal Scientist	Affiliation	No. Sites/ Networks	Area
Alignment Arrays				
	Clarence Allen	Calif. Institute of Technology	24	So CA
	John Galehouse	San Francisco State University	19	C CA
	Art Sylvester	U. C. Santa Barbara	2	So CA
	Beth Brown	U. S. Geological Survey	17	C CA
Dry Tilt				
	Art Sylvester	U. C. Santa Barbara	56	So CA & Mammoth
Gravity				
	Robert Jachens	U. S. Geological Survey	412	So CA
Level Lines				
	Art Sylvester	U. C. Santa Barbara	38	So CA
	Ross Stein	U. S. Geological Survey	2	C CA
			5	So CA
Magnetometers- Survey				
	Malcolm Johnston	U. S. Geological Survey	61	So CA & Mammoth
Resistivity				
	Ted Madden	Mass. Institute of Technology	16	C & So CA
Trilateration				
	Will Prescott	U. S. Geological Survey	49	CA
	Art Sylvester	U. C. Santa Barbara	17	

ANNUAL EARTHQUAKE PROBABILITIES

for selected fault segments of the San Andreas Fault System

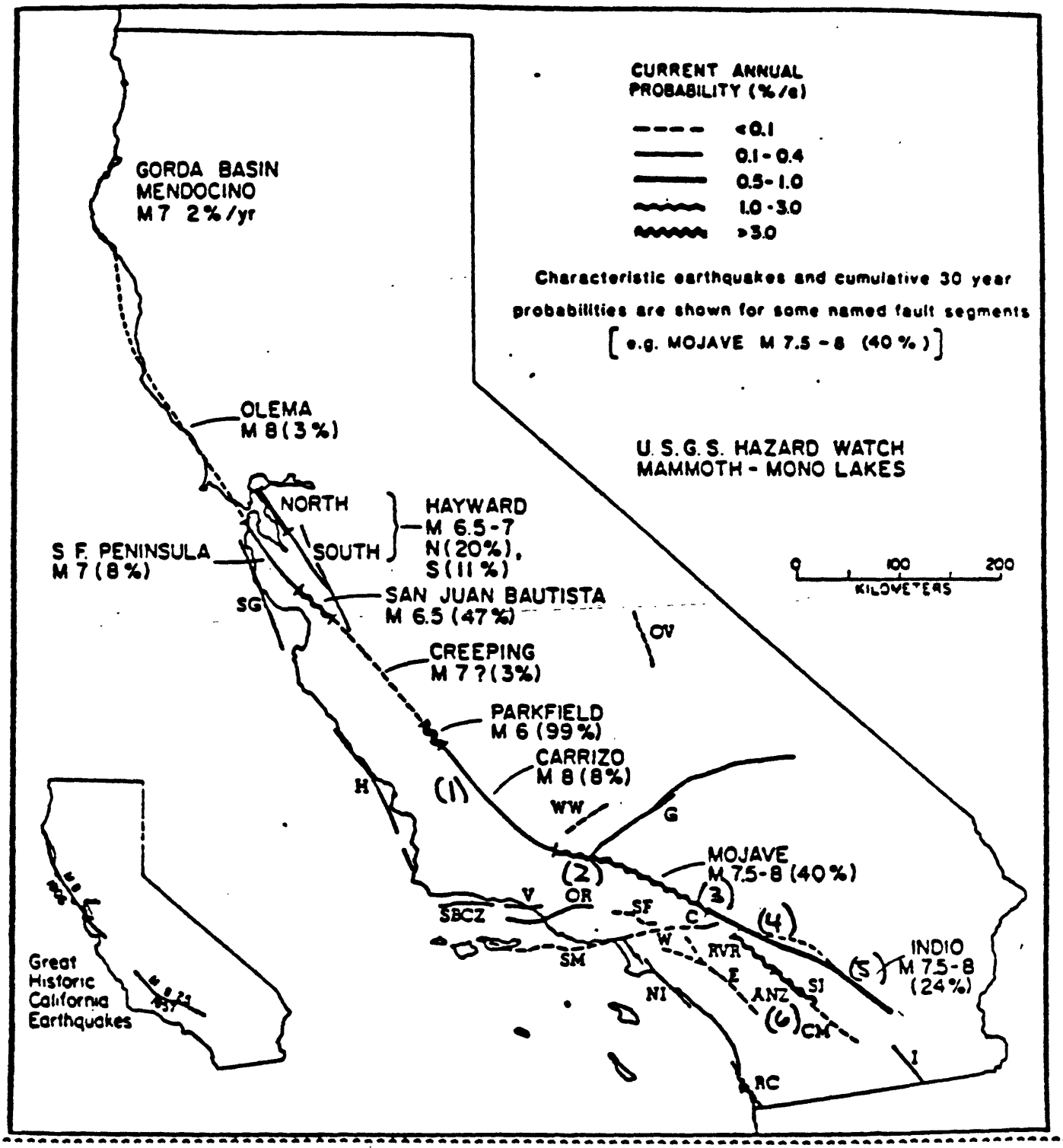

FIGURE 1.

The Road to Parkfield: Origins and Development of an Earthquake Prediction Experiment

W. L. Ellsworth
U.S. Geological Survey
Menlo Park, California

The attempt to predict the next magnitude 5 1/2 - 6 earthquake on the San Andreas fault at Parkfield, California has been a formally organized activity of the National Earthquake Hazards Reduction Program since its inception in 1978. In that year, a new project was created within the U.S. Geological Survey with the stated objective "to predict in advance the next magnitude six (or larger) Parkfield earthquake" (Lindh, et al., 1978). At present, a long-term prediction for the next Parkfield earthquake has been announced (Bakun and McEvilly, 1984; Bakun and Lindh, 1985) which precisely specifies the location and magnitude of the event, and defines a time interval (1988.0 $\pm$ 5.2 years) within which the event should occur. (The probability of a characteristic Parkfield earthquake during the same interval derived from a Poisson model is 31%, and the probability derived from Lindh's (1983) Guassian model with a 30% standard deviation is 67%. Thus the specific forecast differs by factors of only 2-3 from other reasonable alternatives.)

During the intervening seven years there have been many significant advances in our knowledge of earthquakes, and of their causes and effects (Hanks, 1985). In particular, significant progress has been made in understanding the long-term recurrence behavior of faults, which for the entire length of the San Andreas fault can be formally expressed as earthquake occurrence probability (Lindh, 1983; Sykes and Nishenko, 1984). A by-product of this progress in long-term earthquake forecasting — or perhaps despite it — has been the emergence of a scientific consensus on the next critical step for the Earthquake Prediction Program: to measure at the highest precision possible the temporal and spatial changes in the state of the crust before, during and after the next Parkfield earthquake.

The decision to commit the limited discretionary resources of the Earthquake Prediction Program to Parkfield has as long and varied a history as the development of the scientific consensus. By focusing on Parkfield, a deliberate decision was made to either scale-down, or in some cases abandon, other similarly ambitious proposals for earthquake prediction studies elsewhere. The process of arriving at a committment to Parkfield involved a critical series of meetings held in the fall of 1982, at which several proposals for a concentrated earthquake prediction experiment were carefully examined. Specific proposals were considered for the segments of the San Andreas fault to the north and south of San Juan Bautista (Lindh, et al., 1982), Parkfield and, in more general terms, the San Andreas fault in southern California. Parkfield emerged the clear — though not unanimous — choice for a first clustering of prediction-related experiments, chiefly because of the greater uncertainties of the occurrence of an earthquake of sufficient size at any other specific locality.

(For the sake of historical completeness, it should be noted that, in

retrospect, several of the key ingredients in the Parkfield story had also been noted for the segment of the Calaveras fault that ruptured in the M6.1 Morgan Hill earthquake in 1984 (Bakun, et al., 1984). An earlier event (1911) was known, the slip rate of the fault was well-determined, the specific segment of the fault that ruptured had been postulated as the probable break, and a recurrence interval had been established for the adjacent segment to the south from events in 1897 and 1979. What a simple business this would be if we could only run time in reverse! One may conclude that even if the specifics of our physical models are incorrect, a few more well-placed "bets" should yield a scientific bonanza.)

The status of the Parkfield experiment as of early 1985 can, perhaps, be best described as "in process". The region is under continuous seismic analysis by real-time computers in Menlo Park. Six new low-gain 3-component seismic stations have been installed to augment the 24 high-gain vertical component seismometer. The creep meters are also being monitored in real-time by computer, with pre-defined thresholds used to trigger "beepers". Two dilatometers are in operation at Gold Hill, and a third is curing at another site, while efforts continue to site additional dilatometers. Several water wells that produce clear tides are being monitored and more sites will be established this year. The magnetometers network is functional, and being reviewed for possible reconfiguration. The two-color laser observatory is in operation, with measurements being made several times a week. A large-scale trilateration monitor network is also being observed on a bi-monthly schedule. And several other experiments, including a shallow tiltmeter cluster and a surface strainmeter are also in operation. As good as the present effort is, there are many recognized gaps in the experiment and we are working hard to fill them as time and resources permit.

Parkfield represents our clearest and cleanest choice for a focused earthquake prediction experiment. We may not succeed in predicting the time of the next earthquake more precisely than has already been proposed, and forsee the possibility that rupture in the next event may differ significantly from the predicted behavior; but we are resolved to give the monitoring of the fault through the time of the next earthquake our highest priority and our best shot.

REFERENCES

Bakun, W. H., and A. G. Lindh, The Parkfield, California, Prediction experiment: Earthquake Prediction, in press, 1985.

Bakun, W. H., and T. V. McEvilly, Recurrence Models and Parkfield, California earthquakes: Journal of Geophysical Research, v. 89, no. B5, p. 3051-3058, 1984.

Bakun, W. H., M. M. Clark, R. S. Cockerham, W. L. Ellsworth, A. G. Lindh, W. H. Prescott, A. F. Shakal, and P. K. I. K. P. Spudich, The 1984 Morgan Hill, California, Earthquake: Science, v. 225, p. 288-291, 1984.

Hanks, T. C., The National Earthquake Hazards Reduction Program scientific status, 1984: U.S. Geological Survey Circular, 76 p., in press, 1985.

Lindh, A. G., Preliminary assessment of long-term probabilities for large earthquakes along selected fault segments of the San Andreas fault system in California: U.S. Geological Survey Open-File Report 83-63, 14 p., 1983.

Lindh, Allan, Constance Mantis, Peter Evans, and Mark Grossenbaugh, Parkfield Prediction Program: Summaries of Technical Reports Volume VII, National Earthquake Hazards Reduction Program, U.S. Geological Survey, p. 276-280, 1978.

Lindh, A. G., B. L. Moths, W. L. Ellsworth and J. Olson, Historic seismicity of the San Juan Bautista, California region: U.S. Geological Survey Open-File Report 82-180, p. 45-50, 1982.

Sykes, L. R., and S. P. Nishenko, Probabilities of occurrence of large plate rupturing earthquakes for the San Andreas, San Jacinto and Imperial faults, California: Journal of Geophysical Research, v. 89, no. B7, p. 5905-5927, 1984.

in: Summaries of Technical Reports, Volume VII,
National Earthquake Hazards Reduction Program,
December, 1978

Parkfield Prediction Program

8-9930-02098

Allan Lindh, Constance Mantis,
Peter Evans, and Mark Grossenbaugh

Branch of Seismology
U.S. Geological Survey
345 Middlefield Road
Menlo Park, California 94025
(415) 323-8111, ext. 2042

Goals

The principal goal of this project is to predict in advance the next magnitude six (or larger) Parkfield earthquake. The recurrence interval suggests that the chances are better than 50-50 that such an event will occur in the next ten years. Ten years would thus be a nominal estimate for the life of the project. A long-term goal will be to understand the role of the en echelon offset in the SA which spans the Cholame Valley just south of Gold Hill. The foreshocks and epicenter of the 1857 earthquake were located in this vicinity, and by analogy with the Anatolian Fault, may have been located at this offset. I have argued that the 1966 rupture terminated at this point (Lindh and Boore, 1973). Thus any understanding gained concerning the relation of this major discontinuity to the local strain and seismic regime might also pertain to the fundamental question of how great earthquakes like 1857 nucleate, and what relation this process has to that for events of magnitude six or seven.

More immediate short-term goals are:
1) To use existing geodetic and creep data to define as precisely as possible the slip distribution on the SA in the Parkfield area. Using linear inverse theory we will then attempt to design a program of observations to better resolve the slip distribution in time and space (along the fault and with depth) if this appears possible. One additional set of observations that will be undertaken immediately are a few new alignment arrays to fill gaps in our knowledge of the surface slip regime (possible locations are indicated by capital A's in Figure 1). An important question that will have to be faced is whether dislocations in an elastic half-space are an appropriate model, and if not, whether computable alternatives exist. This question is central to the interpretation of point strain measurements, such as those from strain and tilt meters.

2) To adapt the crustal model used by Jerry Eaton in 1966 to the present stations configuration, and to use this to relocate the earthquakes in the Parkfield area since 1969. We will try to fill the gap in '67-'68, between the 1966 aftershock studies and the USGS catalog that begins in

1969. We will also estimate the magnitude threshold to which the catalog is essentially complete, and fill any minor holes that exist. The revised catalog will then be used to compare the seismicity pattern along the fault to the 1966 aftershock pattern, as well as to the slip function obtained in 1). In addition, it will be used to study the time history of such gross characteristics as mean depth, B-slope, clustering in space and time, and spatial migration of hypocenters.

3) The amplitude ratio/focal mechanism study we attempted to initiate this year will be pursued in the Parkfield area (see last year's proposal), along with the zero crossing/stress drop work we tried on the Oroville foreshocks (see semi-annual report). By coordinating our efforts with Bill Bakun's detailed studies of individual events, we hope to quantify what relation, if any, the simple measurements we made at Oroville (P/S amplitude ratios, zero-crossing times and coda lengths) have to source orientation, moment, and duration. In particular, we will look for gradual changes in stress drop and source orientation that might reflect stress accumulation and/or fault zone property changes. As the foreshocks and main events of the last two Parkfield magnitude six events located at approximately the same point (the star in Figure 1 near the north end of the 1966 break) and as microseismicity continues at that point, it seems an ideal place to study the time history of such source characteristics. As the data accumulates it will also provide an opportunity to study the frequency of short term fluctuations in these characteristics. Such short term fluctuations might be useful in identifying immediate foreshocks to a large event, if and when they happen.

The strategy the first year will be to undertake an integrated analysis of the geodetic, creep and seismic data collected for the last ten years and of the strain, tilt and magnetic measurements made by the USGS and CIT in the last few years.

Instruments currently operating in the area are shown in Figure 1, along with the geodetic lines along which yearly measurements are made.

Assuming that the creep data constrain the very shallow slip, we will use Wayne Thatcher's geodetic inversion program to determine how well the results from the geodometer net constrain the slip distribution at depth (2? to 10 km) and whether any further measurements would add significant information in a few years.

A parallel modeling effort will be undertaken with Bill Stuart and Ralph Archuleta, using their 3-D finite-element fault simulation program to model the slip function obtained above with a frictional strength distribution that varies on the fault surface. In particular we will be interested in seeing whether the stronger (or stuck) patches occur at the ends of the 1966 break, near where much of the subsequent micro-seismicity has located.

A second use of the program will be to predict on the basis of Bill's strain-softening/instability model what premonitory deformation would be expected, for a given strength distribution, before the next Parkfield earthquake. The magnitude of these deformations may allow us to assess the adequacy of the observations being made in the area, and hopefully will be of use in sharpening the observational half of the experiment.

The goal is to arrive at an experimental design that will allow us, when the next large earthquake occurs, to distinguish between Bill's instability model, which requires extensive premonitory slip, and the null hypothesis, that an earthquake is just an Heaviside function in time. (We will also consider, of course, any other quantitative models that are proposed.) As the problem is dreadfully non-linear, this will of necessity be an iterative process; our hope is that feed-back loops can be estabilished between the theoretical models and the observational program so that there is some chance of reaching demonstrable conclusions with the expenditure of a finite amount of time, toil and money.

Another important strategic consideration will be to reconcile tidal precision point measurements of tilt and strain, which do not appear to have the long term stability required to measure secular strains, with the very stable geodetic measurements, which are repeated so infrequently as to be of no use in detecting short-term premonitory deformation. The two-color laser would be the slick way out of this problem. It will be a great boon to this project if Parkfield is chosen as the site for one of the new instruments.

Another approach we will try is to tie as many as possible of the point measurements together with short level lines and to expand of the small HP-3800 nets like those Mike Lisowski already has in the Parkfield area. This will allow a direct correction to be made for large non-tectonic drifts, and may also provide a test of the idea that large strains are occurring in and immediately adjacent to the fault zone.

A third approach will be to carefully examine the large quantity of tilt and strain data collected the last year or two by the USGS and Caltech in the Gold Hill area for internal consistency (Figure 1). In addition, three Sachs-Everson down-hole volumetric strain-meters will be installed in the Parkfield area. Each of these sites will also have a shallow 3-component invar wire strain-meter and a small geodetic figure for comparison. It may be however, that the long-term stability question will remain a sticking point and we will eventually be driven to more exotic hardware, like for instance, long-baseline tilt and strain-meters.

Invesitgations

The Parkfield area has been the site of four very similar magnitude six earthquakes in this century. The last three have had similar moments ($\sim 10^{26}$ dyne/cm), and have involved ground breakage along the same section of the San Andreas (SA), along the northeast edge of the Cholame

Valley. At least the last two have had foreshock activity, including one magnitude five foreshock in the final minutes before each main event. In addition the transition from creeping to locked sections of the SA occurs in the Parkfield area, apparently without the complications of slip on subsidiary strands. The northern terminus of the 1857 earthquake is in this area, and it appears to have been the site of several foreshocks and the main epicenter as well (Sieh, 1979).

Surface creep and geodetic measurements make it clear that strain is accumulating along this stretch of the SA, and suggest that the strain gradients are high, both in time and space. We are now past the minimum interval between magnitude six's is this century. As the zone that broke in 1966 has been the site of continuing microseismicity up to the present (including a cluster of activity near the 1966 epicenter), and is already the site of a large number and variety of other measurements, this region seems to us emminently suitable for a detailed prediction experiment. This conclusion is further strengthened by the existence of qualitative evidence that the 1966 event was preceded by accelerating aseismic deformation in the weeks prior to the main event.

We have initiated such an experiment in the Parkfield area. Our intention is that by emphasizing analysis of existing data and by close co-operation with Bill Stuart's modeling efforts, it will be possible to pose answerable questions concerning the slip and/or stress distribution at Parkfield. These questions will then be used to better focus a program of augmented field observations.

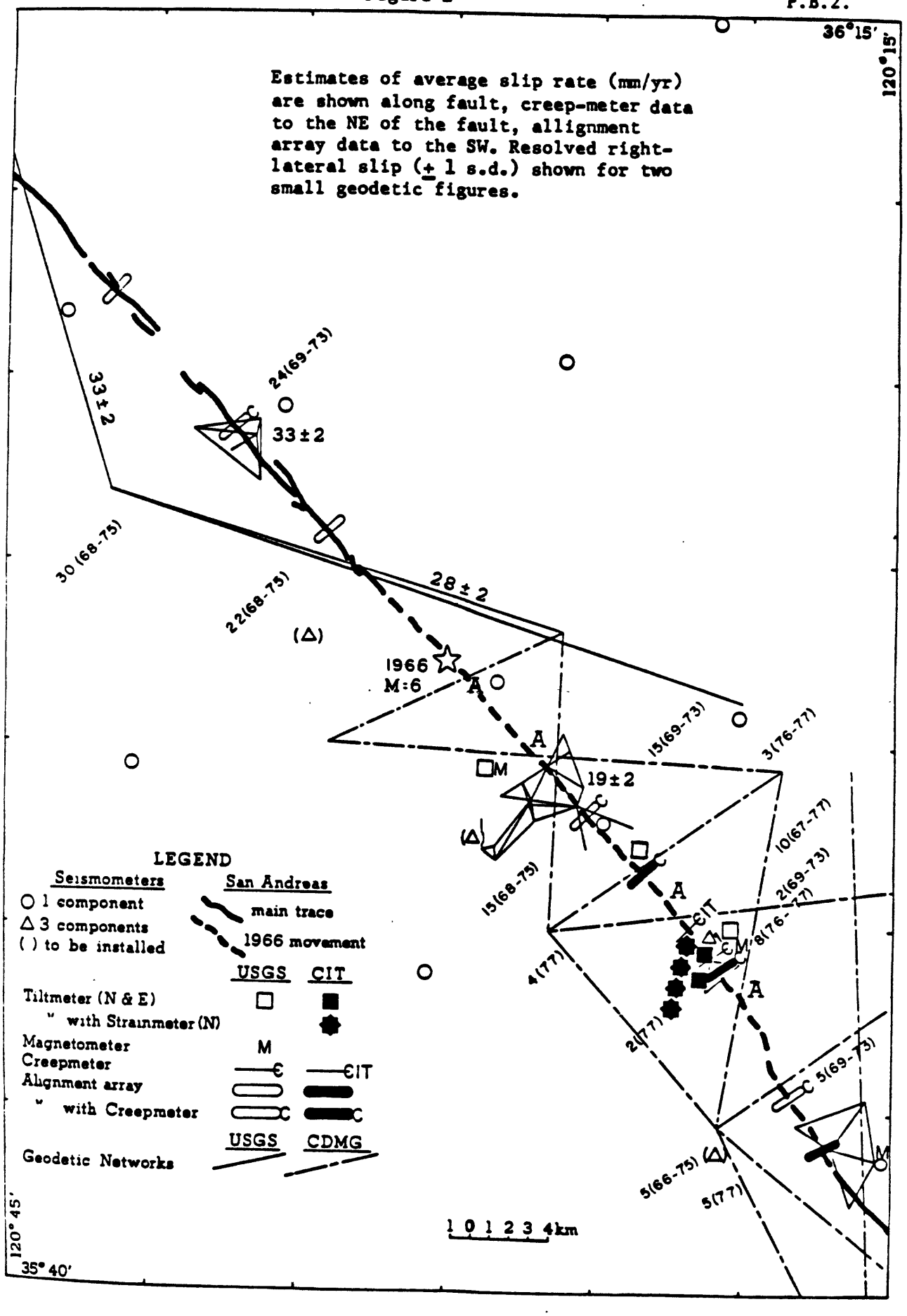
Estimates of average slip rate (mm/yr) are shown along fault, creep-meter data to the NE of the fault, allignment array data to the SW. Resolved right-lateral slip (± 1 s.d.) shown for two small geodetic figures.
36°15'
120°15'
33±2
24(69-73)
33±2
30(68-75)
22(68-75)
28±2
(Δ)
1966
M:6
A
15(69-73)
3(76-77)
M
19±2
(Δ)
10(67-77)
15(68-75)
2(69-73)
4(77)
8(76-77)
2(77)
5(69-73)
5(66-75)
5(77)
LEGEND
Seismometers
○ 1 component
△ 3 components
( ) to be installed
San Andreas
main trace
1966 movement
USGS CIT
Tiltmeter (N & E)
" with Strainmeter (N)
Magnetometer M
Creepmeter
Alignment array
" with Creepmeter
USGS CDMG
Geodetic Networks
1 0 1 2 3 4km
120° 45'
35° 40'

4/16/84

THE PARKFIELD, CALIFORNIA, PREDICTION EXPERIMENT

W. H. Bakun and A. G. Lindh

ABSTRACT

Moderate-size earthquakes occurred on the Parkfield section of the San Andreas fault in central California in 1881, 1901, 1922, 1934, and in 1966. The earlier Parkfield earthquakes were similar to the 1966 event, leading to the hypothesis of a characteristic Parkfield earthquake with recurring, recognizable source features. A simple recurrence model that explains most of the nistoric seismicity near Parkfield implies that the next characteristic Parkfield earthquake will occur within a four year time window centered on 1987-1988. A Parkfield Prediction Experiment, designed to monitor the details of the final stages of the earthquake preparation process is underway. Observations and reports of anomalous seismicity and aseismic slip preceding the last characteristic earthquake in 1966 constitute much of the basis for the design of the Parkfield Prediction Experiment; other design considerations involve testing models of the deformation process leading to failure.

INTRODUCTION

Analysis of the probability of damaging earthquakes in California suggest that the Parkfield-to-Cholame section of the San Andreas fault in central California is the most likely site of a damaging earthquake in the next several years (see figure 1). Lindh (1983) found a 67% probability of a magnitude 6 earthquake at Parkfield in the next 10 years. Available data suggest that a much narrower time window, 1986-1989, for the occurrence of the next Parkfield earthquake can be established. Since this time window is near, and because historic Parkfield earthquakes have been so similar, Parkfield provides a unique opportunity to prepare in detail an experiment to observe the final stages of the earthquake preparation process. The results of this experiment should provide the understanding of that process so critical to the design of earthquake prediction efforts in other areas.

The last damaging Parkfield earthquake, on June 28, 1966, had a Richter local magnitude M_L of 5.6 (Bakun and McEvilly, 1979, 1984) and a seismic moment M_0 of 1.4×10^{25} dyne- cm (Tsai and Aki, 1969). Although large enough to cause significant damage if located in a metropolitan area, the shock caused only minor damage to the large cattle ranches and sturdy wood frame homes in the sparsely-populated Parkfield region. Maximum modified Mercalli intensities of VIII were observed over an area of a few hundred square kilometers centered on Parkfield and the Cholame Valley.

The source of the 1966 earthquake is adequately described for our purposes here by a simple model: unilateral rupture propagation to the southeast over a 20 to 25-km-long section of the San Andreas fault, herein called the rupture

locus, between two geometric discontinuities in the fault trace (Lindh and Boore, 1981). The northwest discontinuity, adjacent to the epicenter of the 1966 shock, is a 5^{o} change in the strike of the fault trace. The term preparation locus will be used to describe the 1 to 2-km-long section of fault that includes both the fault bend and the main shock epicenter. Available data support the view that earlier damaging Parkfield earthquakes were similar to the 1966 event, leading to the hypothesis that Parkfield main shocks have recurring, recognizable source features (Bakun and McEvilly, 1984). Parkfield shocks with these attributes are called characteristic Parkfield earthquakes. Our working hypothesis is that the next damaging Parkfield earthquake will be characteristic, i.e., resembling in detail earlier shocks, in particular the 1966 event for which much detailed information is available (e.g., McEvilly et al., 1967; Brown et al., 1967).

HISTORIC SEISMICITY

Parkfield earthquake sequences with moderate-size main shocks occurred on February 2 in 1881, March 21 in 1901, March 10 in 1922, June 7 in 1934, and June 28 in 1966. Although the Parkfield-to-Cholame section of the San Andreas fault has been tentatively identified as the locus of the probable epicenter of the 1857 Fort Tejon great earthquake and its two moderate-size foreshocks (Sieh, 1978a), data are not sufficient to constrain slip on the San Andreas fault near Parkfield in 1857 (Sieh, 1978b). Epicenters of one, or both, of the 1857 foreshocks as well as the epicenter of the main shock in 1857 might lie on the San Andreas fault southeast of the Parkfield-to-Cholame section.

The times of Parkfield earthquake sequences, including 1857, are plotted in figure 2 against the earthquake sequence counter; i.e., 1857 is number 1, 1881 is number 2, etc. The time between sequences is remarkably similar, with the mean intersequence time = 21.9±3.1 years. Although the time of the 1934 sequence is not consistent with the regular intersequence interval, the time of the 1966 sequence reestablishes the intersequence spacing in that (1966-1922)/2 = 22 years. The two straight lines represent linear regressions of the dates on the counter I. Using all six dates, origin time = 20.8*I+1837.6 (solid line in figure 2) suggesting that the next Parkfield sequence, i.e. number seven in the series, was due in the spring of 1983. Ignoring the apparently anomolous 1934 date, origin time = 21.7*I+1836.2 (dashed line in figure 2), suggesting that the next sequence will occur at the beginning of 1988. Clearly, occurrence of another Parkfield sequence in the next several years would not be unexpected.

THE CHARACTERISTIC PARKFIELD EARTHQUAKE

The 1934 and 1966 Parkfield sequences were remarkably similar. In addition to the common epicenter, magnitude, fault-plane solution and unilateral southeast rupture of the main shocks, identical M_L = 5.1 foreshocks preceded each main shock by 17 minutes (Bakun and McEvilly, 1979, 1984). The lateral extent of aftershock epicenters over the rupture locus in 1966 (McEvilly et al., 1967) repeated that in 1934 (Wilson, 1936).

Much less data are available for Parkfield sequences prior to 1934. Nevertheless, most of the data are consistent with the hypothesis that the

earlier main shocks in 1881, 1901, and 1922 were similar to those in 1934 and 1966. The epicentral location of the main shock in 1922 is constrained by the Love-P_n arrival times at Berkeley, CA (Δ = 240km) to the 18-km-long section of the fault northwest of the preparation locus (Bakun and McEvilly, 1984). The data permit a common epicenter for the 1922, 1934 and 1966 main shocks near the southeast end of the preparation locus. A comparison of seismograms for the 1922, 1934 and 1966 main shocks recorded at the same sites (e.g., see figure 3) suggests that within experimental errors (~ 10-20%), the seismic moment M_0 in 1922 and in 1934 were each equal to the M_0 for 1966 (Bakun and McEvilly, 1984).

Although the features of the main shocks are similar, there are notable differences in the foreshock activity (see figure 4). The 1934 main shock was preceded by a nearly 3-day-long foreshock sequence. The 1934 foreshocks included an M_L 5.0 foreshock 55 hours before the main shock. Whereas the immediate (17 minutes) M_L 5.1 foreshocks in 1934 and 1966 were identical, there was no early foreshock activity in 1966 comparable to that in 1934 (see figure 4). There are no reports of felt foreshocks preceding the main shocks in 1881, 1901, or 1922, so that M_L 5 foreshocks probably did not preceed these early events. Furthermore, there are no foreshocks in 1922 evident on the Berkeley Bosch-Omori seismograms; M_L 4 1/2 Parkfield shocks probably would be noticeable on these records.

The similarities in the main shocks suggest that the Parkfield-to-Cholame section of the San Andreas fault is characterized by recurring earthquakes with predictable features. The notion of a characteristic earthquake with predictable features means that the design of a prediction experiment can be

tailored to the specific features of the recurring characteristic earthquake. Also, as shown in the next section, the hypothesis permits the construction of a recurrence model that can explain most of the historic seismicity at Parkfield.

A Recurrence Model for Parkfield Earthquakes

The limited data available on the recurrence of large and great earthquakes along plate boundaries around the world apparently is consistent with a time-predictable model, for which the time interval between successive shocks is proportional to the coseismic displacement of the preceding earthquake (Shimazaki and Nakata, 1980; Sykes and Quittmeyer, 1981). The fundamental principles of the time-predictable model are contained in Reid's (1910) analysis of the mechanics of the 1906 California earthquake. That is, an earthquake occurs when the strain accumulated since the preceding earthquake results in sufficient stress to rupture the fault surface. Adding the concepts of a constant failure stress threshold, a constant rate of strain accumulation, and variable stress drop results in the time-predictable model. Unfortunately this simple model is not supported by the data available for the last three Parkfield earthquakes: although comparable coseismic displacements in 1922, 1934, and 1966 are inferred from the observations, the time intervals differ by more than a factor of 2 (12 yrs versus 32 yrs).

However, simple adjustments to the assumptions that drew the time-predictable model from Reid's analysis result in another model that we call the Parkfield Recurrence Model, whic accounts for the historic seismic

activity at Parkfield. Like the time-predictable model, the Parkfield recurrence model assumes a constant loading rate and an upper bound stress threshold σ_1, corresponding to the failure or yield stress of the fault. Whereas the time-predictable model permits variable stress drop, the Parkfield recurrence model assumes a characteristic earthquake (constant stress drop) and permits failure before σ_1 is reached. Of course such a model is useful in a predictive sense only if these early failures occur infrequently. The Parkfield recurrence model is illustrated in figure 5. The constant stress threshold at which most characteristic earthquakes occur is represented by σ_1. A constant loading rate of 3 cm/yr was used to match the rate of relative plate motion across the creeping section of the San Andreas fault to the northwest of the Parkfield section (Burford and Harsh, 1980). We assume that the Parkfield earthquakes in 1881, 1901, 1922, and 1934 were identical, with 60 cm of coseismic slip representing a constant average static stress drop of a few tens of bars. We use a 20% larger coseismic slip for 1966, consistent with the marginally larger seismic moment in 1966 (Bakun and McEvilly, 1984).

A simple physical model can qualitatively account for the features of the Parkfield recurrence model. Let σ = the upper stress threshold σ_1 correspond to times when the failure stress is approached generally over the entire fault, at which times failure must occur. That is, there are no late characteristic Parkfield earthquakes. Following Brune (1979), we can devise a triggering scenario that permits the occasional early characteristic earthquake. Consider an asperity, i.e., the preparation locus, adjacent to a weak, creeping fault section, i.e., the rupture locus. If a local stress concentration at the asperity exceeds the failure stress there, then

the rupture in a resulting relatively high-stress drop small shock might easily extend into the weak rupture locus and continue until resistance to rupture is sufficient to stop the earthquake (e.g., Husseini et al., 1975; Das, 1976). (At Parkfield, the geometrical barrier at the southeast end of the rupture locus provides sufficient resistance to rupture to stop the characteristic Parkfield earthquakes.) Thus a smaller Parkfield shock might grow into a characteristic earthquake when the failure stress is approached only locally in the preparation locus. Local, rather than general approach of the failure stress, would correspond to $\bar{\sigma} < \bar{\sigma}_i$.

A triggering mechanism for the occasional early characteristic Parkfield is easily seen in its only example, the 1934 event. The sequence of foreshocks located near the preparation locus (Wilson, 1936) in the 3 days just before the 1934 main shock is a clear expression of localized failure. Apparently these foreshocks in 1934 were sufficient to alter the stress field at the main shock focus so that the trigger mechanism for an early characteristic earthquake outlined above could occur. Clearly the location and source mechanisms of the nearby foreshocks control their effect on the stress field within the preparation locus. Note that the early (55 hours) M_L 5.0 foreshock in 1934 was characterized by unilateral southeast rupture expansion toward the preparation locus (Bakun and McEvilly, 1981), a particularly efficient mechanism for increasing dynamic right-lateral shear stress in the preparation locus. The epicenter of the immediate (17 minutes) M_L 5.1 foreshock in 1934 was 1-2 km northwest of the main shock epicenter so that it too was favorably situated to increase right-lateral shear stress in the preparation locus. While the foreshock swarm is the immediate triggering

mechanism, we do not understand the conditions that led to the earthquake sequence. Accelerated loading rate associated with nonuniform regional strain accumulation (Thatcher, 1982) and/or accelerated fault creep near the preparation locus as well as temporal changes in the failure stress associated with fluctuations in pore pressure, etc. must be considered.

The recurrence of $M_L \geq 4$ earthquakes since 1930 is shown by the stick-plot diagram at the bottom of figure 5. The 10-12 years following the 1934 and 1966 Parkfield earthquakes are relatively quiet. Earthquakes with $M_L > 4.0$ tend to occur at a higher rate after exceeds a second stress threshold σ_2. Apparently $\sigma = \sigma_2$ corresponds to local stress concentrations approaching the failure stress. The sequence of M_L 3-5 foreshocks in 1934 at $\sigma \simeq \sigma_2$ (see figure 5) suggest that under at least some conditions a characteristic Parkfield earthquake can occur at $\sigma = \sigma_2$. According to the Parkfield recurrence model shown in figure 5, the lower stress threshold σ_2 was reached in 1975, when $M_L \geq 4$ Parkfield earthquakes again occurred. That is, an early characteristic earthquake this cycle might have occurred as early as 1975.

The stress threshold σ_1, at which the next characteristic Parkfield earthquake must occur, should be reached early in 1988. Since the 1934 shock did not occur at $\sigma = \sigma_1$, it is ignored in estimating the uncertainty in the predicted time of the next characteristic shock. The appropriate relation, origin time = 21.7*I + 1836.2, where I = characteristic earthquake counter (dashed line in figure 2), results in observed-predicted occurrence times of -0.9 yr for 1857, 1.5 yr for 1881, -0.1 yr for 1901, -0.8 yr for 1922, and 0.2 yr for 1966. The rms difference is 0.9 yr. Using 2 std dev. to define the

duration of the time window, these calculations imply that the next Parkfield earthquake should occur in 1988.0± 1.8, i.e., between 1986 and 1989.

RECENT SEISMICITY

Although earthquakes occur throughout central California, most of the shocks in recent years lie along the San Andreas fault (see figure 6). Not shown here are the sequences of earthquakes east of the San Andreas near New Idria in October 1982 (M_L5.4) and near Coalinga in May 1983 (M_L6.5). Earthquakes on the San Andreas are shown as a lineation of epicenters 3-5 km southwest of the San Andreas fault trace. This apparent mislocation is presumably the result of lateral variations in crustal velocity not adequately modeled in the location algorithm. Most of the shocks on the San Andreas occur on the creeping section to the northwest of the preparation locus. The section southeast of Cholame that broke during the great Fort Tejon earthquake of 1857 is currently locked, with no measureable fault creep and only infrequent small shocks. A cross section of the seismicity along the fault (figure 7) illustrates the predominance of the activity to the northwest of the preparation locus, defined by the locations of the main shock and the immediate M_L5.1 foreshock in 1966. This activity northwest of the preparation locus is concentrated at focal depths less than about 5 km. Focal depths of the main shock and the immediate foreshock in 1966 are about 8 km (Lindh et al., 1983), deeper than most of the events to the northwest of the preparation locus and deeper than the majority of aftershocks in the rupture locus (see figure 7)). The recent clusters of seismicity within the 1966 aftershock zone (shaded area in figure 7) occur at the concentrations of aftershocks identified by Eaton et al. (1970).

Prominent features of the seismicity near the 1966 hypocenter are illustrated in the schematic cross-section shown in figure 8. Since 1975 a number of magnitude 4 to 5 earthquakes have occurred near the preparation locus. This is the seismicity that, according to the Parkfield recurrence model shown in figure 5, occurred at σ greater than the second stress threshhold σ_2. The 1934 and 1966 Parkfield sequences were proceded by M_L5.1 foreshocks located at the northwest edge of the preparation locus. The immediate foreshocks had larger stress drops than had other M_L5 earthquakes that occurred in the area in the past 50 years (Bakun and McEvilly, 1981). These other M_L5 earthquakes all occurred a few kilometers northwest or southeast of the preparation locus (Bakun and McEvilly, 1981). It is not clear whether the larger stress drops of the immediate foreshocks result from their location at the edge of the preparation locus or because they preceded their respective main shocks by only 17 minutes. Note that the early M_L5 foreshock located 2 kilometers northwest of the preparation locus that preceded the 1934 earthquake by 55 hours was a relatively low stress drop source (Bakun and McEvilly, 1981). A magnitude 4 earthquake in June 1982 near the same location and the magnitude 5 shock in September 1975 located 5 km northwest of the preparation locus were lower stress drop sources as well (O'Neill, 1984; Bakun and McEvilly, 1981). Stress drops for a number of smaller earthquakes that have occurred near the preparation locus indicate a similar spatial pattern (see figure 9). Lower stress drop sources tend to occur around the higher stress drop sources. Note that the focal depths of the main shock and immediate foreshock in 1966 are relatively uncertain so that the hypocenters of these events whose epicenters define the extent of the

preparation locus might lie within the group of higher stress drop sources shown in figure 9. The implication is that the preparation locus is characterized by relatively high stress drop sources, whether or not the sources are foreshocks. Under this interpretation, the immediate foreshocks in 1934 and in 1966 were relatively high stress drop sources because of their location at the edge of the preparation locus rather than because they immediately preceded the main shocks.

The historic seismicity suggests that the preparation locus is critical in the nucleation of characteristic Parkfield earthquakes. The last two characteristic earthquakes, in 1934 and in 1966, were preceded by foreshocks within the preparation locus. These events, like other shocks within the preparation locus, are relatively high stress drop sources, consistent with the notion that the 5^{0} bend in the fault at the preparation locus is the point where stress is concentrated. Clearly any earthquakes located in the preparation locus, or any other anomalous behavior there, might be precursors to the next characteristic Parkfield earthquake.

SEISMIC INSTRUMENTATION

The seismic instrumentation now deployed near Parkfield (see figure 10) is focused to monitor the details of seismic activity in and near the preparation locus. Eleven seismographs of the U.S. Geological Survey's (USGS) central California seismic network (CALNET) are located within a few focal depths of the preparation and rupture loci. In addition, ten Terra-Technology DCS-302 digital event recorders are deployed in a temporary network near the

preparation locus; these temporary stations are being replaced by the more-reliable 3-component low-gain CALNET stations. The dense seismograph coverage around the preparation locus should provide documentation of any seismic precursors to the next Parkfield characteristic earthquake.

In addition to the seismograph networks, nearly 50 SMA-1 strong-motion accelerographs are deployed near the rupture locus (see figure 10). The conception and design of this strong-motion network was a cooperative effort of the USGS and the California Division of Mines and Geology (CDMG). The network is operated and maintained by the CDMG. A much sparser strong-motion network was operated near the southeast end of the rupture locus during the 1966 sequence of earthquakes (Murray, 1967) by the U.S. Coast and Geodetic Survey and the California Department of Water Resources. Data recorded by that network was the basis of important research on the focal mechanism of earthquakes and the interpretation of near-field strong motion recordings (eg., Aki, 1968; Haskell, 1969; Boore et al. 1971; Lindh and Boore, 1981). While data from that earlier sparse strong-motion network stimulated much discussion, it left unresolved some important questions. In particular, the location of the southeast end of the rupture locus in 1966 is uncertain; the current strong-motion network shown in figure 10 is designed to provide definitive answers to some of these questions.

STRAIN MEASUREMENTS

Reports consistent with signficant precursory aseismic slip along the rupture locus in 1966 provide a strong incentive to deploy strain-measuring

instrumentation near the rupture and preparation loci. An irrigation pipeline that crosses the main trace of the San Andreas in the rupture locus near creepmeter XCK (see figure 11) broke and separated about 9 hours before the occurrence of the main shock in 1966. Brown et al. (1967) attribute the break to 1-2 feet of southeast movement of the northeast end relative to the southwest end. This movement is consistent with the right lateral strike-slip displacement across the fault observed in the 1966 afterslip (Brown et al., 1967) and on creepmeter recordings near Parkfield since the early 1970s (Burford and Harsh, 1980). However, the time history of the movement that resulted in the broken irrigation pipe is unknown; perhaps only a small fraction of the postulated 1-2 feet of displacement occurred in the days and weeks just before the 1966 earthquakes.

Also of interest are the reports of very fresh appearing en echelon cracks observed in the rupture locus near creepmeter XUK (see figure 11) twelve days before the 1966 earthquakes (Brown et. al., 1967). (Note that cracks tend to appear each spring in the Cholame Valley (R. Burford, personal communication, 1982) as the clay soil desiccates following the winter rains.) The discovery of the cracks in June 1966 by delegates to the Second United States-Japan Conference of Research Related to Earthquake Prediction led to the deployment of a microearthquake study in the area on 18-19 June 1966, eight days before the 1966 sequence began; a 24-hour record from that study shows no identifiable magnitude $\geq$ 0 earthquakes within 24 km (Allen and Smith, 1966). Thus, if of tectonic origin, the en echelon cracks resulted from aseismic slip or fault creep in the rupture locus. The occurrence of 1-2cm of fault creep, inferred from the en echelon cracks, would be 4-8 times the annual creep rate

at Parkfield.

An optimistic interpretation of the broken irrigation pipeline and the fresh en echelon cracks described above is that significant anomalous precursory fault creep occurred at least in the rupture locus in the days and weeks just before the 1966 earthquake. If comparable aseismic slip precedes the next Parkfield earthquake, the strain measuring instruments deployed along the rupture locus (see figure 11) will provide clear precursory signals that might be used to issue a short-term prediction. Six creepmeters (see Burford and Harsh, 1980) span the main trace of the San Andreas fault in the rupture locus. Signals from these sensors are recorded on site and also are telemetered to the U.S.G.S. analysis facilities in Menlo Park, California.

Line lengths will be measured each night on a two-color laser distance measuring instrument located at the center of the radial array shown in figure 10; this instrument provides long term repeatability at the 10^{-7} level on lines of 3-8 km length. The two-color laser project is a cooperative effort of the University of Colorado and the U.S. Geological Survey. Two Sacks-Evertson volumetric borehole strainmeters are now installed near the southeast end of the rupture locus (DGH in figure 10); the borehole strainmeters have a sensitivity better than 10^{-10} and are isolated from first order surface noise sources such as rain and temperature. The borehole dilatometer project is a cooperative effort of the Carnegie Institute, Washington, D.C., and the U.S. Geological Survey. The two-color laser geodimeter and borehole strainmeter observations should provide corroborative evidence of changes in seismicity and/or creep rate. On a more fundamental basis, they provide the means to define any tectonic deformation leading up to the next characteristic Parkfield earthquake.

DISCUSSION

Although our understanding of Parkfield earthquakes is far from complete, the available information summarized in this paper suggest some guidelines for short-term prediction of the next characteristic Parkfield earthquake.

SCENARIO 1: FORESHOCKS IN THE PREPARATION LOCUS, FAULT CREEP IN THE RUPTURE LOCUS. Based on the observations in 1966, we might expect significant foreshock activity in the preparation locus in the hours and minutes before the next characteristic shock and perhaps significant fault creep in the rupture locus in the weeks and days before the event. If such precursors occur, then the current deployment of instrumentation shown in figures 10 and 11 should unambiguously capture the short-term precursory signals and might provide sufficient evidence to support a short-term prediction.

SCENARIO 2: NO FORESHOCKS, NO FAULT CREEP IN THE RUPTURE LOCUS. According to the Parkfield recurrence model shown in figure 5, the occurrence times of the Parkfield sequences in 1881, 1901, 1922, and 1966 were not anomalous. While the 1966 event was preceded by significant foreshock activity, the absence of reports of felt foreshocks in 1881, 1901, and 1922 suggests that these events were not preceded by M_L 5 foreshocks. Whereas the evidence for significant precursory fault creep in the rupture locus before the 1966 event is ambiguous, there is no information at all concerning analogous changes before the 1881, 1901, or 1922 earthquakes. Clearly the worst short-term prediction scenario - no foreshocks and no fault creep - would probably lead to the occurrence of the next characteristic shock without a short-term prediction.

Note however that the epicenter of the main shock in 1922 occurred near

the preparation locus. It seems reasonable to assume that some precursory changes, albeit without $M_L \geq 4\ 1/2$ foreshocks, occurred near the preparation locus in 1922. Under the characteristic earthquake hypothesis, the epicenter of the next characteristic Parkfield earthquake will be located near the preparation locus. Hence precursory changes, with or without foreshocks, in the preparation locus are likely. Whereas the two-color laser and dilatometers are favorably sited to detect deformation along the rupture locus, they are relatively insensitive to strain or creep in the preparation locus. Thus, if the only precursors are less-than-gross deformations in the preparation locus (scenario 2), the current instrumentation would likely fail to provide evidence of that deformation sufficient to permit a short-term prediction. Additional strain-measuring instrumentation near the preparation locus would significantly increase our ability to detect precursors in the worst-case short-term prediction scenario of no foreshocks and no significant fault creep along the rupture locus.

SCENARIO 3: EARLY (1934-LIKE) OCCURRENCE. Scenarios 1 and 2 dealt with circumstances likely to precede a characteristic Parkfield earthquake in 1986-1989, i.e., when $\sigma \tilde{\geq} \sigma_f$. The next characteristic Parkfield earthquake might occur early, i.e. at $\sigma < \sigma_f$, as in 1934. Could such an earthquake be predicted? Unfortunately, data from only one such occurrence, in 1934, is available to address that question. Fortunately, the foreshock swarm in 1934 was so pronounced and prolonged (see figure 4) that it would be easy to recognize a repeat of the sequence of events in 1934, even if no precursory fault creep occurred in the rupture locus. Note the failure of isolated M_L 5 Parkfield shocks in 1939, 1956, and 1975 (see figure 4) to be

followed by early characteristic Parkfield earthquakes. This admittedly limited data set suggests that not only are early characteristic Parkfield earthquakes preceded by significant prolonged foreshock activity, but that M_L 5 Parkfield earthquakes either isolated in time, e.g., 1939 and 1956 in figure 4, or only followed within a few hours by small aftershocks, e.g., 1975 in figure 4, are not sufficient in themselves to warrant the short-term prediction of a characteristic Parkfield earthquake. Of course the next characteristic Parkfield earthquake can only be early by at most 3 or 4 years in contrast to the 10-year-advance of the 1934 sequence; perhaps the sequence of events in 1934 cannot be used to anticipate the circumstances preceding a characteristic earthquake early by only a few years.

SCENARIO 4: A CHARACTERISTIC PARKFIELD EARTHQUAKE TRIGGERS A LARGER SHOCK. Scenarios 1, 2, and 3 describe circumstances that might precede the next characteristic earthquake, i.e., an M_L 5.6 shock bound by the geometrical barriers at the ends of the rupture locus. In this final scenario, we consider the situation where the characteristic earthquake breaks through the right-step en echelon offset at the southeast end of the rupture locus and continues southeast along the San Andreas fault, growing into a major earthquake. Mechanisms for rupture continuing through an unbroken, or broken, asperity have been developed by Das and Aki (1977). Alternatively, the characteristic earthquake might stop at the echelon offset, and, in analogy to the triggering mechanism of the early M_L 5.0 foreshock in 1934, increase the right-lateral shear stress on the fault southeast of the rupture locus so that another shock eventually starting there would rupture to the southeast. The latter case has been suggested (Sieh, 1978a; Lindh and Boore,

1981) as the triggering mechanism for the great Fort Tejon earthquake of 1857.

How might scenario 4 be discriminated in advance? Clearly this scenario presents technical, social, and political problems of the most serious nature. Slip in 1857 along the 50-km-long section of the San Andreas southeast of Cholame was about 3 1/2 m, significantly less than the 9 m offset further to the southeast (Sieh, 1978b). Continuation of a Parkfield earthquake to the southeast might result in a rupture length of about 90 km and offsets of about 3 1/2 m to the southeast of Cholame (Sieh and Jahns, 1984). Such an event would perhaps be as large as surface-wave magnitude M_S 7 1/2 (Sieh and Jahns, 1984). Social and economic consequences of such an earthquake would certainly be more severe than for the characteristic Parkfield earthquake considered in the first three scenarios. Since the average Holocene offset rate across the San Andreas fault at Wallace Creek is 3.5 cm/yr (Sieh and Jahns, 1984), it seems likely that the 3 1/2 m of slip in 1857 largely has been recovered so that the possibility of an earthquake breaking this segment must be taken seriously. Unfortunately, there is little data available to suggest what precursors might discriminate scenario 4 from scenarios 1, 2, or 3. Models of rupture through asperities (e.g., Das and Aki, 1977) suggest that minor differences in the stress field near the asperity, the strength of the asperity, and the dynamic stress ahead of the rupture could all be important. Although foreshocks and/or deformation at the southeast end of the Parkfield rupture zone might portend a shock significantly larger than a characteristic Parkfield earthquake, there is certainly no evidence that such need be the case.

References

Aki, K., Seismic displacements near a fault, J. Geophys. Res., 73, 5339-5376, 1968.

Allen, C. R., and S. W. Smith, Pre-earthquake and post-earthquake surficial displacements, in Parkfield earthquakes of June 27-29, 1966, Monterey and San Luis Obispo Counties, California - preliminary report, Bull. Seism. Soc. Am. 56, 966-967, 1966.

Bakun, W. H., and T. V. McEvilly, P-wave spectra for M_L foreshocks, aftershocks, and isolated earthquakes near Parkfield, California, Bull. Seism. Soc. Am. 71, 423-436, 1981.

Bakun, W. H., and T. V. McEvilly, Recurrence models and Parkfield, California, earthquakes, J. Geophys. Res. 89, in press, 1984.

Bakun, W. H., and T. V. McEvilly, Earthquakes near Parkfield, California: comparing the 1934 and 1966 sequences, Science, 205, 1375-1377, 1979.

Boore, D. M., K. Aki, and T. Todd, A two-dimensional moving dislocation model for a strike-slip fault, Bull. Seism. Soc. Am, 61, 177-194, 1971.

Brown, R. D., Jr., J. G. Vedder, R. E. Wallace, E. F. Roth, R. F. Yerkes, R. O. Castle, A. O. Waananen, R. W. Page, and J. P. Eaton, The Parkfield-Cholame California, earthquakes of June-August 1966-Surface geologic effects water resources aspects, and preliminary seismic data, U.S. Geol. Survey Prof. Paper 579, 66 pp., 1967.

Brune, J. N., Implications of earthquake triggering and rupture propagation for earthquake prediction based on premonitory phenomena, J. Geophys. Res. 84, 2195-2198, 1979.

Buhr, G.S., and A. G. Lindh, Seismicity of the Parkfield, California, region 1969 to 1979, U.S. Geol. Surv. Open-File Report 82-205, 89 pp., 1982

Das, S., A numerical study of propagation and earthquake source mechanism, ScD. Thesis, Massachusetts Institute of Technology, Cambridge, 1976.

Das, S., and K. Aki, Fault plane with barriers: a versatile earthquake model, J. Geophys. Res. 82, 5658-5670, 1977.

Eaton, J. P., M. E. O'Neill, and J. N. Murdock, Aftershocks of the 1966 Parkfield-Cholame, California, earthquake: a detailed study, Bull. Seism. Soc. Am., 60, 1161-1197, 1970.

Haskell, N. A., Elastic displacement in the near-field of a propagating fault, Bull. Seism. Soc. Am., 59 865-908, 1969.

Husseini, M. I., D. B. Jovanovich, M. J. Randall, and L. B. Freund, The fracture energy of earthquakes, Geophys. J. 43, 367-385, 1975.

Lindh, A. G., M. E. O'Neill, W. H. Bakun, and D. B. Reneau, Seismicity patterns near Parkfield, California, (abs.): Earthquake Notes 54, 61, 1983.

Lindh, A. G., and D. M. Boore, Control of rupture by fault geometry during the 1966 Parkfield earthquake, Bull. Seism. Soc. Am. 71, 95-116, 1981.

Lindh, A. G., Preliminary assessment of long-term probabilities for large earthquakes along selected fault segments of the San Andreas fault system in California, U.S. Geol. Surv. Open-File Report 83-63, 14 pp, 1983.

Murray, G. F., Note on strong motion records from the June 1966 Parkfield, California, earthquake sequence, Bull. Seism. Soc. Am 57, 1259-1266, 1967.

McEvilly, T. V., W. H. Bakun, and K. B. Casaday, The Parkfield, California, earthquakes of 1966, Bull. Seism. Soc. Am., 57, 1221-1244, 1967.

O'Neill, M. E., Source dimensions and stress drops of small earthquakes near Parkfield, California, Bull. Seism. Soc. Am. 74, 27-40, 1984.

Reid, H. F., The California earthquake of April 18, 1906, II, Mechanics of the Earthquake, Carnegie Inst. of Washington, Washington, D.C., 1910.

Shimazaki, K. and T. Nakata, Time-predictable recurrence model for large earthquakes, Geophys. Res. Lett., 7, 279-282, 1980.

Sieh, K. E., Centaral California foreshocks of the great 1857 earthquake, Bull. Seism. Soc. Am., 68, 1731-1749, 1978a.

Sieh, K. E., Slip along the San Andreas fault associated with the great 1857 earthquake, Bull. Seism. Soc. Am. 68, 1421-1448, 1978b.

Sieh, K. E., and R. H. Jahns, Holocene activity of the San Andreas fault at Wallace Creek, California, Geol. Soc. Am. Bull., in press, 1984.

Sykes, L. R., and R. C. Quittmeyer, Repeat times of great earthquakes along simple plate boundaries, Third Maurice Ewing Symposium of Earthquake Prediction, 4, edited by D. W. Simpson and P. G. Richards, AGU, Washington, D.C., 1981.

Thatcher, W., Seismic triggering and earthquake prediction, Nature, 299, 12-13, 1982.

Tsai, Y. B., and K. Aki, Simultaneous determination of the seismic moment and attenuation of seismic surface waves, Bull. Seism. Soc. Am., 59 275-287, 1969.

Wilson, J. T., Foreshocks and aftershocks of the Nevada earthquake of December 20, 1932 and the Parkfield earthquake of June 7, 1934, Bull. Seism. Soc. Am., 26, 189-194, 1936.

Figure Captions

Figure 1. Annual earthquake probabilities for selected segments of the San Andreas fault system in California (Taken from Lindh, 1983). These estimates are preliminary and should only be used to obtain an overview of the relative earthquake likelihood for different individual fault segments.

Figure 2. Series of earthquake sequence at Parkfield since 1850 (taken from Bakun and McEvilly, 1984). Solid line is the linear regression of the time of the sequence using the last six sequences. Dashed line is the linear regression obtained without the 1934 sequence. The anticipated time of the seventh, i.e., the next, Parkfield sequence for the two regressions is 1983.2 and 1988.0.

Figure 3. Surface waves recorded on the De Bilt, the Netherlands, east-west (DBN-EW) and north-south (DBN-NS) component Galitzin seismographs for the 1922, 1934, and 1966 Parkfield events (taken from Bakun and McEvilly, 1984). Amplitude and time scales are constant. Brackets indicate the Love- and Rayleigh-wave phases.

Figure 4. Parkfield seismicity relative to the origin times of M_L 5 shocks in 1934, 1939, 1956, 1966, and 1975. The times in 1934 are relative to the origin time of the early M_L 5.0 foreshock; felt foreshocks in 1934 for which Buhr and Lindh (1982) assign no magnitude are shown as M_L 3 events. Except for the aftershock sequences in 1934 and 1966, no known $M_L \geq 3$ Parkfield earthquakes occurred within several days of the 75-hour-long time intervals shown.

Figure 5. The Parkfield recurrence model. σ_1 represents the failure stress of the fault. Constant 3cm/yr loading rate and 60cm coseismic slip for the Parkfield earthquake sequences in 1881, 1901, 1922 and 1934 are assumed; a 20% larger coseismic slip was used for 1966. According to the model, the next Parkfield sequence is expected in 1988 $\pm$ 2 yr. $M_L > 4.0$ shocks since 1930 are shown at bottom. $M_L > 4$ shocks tend to occur when the stress exceeds σ_2.

Figure 6. Earthquake epicenters for 1969-1981 and the location of permanent seismographs in central California relative to geologic features. Most of the area shown is blanketed by Cretaceous and Tertiary marine sediments. Large outcrops of Franciscan melange (Fr) of Mesozoic age are shown, as is the western edge of the San Juaquin Valley, marking the boundary between Tertiary sediments and Quaternary alluvium. Symbols refer to the earthquake focal depths (..., 9, A, B, ...for...,

9-10 km, 10-11 km, 11-12 km,...). Symbol size is proportional to magnitude (see key). Epicenters were obtained using a one-dimensional crustal velocity model; the band of epicenters located on the San Andreas fault are displaced 3-5 km to the southwest because the higher crustal velocity southwest of the fault are not properly accounted for in the location procedure. Priest Valley (PRI) operated by the Univerity of California Berkeley Seismographic Station and the CALNET station at Gold Hill (GDH) were seismograph stations installed before the 1966 Parkfield sequence.

Figure 7. Cross section of the seismicity along the San Andreas fault near Parkfield for the years 1975-1980. The hypocenter of the main shock and the M_L 5.1 immediate foreshock in 1966 are shown as stars. Symbol size is proportional to magnitude. No vertical exaggeration.

Figure 8. Schematic cross section of seismicity ($M_L > 3$) along the San Andreas fault near Parkfield for 1969-1983. No vertical exaggeration. The shaded vertical band corresponds approximately to the location of a 5° bend in the surface trace of the fault. The preparation locus is inferred to lie within the shaded region between the hypocenters of the main shock and the M_L 5.1 immediate foreshock in 1966 (the two stars). The aftershocks in 1966, i.e., the rupture locus, lie southeast of

the preparation locus at depths shallower than 8-10 km. Since 1975, M_L 3-5 earthquakes have occurred near the preparation locus; these sequences are shown together with estimates of their source dimensions based on aftershock locations.

Figure 9. Cross section along the San Andreas fault zone near Parkfield showing the distribution of static stress drops for a number of earthquakes in 1977-1982 (taken from O'Neill, 1984). The numbers next to the symbols are stress drops in bars. The hypocenter of the main shock and the M_L 5.1 immediate foreshock in 1966 are shown as filled circles. Focal depths of the 1966 shocks are uncertain to within 1-2 km so that their hypocenters might easily coincide with the locus of greater stress drop sources shown as filled triangles.

Figure 10. Seismograph and accelerograph deployment along the Parkfield-to-Cholame section of the San Andreas fault relative to the preparation locus and rupture locus of the characteristic Parkfield earthquake. The epicenter of the 1966 main shock is shown as a star. The location of the southeast end of the rupture locus is problematic; in 1966, numerous aftershocks and surface cracks were observed over the 20-km-long section (cross hatching) immediately southeast of the preparation locus. Surface cracks and some small aftershocks were observed over a 15-km-long section further to the southeast.

Figure 11. Strain-measuring instrument deployment along the Parkfield-to-Cholame section of the San Andreas fault relative to the preparation locus and rupture locus of the characteristic Parkfield earthquake (see caption for figure 10). Names of sites of invar-wire strainmeters, bubble-level tiltmeters, Sacks-Evertsen dilatometers and creepmeters begin with S, T, D, and X respectively. Creepmeter XMM is located at the epicenter of the 1966 main shock.

TABLE 1. $M_L \geq 4$ Earthquakes Near Parkfield (1930-1983)*

#	YEAR	MO-DAY	ORIGIN TIME HR-MIN(OCT)	LATITUDE (°N)	LONGITUDE (°W)	M_L
1	1934	06-05	21-48	35°48.0'	120°20.0'	5.0
2	1934	06-05	22-52	35°48.0'	120°20.0'	4.0
3	1934	06-08	04-30	35°48.0'	120°20.0'	5.1**
4	1934	06-08	04-47	35°48.0'	120°20.0'	5.6***
5	1934	06-08	05-42	35°48.0'	120°20.0'	4.5
6	1934	06-08	09-30	35°48.0'	120°20.0'	4.0
7	1934	06-08	23-23	35°48.0'	120°20.0'	4.0
8	1934	06-10	08-03	35°48.0'	120°20.0'	4.5
9	1934	06-14	14-55	35°48.0'	120°20.0'	4.0
10	1934	06-14	15-54	35°48.0'	120°20.0'	4.0
11	1934	06-14	19-26	35°48.0'	120°20.0'	4.5
12	1934	12-02	16-07	35°58.0'	120°35.0'	4.0
13	1934	12-24	16-26	35°56.0'	120°29.0'	4.7**
14	1935	01-06	04-04	35°56.0'	120°29.0'	4.0
15	1935	10-22	18-37	35°55.0'	120°29.0'	4.0
16	1937	02-20	09-58	35°56.0'	120°29.0'	4.0
17	1938	11-22	15-30	35°52.7'	120°28.13'	4.2
18	1939	05-02	18-49	35°59.2'	120°21.28'	4.0
19	1939	12-28	12-15	35°58.17'	120°24.62'	5.2
20	1941	12-22	00-54	35°56.0'	120°29.0'	4.0
21	1942	10-31	10-51	36°01.86'	120°25.71'	4.0
22	1953	05-28	03-51	35°57.0'	120°28.98'	4.3
23	1953	06-22	15-22	35°55.9'	120°25.8'	4.4
24	1954	03-09	19-55	36°00.0'	120°20.0'	4.0
25	1956	11-16	03-23	35°57.9'	120°25.7'	5.0
26	1956	12-11	10-56	35°56.6'	120°28.0'	4.0
27	1958	09-01	11-31	36°06.0'	120°29.91'	4.6
28	1961	07-31	00-07	35°49.4'	120°15.8'	4.7
29	1961	12-14	11-51	36°00.0'	120°30.0'	4.0
30	1966	06-28	04-08	35°56.6'	120°30.5'	5.1
31	1966	06-28	04-26	35°56.0'	120°29.6'	5.6
32	1966	06-28	04-28	35°55.9'	120°29.6'	4.5
33	1966	06-28	04-32	35°48.9'	120°16.8'	4.0
34	1966	06-28	04-34	35°48.9'	120°16.8'	4.0
35	1966	06-29	02-19	35°55.8'	120°27.5'	4.0
36	1966	06-29	19-53	35°56.8'	120°28.6'	4.9**
37	1966	06-30	01-17	35°52.0'	120°21.5'	4.2
38	1966	10-27	12-06	35°56.9'	120°41.4'	4.2
39	1967	07-24	07-08	35°55.7'	120°26.25'	4.1
40	1967	08-12	18-57	35°51.2'	120°23.09'	4.2
41	1967	12-21	23-58	35°45.3'	120°26.8'	4.3
42	1967	12-31	23-48	35°55.31'	120°27.15'	4.5
43	1975	01-06	11-17	35°56.78'	120°30.90	4.4
44	1975	09-13	21-20	35°59.54'	120°33.22'	4.9**
45	1977	01-24	18-05	35°47.23'	120°20.96'	4.0
46	1977	11-29	16-42	35°56.51'	120°29.59'	4.1
47	1977	12-28	02-59	35°48.49'	120°21.89'	4.0
48	1982	06-25	03-58	35°58.32'	120°31.38'	4.0

* Events for 1930-1979 taken from Buhr and Lindh (1982). Locations for early events are approximate. Data for 1980-1983 taken from preliminary USGS earthquake catalogs.

** M_L taken from Bakun and McEvilly (1981).

*** M_L taken from Bakun and McEvilly (1984).

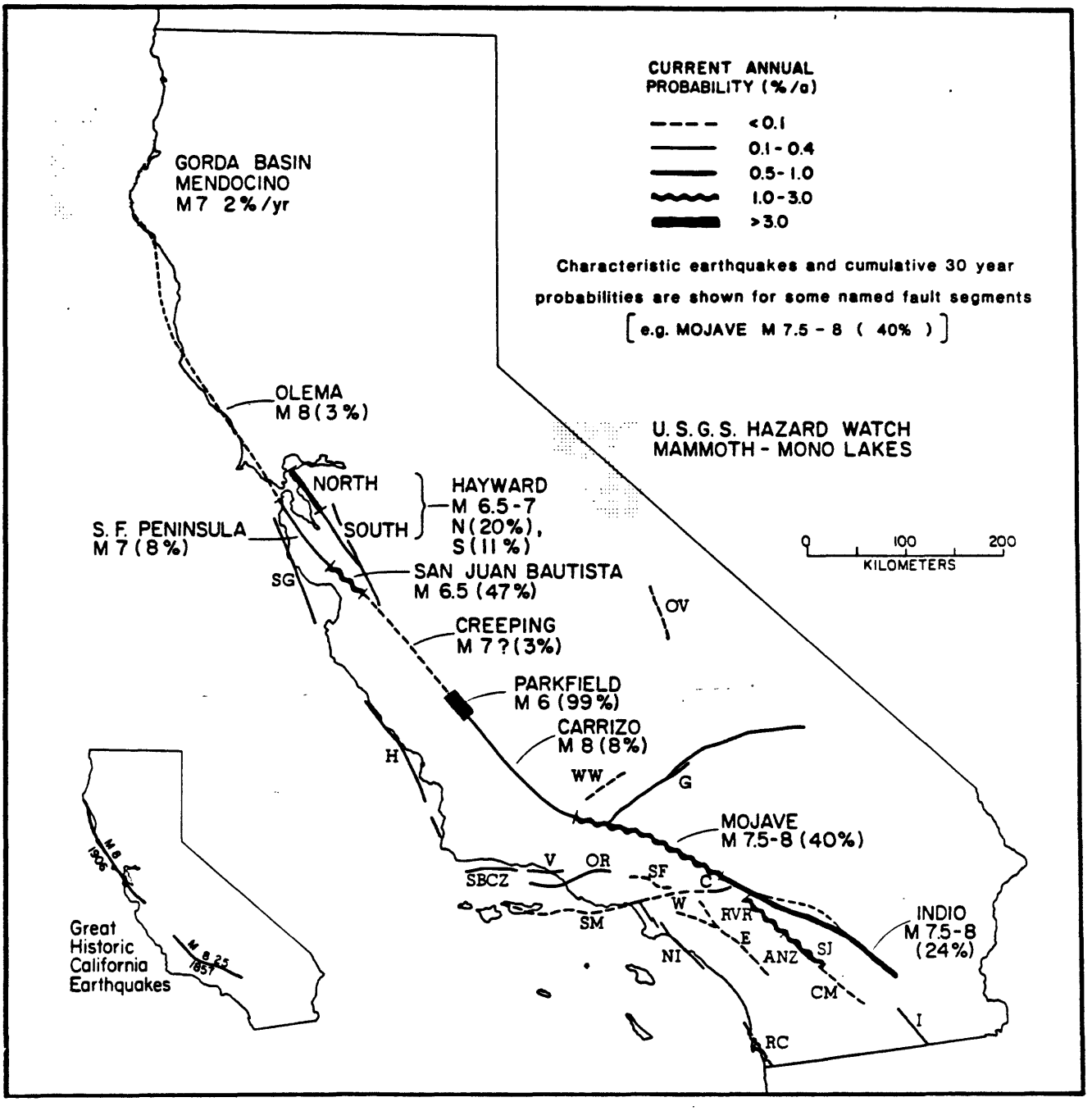
CURRENT ANNUAL PROBABILITY (%/a)
<0.1
0.1 - 0.4
0.5 - 1.0
1.0 - 3.0
>3.0
Characteristic earthquakes and cumulative 30 year probabilities are shown for some named fault segments
[e.g. MOJAVE M 7.5 - 8 (40%)]
GORDA BASIN
MENDOCINO
M 7 2%/yr
OLEMA
M 8 (3%)
NORTH
SOUTH
HAYWARD
M 6.5-7
N(20%),
S(11%)
S. F. PENINSULA
M 7 (8%)
SAN JUAN BAUTISTA
M 6.5 (47%)
CREEPING
M 7?(3%)
PARKFIELD
M 6 (99%)
CARRIZO
M 8 (8%)
MOJAVE
M 7.5-8 (40%)
INDIO
M 7.5-8
(24%)
U. S. G. S. HAZARD WATCH
MAMMOTH - MONO LAKES
0 100 200
KILOMETERS
SG
OV
H
WW
G
V
OR
SF
C
SBCZ
SM
W
RVR
E
ANZ
SJ
NI
CM
I
RC
Great
Historic
California
Earthquakes
M 8
1906
M 8.25
1857

Figure 1

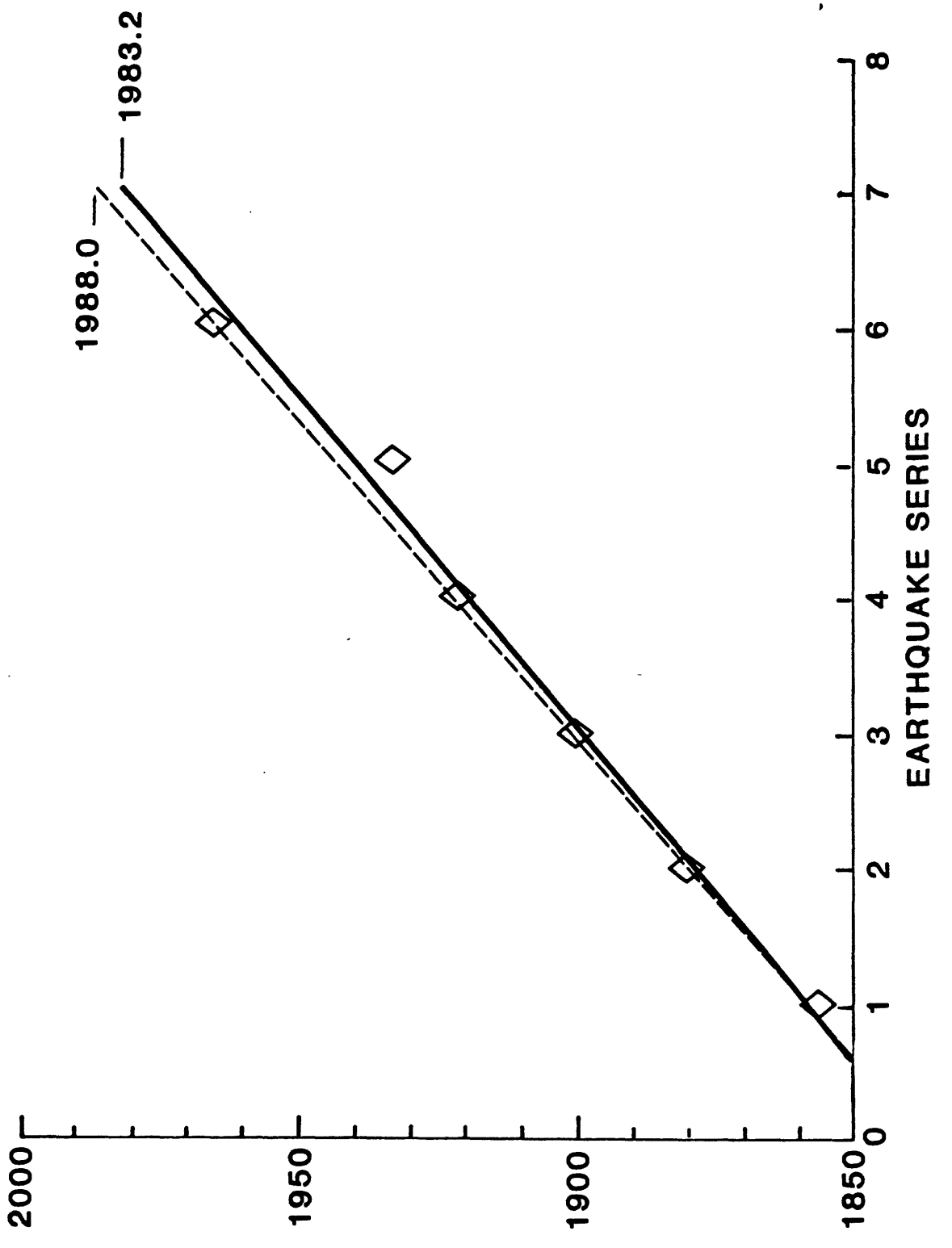
1983.2
1988.0
2000
1950
1900
1850
0
1
2
3
4
5
6
7
8
EARTHQUAKE SERIES

Figure 2

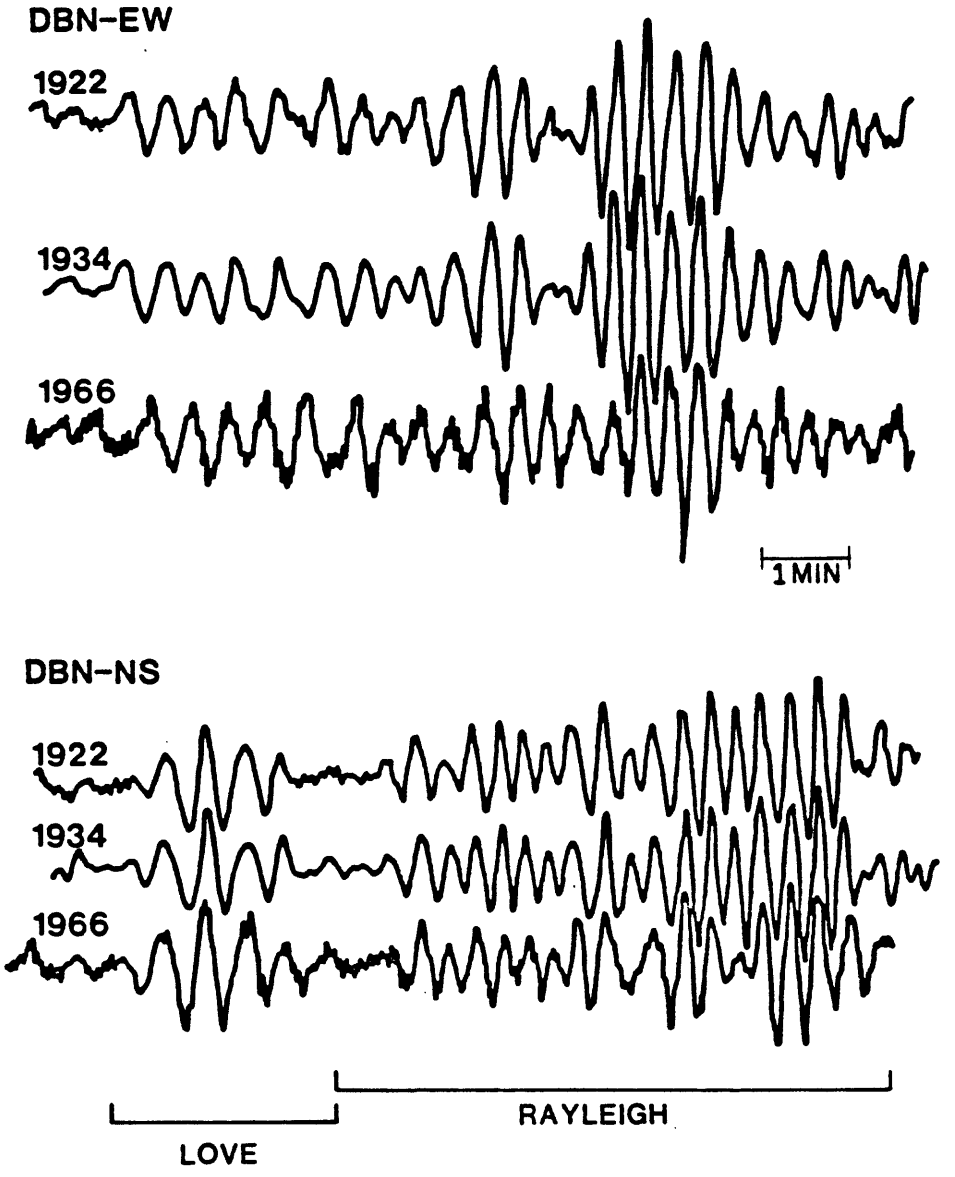
DBN-EW
1922
1934
1966
1 MIN
DBN-NS
1922
1934
1966
RAYLEIGH
LOVE

Figure 3

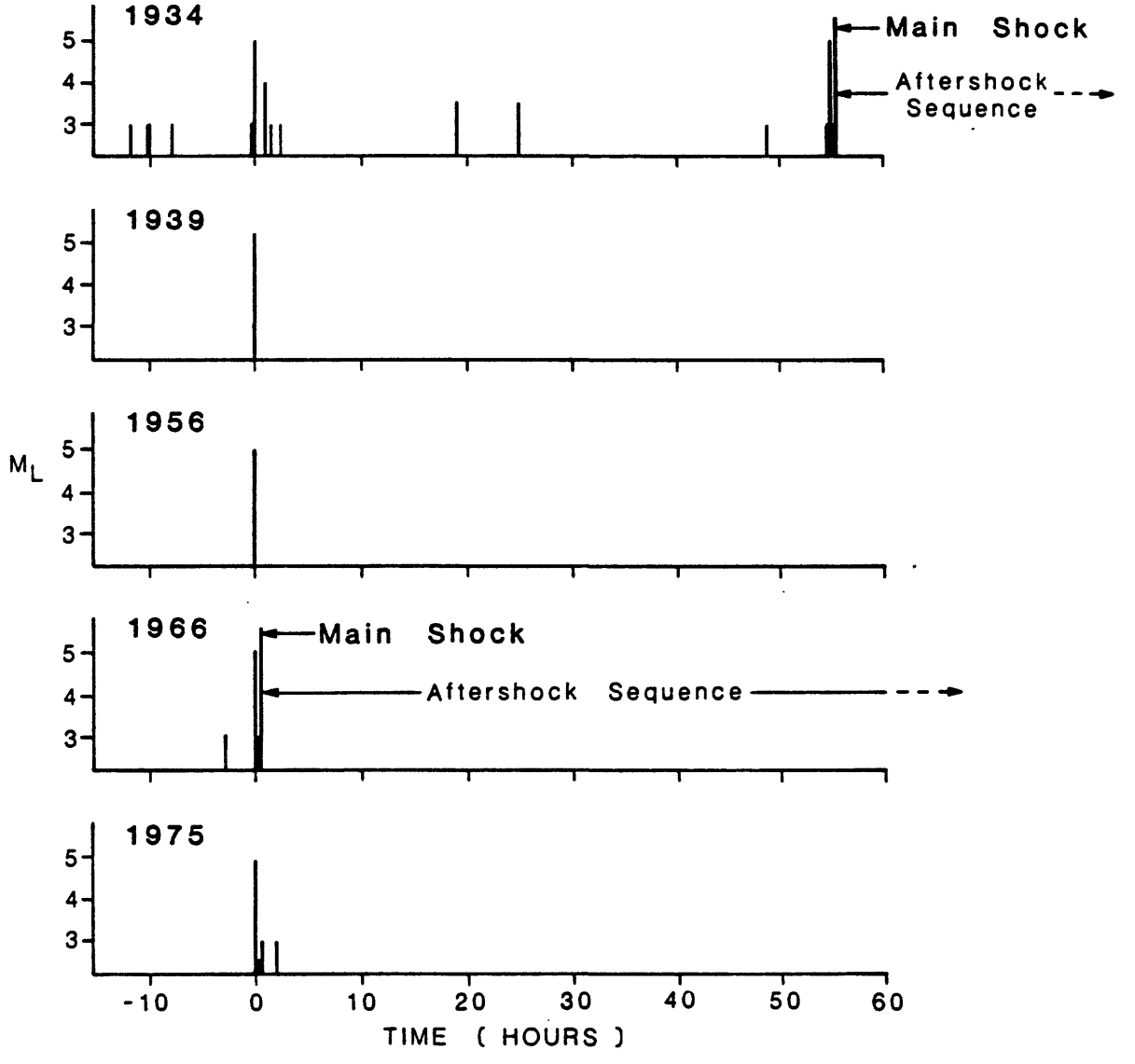
1934
Main Shock
Aftershock Sequence
1939
1956
1966
Main Shock
Aftershock Sequence
1975
5
4
3
M_L
-10
0
10
20
30
40
50
60
TIME (HOURS)

Figure 4

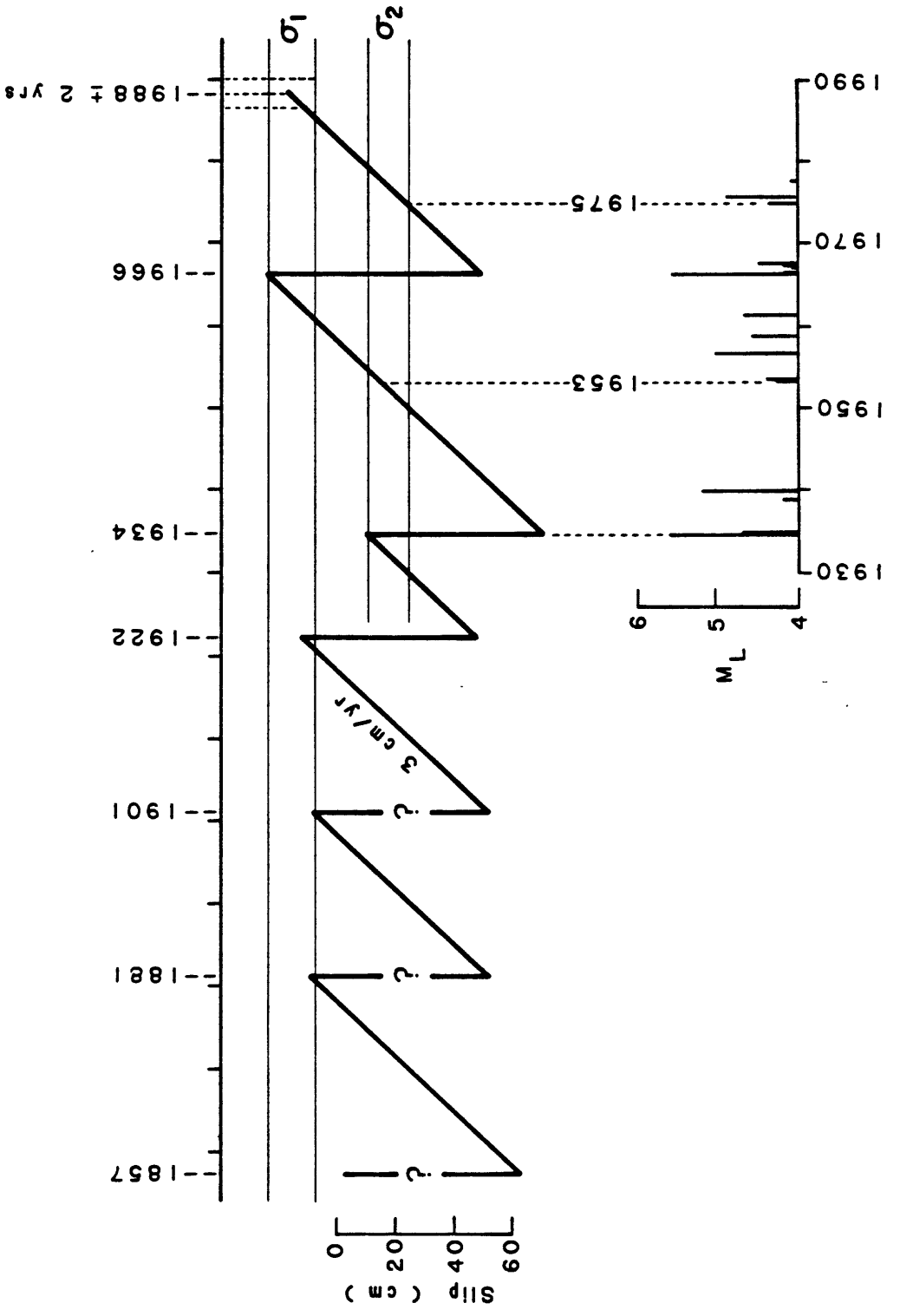
σ1
σ2
1988 ± 2 yrs
1966
1934
1922
1901
1881
1857
3 cm/yr
?
?
?
0
20
40
60
Slip (cm)
1990
1970
1950
1930
1975
1953
6
5
4
ML

Figure 5

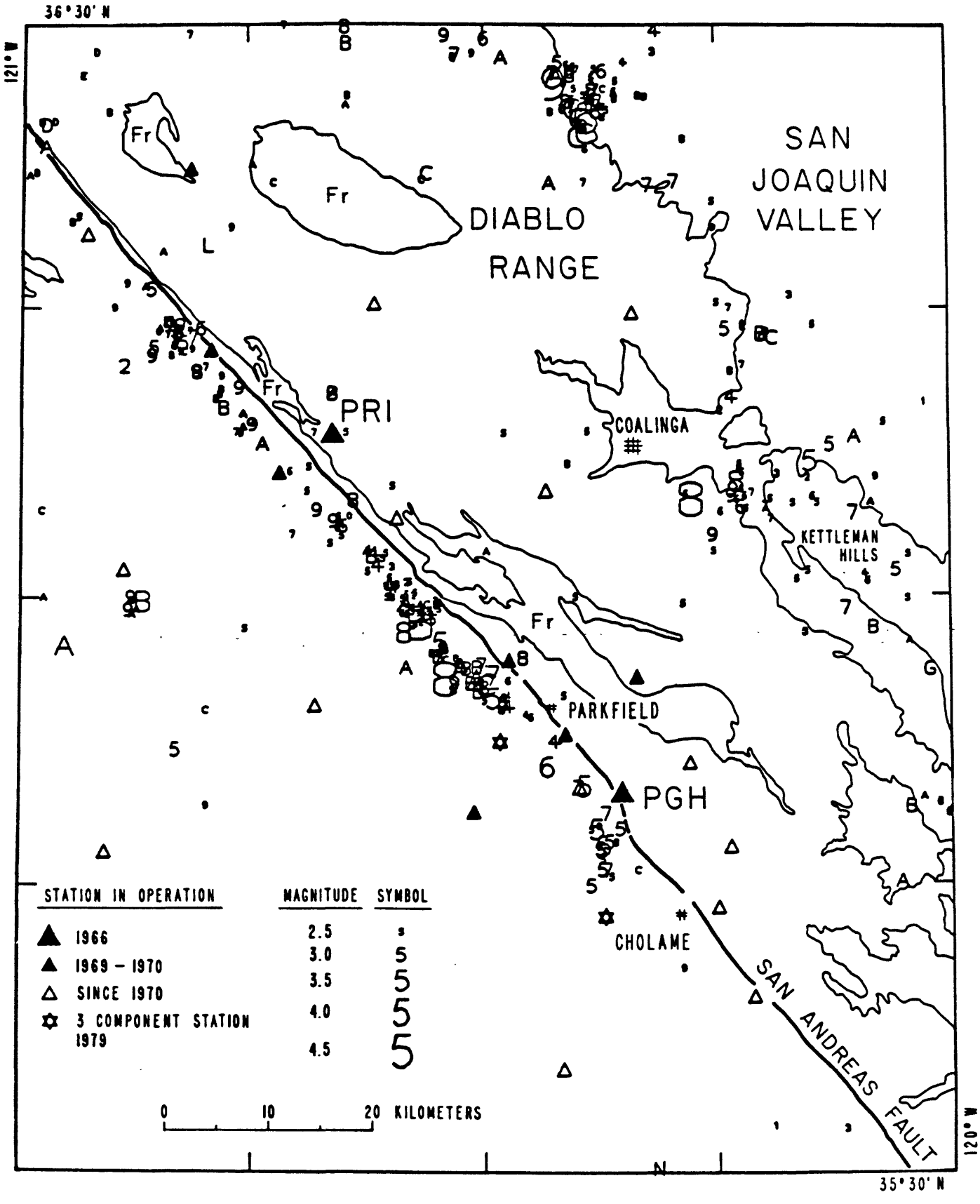
36°30' N
121° W
SAN
JOAQUIN
VALLEY
DIABLO
RANGE
Fr
PRI
COALINGA
KETTLEMAN
HILLS
PARKFIELD
PGH
CHOLAME
SAN ANDREAS FAULT
120° W
35°30' N
STATION IN OPERATION
1966
1969 – 1970
SINCE 1970
3 COMPONENT STATION
1979
MAGNITUDE
SYMBOL
2.5
3.0
3.5
4.0
4.5
0
10
20 KILOMETERS

Figure 6

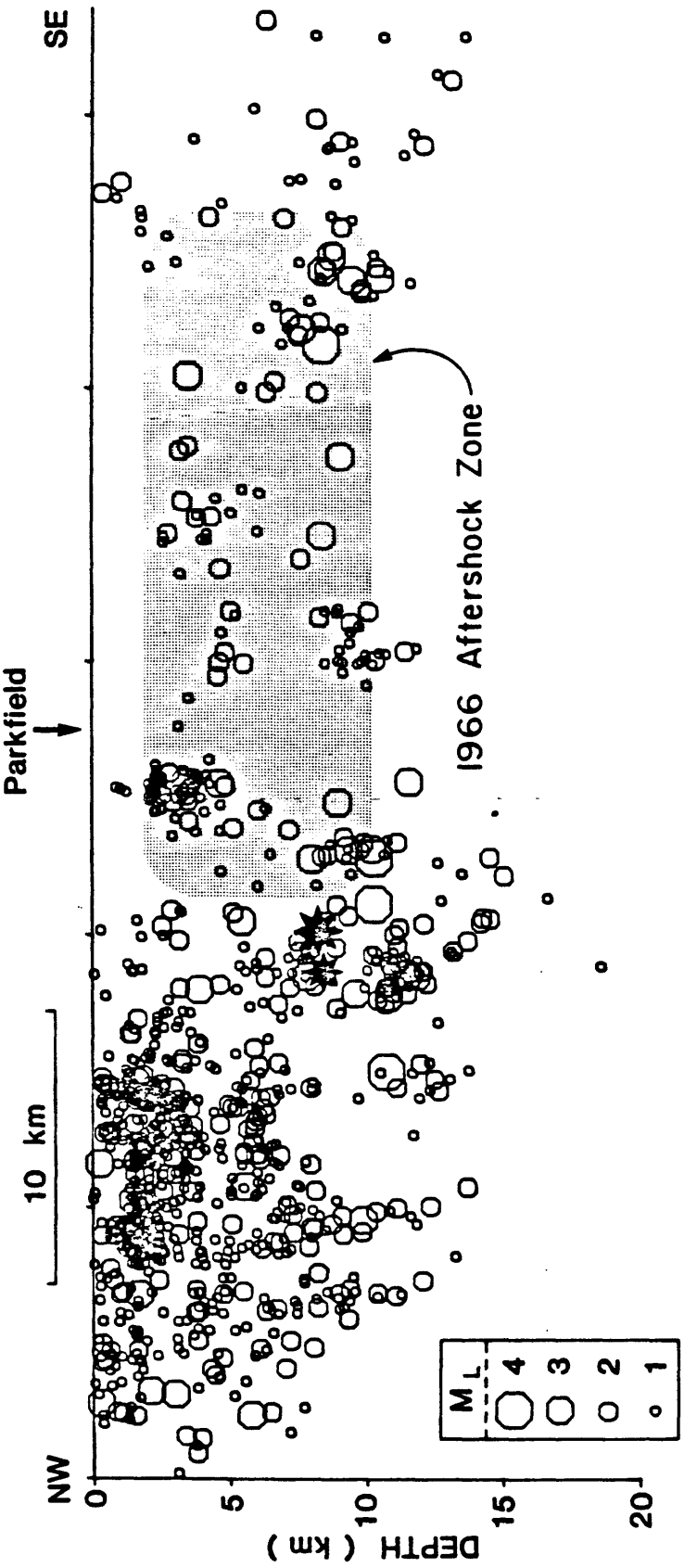
SE
NW
Parkfield
1966 Aftershock Zone
10 km
DEPTH (km)
0
5
10
15
20
M_L
4
3
2
1

Figure 7

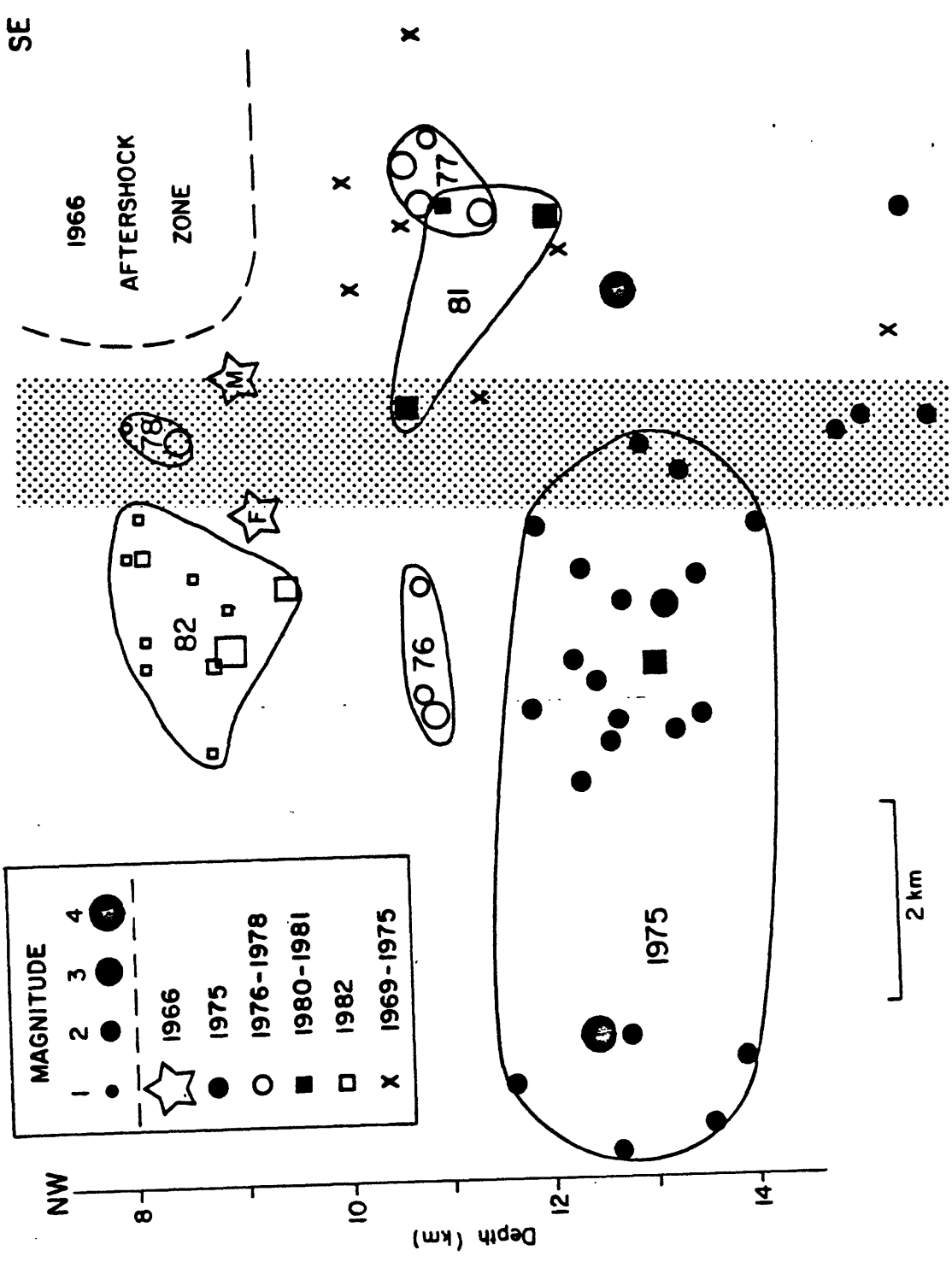
SE
1966
AFTERSHOCK
ZONE
M
F
78
82
76
77
81
1975
MAGNITUDE
1
2
3
4
1966
1975
1976-1978
1980-1981
1982
1969-1975
2 km
NW
8
10
12
14
Depth (km)

Figure 8

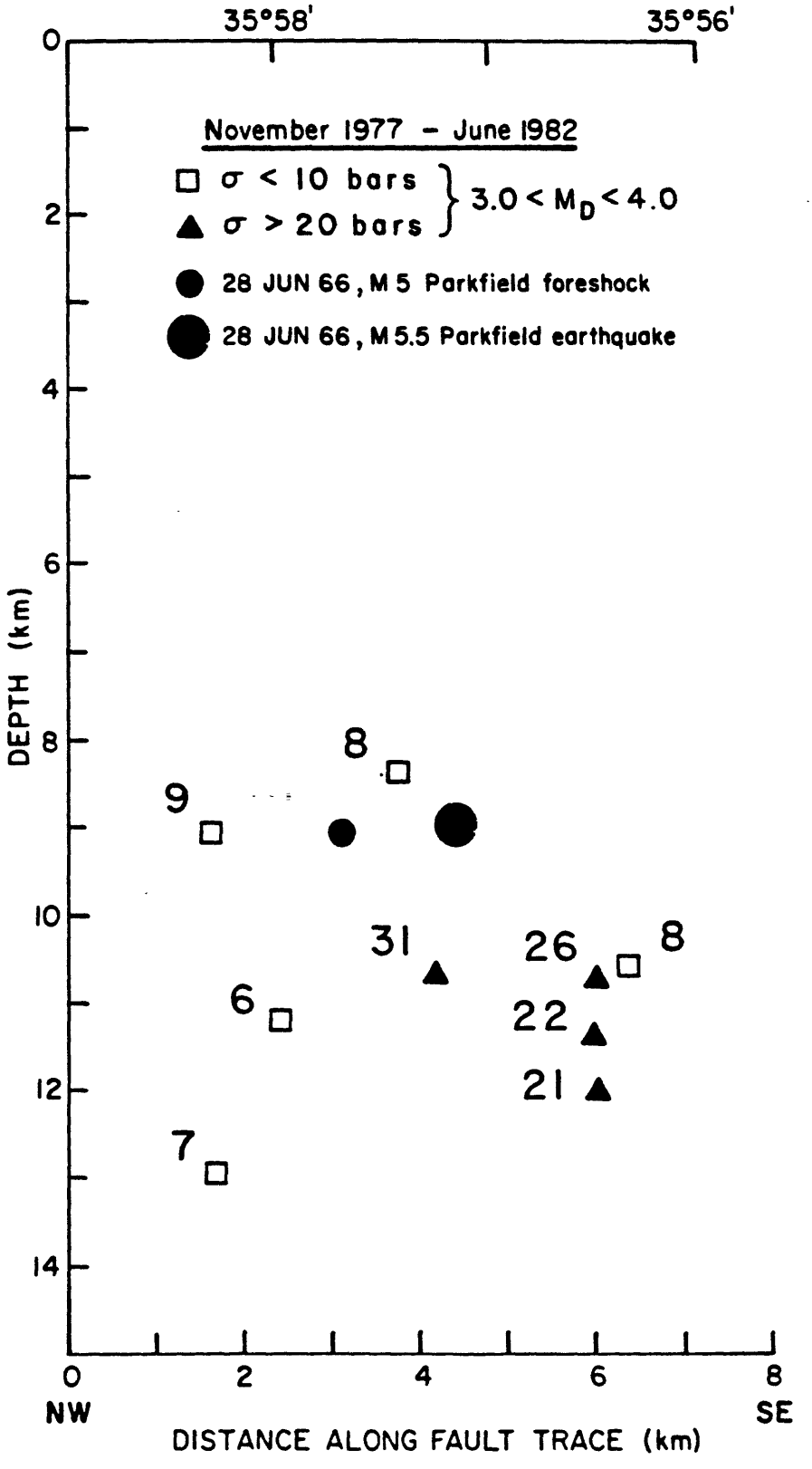
35°58'
35°56'
November 1977 - June 1982
□ σ < 10 bars
▲ σ > 20 bars
3.0 < M_D < 4.0
28 JUN 66, M 5 Parkfield foreshock
28 JUN 66, M 5.5 Parkfield earthquake
DEPTH (km)
0
2
4
6
8
10
12
14
8
9
31
26
8
6
22
21
7
0
2
4
6
8
NW
SE
DISTANCE ALONG FAULT TRACE (km)

Figure 9

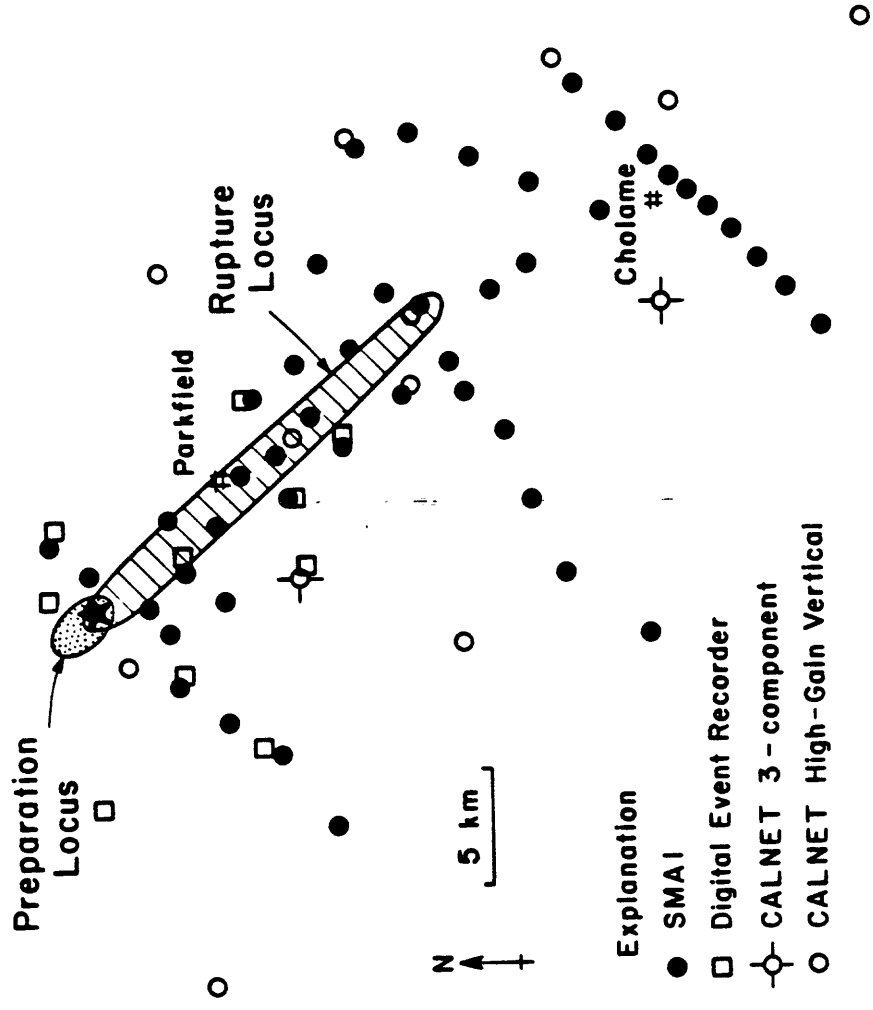
Preparation Locus
Parkfield
Rupture Locus
Cholame
5 km
N
Explanation
SMAI
Digital Event Recorder
CALNET 3-component
CALNET High-Gain Vertical

Figure 15

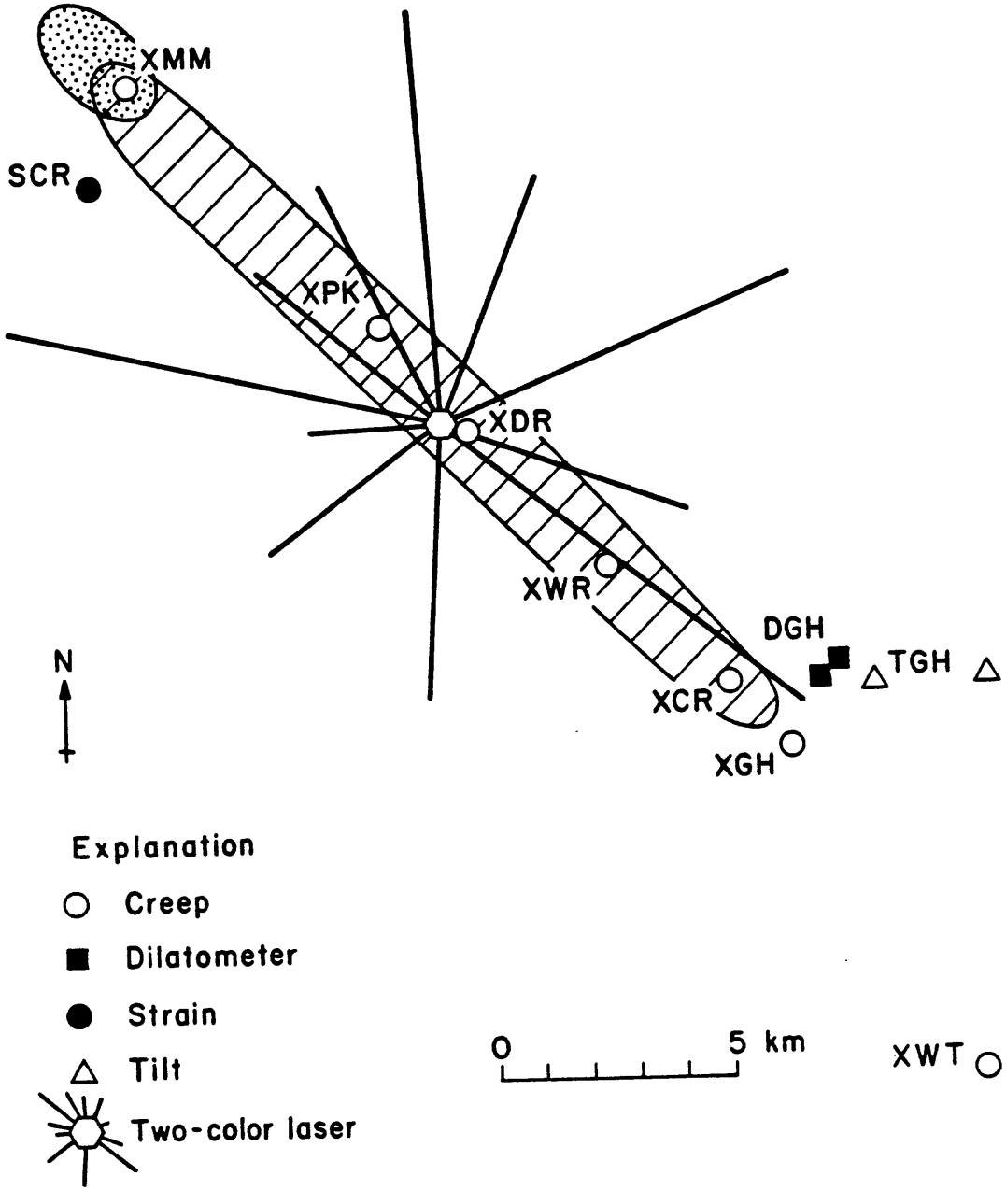
XMM
SCR
XPK
XDR
XWR
DGH
TGH
XCR
XGH
N
Explanation
Creep
Dilatometer
Strain
Tilt
Two-color laser
0
5 km
XWT

Figure 11

EXTENDED ABSTRACTS

Special Study Area in Southern California
San Jacinto Fault Zone

Tom Hanks and Chris Sanders, Principal Speakers
Rob Wesson, Reporter

The San Jacinto fault zone has been the highest producer of earthquakes near magnitude 6 and above of any fault zone of comparable extent in California since about 1890. Extending about 250 km southeast from the San Andreas fault in the vicinity of Cajon Pass, the San Jacinto Fault has produced at least five, probably seven and possibly as many as 10 earthquakes of magnitude near 6 and above. Owing to sparse settlement, pre-instrumental locations based on intensity distributions- - particularly prior to 1899 - - lead to uncertainty about assigning earthquakes to the fault, especially at the north end where the earthquakes may be located on the San Andreas or other faults. All large earthquakes since 1937 have occurred along the southern half of the zone, south of Anza.

Geological studies by Bob Sharp suggest a long-term slip rate of 8-12 mm/yr in the central part of the fault. Geodetic studies by King and Savage indicate a rate of accumulation of right lateral shear strain of about 0.3 strain/yr. Surface creep is observed to be zero since 1970 by Allen and others.

Seismic gaps

Three possible seismic slip gaps are suggested: Cajon-Pass to Riverside, Anza, and south of Superstition Mountain. Except in these gaps, the San Jacinto fault has experienced average seismic slip since 1890 of about 1 m. Even if the earthquakes with uncertain locations are assigned to the gaps, the gaps still lag behind the rest of the fault.

A 20-km long segment of fault within the northern end of the Anza seismic slip gap is also currently a gap for small earthquakes, marked at both ends by regions of high seismicity.

Geologic complexity and uncertainties at the northwest and southeast ends the San Jacinto fault may complicate interpretations based on a simple slip budget, but the region of the fault near Anza is a straight segment believed to be a single strand, bounded by complexity on the northwest and southeast.

It is not clear why any of these gaps exist but normal stress and fault complexity may play roles.

Evidence for imminence

The evidence for the imminence of a magnitude 6 earthquake includes 1) the absence of any significant seismic slip along a segment that is judged to have accumulated at least one meter-slip equivalent of seismic strain. 2) possible temporal seismicity patterns and 3) off fault seismicity at Cahuilla, in a small area that may be interpreted as a "stress meter."

Additional work indicated

The main questions surrounding the Anza gap and the whole northern San Jacinto fault are 1) Did significant slip occur in the Anza gap in the 19th century? 2) What is the recurrence rate? 3) Is the high rate of seismic slip along most of the fault over the last century a stable property, or a phenomenon that has now played out? Geologic investigations such as trenching in the Anza gap, if possible, seem to be suggested.

Conclusion

Based on the slip rate, and history of the last 90 years the northern San Jacinto fault, and Anza gap in particular, seems to be a likely location for a magnitude 6-7 earthquake in the near future. Existing information and instrumentation, location of fault in crystalline rock, and relative simplicity of the fault zone (at least distant from Cajon Pass) all argue in favor of the region as a site for designation as a special study area.

WORKSHOP ON

SPECIAL STUDY AREAS IN SOUTHERN CALIFORNIA

SUMMARY

Southern San Andreas fault - Tejon Pass to San Bernardino
Central San Andreas fault - Parkfield to Tejon Pass

Special studies along segments of the San Andreas fault between Parkfield and San Bernardino should consider four primary approaches, a discussion of which follows:

1 **Regional Outlook** -- If the large southern California earthquakes of 1857. 1872, 1927 and 1952 were to recur today, it is quite possible that we would predict only the 1857 event. The other events were located in areas away from the San Andreas fault where our monitoring equipment is currently sparse. More than a decade of effort clearly shows that there are more than 95 active faults in the Los Angeles Basin. A M6.5 earthquake on a fault system such as the Newport-Inglewood could have as large an impact on Los Angeles as an M8 earthquake on the San Andreas fault, located about 30 miles to the northeast. Consideration, therefore, should be given to a regional monitoring scheme that includes the San Andreas and San Jacinto faults and other structures as well. Detecting earthquake precursors is not easy and if we are not to miss a major earthquake, selective equipment upgrading should be done throughout southern California.

Studies should be geared to maintaining a regional perspective in order to gain a comprehensive picture of the earthquake process and the inter-

relationship of individual segments of the San Andreas system. Greater understanding of the slip rates of individual fault segments and of the variation of those rates with time (uniform(?)) are necessary in order to understand the long-term behavior of the San Andreas fault and major changes between active and "inactive" segments In addition, they provide important data on the kinematic character of multiple segments of fault systems for forecast modelling such as time - dependent and instability models. A regional approach also provides greater latitude for developing new, innovative instruments, and would allow us to coordinate experiments that employ these instruments.

2. **Pre- or syn- cluster developmental program** -- In order to best determine where instrument clusters should be installed, a developmental program should be initiated to address specific problems and to formulate models of how data should be collected. Of particular importance, is the continuation of geologic mapping and trenching of the type being done by Kerry Sieh, John Matti, Joe Ziony, and others to accurately map geologic units and the structural framework, to determine the chronologic history of fault activity, to establish local and regional fault slip rates, and to calculate earthquake recurrence intervals Groups of people should be identified for coordinated pre- and syn- cluster studies. From the standpoint of political support it should be kept in mind that Congress associates an augmented earthquake prediction program with increased monitoring focused on areas of high seismic potential. The program design, therefore, should include the simultaneous development of clusters and pre-cluster investigations.

Problems to be addressed include:

a. Determination of the long-term tectonic behavior of the San Andreas fault. From Cholame to Tejon Pass M8 events occur about every 250-450 years, with surface offsets on the order of 7m. Between Tejon Pass and Cajon Pass, on the other hand, there is about 145 years between M8 events and these are associated with surface offsets of about 3.5m. The entire interval, however, is believed to have a relatively uniform fault slip rate of 35mm/yr and there are no obvious gross differences in surface geology or in strain levels at the Garlock fault (Tejon Pass) where the seismic character of the fault changes. What, then, are the reasons for these changes? And what are the coupling mechanisms between segments that allow ruptures to propagate long distances during great earthquakes?

b. Between Parkfield and San Bernardino do fault ruptures begin in generally simple or complex areas?

c. Creep is occurring on the southern San Andreas fault from Thousand Palms to Bombay Beach (on the Salton Sea). Apparently, there is no current seismicity along this stretch of the fault. Why is this segment of the creeping fault aseismic while the central California creeping segment displays relatively abundant low-magnitude seismicity?

d. What mechanisms control how fault segments interact and how is total fault slip accommodated by tangential or en echelon systems? Why do events migrate and what controls the migration rate?

e. What effects do secondary structures and seismicity have on the occurrence, size, and nucleation point of major earthquakes?

f. Are premonitory signals present in our micro-earthquakes?

g. If the crust is locked at depths shallower than 20-25KM from Tejon Pass to Cajon Pass as geodetic data suggest, then it seems that prior to a large event the lower part of this zone must break (because recent earthquakes do not involve a thickness as large as 25KM). What experiments might we initiate to detect this premonitory rupture?

h. How do we determine that part of the strain budget that is accommodated by folding and minor fracturing as compared to faulting?

3. **Instrumentation at Parkfield** -- The current monitoring network at Parkfield is insufficient and should be augmented before a major effort is made to add new clusters in southern California. Our achievements at Parkfield may well determine our ability to secure new funding for an operational prediction network for southern California. What we learn at Parkfield may not be transferable to southern California but it should provide a good physical model that assists our research in network deployment strategy. Sufficient instrumentation at Parkfield is also

important to be able to properly evaluate the likelihood of a "run-on" of the expected Parkfield earthquake for 20 or so miles to the southeast, possibly producing an earthquake as large as M7

4. **Suggested cluster sites** -- Sites of concentrated monitoring in southern California probably should not be developed as replicates of the Parkfield cluster. Each new site will be tectonically and seismologically unique and so monitoring must be tailored to the physical characteristics and the logistical realities of the site.

The suggested sites are listed in the order in which they were mentioned most frequently, beginning with those mentioned the most.

a. Cajon Pass

The region from Pallet Creek to Cajon Pass was considered by many to be one of the strongest candidates for a cluster. It is the location where the fault rupture associated with the 1857 earthquake terminated and it marks a transition from a generally simple to complex segments of the San Andreas fault. It is, of course, the junction of the San Andreas and the San Jacinto fault systems and the seismicity increases south of the pass Recent movement on the San Jacinto fault may have produced sinuous bulges on the San Andreas fault, thus affecting the seismic potential at this location In terms of monitoring, we already have a baseline of data from the 2-color laser operations at nearby Pearblossum. In addition, downhole experiments and the development of a deep earth observatory in the Cajon Pass drill hole will provide data valuable for a more

comprehensive evaluation of the tectonic and seismologic environment.

b. Cholame area, southeast of Parkfield

The concern of a run-on of the next Parkfield earthquake argues that the area where the potential fault rupture will occur be adequately instrumented. The same area could possibly be the nucleation point of a repeat of the 1857 earthquake as well and so instrumentation should be increased in an effort to detect precursors.

c. Tejon Pass

The seismic and tectonic character of the San Andreas fault change across the Garlock fault. How do these changes affect earthquake potential on the San Andreas and how dangerous is the Garlock fault and the Big Pine fault? The intersection of major faults and the change in seismic character support the installation of a cluster between Tejon Pass and Lake Hughes.

d. Mojave

A cluster on a relatively simple stretch of the San Andreas fault may provide valuable data that can be applied to a better understanding of earthquake generation on more complex segments of the fault.

SESSION 3:

SAN BERNARDINO TO SALTON SEA

Speakers: Matti, Sieh, Johnson, Seeber

Reporter: Jim Dieterich

SAN GORGONIO PASS

John Matti described recent work and summarized his thinking on the geology and current tectonic elements of the greater San Gorgonio Pass region. This is an extremely complicated area with distributed faulting on several active strands and many old and probably inactive faults. An important question for understanding the current tectonics of this region and for planning possible monitoring sites is: How is the the San Andreas slip passed through this complicated region? Other related questions pertain to the behavior of this region at the time of a large earthquake: Would this region respond by "shattering" or would there be a single through going fault plane? Can earthquake slip propagate through this region to permit failure of the entire southern San Andreas or will this region form a temporary barrier to earthquake slip? Is this region likely to be the nucleation point for large earthquakes propagating either north or south along the San Andreas?

At Cajon Pass, Holocene (?) slip rate on the San Andreas is approximately 25 mm/yr (from the work of Welden and Sieh). To the south of Cajon the San Andreas splits into the northerly Mill Creek strand which appears to be inactive and the southerly San Bernardino strand which is active. Slip rate on the San Bernardino strand is approximately 25 mm/yr (Rasmussen, 1982), but slip appears to die out as the fault is followed to the south. South of Crafton Hills the trace of the San Bernardino strand joins the Wilson Creek strand and both appear to be inactive. At Crafton Hills there is a system of NE-SW trending normal faults that form a horst and graben complex immediately south of the San Bernardino strand. The Crafton Hills horst and graben complex appears to take up the slip on the San Bernardino strand and transfers it to the E-W faults of the San Gorgonio fault system.

The faults of the San Gorgonio system show evidence of Quaternary activity and include both thrust and strike slip types. The rate of right lateral motion on the San Gorgonio system is not well established and there was some discussion of the details of this point. Matti proposed that possibly 10mm/yr of slip occurs on these faults with the remaining 15mm/yr being added to the rate of San Jacinto fault in this region. This would give the San Jacinto a slip rate of 25mm/yr in this section. An alternate interpretation that appeared to favored by several of the participants is that the faults of the San Gorgonio system can account for the full 25mm/yr of slip that occurs on the San Bernardino strand of the San Andreas to the NW and on the Salton section of the San Andreas to the SE. By this latter interpretation the San Jacinto fault would

presumably have a uniform 10mm/yr of slip in this area and to the south.

To the east the faults of the San Gorgonio Pass system join the SE trending Coachella Valley segment of the Banning fault which in turn joins the northern end of the Salton section of the San Andreas. The Coachella Valley segement of the Banning fault is actively creeping now at 2mm/yr (C. Allen) and according to Matti's interpretation the average slip rate through this region is 25mm/yr. The latter rate is distributed principally between the Coachella Valley sections of the Banning and an active section of the San Andreas that may extend a short distance north of the Banning.

INDIO SEGMENT

Kerry Sieh discussed the historic and prehistoric record of slip on the Indio segment of the San Andreas fault. Sieh interprets this section of the San Andreas as one of the sections most likely to generate a large earthquake in the next 50 years. At many locations along this section surface features are offset by 3-6m. These offsets may be caused by creep, by prehistoric earthquakes or some combination of both. At Indio, the current creep rate is 1-3mm/yr and the average prehistoric slip rate is 23-35mm/yr. It is known that creep is presently occuring at many other locations and 2-3mm/yr seems to be a representative number. A noteworthy exception to this occurred at Mecca Beach where the creepmeter recorded three creep events in 1984 for a total slip in one year in excess of 10mm. If the offset features have a seismic origin, then the seismic slip must 3-6m or less. Taking an average slip rate of 25mm/y yields a maximum hypothetical earthquake recurrence time of 130-200yrs. There has been no large historic earthquakes which raises the question: Is an earthquake overdue?

A site near Indio that is under study by Sieh provides some new information to estimate the current seismic potential of this section of the San Andreas. The site is an alluvial channel cut through the shore bar of ancient Lake Cahuilla. The San Andreas fault at this site consists of four strands only two of which have been excavated. There is evidence for as many as five fault offset events. The data for two of these events is reasonably good and indicates large components of those slip events may have occured as seismic slip and not as creep. The interevent time is approximately 130-150 years. The amount of slip in these events is poorly constrained because only two of the strands have been excavated, but there has been a minimum of 2.7m since about 1630 A.D. and a minimum of 0.9m since about 1720 A.D.. Sieh indicated that work is continuing at this site and additional data should be forthcoming in 1985 and1986.

Finally, there was some discussion of the of the signifance of creep on this segement. The creep observations might be interpreted as premonitory to a large eathquake that is due or it might be interpreted as the passive response of the fault to strain. The distinctions have obvious important implications.

INTERACTION BETWEEN INDIO AND IMPERIAL SEGMENTS

Carl Johnson briefly discussed possible interactions between the the Imperial fault and the

southernmost section of the San Andreas fault. Slip on the two faults apparently links through the Brawley seismic zone which is an area of extensional tectonics. An analogous extensional zone offsets the Imperial fault to south. Johnson noted several characteristics of the southern end of the San Andreas and the northern end of the Brawley seismic zone that he interprets to indicate that this could be the point of nucleation of an earthquake sometime soon. The Imperial earthquakes of 1940 and 1979 nucleated at the northern and southern ends respectively of the Imperial fault at the tips of the extensional zones. The 1980 earthquake in Mexico nucleated at the corresponding southern tip of the southern extensional zone that offsets the Imperial fault. Hence, a case can be made that the larger earthquakes tend to nucleate at the tips of the extensional zones that transfers slip from one strike slip fault to another. The remaining extensional tip at the northern end of the Brawley seismic zone is the only one that has not nucleated an earthquake. In recent years the Brawley zone has been an area of high seismicity. Finally, and most recently, a new area of seismicity has been evolving off the southernmost end of the Indio section of the San Andreas, extending somewhat SE of the point of intersection of the Brawley seismic zone.

EASTERN TRANSVERSE RANGES SEISMICITY

Leonardo Seeber discussed recent results of analysis of the seismicity of the region adjacent to and NE of the Indio section of the San Andreas. Seismicity of this region is diffuse and is entirely to the NE of the trace of the San Andreas fault. The work described by Seeber suggests that the earthquakes can be divided into subgroups that have consistent first motion solutions and when thus grouped form linear patterns of fault zones. Treated in this manner a number of left lateral strike slip zones trending E-W or NE-SW. There was some discussion of the results and the methods of data reduction employed in this study. Interactions of these lesser faults to the NE of the San Andreas could have a bearing on the preparation of the San Andreas for large earthquake.

REPORT ON ROGER BILHAM'S IDEAS FOR THE INDIO SECTION

A brief decription was given of Roger Bilham's ideas correlating the geometry of the subsections of the Indio segment, topography and character of observed creep. Two distinct alternating trends of the fault can be discerned striking N40W and N48W. Areas of youthful hills occur opposite the N48W sections. The uplift presumably arises because of convergent interference on the fault. Continuous creep occurs on the N40W sections and triggered slip following larger regional events is restricted to the N48W sections. The suggestion of Bilham as presented here is that the strain patterns arising from fault geometry could be an element of a monitoring strategy for this section. There was discussion of the validity of the correlations of creep character and fault orientation.

SAN JACINTO FAULT ZONE

San Jacinto Fault Zone

The San Jacinto fault zone is the most seismically active fault zone in California. Since 1899 at least five and probably seven large earthquakes (M 6-7) were caused by fault rupture in this zone. The 1899 (M 7) and 1918 (M 6.8) earthquakes extensively damaged the towns of San Jacinto and Hemet and were probably caused by rupture of the 60 km segment of the fault zone centered on these towns. A smaller earthquake in 1923 (M 6¼) was most likely located on the San Jacinto fault near Riverside just northwest of the 1899-1918 rupture zone. Since 1937 all large earthquakes have occured in the southeastern half of the fault zone. Large events in 1937 (M_L 6.0) and 1954 (M_L 6.2) were caused by rupture of segments of the San Jacinto (Clark) fault, and the 1968 (M_L 6.8) Borrego Mountain earthquake was caused by rupture of the southern part of the Coyote Creek fault. A large earthquake in 1942 (M_L 6.5) was very likely located on the Superstition Mountain fault just southeast of the 1968 rupture.

The seismic moments of these large earthquakes have been determined (Hanks, Thatcher, and Hileman, 1975). Using these moment values Thatcher, Hileman, and Hanks (1975) estimated the amount and distribution of seismic slip along the San Jacinto fault zone. They noticed two significant gaps in seismic slip, one between Cajon Pass and Riverside (the fault zone section northwest of the 1899-1918 ruptures), and the other from Anza to Coyote Mountain (the fault zone section between the 1899-1918 and 1954-1968 ruptures). In essence the 1899-1918 and 1954-1968 fault zone segments have ruptured about one meter and the adjoining seismic-slip gaps have not.

The seismicity since 1977 (well located hypocenters, catalog complete above M 2) is generally concentrated in certain segments of the fault zone with quiet segments intervening. The most distinct quiet segment (called the Anza seismic gap by Sanders and Kanamori, 1984) is located between the two currently most seismically active segments of the fault zone. This seismicity gap is coincident with the northwest 20 km of the Anza to Coyote Mountain seismic-slip gap identified by Thatcher et al. (1975).

Sanders and Kanamori (1984) studied various aspects of the seismicity, geology, and geodetic results and concluded that the Anza seismic gap is seismogenic and highly stressed but at present locked by some mechanism. They suggested that the locked nature of the fault here may be due to relatively high compressive stress normal to the fault resulting from the convergent geometries of the local faults and the oblique orientation of the regional maximum compressive stress. They also noted another interesting aspect of the seismicity near Anza. The area of ground beneath the town of Cahuilla, about 10-15 km southwest of the center of the Anza seismic gap, was in 1980-1981 the site of an intense swarm of small earthquakes. This area was also the site of a swarm of M 3-4 earthquakes about a year and a half before the nearby 1937 event, and prior to the nearby 1918 event a weather station at Cahuilla reported a very high level of small, local, felt earthquakes. These data suggest that the ground beneath Cahuilla may be very sensitive to stress buildup prior to nearby large earthquakes. If this is true then the recent swarm activity at Cahuilla, which is the first there since 1935, may be indicating present high shear stresses on the faults near the Anza seismic gap.

Other relatively quiescent segments in the recent seismicity coincide with the 1899-1918, the 1954, and the 1968 rupture zones.

Presently seismically active areas in the fault zone are the stretch near Riverside coincident with the proposed rupture zone of the 1923 earthquake; the two segments bounding the Anza seismic gap, the southeast of which is partly coincident with the 1937 rupture zone; the unmapped extension of the San Jacinto fault coincident with the southeast end of the 1954 rupture; and the northwest end of the Superstition Mountain fault near the possible epicenter of the 1942 earthquake. Thus we see that the presently seismically active stretches of the San Jacinto

fault zone are located at the ends of the rupture zones of the largest large historic earthquakes (1899-1918, 1954, 1968 had large moments) or coincident with the rupture zones of the smaller large historic earthquakes (1923 and 1937 had small moments).

The historic large earthquakes in the San Jacinto fault zone have all occured on separate fault segments in the zone. No segment has ruptured twice. The seismic moments of these large events coupled with their locations and rupture areas indicate that two 40-60 km long seismic-slip gaps exist. If the seismic gap hypothesis holds we would expect future large earthquakes to occur within these gaps.

THE DIGITAL ARRAY AT ANZA, CA: PROCESSING AND INITIAL INTERPRETATION OF SOURCE PARAMETERS

Jon Fletcher, Linda Haar, Thomas Hanks, Lawrence Baker
at the U. S. Geological Survey
345 Middlefield Road, Menlo Park, CA 94025

Frank Vernon, Jon Berger, and James Brune
at IGPP of the University of California
San Diego, La Jolla, CA

ABSTRACT

Seismicity along the San Jacinto fault suggests that a 40-km-long section near the town of Anza may constitute a gap in the occurrence of $M_L = 6$ to 7 earthquakes. The potential for a gap-filling shock and the high rate of seismicity at the southern end of the gap (5 events of $4.0 \leq M_L \leq 5.5$ since 1970) provided the impetus for deploying a digital seismic array to collect high-quality ground motion recordings of all events $2 \leq M_L \leq 4.5$ (on-scale recording for shocks with magnitudes above $M_L = 4$ can be obtained from an existing array of eight strong motion accelerographs). The Anza site also had the advantage of being in the southern Californian batholith, which appears to be relatively homogeneous compared to the Franciscan/Gablian contrast of the central San Andreas; we expected the granitic rocks of the batholith would yield relatively accurate earthquake locations and efficiently propagate high frequencies.

The field instrumentation is specifically designed for broad-band recording (up to 70 Hz) and high dynamic range (96 dB in the onsite digitizer alone), since both are necessary for determining the rupture history of earthquakes. Both local VHF and microwave digital telemetry transmit the data from the Anza region to San Diego for computer data logging. In the first 30 months of the array's operation approximately 292 events have been recorded, located, and processed for source parameters.

Most events occur in one of five clusters, or in a diffuse zone near the Buck Ridge fault. Two of these clusters are located at right-stepping *en echelon* offsets (Coyote Creek–San Jacinto and San Jacinto–Hot Springs); two others are directly below and about 8 km west of Anza respectively. The fifth cluster is just to the northeast of the Hot Springs fault. Although event depths are generally between 11 and 14 km, at the southern end of the Hot Springs fault, depths extend to 18 km; these are some of the deepest strike-slip earthquakes on the San Andreas system.

We calculate source parameters such as the scalar moment and stress drop for the analysis of high frequency waves, scaling relations, and earthquake interaction. The largest event recorded thus far had a moment of 4.4×10^{21} dyne-cm ($M = 3.8$) and a stress drop of 55 bars. Both a_{rms} and Brune stress drops increase with moment; source radius increases only slowly with moment. The maximum values of both the Brune and a_{rms} stress drops

increase with depth down to 10 km, remain approximately constant to 14 km and may decrease below 14 km. The data suggest that stress drops of a group of earthquakes can be related to the strength of the upper crust calculated from frictional and quasi-plastic flow laws, although individual events may not be. Stress drops on the San Jacinto fault are high compared to those on the central creeping section of the San Andreas where stress drops are about ten bars or less (*Bakun and McLaren*, 1984). This observation is consistent with the relative rupture area of events of equal M_L (5.5) and may be related to the lithologic differences between the two fault segments, and the amount of normal stress compared to shear stress.

In this paper we discuss the seismological and geological background that both provided the impetus to install an array at Anza and describes the tectonic style within which we will interpret the seismic data from the array: this paper is intended to be a point of departure for future work on Anza. Following this background discussion we give the processing procedures which we use to calculate source parameters from the seismic data. Finally we attempt to correlate the estimates of stress release to the estimate of tectonic stress for major strike-slip faults in California.

HISTORICAL SEISMICITY

Based on the spatial distribution and inferred rupture lengths of nine moderate ($6 \leq M_L \leq 7$) earthquakes, *Thatcher et al.* (1975) interpreted the 50-km-long section of the San Jacinto fault just east of Anza as a seismic gap. The gap is bounded by four events to the northwest and two to the southeast. The former four events, which occurred in 1890, 1899, 1918, and 1923 were located along a 75-km-long section of the San Jacinto fault between a point just north of Anza and San Bernardino; they were assumed to have released the stress along this zone (see Fig. 1). The location of the 1890 event is based only on intensity reports at distant cities. Local as well as distant intensity data were used to locate the three later events. Ground cracking was observed for the 1918 event near the town of San Jacinto.

Instrumental records exist for the 1918 and 1923 events so that the moments for these events (for determining the amount of slip) are relatively well known, but the moments for the 1899 and particularly the 1890 event are not: their moments are fixed only by the similarity of the distribution of intensity data of these events compared to those of the 1918 and 1923 events. Additional field reports by *Claypole* (1900), *Rolfe and Strong* (1919), and work by *Real et al.* (1978), *Toppazada et al.* (1978), and *Toppazada et al.* (1979) support the conclusions of *Thatcher et al.* (1975) that the southern end of the zone that ruptured in the 1890, 1899, 1918, and 1923 events ended just north of Anza near the terminus of the Hot Springs fault.

Only two earthquakes (1937 and 1968 events) located along the southern portion of the San Jacinto fault system had moments large enough to have accounted for significant

INTRODUCTION

Aftershock studies have provided a large collection of high quality digital earthquake recordings. These data have been used in numerous seismological investigations including studies of stress in the upper crust, earthquake source parameter scaling relations, site effects, and frequency dependence of Q. However, recording only aftershocks limits the magnitude range and ultimately the completeness of the data set. More specifically, "aftershock chasing" suffers from the loss of recordings of the greatest ground shaking and, because maintaining ten or more digital recorders in the field is labor-intensive, data-sets obtained in this way cover a very limited time span. Thus seismic data that covers even a small part of the earthquake cycle must come from permanent arrays. One purpose of the Anza array is to provide a precise set of source parameters, complete above some minimum magnitude, that spans the precursory phase of the earthquake cycle.

The design of the digitizer/telemetry unit for the Anza field sites and of the minicomputer-based data logger was started as a joint project between personnel at the USGS facility at Menlo Park, CA and the Institute of Planetary Physics at the University of California, San Diego. Details of the field electronics and computer system are described by *Berger et al.* (1984) and will not be repeated here except to mention the essential recording characteristics. The Anza array is a local short-period array of 10 three-component stations with an on-site 16-bit (96 dB dynamic range) analog-to-digital converter. Each component is digitized at a rate of 250 samples/sec; a 62 Hz lowpass filter prevents aliasing. Thus the bandwidth of each seismogram ranges from the geophone natural period of 2 Hz to about 60 Hz (uncorrected).

Complementing the quality of the data, we have engineered a processing system that requires interaction for rendering seismological judgement when necessary but which otherwise is as automated as possible for the initial storing of data files to the archiving of source parameters. Interaction is required for picking arrival times, spectral windows, and spectral parameters to insure that the resulting data are as unbiased as possible, because no picking algorithm based on a particular model is used. P- wave as well as S-wave data sets are compiled and are a resource we intend to exploit for studying many important problems in source and wave propagation disciplines.

slip. The Borrego Mtn. event (April 9, 1968, $M_L = 6.4$) (*Hanks et al.*, 1975; Thatcher *et al.*, 1975), however, had a moment 40 times that of the 1937 event. Surface cracks were observed over a 33 km length (*Allen and Nordquist*, 1972) but the later aftershocks appeared to extend the rupture an additional 15 to 20 km to the northwest culminating in a large aftershock in 1969 (see Fig. 1). Even though the shock in 1937 appears to have occurred in the gap inferred by *Thatcher et al.* (1975), its small moment precludes the possibility that significant strain was released here. Furthermore locations are too inaccurate to determine which fault segment (Coyote Creek, San Jacinto, or Buck Ridge) the 1937 shock ruptured. These observations suggest that significant strain has yet to be released along a 40-km-long zone that extends approximately from the southern terminus of the Hot Springs fault to the location of the 1969 aftershock of the Borrego Mtn. earthquake.

GEOLOGY AND GEOPHYSICS

San Jacinto Fault

The San Jacinto fault is a major linear fault segment in southern California that extends for over 160 km southwest from the San Gabrial Mountains Its geometry is complex with several fault strands such as the Hot Springs fault to the northeast of Anza and San Jacinto; the Buck Ridge fault, also to the northeast near Pinyon Flat; and the Coyote Creek fault, an *en echelon* break to the southwest (see Fig. 1). The sense of displacement is predominantly right-lateral strike-slip with approximately 24 km total displacement since the mid-Cretaceous. Some thrusting is found near Table Mtn. and White Wash, both of which are near the point of trifurcation just east of Anza (*Sharp*, 1967). Stratigraphically the west side of the fault has been raised 1.6 to 3.2 km higher than the eastern side even though the east side is now topographically higher.

The rock type for the region near Anza is unusual compared to much of the San Andreas fault system in that a similar competent rock is exposed on both sides of the fault (Fig. 2). The southern California batholith (*Sharp*, 1967) which is composed of gabbroic, tonalitic, granodioritic, and adamellite plutons intrude the prebatholithic metasedimentary and metavolcanic rocks. Shallow deposits of Pleistocene gravels are also found along the fault zone east of Anza (seismic stations that are generally within the zone of Pleistocene

gravels have been sited on hard rock outcroppings).

As no creep (aseismic slip) has been detected in this area (*Allen et al.*, 1983) the entire slip budget of the fault can presumably be computed by summing the moments of earthquakes that occur on the faults; this is an important consideration for studying fault zone interactions.

Slip Rate and Geodetic Strain Accumulation

Estimates of the slip rate come from observations of gravel deposit offsets as well as total offsets of more regional geologic formations (*Sharp*, 1967, 1981). Horizontal offsets between 5.6 and 8.6 km in 0.73 m.y. converts to 8 to 12 mm/yr average slip rate for the late Pleistocene. However *Sharp* (1981) also found slip rates to be variable with a period of low slip rate (1–2 mm/yr) between 4000 BC and 1600 AD. Within the last 200 to 500 years rates have increased again to 3 to 5 mm/yr. The offset of crystalline rock masses suggests a total offset of about 24 km. *Sharp* (1967) gives the age of the San Jacinto fault as younger than mid-Cretaceous based on the oldest offset rock units. But a minimum age of Pliocene is suggested by dividing the total displacement by the minimum Quaternary slip rate. *King and Savage* (1984) have calculated the strain accumulation in a band across the Elsinore, the San Jacinto, and San Andreas faults. Maxima in rates of shear strain accumulation of 0.35 and 0.4 urad/yr were found for the San Jacinto and San Andreas faults, respectively.

Heat Flow

In contrast to the lack of a heat flow anomaly centered on the San Andreas in central California (*Lachenbruch and Sass*, 1980) a heat flow anomaly has been detected on the San Jacinto fault (*Lee*, 1983). The half width of this anomaly is about 14 km and is .032 watts/m^2 above a regional value of .042 watts/m^2. A slip rate of 2.5 cm/yr implies a shear stress of 28 to 63 MPa (1 MPa = 10 bars). Lee favors a range of 30 to 40 MPa and believes the anomaly to be generated as a result of shear stress heating on the San Jacinto fault. On the San Andreas, however, the lack of a heat flow anomaly centered on the San Andreas and the broad anomaly over the Coast Ranges suggests an upper bound of about 20 MPa for the shear stress-producing fault slip (*Lachenbruch and Sass*, 1980).

Lee (1983) assumed a slip rate of 2.5 cm/yr for his calculation of shear stress, which he obtained from geodetic work across the Borrego Valley (*Whitten*, 1956), and summing the moments for events between 1912 and 1963 (*Brune*, 1968) but using the rigidity and fault dimensions of *Thatcher et al.* (1975). However Sharp's work suggests a rate of 1.0 cm/yr would be more reasonable. The shear stress τ is obtained from the mean heat generation/unit of fault surface (Q) and the slip (u) by:

$$\tau = Q/u$$

If 1.5 cm/yr is more representative of the actual slip at Anza then τ increases from 48 MPa to 69 MPa. The high shear stress on the San Jacinto fault inferred from *Lee* (1983) is in agreement with the small source dimensions inferred by *Sanders and Kanamori* (1984) for events on the San Jacinto fault compared to those on the central section of the San Andreas for the same M_L. On the other hand the impulsive high-frequency waveforms recorded by the Anza array (*Berger et al.*, 1984) and noted by others (*Brune and Hartzell*, 1979) are usually associated with areas of low heat flow (*e.g., Molnar and Oliver*, 1969).

RECENT SEISMICITY

Although the Anza gap is deficient in slip, it is not aseismic. Figure 3 shows epicenters of all earthquakes with $M_L > 3$ since 1970 from the SCARLET short-period array. Highlighted are the $M_L > 4$ events, which now total 8 since 1970. The triangular block south of the trifurcation point appears particularly active; 5 of the 8 events occurred there. In contrast to the seismicity of this block is the aseismic nature of the linear strand of the San Jacinto fault just to the north; the 1982 $M_L = 4.8$ shock does not appear to be on the San Jacinto (*Sanders and Kanamori*, 1984).

The microearthquake activity shown in Fig. 4a mimics patterns defined by the larger events with the trifurcation block again showing the most activity. Much of the seismicity in Fig. 4a occurs in concentrated clusters with diameters of 10 to 15 km which we denote: Hot Springs (HS), Cahuilla (CA), Anza (AN), and Table Mtn. (TB). Clusters HS and TB are at right-stepping *en echelon* offsets where additional components of tensional stress are expected that may promote earthquake activity (*Segall and Pollard*, 1980). Cluster

CA has been active before some of the larger earthquakes on the San Jacinto and thus has been called a stress meter by *Sanders and Kanamori* (1984). This cluster tends to be very swarm-like, displaying occasional bursts of very intense activity mostly below $M_L \sim 3$. The AN cluster appears to be near to, but not on, the San Jacinto and may be part of a cross-cutting trend which includes cluster CA. The block between the San Jacinto and Buck Ridge faults is also quite active; part of this activity is from the aftershocks of the Feb. 25, 1980 event ($M_L = 5.5$). Plotted in cross section (Fig. 4b) from northwest to southeast, the hypocenters extend to depths of 18 to 20 km at cluster HS and to 15 km in the trifurcation block. These are some of the deepest strike-slip earthquakes in California.

Accumulated Slip From Microearthquakes

Does the occurrence of these magnitude 2 to 5.5 events relieve a significant portion of the accumulated strain in the triangular block south of the trifurcation point? Using the formula of *Hanks and Kanamori* (1979) the magnitudes of 4.0 and larger events contained in the catalog of earthquake epicenters for southern California from 1934 were converted to moments and then summed. Slip was apportioned along a fault 48 km long and 18 km deep. Over the time period of 48 years, 3.2 cm of slip was released along the fault zone; this is less than 0.1 cm per year. If the slip is confined to just the triangular block south of the trifurcation point then about 2.5 mm/yr is released, which is still a factor of four less than the long-term geologic slip rates of at least 1 cm/yr average slip rate estimated by *Sharp* (1981) for the last 750,000 years. Hence the slip rate accounted for by these intermediate magnitude events is small compared to the long-term geologic slip rates.

PROCESSING SCHEME FOR ANZA SEISMOGRAMS

Magnetic tapes of earthquake time series from the data-logger are sent to Menlo Park every three to four weeks for processing with a standardized set of computer programs that yield the desired earthquake source parameters. The programs were written to reflect the high quality of the incoming seismic data as well as our need for highly precise source parameters. Both time domain and spectral analysis are employed where appropriate and both P-wave (from vertical component) and S-wave (from horizontal components)

estimates are determined for most quantities. The following is a short synopsis of the processing procedure.

Location Procedure

Hardcopy plots are made of each event file on the raw data tape to sort the valid earthquakes with adequate signal-to-noise from false triggers. Events judged to be both of adequate signal-to-noise ratio and within the study area are transferred to disk. Times are picked from these traces interactively on a raster scan display screen, where traces are stretched to the optimum time scale for picking high frequency arrivals. Both P- and S-wave arrivals are picked and given weights of from 0 to 4; generally S-picks receive lower weights compared to P-picks. The program Hypoinverse (*Klein*, 1978) with the crustal structure of *Hartzell and Brune* (1979) is used to invert for the hypocentral coordinates.

RMS errors for most of the events (using ten stations) are about 0.1 sec or less. The parameter ERH (*Lee and Lahr*, 1972), which gives an estimate of the standard deviation of the surface coordinates is usually less than 1.5 km for events that are inside the array. ERZ (similar to ERH, but for depth) varies between 1 and 3 km for the more stable solutions. These values suggest location accuracies of a few kilometers or less in plan and in depth.

The Anza array solutions may be compared to those from the USGS/Caltech array in southern California, which uses a more regional network of stations. Table 1 compares the hypocenters for 10 events that have been located by both seismic arrays. The average of the horizontal differences is 1.39 km and 1.40 km is the average discrepancy in depth. Both of these values are remarkably small considering the different crustal models and data sets used. The arrivals are read with an accuracy of 0.01 sec (or 50 m at 5 km/sec), however, suggesting that the precision of relative hypocentral locations within restricted regions could be much better than 1 km.

Moments, Source Radii and Brune Stress Drops

Our calculation of these parameters follows closely that of *Fletcher* (1983) and *Fletcher et al.* (1984) and uses *Brune* (1970) as its basis. Weights are assigned to the spectral picks (see *Haar et al.*, 1984, for a description of the weights) and then weighted averages are computed for the moment (M_o), source radius (r_o), and stress drop ($\Delta\sigma$).

$$M_{oi} = \frac{4\pi\rho\,(\alpha,\beta)^3 R_i \Omega_{oi}\,(p,s)}{F_i\,(\theta,\phi)} \tag{1}$$

$$\log \overline{M}_o = \sum_{i=1}^{n} \frac{\omega_i \log M_{oi}}{\omega_i} \tag{2}$$

$$\bar{r}_o = \frac{1}{n} \sum_{i=1}^{n} \frac{2.34\,\beta}{2\pi f_{ci}} \tag{3}$$

$$\Delta\sigma = \frac{7}{16} \frac{\overline{M}_o}{\bar{r}_o^3} \tag{4}$$

where R = hypocentral distance, Ω_o = asymptotic long-period level, F_i = the radiation pattern correction, ω = weight, f_c = corner frequency, and i indicates component. Total weight is also noted for each calculated quantity. Weights were implemented to decrease the importance of spectra which did not conform closely to the Brune model. *Fletcher et al.* (1984) showed that the random error was not strongly affected by using weights, but that for those data sets with a small number of components misinterpretations at a few stations could lead to systematic biases.

a_{rms} Stress Drop and Energy

When time series windows are picked for spectral analysis, windows are chosen for computing energy and a_{rms}. *P*-waves are interpreted just from vertical components, *S*-waves from the horizontal components. For the calculation of the *rms* of acceleration and seismic energy, windows are chosen to include the high frequency arrivals that usually accompany the body waves whereas spectral windows are usually 2 to 3 times longer. Both of these parameters may be in error if the window is not chosen with respect to the initial body-wave arrival. For example a_{rms} is defined as

$$a_{rms} = \left[1/T_d \int_o^{T_d} a^2(t)dt \right]^{1/2}$$

where T_d = duration of high frequencies associated with direct arrivals; a_{rms} would have too low a value if smaller amplitudes were averaged in. On the other hand energy which is derived from the integrated squared velocity

$$I = \int_o^{T_d} (v(t))^2 \, dt$$

increases with increasing window size. Stress drop is determined from a_{rms} from

$$\Delta\sigma = 2.23 \, \rho R \left[\frac{-4}{5} f_c + \frac{2\eta}{2\eta - 1} f_{\max} \right]^{-1/2} a_{rms} \, f_c^{1/2} \, w_c < w_m$$

where ρ = density, $f_{\max}$ = transition from a flat to a decreasing function with higher frequency in body wave acceleration, and η is the order of the roll-off of acceleration spectra above $f_{\max}$ (*Fletcher et al.*, 1984). In this derivation straight line segments are used to define the shape of the spectrum and $T_d \equiv 1/f_c$. In practice T_d is usually greater than $1/f_c$, which may introduce errors.

Seismic energy of wave-type E_c, calculated from component i is

$$E_s^i = 4\pi < F^i >^2 \left(\frac{R(x,\xi)}{F^i(\theta,\phi)} \right)^2 E_i^*$$

where $< F^i >$ is the average of the radiation pattern correction, and E_i^* is the energy flux corrected for attenuation (noted by the asterisk), and $E_i^* = \rho c I^*$. Energy has been corrected for attenuation in the frequency domain assuming a frequency independent Q of 300, but we suspect this correction is too severe and are presently exploring alternatives. Also, a baseline is removed from the velocity time series. Average radiation pattern

corrections will be used ($< F_p > = \sqrt{4/15}, < F_s > = \sqrt{2/5}$) (*Boatwright and Fletcher*), 1984) until focal mechanisms are determined for individual events.

Estimates of Error

We use the term relative uncertainty (η) to describe the error in our moment measurements. It is calculated from the standard deviation by:

$$\eta = \frac{10^{\sigma}}{\sqrt{(N)}\, M_o}$$

where σ is the standard deviation of the linear average of the logarithms of a parameter determined at each component. Geometric, rather than arithmetic means are used in calculating moment because the range of the ensemble is orders of magnitude (typically 2) and thought to be logarithmically distributed. Using a suite of 11 events (see Table 2) recorded in June of 1984, when all stations were installed, the average relative uncertainty was .39 (S-waves); *i.e.*, the relative uncertainty was about 39% of the mean. η was high at .59 for P-waves: this increase is in part caused by the lower number of vertical components available. Both P-waves and S-waves should yield the same value of moment and we test for agreement to judge the level of systematic errors that would affect the S-waves. For these 11 events the average of the differences between the P- and S-wave estimates of moment is 37%. 70% of the time the S-wave estimate is greater than the P-wave estimate. For 60% of these events, however, the deviation is less than 50%. Both the lack of radiation pattern corrections and S-wave amplification at sites near the trifurcation point undoubtedly contribute to this systematic bias.

In spite of the difficulty in determining corner frequency from displacement spectra, source radius is relatively well determined with an average relative uncertainty of .16 of P-wave data and .12 for S-waves. The smallness of these errors is surprising. Apparently the source radii are only varying by factors of 2 or 3 instead of 10 or more as do the estimates of moment. Using the rule for propagation of error (*Beers*, 1957)

$$\eta_\sigma = \sqrt{(\eta_m)^2 + 9(\eta_r)^2}$$

where η_m is the relative error associated with moment and η_σ is the relative error associated with source radius. We find that the average relative uncertainty for stress drop would be 53% of the mean.

SEISMICITY AT ANZA SINCE OCT. 1982

Figure 5 shows the epicenters plotted around the San Jacinto fault: moment is used as the gauge of earthquake size. Moments range from 1.3×10^{17} ($M = .7$) to 4.4×10^{21} ($M = 3.8$) dyne-cm. This plot is very similar to Fig. 4a with concentrations in seismicity at clusters HS, CA, AN, and TB. The seismicity at cluster HS now appears as two distinct clusters; we will continue to call the seismicity between the Hot Springs fault and the San Jacinto fault the Hot Springs cluster, but we will call the seismicity to the northeast of the Hot Springs fault the Keen (KN) cluster. We make this distinction because of their separation in both plan and depth. Also note that the epicenters are more numerous between the Elsinore and San Jacinto than between the San Jacinto and the San Andreas. An apparent lineation of earthquakes trends east of TB into the Pinyon block.

No mainshock-aftershock sequences lasting longer than a few hours have occurred during this time period. Rather, seismic activity continues at the loci previously identified in Fig. 4a: some of these loci, such as TB, apparently have been continually active at least since 1968 (*Arabasz et al.*, 1970). The largest event since October, 1982, occurred at the HS cluster, but most clusters have at least one event with moment greater than 1×10^{20} dyne-cm, which is large for this data set. The diffuse seismicity of Fig. 4a at HS and at the trifurcation block is not apparent in Fig. 5, but this may be due to the smaller number of epicenters in Fig. 5 compared to Fig. 4a.

Viewed in cross section (Fig. 6) the clusters at HS and KN are distinct; one is centered at 13 km and the other at 17 km depth. Some of the most southwesterly hypocenters of the HS cluster may be on the San Jacinto fault if we assume a dip of 85° to the NE (*Sanders and Kanamori*, 1984), but most events occur between the two faults. The Cahuilla events, however, are shallow compared to other events in the area, and are distributed from near the surface to 9 km deep (Fig. 7). The deepening trend that extends from cluster CA to

AN is intriguing for its eye-catching similarity to a Benioff zone, but this trend appears to be more related to varying modes of failure (cluster CA is located near geothermal hot springs). A few smaller events (for which no source parameters have been calculated) fill in the gaps between the two clusters. The largest events in Figure 7 locate at cluster AN; only small events extend into the Pinyon block.

A cross section of the trifurcation block reveals some possible lineations which coincide with the Coyote Creek and Buck Ridge faults. On the left portion of Fig. 8 there is a vertical line of epicenters beneath the 8 km tic mark. This is cluster TB which is off the end of the Coyote Creek fault. The largest event under about the 13 to 18 km tic marks define a trend that dips at about 64° to the southwest. Although these events are close to the Buck Ridge fault, the surface projection is considerably east of the geologic expression of the Buck Ridge fault which suggests either a bias in the locations or a steepening of the fault near the surface.

Viewed in cross section along the fault (Fig. 9) the recent hypocenters on the San Jacinto show a pattern that is similar to the one in Figure 4b. Seismicity is concentrated in the Hot Springs area and trifurcation block with a zone that is aseismic in between.

STRESS DROPS

Scaling of Anza source spectra is shown in Figure 10 where the log of moment is plotted as a function of the log of source radius (*Hanks and Thatcher*, 1972). Figure 10 shows that in the moment range of 10^{17} to 10^{21} dyne-cm the Anza events generally display increasing stress drop with increasing moment. Earthquakes at Cahuilla are notably lower in stress drop than are events from the other areas. This difference is most apparent at the larger moments. The largest Cahuilla events have stress drops of 1 to 10 bars whereas the events from other areas have stress drops that are close to or greater than 100 bars.

The dependence of stress drop on moment corresponds to a nearly constant source radius or corner frequency observed over a wide range in moment and is similar to that noted by *Fletcher* (1982), *Archuleta et al.* (1983), *Tucker and Brune* (1977) and *Rautian et al.* (1978). *Hanks* (1982) observed that acceleration spectra do not continue at a constant level (*i.e.*, in agreement with ω^{-2} model of displacement spectra) much beyond

10 to 30 Hz depending on whether the receiver site was underlain by hard or soft rock. Hanks called the point of departure f_{max}. It can be interpreted as the frequency above which attenuation weakens the high frequencies. *Anderson and Hough* (1984) fit the high frequency decay above some equivalent f_{max} with spectral decay parameters called κ. Particularly for strong motion data from the San Fernando earthquake κ increased with epicentral distance suggesting that κ represent an attenuation mechanism: its non-zero intercept at zero epicentral distance represents a constant site specific attenuation. In both cases attenuation provides a mechanism that would limit the upper ranges of corner frequencies.

f_{max} was calculated for S-waves for each station at Anza by observing when acceleration spectra (calculated from velocity) start to fall off to higher frequencies from a constant level. Between 5 and 10 measurements were taken for each station and averaged to obtain a final value. These values are shown in Fig. 11 along with the corner frequencies calculated for that component for a large subset of the data. For most stations f_{max} does represent an upper limit to the corner frequencies observed at that station suggesting that for some events the low corners observed at stations with low f_{max}s may be biasing source parameter estimates for small events. Consequently we have recalculated all events, but only using data from stations where f_{max}s are greater than 30 Hz which should provide a reasonable gap in frequency between the average corner observed in Fig. 10 and the average f_{max} of the data set. The moment and source radius are replotted in Fig. 12 and a shift to higher average corner frequency/source radius is apparent in Fig. 12 compared to Fig. 10. Nevertheless the overall range of stress drops has not significantly changed. A side effect of reducing the number of stations from which data are taken is a large increase in the error. We consider it a matter of further research to measure the site- and path-dependent attenuation, but for the rest of the analysis we will continue to use the source parameters calculated using all of the stations

Recent studies of attenuation of high frequencies offer conflicting results. Data from downhole geophones at Parkfield, CA (*Malin*, personal communication) suggests that measurements made near the earth's surface may be diminished in high-frequencies. On the other hand, although data from Mammoth Lakes (*Archuleta*, personal communication)—

where both a downhole force balance accelerometer (at a depth of 600 m) and a surface station were installed—showed large amplifications at the surface no gross attenuation of high frequencies in the upper 600 km was observed. These apparently conflicting results in conjunction with the differences in geology at these two sites suggests that the effects of the near surface are not uniform; it would seem that Anza, which has granite exposed at the surface at most sites, would be the least affected. Nevertheless our understanding of these near-surface phenomena are limited and require actual measurement.

Scattering has recently been shown to cause a diminution of the high frequencies in body waves; the high-frequency energy appears to be transferred to the coda (*Frankel and Clayton*, 1984; *Richards and Menke*, 1984). Such a mechanism would help to explain the common observation that body wave records frequently start as long period, but end in higher frequencies. Most body wave spectra include enough coda that if the high frequencies are simply shifted in time (phase), the amplitude spectra should still resemble that of the original pulse. Particularly in regions where intrinsic attenuation is low, scattering must effect pulse shapes. Scattering mechanisms are very difficult to quantify due to the lack of a quantifiable distribution of scatterers in the real earth's crust.

Depth Dependence

Shear stress in the brittle crust increases approximately linearly with depth (*McGarr*, 1980). Similarly crustal strength is expected to increase linearly with depth (*e.g.*, *Sibson*, 1974). If the Brune stress drop is related to either the absolute crustal stress or to strength then some depth dependence is anticipated. Figure 13 shows the Brune stress drop again separated into source regions plotted against depth to determine empirically whether or not crustal stress or strength is related to seismic stress drops. An envelope around the maximum value increases with depth to about 9 km, stays approximately constant to 14 km, and then decreases slightly at deeper levels. Figure 13 also shows the stress drops calculated using the a_{rms} method (*Hanks and McGuire*, 1981) to show that a crude attempt to take into account f_{max} does not alter the essential result.

Some of the regions separate out distinctly. The most obvious is the Cahuilla region which occupies all of the shallow depths and their maximum stress drops are smaller than

at the other locales. Anza region data is found mostly at the mid-depth (6 to to 11 km) and the deeper events are almost all from the Hot Springs region. Buck Ridge events seem to span these two data sets.

Crustal Strength Versus Depth

Strength, which refers to the maximum stress difference ($\sigma_1 - \sigma_3$) that a rock can sustain can be calculated for the crust using Byerlee's law in the upper, brittle part and an exponential flow law below (*Sibson*, 1974; *Brace and Kohlstedt*, 1980; *Goetz and Evans*, 1976). Figure 13d shows profile strength vs. depth for compressional, strike-slip, and tensional regimes under hydrostatic pressure. The temperature profile is from *Brace and Kohlstedt* (1980). There are several similarities between the crustal strength curves in Fig. 13d and the stress drops plotted in Fig. 13a,b and the number of earthquakes versus depth in Fig. 13c. Stress drops are much smaller near the earth's surface and increase with depth. The peak in the number of earthquakes at different depth intervals is a maximum at 14 to 15 km and the maximum stress drop is also between 14 to 15 km (Fig. 13). *Sibson* (1982) and *Meissner and Strehlau* (1982) have noted that 10 km seems to be an appropriate depth for nucleation of large earthquakes and the brittle-ductile transition for much of the San Andreas. Some evidence suggests, however, that the elastic portion may extend to about 15 km at Anza. First there is a strong peak in the number of earthquakes at a depth of 14 to 15 km and second the Feb. 25, 1980 event, which had a stress drop of 420 bars (see APPENDIX I), had a depth of between 14 and 15 km. *Sibson* (1982, 1984) shows that the depth to the peak in shear strength can be depressed by assuming lower (colder) geotherms and lower strain rates. Geotherms may be depressed by the southern Californian batholith. *Lee* (1983) observed a high heat flow anomaly over the San Jacinto fault, which would appear inconsistent with the greater depth of Anza events. Lee's data is confined to a single profile of data across the fault near the intersection of the Buck Ridge fault and may represent a very localized anomaly. Strain ratio is less to the northeast of the San Jacinto fault (*King and Savage*, 1983) whereas *Sibson* (1984) suggests a greater strain rate is needed to depress the frictional/quasi-plastic (FR/QP) transition.

A third possibility is the mineral composition of the rocks (the batholithic rocks

are quartz diorites (*Sharp*, personal communication) with a 40 to 60% feldspar content). According to *Sibson* (1984) an increasing percentage of feldspar (especially plagioclase) will lower the FR/QP transition. This feldspar content compares with a 20 to 60% content for Graywacke, a major constituent of the Franciscan Formation of central California (*Barth*, 1982). Composition could easily change with depth, however, which makes it difficult to draw any conclusions on the specific reason for greater depth of Anza earthquakes.

SUMMARY

Historical and recent seismicity suggest that a 40-km-long section of the San Jacinto fault adjacent to the town of Anza is a seismic gap and has accordingly been chosen as the site of a digital short-period array. Seismicity recorded from Oct. 1982 to Nov. 1984 show:

1. Epicenters group into clusters, many of which do not appear to be directly on the fault.
2. Two clusters at Hot Springs and Table Mtn. coincide with right-stepping fault offsets.
3. Hypocenters at Keen are unusually deep extending down to 18 km.
4. A vertical lineation at the southwestern edge of the trifurcation block coincides with the Coyote Creek fault and a 65° dipping trend further to the east is presumably indicating the deep extension of the Buck Ridge fault.
5. Source radii determined from the Anza data set appear to be approximately constant from 10^{17} to 10^{20} dyne-cm. If corner frequencies from low f_{max} stations are pruned from the data set then the recalculated source radii decrease for the smaller events. Apparently some stations are affected by attenuation. The recalculated source radii are less constant than those calculated using the whole data set, but still yield stress drops that range from less than 1 bar to slightly greater than 100 bars.
6. Maximum stress drops tend to increase with depth to 10 km, are approximately constant from 10 to 15 km and diminish slightly below that. The largest recent event had a stress drop of about 400 bars and a depth of 14.2 km which is coincident with a peak in the distribution of earthquake hypocenters with depth. Qualitatively,

curves of crustal strength versus depth (*Sibson*, 1982) agree with the envelope of stress drops and the distribution of earthquake depths.

ACKNOWLEDGEMENTS

Many of the formula for processing Anza seismograms over many components were worked out in collaboration with Jack Boatwright of the Survey. In a review of this paper D. J. Andrews derived the following expression for the relative uncertainty η.

If

$$X = \frac{1}{N} \sum_n \log M_o$$

and

$$M_o \pm \Delta M_o = 10^x \cdot 10^{\Delta x} = M_o \cdot 10^{\pm \sigma}$$

$$\log M_o \pm 0.43 \frac{\Delta M_o}{M_o} = \log M_o \pm \sigma$$

then

$$\eta = \frac{\Delta M_o}{M_o \sqrt{N}} = 2.3 \frac{\sigma}{\sqrt{N}} \quad .$$

The above formula will be used for future calculation of source parameters using the Anza data.

REFERENCES

Allen, C. R. and J. M. Nordquist, 1972, Foreshock, main shock, and larger aftershocks of the Borrego Mountain earthquake, *U. S. Geol. Surv. Prof. Pap.*, **787**, 16–23.

Allen, C. R. and K. E. Sieh, 1983, Creep and strain studies in southern California, Summaries of technical reports Vol. XVI, *U. S. Geol. Surv. Open-File Rep.*, **83–525**, 161–164.

Arabasz, W. J., J. N. Brune, and G. R. Engen, 1970, Locations of small earthquakes near the trifurcation of the San Jacinto fault southeast of Anza, California, *Bull. Seismol. Soc. Am.*, **60**, 617–627.

Archuleta, R. J. and S. Day, 1980, Dynamic rupture in a layered medium: The 1966 Parkfield earthquake, *Bull. Seismol. Soc. Am.*, **70**, 671–689.

Archuleta, R. J., E. Cranswick, C. Mueller, and P. Spudich, 1982, Source parameters of the 1980 Mammoth Lakes, California, earthquake sequence, *J. Geophys. Res.*, **87**, 4595–4607.

Barth, T. F. W., 1962, Theoretical Petrology, *John Wiley and Sons*, 416 p.

Berger, J., L. M. Baker, J. N. Brune, J. B. Fletcher, T. C. Hanks, and F. L. Vernon, III, 1984, The Anza array: A high-dynamic-range, broadband, digitally-radiotelemetered seismic array, *Bull. Seismol. Soc. Am.*, **74**, 1469–1481.

Boatwright J. and J. B. Fletcher, 1984, The partition of radiated P and S waves, *Bull. Seismol. Soc. Am.*, **74**, 361–376.

Brace, W. F. and D. L. Kohlstedt, 1980, Limits on lithospheric stress imposed by laboratory experiments, *J. Geophys. Res.*, **85**, 6248–6252.

Brune, J. N., 1968, Seismic moment, seismicity, and rate of slip along the San Andreas fault, California, *J. Geophys. Res.*, **74**, 3821–3827.

Brune, J. N., 1970, Tectonic stress and the spectra of seismic shear waves from earthquakes, *J. Geophys. Res.*, **75**, 4997–5009.

Brune, J. N., 1971, Corrections, *J. Geophys. Res.*, **76**, 5002.

Claypole, E. W., 1900, The earthquake at San Jacinto, December 25, 1899, *The American Geologist*, **25**, 106–108.

Fletcher, J. B., 1983, A comparison between the tectonic stress measured *in situ* and stress parameters from induced seismicity at Monticello, South Carolina, *J. Geophys. Res.*, **87**, 6931–6944.

Fletcher, J. B., J. Boatwright, and W. B. Joyner, 1983, Depth dependence of source parameters at Monticello, South Carolina, *Bull. Seismol. Soc. Am.*, **74**, 1735–1751.

Fletcher, J. B., J. Boatwright, L. Haar, T. Hanks, and A. McGarr, 1984, Source parameters for aftershocks of the Oroville, California earthquake, *Bull. Seismol. Soc. Am.*, **74**, 1101–1123.

Frankel, A. and R. W. Clayton, 1984, A finite-difference simulation of wave propagation in two-dimensional random media, *Bull. Seismol. Soc. Am.*, **74**, 2167–2186.

Goetze, C. and B. Evans, 1979, Stress and temperature in the bending lithosphere as constrained by experimental rock mechanics, *J. Geophys. Res.*, **59**, 463–478.

Haar, L. C., J. B. Fletcher, and C. S. Mueller, 1984, The 1982 Enola, Arkansas, swarm and scaling of ground motion in eastern United States, *Bull. Seismol. Soc. Am.*, **74**, 2463–2482.

Hanks, T. C., 1982, $f_{\max}$, *Bull. Seismol. Soc. Am.*, **72**, Part A, 1867–1880.

Hanks, T. C., 1983, $\overline{a_{rms}}$ and seismic source studies, *Proc. First Int. Symp. on Rockbursts and Seismicity in Mines, Symposium Series*, **No. 6**, S. Afr. Inst. Mines and Metallurgy, 1984.

Hanks, T. C. and H. Kanamori, 1979, A moment-magnitude scale, *J. Geophys. Res.*, **84**, 2348–2350.

Hanks, T. C. and R. K. McGuire, 1981, The character of high-frequency strong ground motion, *Bull. Seismol. Soc. Am.*, **71**, 2071–2095.

Hanks, T. C., J. A. Hileman, and W. Thatcher, 1975, Seismic moments of the larger earthquakes of the southern California region, *Geol. Soc. Amer. Bull.*, **86**, 1131–1139.

Hanks, T. C. and W. Thatcher, 1972, A graphical representation of seismic source parameters, *J. Geophys. Res.*, **77**, 4393–4405.

Hartzell, S. H. and J. W. Brune, 1979, The Horse Canyon earthquake of August 2, 1975–Two stage stress-release process in a strike-slip earthquake, *Bull. Seismol. Soc. Am.*, **69**, 1161–1173.

King, W. E. and J. C. Savage, 1983, Strain rate profile across the Elsinore, San Jacinto, and San Andreas faults near Palm Springs, California 1973–1981, *Geophys. Res. Lett.*, **10(1)**, 55–57.

Klein, F. W., 1978, Hypocenter location program HYPOINVERSE Part I: User's guide to versions 1, 2, 3, and 4, *U. S. Geol. Surv. Open-File Rep.*, **78–694**.

Lachenbruch, A. H. and J. H. Sass, 1980, Heat flow and energetics of the San Andreas fault zone, *J. Geophys. Res.*, **85**, 6185–6222.

Lee, T.-C., 1983, Heat flow through the San Jacinto fault zone, southern California, *J. Geophys. Res.*, **72**, 721–731.

Lee, W. H. K. and J. C. Lake, 1975, HYPO71 (Revised): A computer program for determining hypocenter, magnitude, and first motion pattern of local earthquakes, *U. S. Geol. Surv. Open-File Rep.*, **75–311**.

McGarr, A., 1980, Some constraints on levels of shear stress in the crust from observations and theory, *J. Geophys. Res.*, **85**, 6231–6238.

Meissner, R. and J. Streklau, 1982, Limits of stresses in continental crusts and their relation to the depth-frequency distribution of shallow earthquakes, *Tectonics*, **1**, 73–89.

Molnar, P. and J. Oliver, 1969, Lateral variations of attenuation in the upper mantle and discontinuities in the lithosphere, *J. Geophys. Res.*, **74**, 2648–2682.

Rautian, T. G., V. I. Khaltium, V. G. Martynov, and P. Molnar, 1978, Preliminary analysis of the spectral content of P and S waves from local earthquakes in the Garm, Takjikistan region, *Bull. Seismol. Soc. Am.*, **68**, 949–971.

Real, C. R., T. R. Toppozada, and D. L. Parke, 1978, Earthquake catalogue of California January 1, 1900–December 31, 1974, *California Division of Mines and Geology Special Publication*, **52**, 15 p.

Richards, P. G. and W. Menke, 1983, The apparent attenuation of a scattering medium, *Bull. Seismol. Soc. Am.*, **73**, 1005–1021.

Rolfe, F. and A. M. Strong, 1918, The earthquake of April 21, 1918, in the San Jacinto Mountains, *Bull. Seismol. Soc. Am.*, **8**, 63–67.

Sanders, C. O. and H. Kanamori, 1983, A seismotectonic analysis of the Anza seismic gap, San Jacinto fault zone, southern California, *J. Geophys. Res.*, **89**, 5873–5890.

Segall, P. and D. D. Pollard, 1980, Mechanics of discontinuous faults, *J. Geophys. Res.*, **85**, 4337–4350.

Sharp, R. V., 1967, San Jacinto fault zone in the Peninsular Ranges of southern California, *Geol. Soc. Amer. Bull.*, **78**, 705–750.

Sharp, R. V., 1981, Variable rates of late Quaternary strike slip on the San Jacinto fault zone, southern California, *J. Geophys. Res.*, **86**, 1754–1762.

Sibson, R. H., 1974, Frictional constraints on thrust, wrench, and normal faults, *Nature*, **249**, 542–544.

Sibson, R. H., 1982, Fault zone models, heat flow, and the depth distribution of earthquakes in the continental crust of the United States, *Bull. Seismol. Soc. Am.*, **72**, 151–163.

Thatcher, W., J. A. Hileman, and T. C. Hanks, 1975, Seismic slip distribution along the San Jacinto fault zone, southern California, and its implications, *Geol. Soc. Amer. Bull.*, **86**, 1140–1146.

Toppozada, T. R. and D. L. Parke, 1982, Areas damaged by California earthquakes 1900–1949, Annual technical report to the U. S. Geological Survey, *California Division of Mines and Geology Open-File Report*, **82–17 SAC**, 65 p.

Toppozada, T. R., C. R. Real, S. P. Begore, and D. L. Parke, 1979, Compilation of pre-1900 California earthquake history, Annual technical report–fiscal year 1978–1979, *California Division of Mines and Geology Open-File Report*, **79–6 SAC**.

Townley, S. D. and M. W. Allen, 1939, Descriptive catalogue of earthquakes of the Pacific Coast of the United States 1769 to 1928, *Bull. Seismol. Soc. Am.*, **29**, 1–293.

Tucker, B. E. and J. N. Brune, 1973, S-wave spectra and source parameters for aftershocks of the San Fernando earthquake of February 9, 1971, *in Geological and Geophysical Studies*, **Vol. 3**, San Fernando Earthquake of February 9, 1971, National Oceanic and Atmospheric Administration, Washington, D.C.

Whitten, C. A., 1956, Crustal movements in California and Nevada, *Trans. Am. Geophys. Un.*, **37**, 393–398.

TABLE 1

COMPARISON OF USGS AND USGS/CALTECH HYPOCENTRAL COORDINATES

	USGS					USGS/CALTECH			
Origin Time	Lat. 33°	Lon. 116°	Depth (km)	Sta.	M	Lat. 33°	Lon. 116°	Depth (km)	Qual.
10/17/82									
10.13	31.94′	28.08′	7.34	7	2.9	30.92′	27.33′	8.08	A
10/18/82									
22.36	29.59′	33.70′	9.89	5	2.6	28.28′	33.72′	11.44	A
10/16/83									
06.29	34.43′	39.01′	12.90	9	1.7	34.13′	38.47′	13.43	A
10/18/83									
23.33	29.89′	29.13′	9.36	8	1.6	29.47′	28.99′	11.73	A
10/21/83									
20.53	39.10′	42.96′	14.00	8	1.9	39.53′	43.09′	14.04	A
10/23/83									
10.57	38.99′	43.41′	14.01	8	1.6	39.46′	43.04′	11.80	A
10/27/83									
13.13	28.86′	33.35′	10.43	9	2.1	28.04′	34.01′	12.29	A
10/29/83									
12.21	26.57′	28.45′	11.74	8	2.0	25.21′	11.15′	11.15	A
10/30/83									
01.15	32.91′	45.96′	4.48	8	2.0	32.99′	46.71′	2.90	A
11/09/83									
23.33	43.43′	46.00′	17.32	8	2.3	42.78′	46.01′	14.77	A

TABLE 2

COMPARISON OF SOURCE PARAMETER ESTIMATES AND ERRORS

Event	M_o–P	M_o–S	R(p)	R(s)	$\Delta\sigma$(p)	$\Delta\sigma$(s)	$\Sigma\omega$(p)	Σ(
6/20	4.26E18	4.02E18	1.8E4	1.6E4	.32	.39	4.3	8.:
20.13	.88	.31	.22	.13				
6/21	1.45E19	1.50E19	1.27E4	1.63E4	3.1	1.5	8.3	16
23.49	.37	.39	.12	.14				
6/22	4.7E19	8.02E19	1.75E4	1.74E4	3.9	6.6	5.7	15
18.13	.36	.81	.19	.08				
6/22	1.87E20	3.33E20	1.65E4	2.02E4	18.2	17.7	8.7	17
22.18	1.0	.46	.17	.10				
6/24	1.82E19	1.55E19	1.45E4	1.59E4	2.6	1.7	6.3	12
7.48	.58	.27	.08	0.8				
6/25	2.99E20	4.68E20	2.64E4	2.62E4	7.12	11.4	6.3	15
21.57	.60	.30	.13	.08				
6/20	1.88E18	3.14E18	1.12E4	1.45E4	.59	.45	4.7	8.'
18.43	.3	.23	.22	.20				
06/27	1.34E19	1.69E19	1.59E4	2.16E4	1.5	.7	3.3	9.(
6.13	.24	.26	.15	.14				
6/28	9.4E18	2.92E18	1.23E4	1.19E4	2.2	.76	7.3	10
19.02	.46	.46	.17	.18				
6/29	1.92E19	1.70E19	1.22E4	1.63E4	4.6	1.7	7.7	17
5.20	.54	.38	.14	.11				
6/29	1.17E19	1.52E19	1.53E4	1.70E4	1.4	1.4	5.0	13
13.56	1.2	.48	.13	.13				

APPENDIX I

Source Parameters for the Feb. 25, 1980 Earthquake

The 1980 event is the largest recent event at Anza. *Sanders and Kanamori* (1983) point out that the size of the aftershock zone and number of large aftershocks are in sharp contrast to say those of the Parkfield earthquake (M_L = 5.5, 1966). For example the rupture surface for the 1980 event is only 5 km across and is 6 times smaller than that of the Parkfield event (*Archuleta and Day*, 1980). We can calculate the stress drop from the seven strong motion records available for that event. Table 3 shows the moment, source radius, and stress drop using the Brune model and the spectral parameters for the 1980 event.

As the local Richter magnitude is essentially a measure of the high frequency radiation at about 1 Hz the similar M_L versus the difference in two orders in moment for these two events reflects the much higher stress drop of 42 MPa for the 1980 event compared to a few MPa for the 1966 Parkfield earthquake.

TABLE 3

SOURCE AND SPECTRAL PARAMETERS FOR FEB. 22, 1980 EVENT

Station Component	Distance (km)	Omega (cm-sec)	Corner F (Hz)	Moment (dyne-cm)	Source R (km)
BO					
315	40.8	7.5×10^{-3}	4.1	5.6×10^{22}	0.32
225	40.8	7.5×10^{-2}	1.5	5.6×10^{23}	0.87
PIN					
135	18.8	5.8×10^{-2}	2.7	2.0×10^{23}	0.48
045	18.8	1.9×10^{-2}	2.7	6.6×10^{22}	0.48
RDA					
135	24.0	4.2×10^{-2}	2.7	1.8×10^{23}	0.48
045	24.0	1.4×10^{-1}	1.9	6.2×10^{23}	0.69
ANZ					
045	21.0	1.3×10^{-1}	1.3	5.0×10^{23}	1.00

AVERAGE S-WAVE MOMENT = 2.2×10^{23} dyne-cm.

AVERAGE S-WAVE SOURCE RADIUS = 0.63 km.

STRESS DROP = 420 bars.

FIGURE CAPTIONS

Figure 1. Historical and recent large earthquakes near Anza. The locations of the 1890, 1899, and 1918 events are inferred from intensity reports. Circles are epicenters for earthquakes with $M > 4.5$ that occurred from 1932 to 1974. The slip gap is the section of the San Jacinto fault, which has had no large earthquake since the 1800's. The seismic gap is a subset of the slip gap and is presently aseismic. The triangular block just south of the seismic gap is seismically active for earthquakes with $M_L \lesssim 5.5$.

Figure 2. Locations of the digital 3-component seismographs as well as the pre-existing Kinemetrics SMA-1B. The stippled area marks the location of the southern California batholith.

Figure 3. Moderate-sized earthquakes at Anza. Those with $M_L > 4.0$ have been identified by the origin times and M_L. Eight $M_L > 4.0$ events have occurred since 1970 for an average of one every two years. The last occurred in June 1982. Triangles note the location of the first seven digital stations to be installed.

Figure 4a. Microearthquake locations from the SCARLET array ($M_L > 2.0$) for 1977 to 1982 with a quality factor of B or greater. Hypocentral depths appear to be considerably more precise after 1977 than before as judged by the number of depths at the trial solution.

Figure 4b. View of the San Jacinto fault from the southwest. Cluster of seismicity at 29 km (horizontal scale) is not on the San Jacinto fault. Note the quiescent section from 21 km to 39 km, and the activity southeast of 40 km. Seismicity tends to concentrate at the deepest interval, which is 15 to 20 km at the NW and 10 to 13 km at the SE end.

Figure 5. Epicenters of events located by the digital 3-component array from Oct. 1982 to Nov. 1984. The size of the circles is proportional to the logarithm of the moment; the largest is 4.4×10^{21} dyne-cm (M = 3.8). Digital array stations

are noted by a 3-letter code whereas strong-motion stations are given by a 3- or 4-digit number. Note that events tend to concentrate at clusters.

Figure 6. Cross section through the cluster at the southern terminus of the Hot Springs fault. Hypocenters within 5 km of the plane are included in the plot. The 18- to 20-km depths are some of the deepest events along the San Andreas system.

Figure 7. Cross section through Cahuilla and Anza. Events at Cahuilla are shallow compared to those closer to the San Jacinto fault. Cahuilla tends to be active in swarm sequences, and is located at hot springs.

Figure 8. Cross section through the northern end of the Coyote Creek fault, southern end of the San Jacinto, and the Buck Ridge fault.

Figure 9. Cross section coincident with the San Jacinto fault. The vertical line of events in the seismic gap (see Fig. 1) is not on the fault. The seismic gap appears to have a trapezoidal shape narrowing towards the surface.

Figure 10. Source radius versus moment for the data period Oct. 1982 to Nov. 1984 (for subsequent plots as well). Most source radii are larger than 60 m, which corresponds to 22 Hz. Four stations have f_{max}'s below 25 Hz. The tendency for the source radii to vary slowly with moment yields stress drops that increase with moment. Data are from S-waves. Radii are in units of centimeters. Data have been separated by clusters.

Figure 11. Corner frequencies and f_{max} for each station. f_{max} is calculated from acceleration spectra for a small group of events at each station. Corner frequencies are for S-waves from the N45°E component for about half of the total data set. Note that f_{max} does seem to be an upper limit to the corner frequencies at that station. Also note that for the higher f_{max} stations the average corner frequencies are about the same as that for the lower f_{max} station.

Figure 12. Source radius as a function of moment, but only using spectral data from stations that have an S-wave f_{max} of 30 Hz or higher. Particularly for the

smaller events source radii are generally smaller compared to those in Fig. 10. The range of stress drops, however, has not changed.

Figure 13a. Brune stress drops versus depth. Note that the maximum envelope increases with depth to about 10 km, appears constant from 10 to 14 km, and decreases below. A $M_L = 5.5$ event (Feb. 25, 1980) recorded on SMA-1's had a stress drop of 420 bars and a depth of about 14 km (not plotted). This event suggests a more complete catalogue may extend the increase in stress drop versus depth curve to 14 km.

Figure 13b. a_{rms} stress drops versus depth. Note the similarity to Fig. 14a. The calculation of a_{rms} stress drops include a correction for $f_{\max}$.

Figure 13c. Number of earthquakes versus depth. Note the peak at 14 km.

Figure 13d. Shear strength versus depth computed using a strain rate and heat flow profile from Brace and Kohlstedt (1980), and the model of Sibson (1976, 1982).

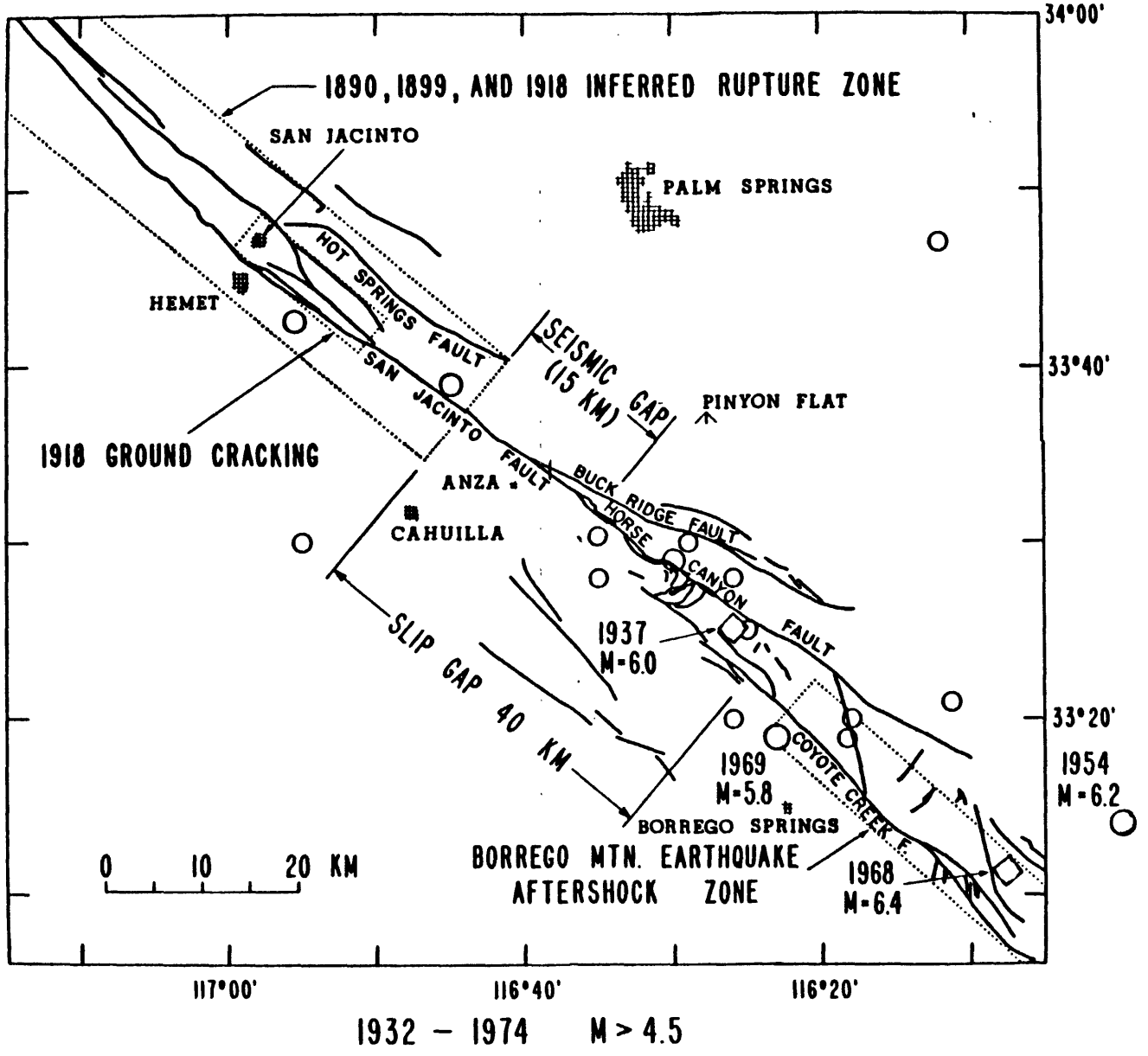

1932 – 1974 M > 4.5

fig 1

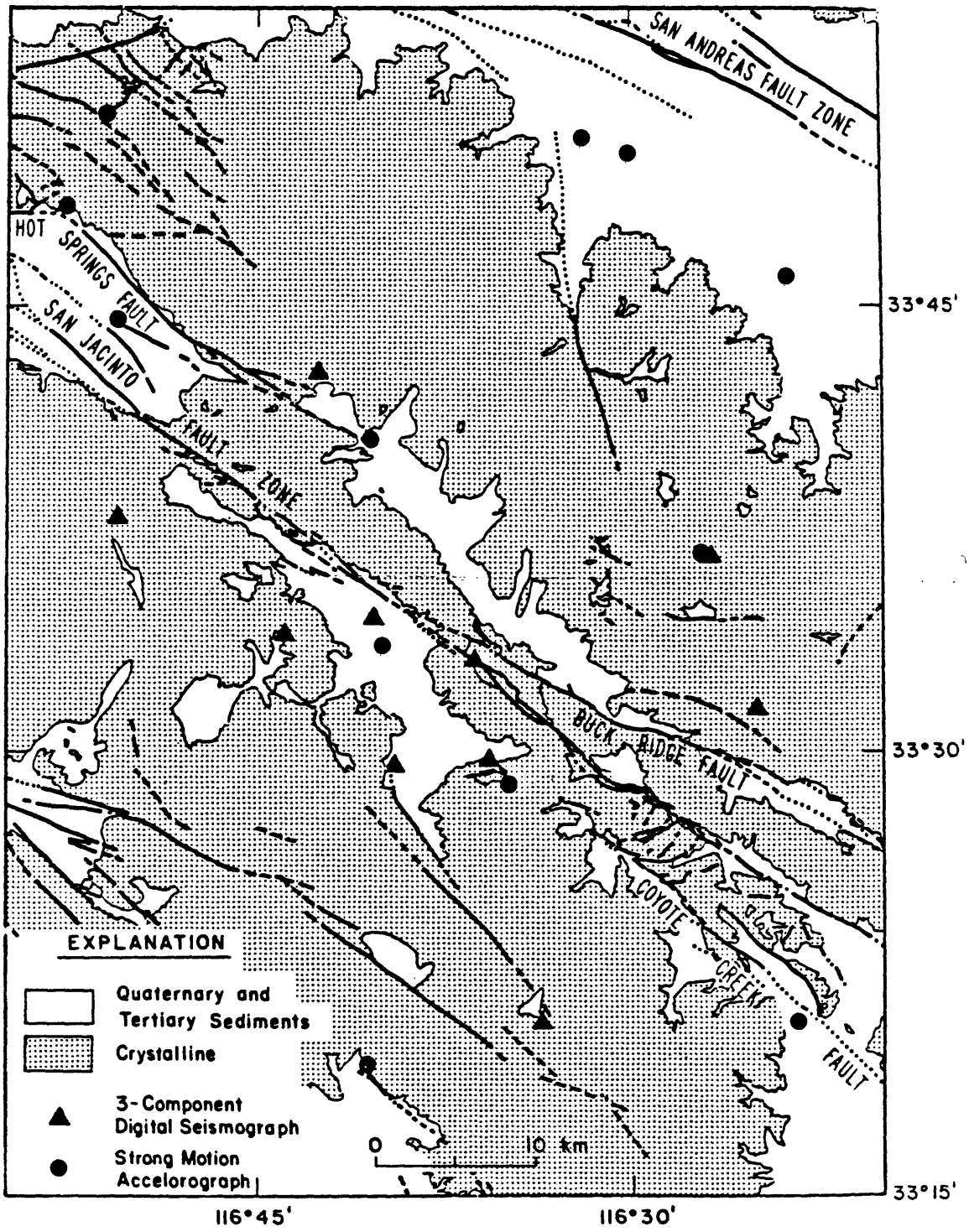
SAN ANDREAS FAULT ZONE
HOT SPRINGS FAULT
SAN JACINTO FAULT ZONE
BUCK RIDGE FAULT
COYOTE CREEK FAULT
33°45'
33°30'
33°15'
116°45'
116°30'
EXPLANATION
Quaternary and Tertiary Sediments
Crystalline
3-Component Digital Seismograph
Strong Motion Accelerograph
0
10 km

fig 2

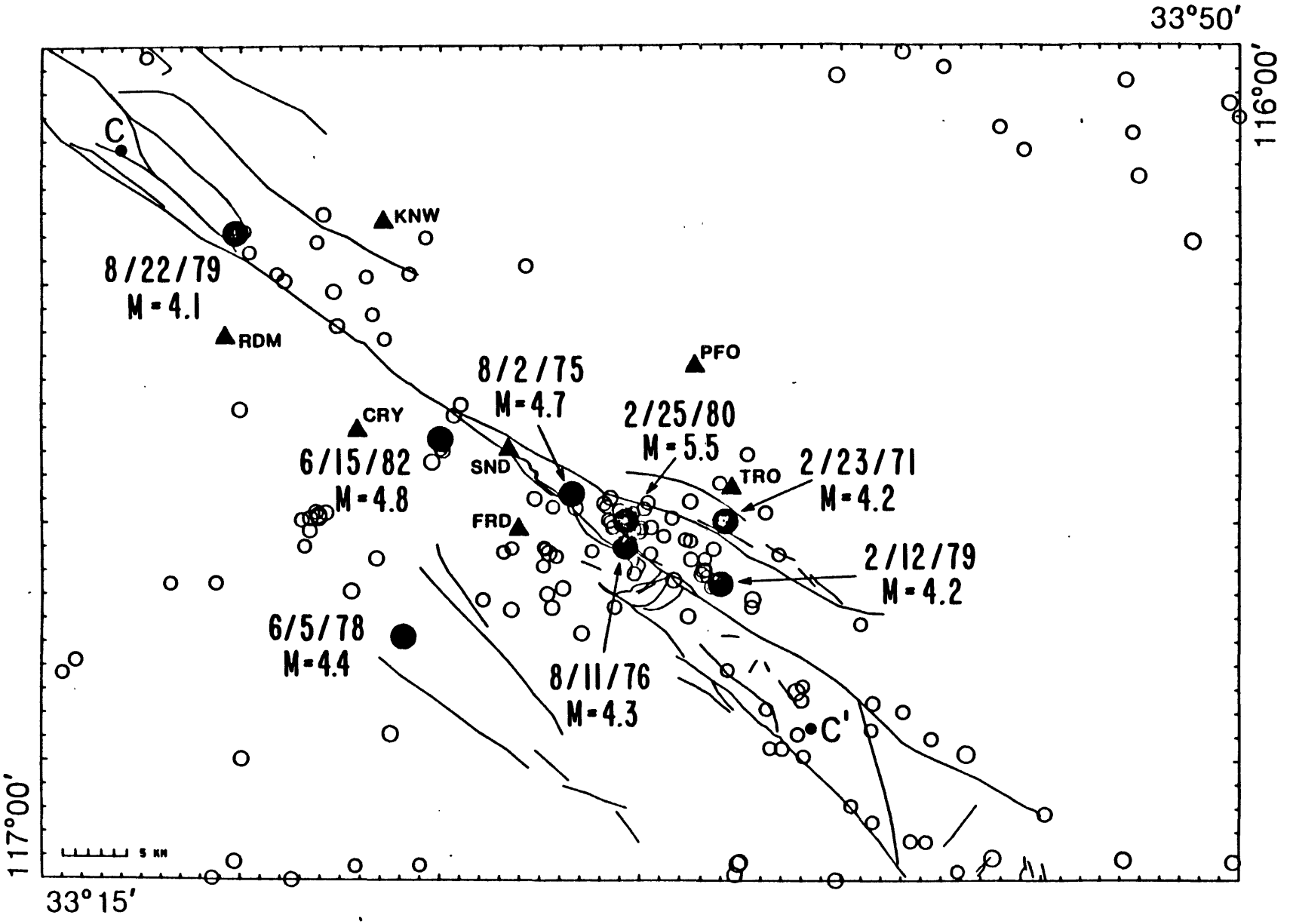

1970 - 1982 M > 3.0

fig 3

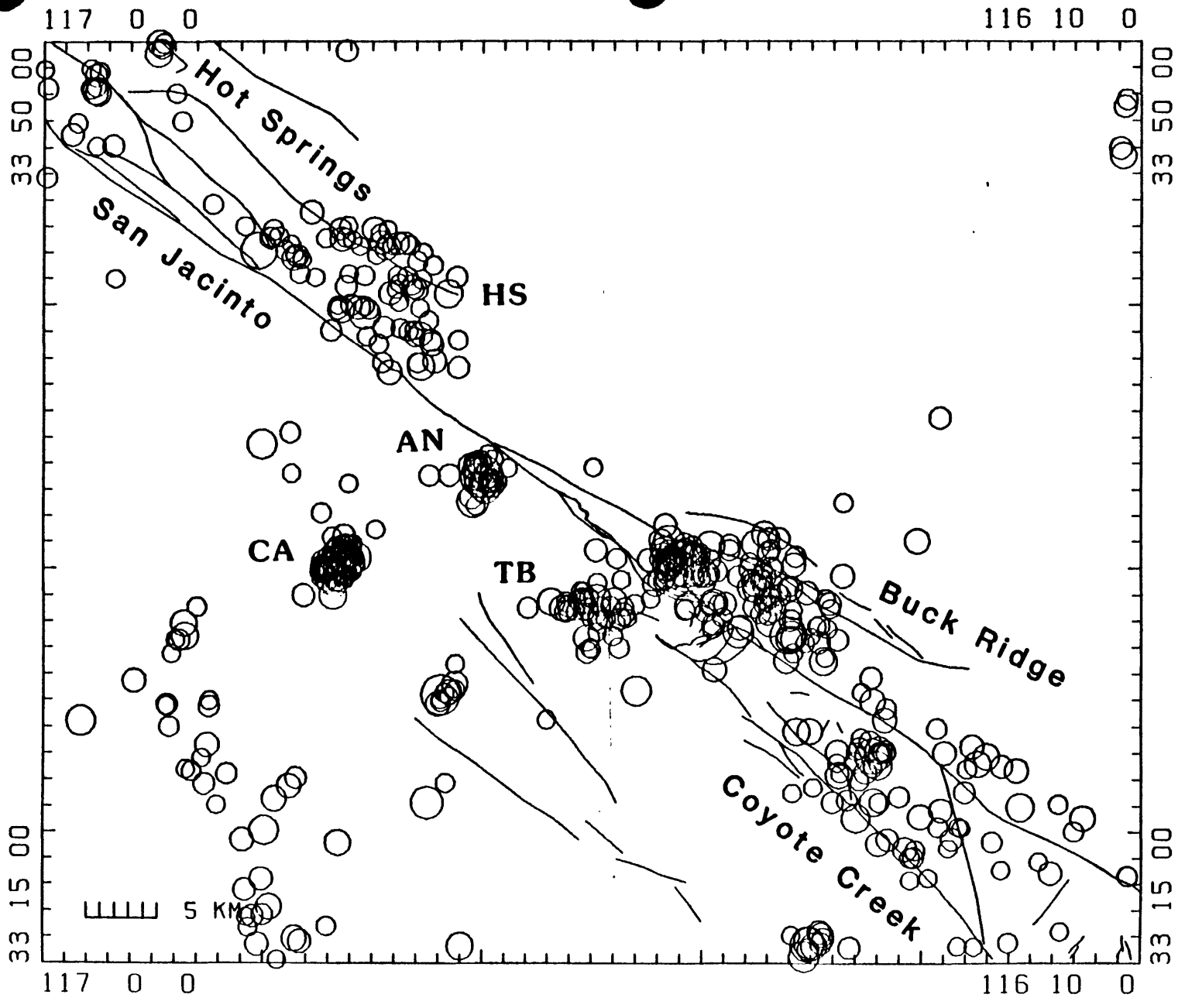

1977 to 1982 Qual A,B M greater than 2.0

fig 4a

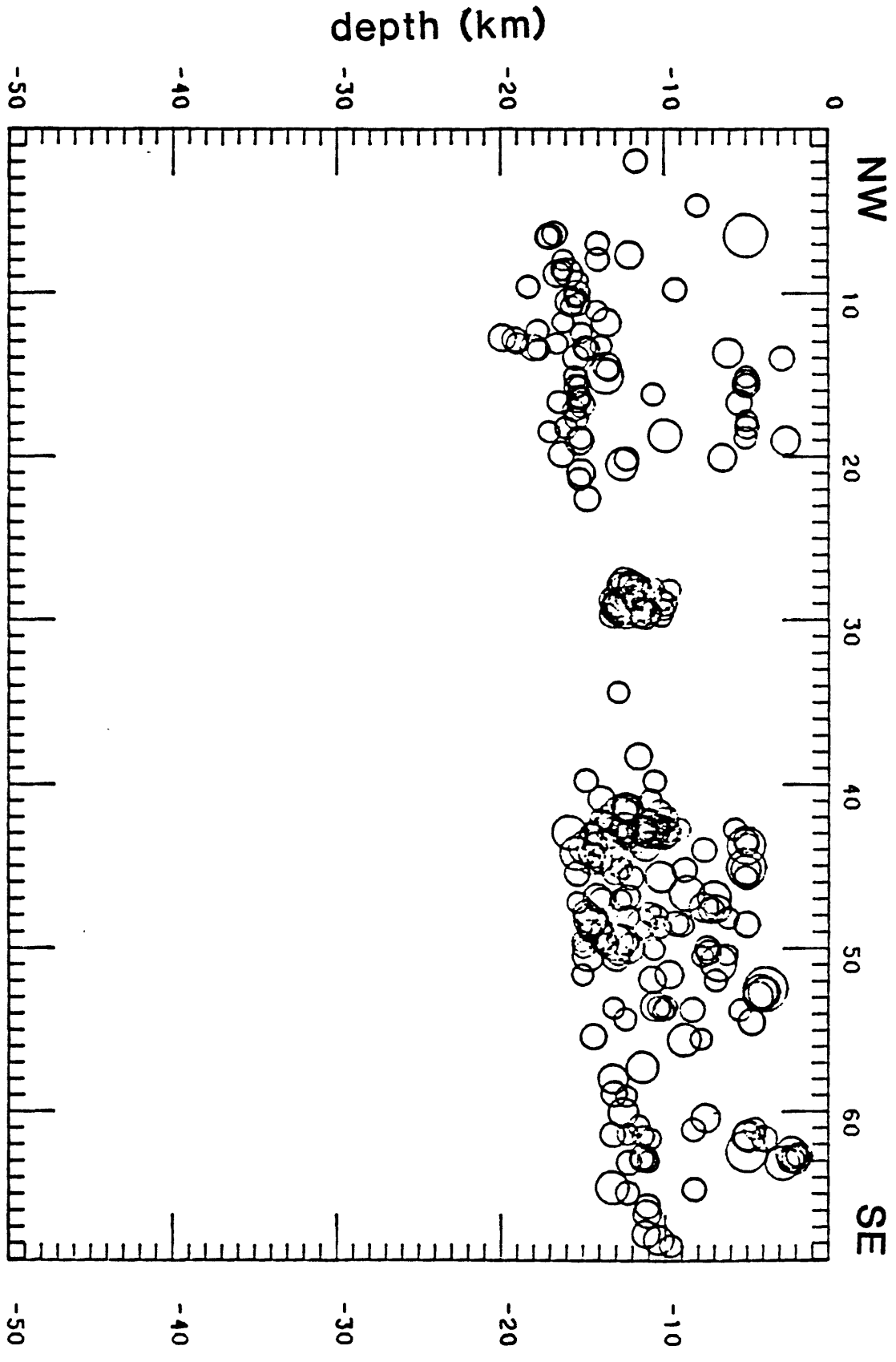

Fig. 4b

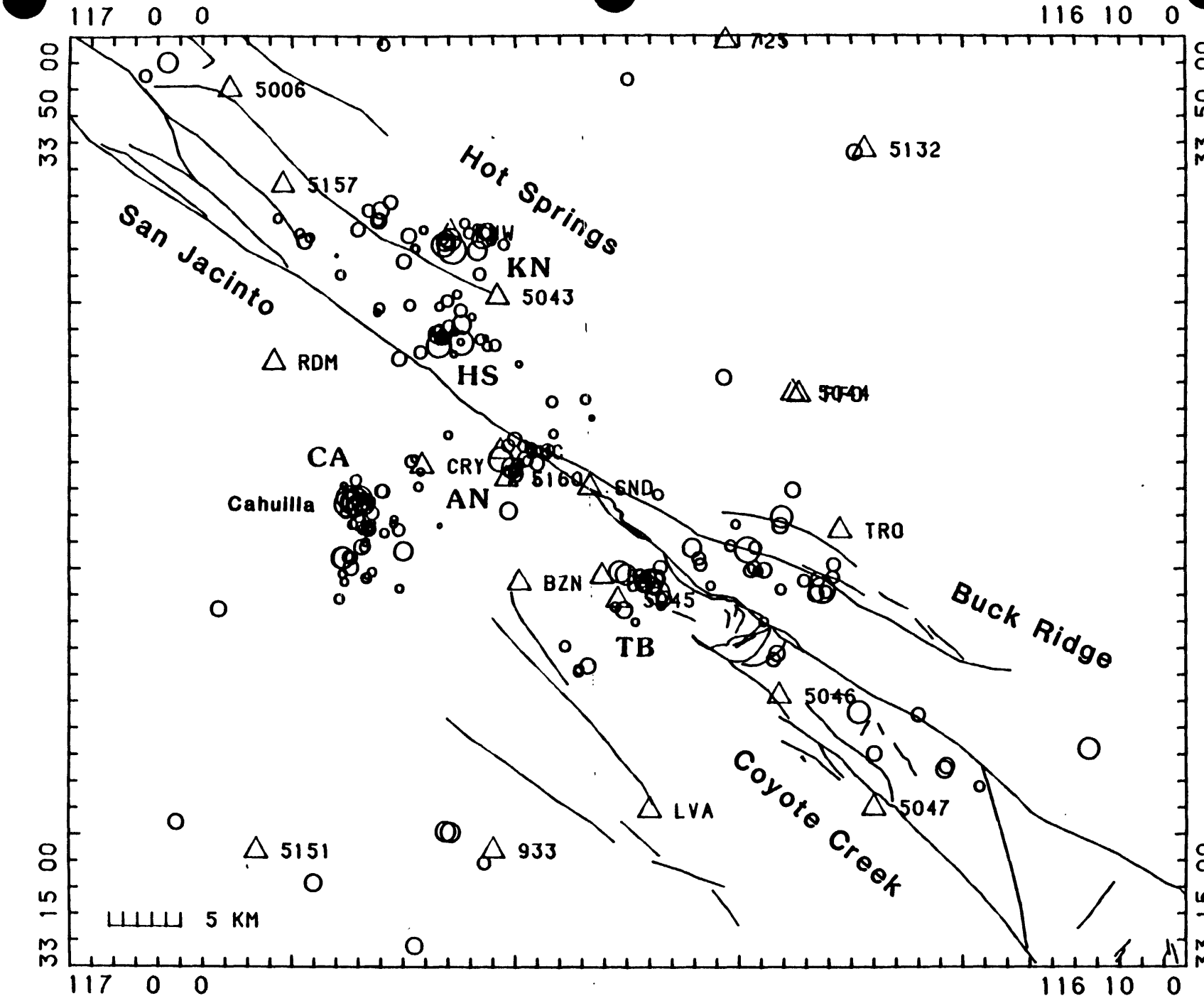
117 0 0
116 10 0
33 50 00
33 15 00
5006
5157
5043
5132
RDM
5160
SND
TRO
BZN
5045
5046
5047
LVA
5151
933
KN
HS
CA
AN
CRY
Cahuilla
TB
Hot Springs
San Jacinto
Buck Ridge
Coyote Creek
5 KM

128

fig 5

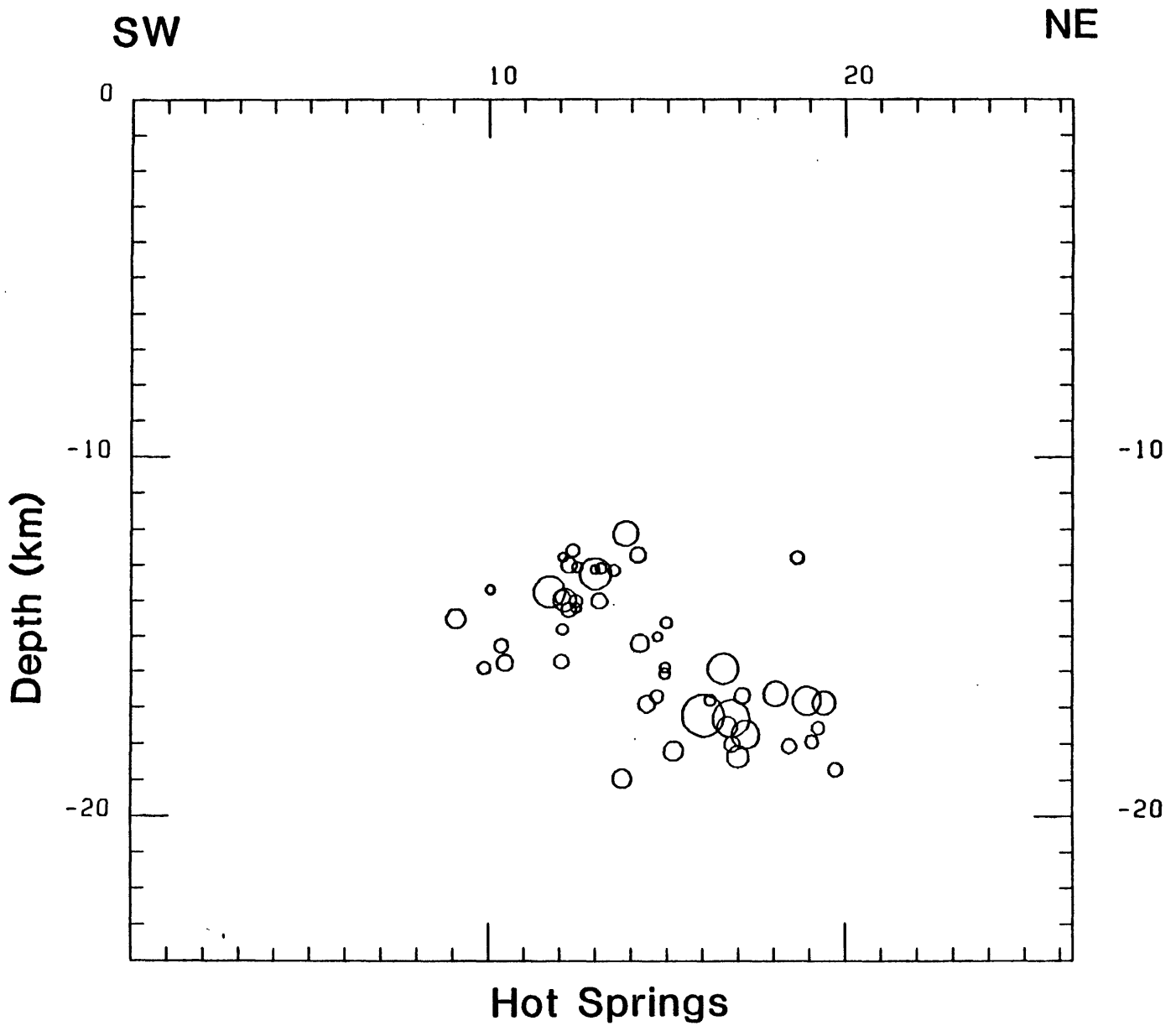

fig 6

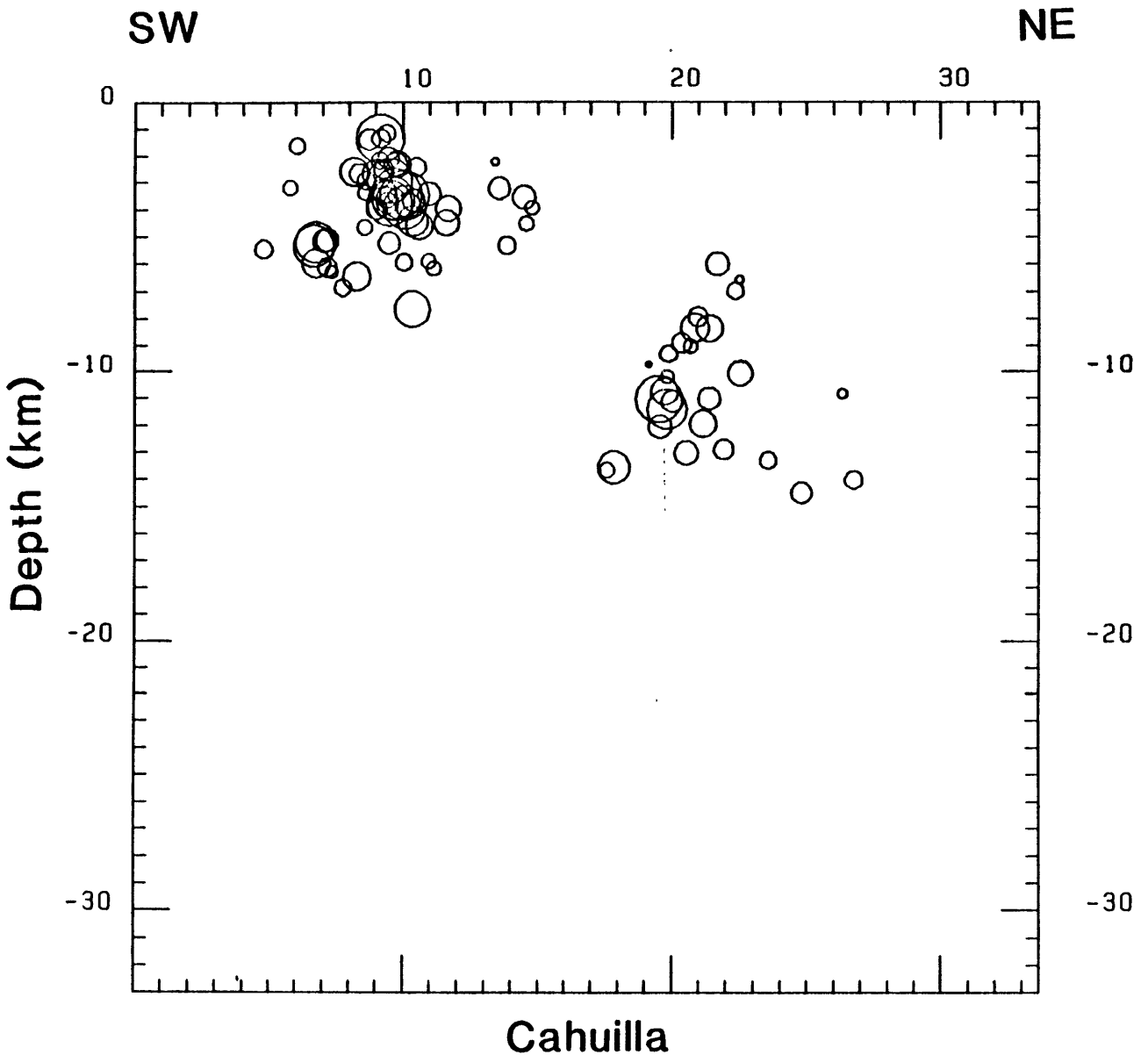

fig 7

fig 8

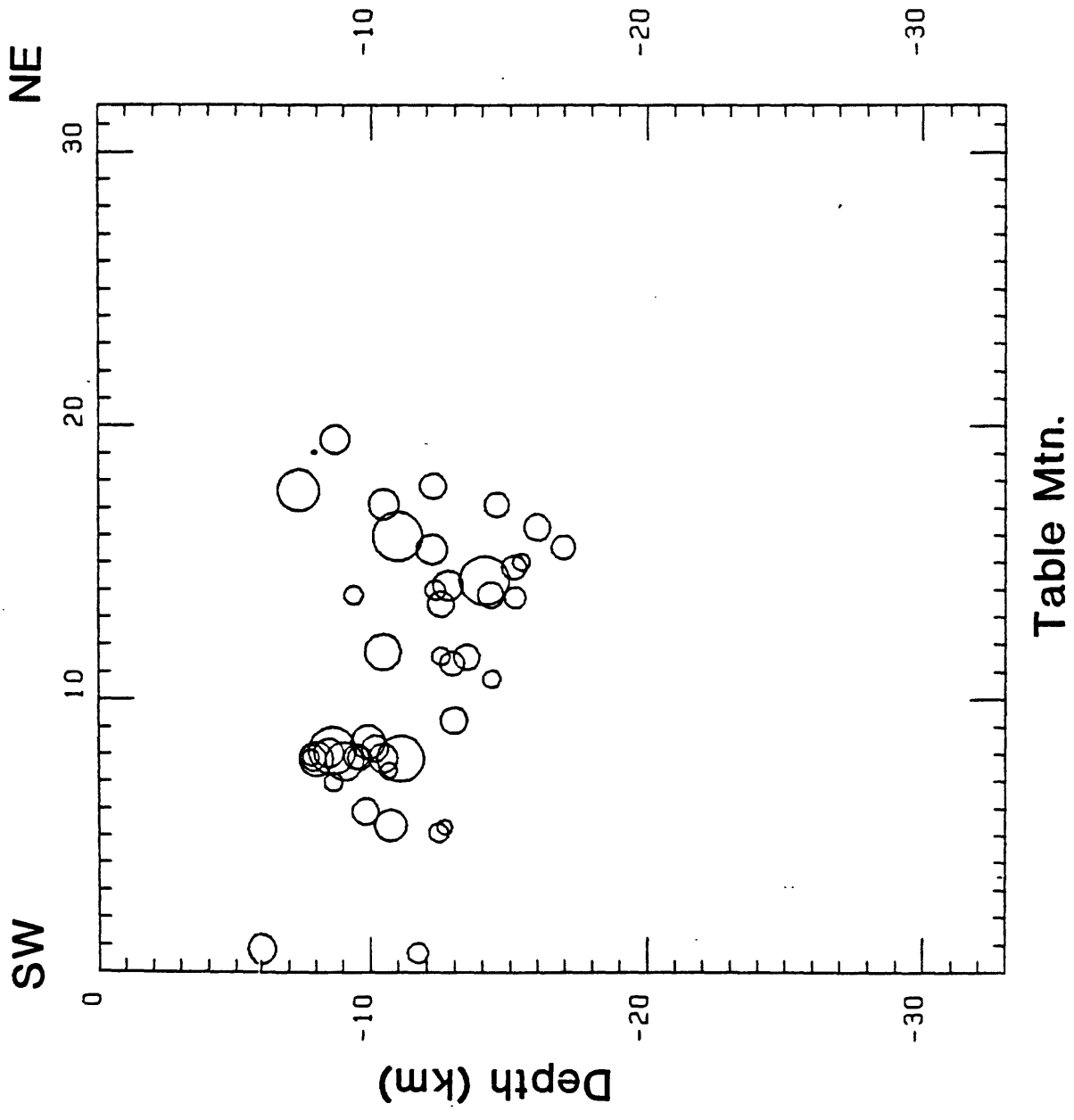

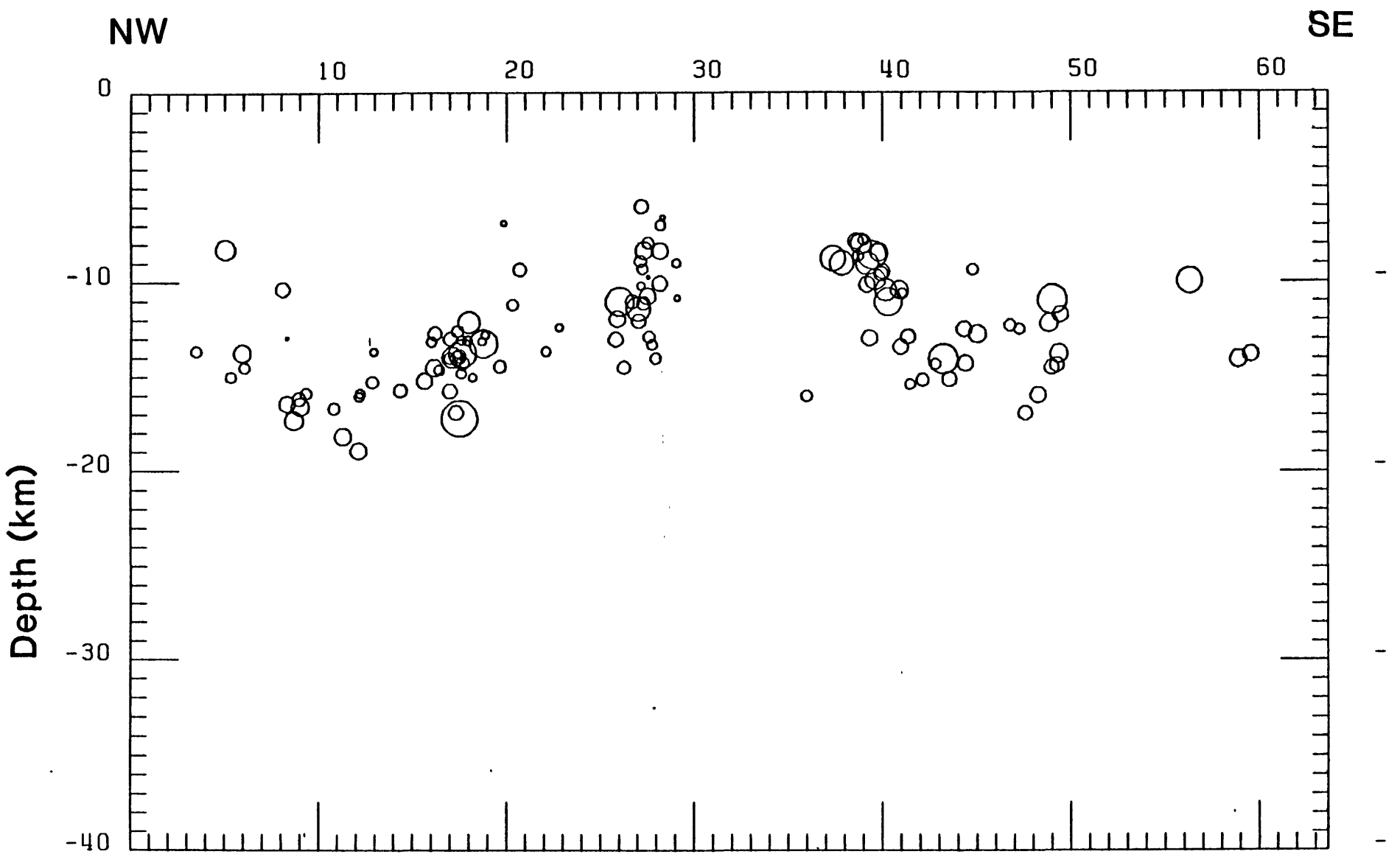

fig 9

Moment vs Source Radius

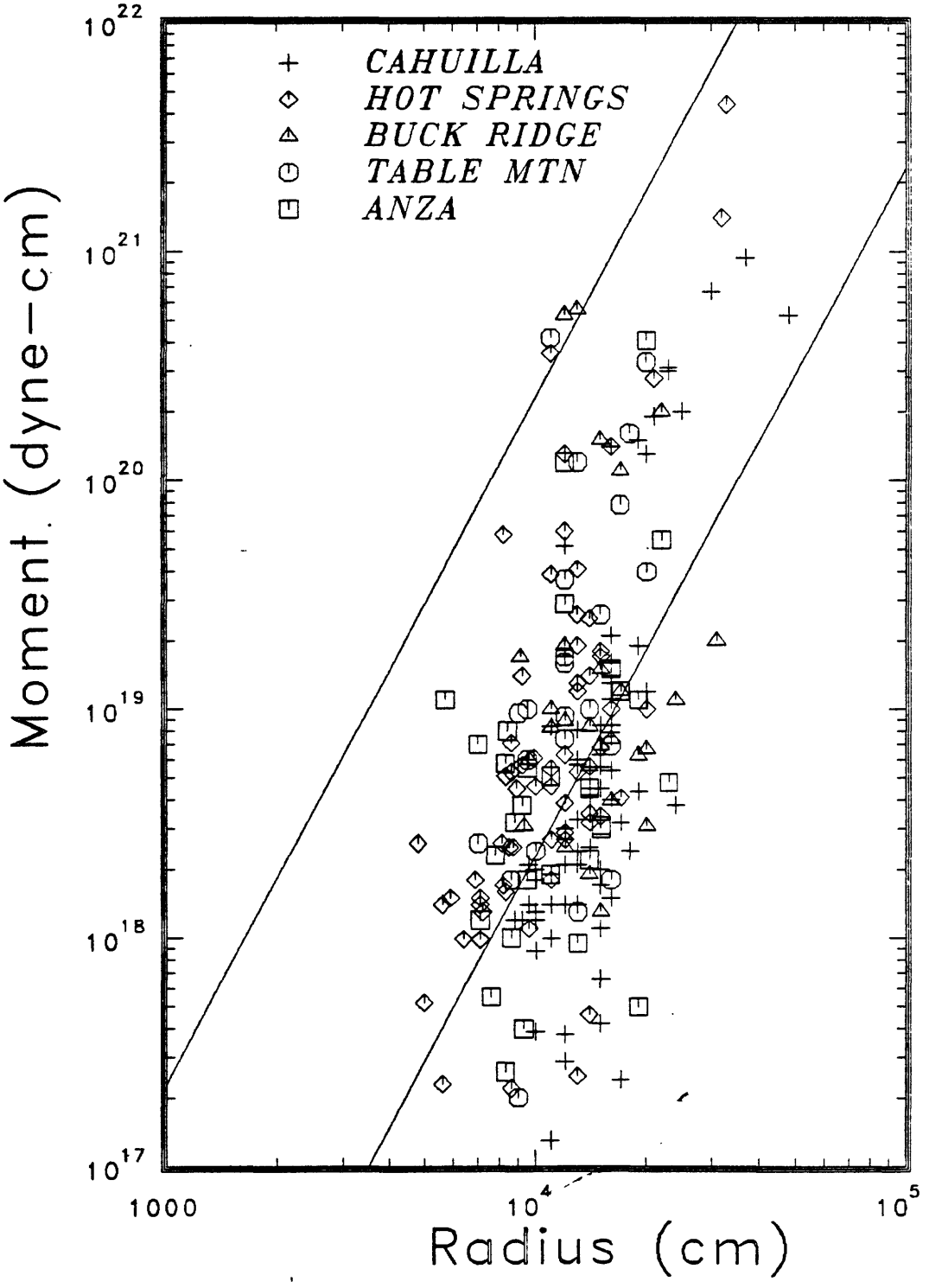

fig 10

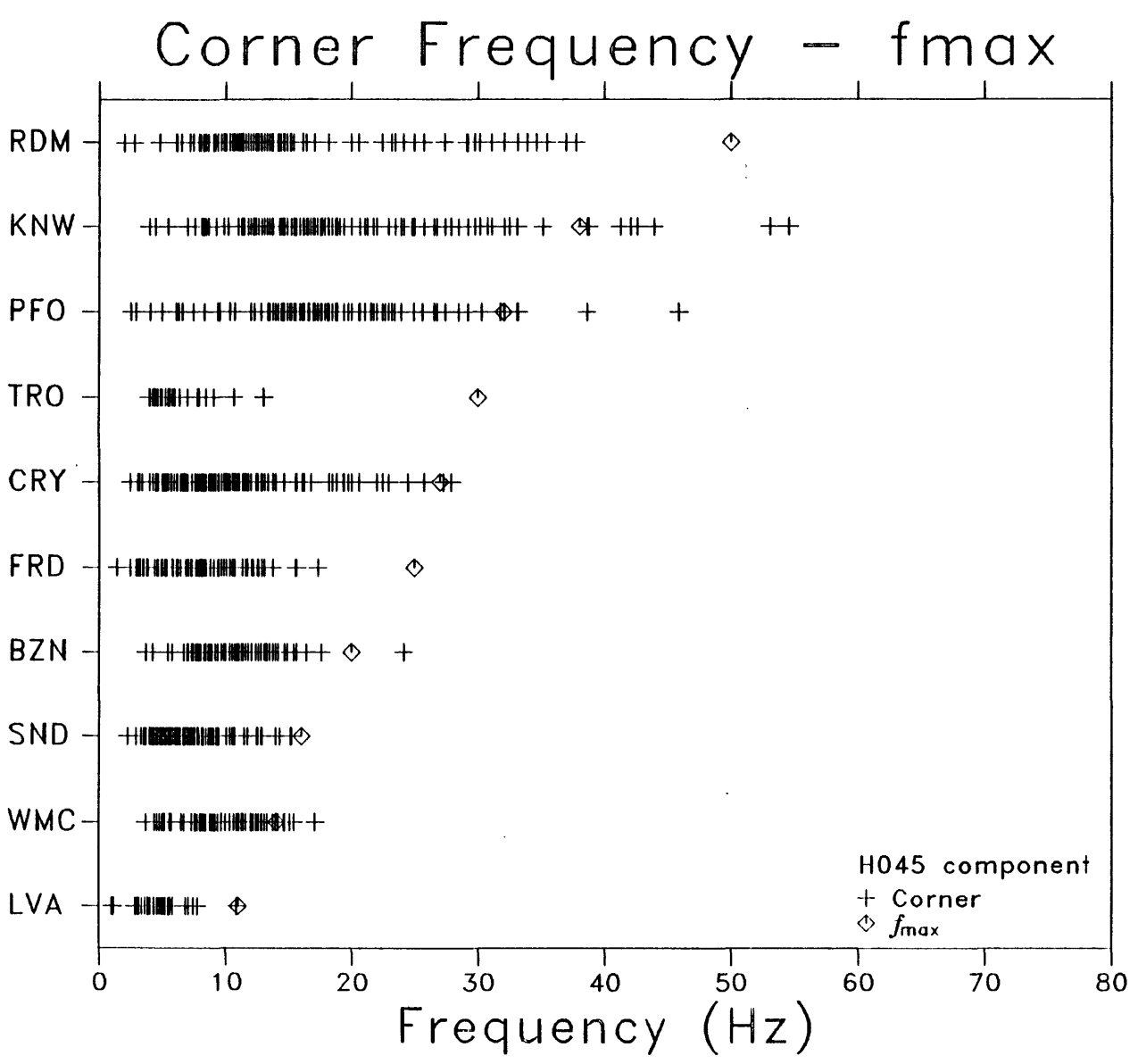
USGS CFPlot (27-Jun-85) -- 28-JUN-85 11:18:01
Tinker file: GSRSX0::DR3:[70,67]ANZATOT.PIK;2
fmax file: PUB1:[FLETCHER.CFPLOT]FMAX.DAT;5
Corner Frequency - fmax
RDM
KNW
PFO
TRO
CRY
FRD
BZN
SND
WMC
LVA
H045 component
+ Corner
◇ fmax
0
10
20
30
40
50
60
70
80
Frequency (Hz)

fig 11

Stations fmax greater than 30H

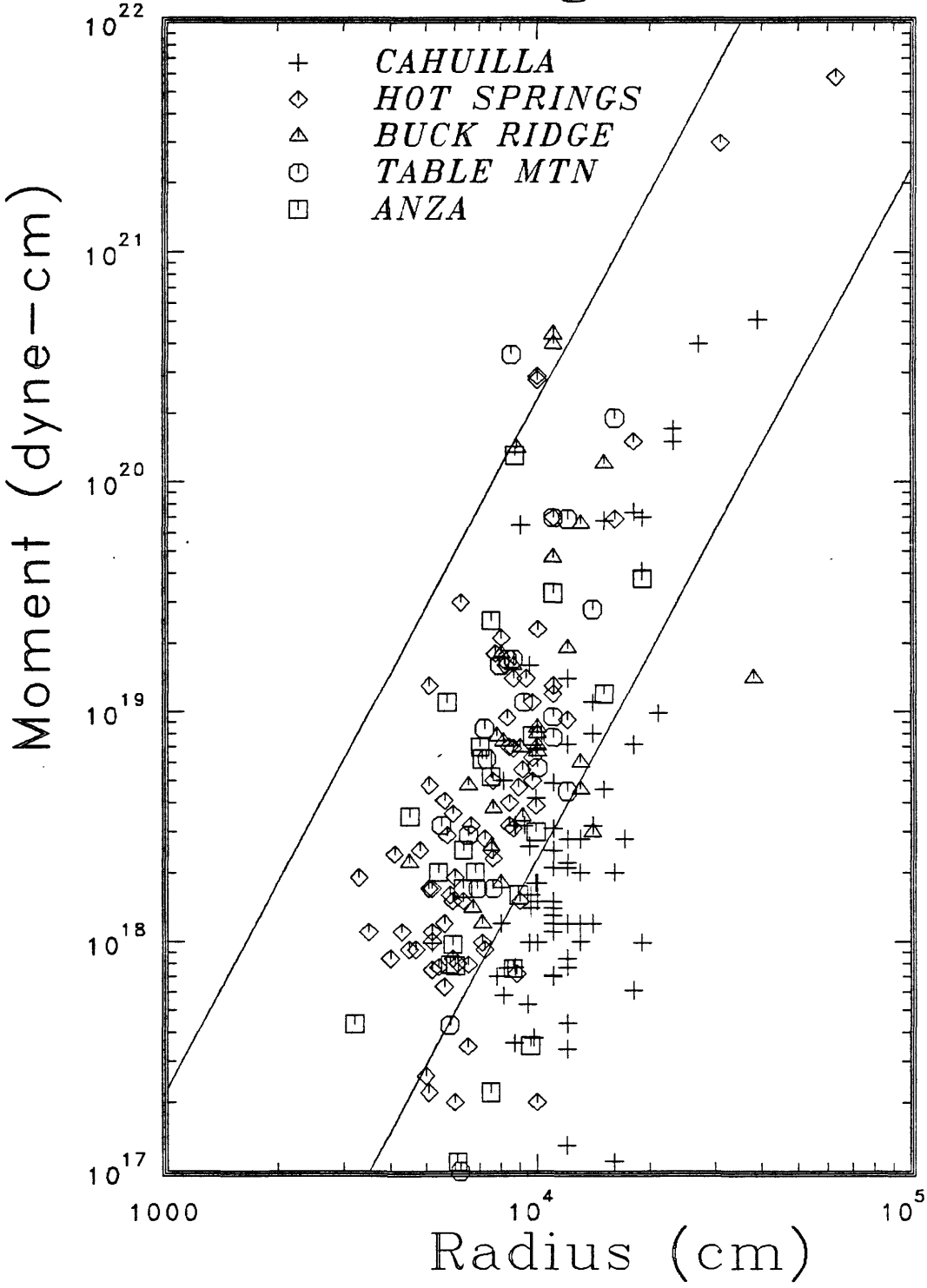

fig 12

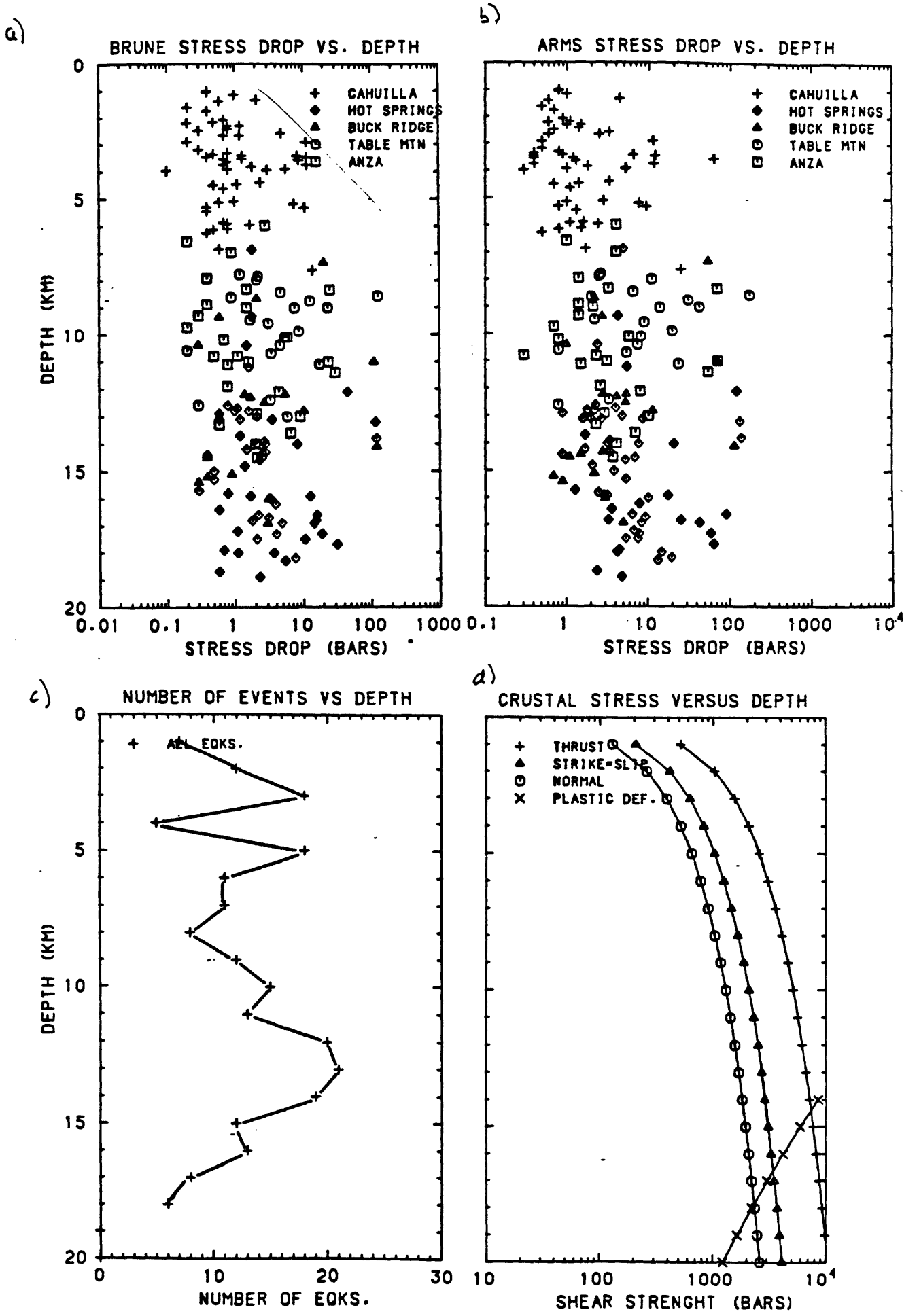
a)
BRUNE STRESS DROP VS. DEPTH
CAHUILLA
HOT SPRINGS
BUCK RIDGE
TABLE MTN
ANZA
DEPTH (KM)
0
5
10
15
20
0.01
0.1
1
10
100
1000
STRESS DROP (BARS)
b)
ARMS STRESS DROP VS. DEPTH
CAHUILLA
HOT SPRINGS
BUCK RIDGE
TABLE MTN
ANZA
0.1
1
10
100
1000
10^4
STRESS DROP (BARS)
c)
NUMBER OF EVENTS VS DEPTH
ALL EQKS.
DEPTH (KM)
0
5
10
15
20
0
10
20
30
NUMBER OF EQKS.
d)
CRUSTAL STRESS VERSUS DEPTH
THRUST
STRIKE-SLIP
NORMAL
PLASTIC DEF.
10
100
1000
10^4
SHEAR STRENGHT (BARS)

SOUTHERN SAN ANDREAS SYSTEM

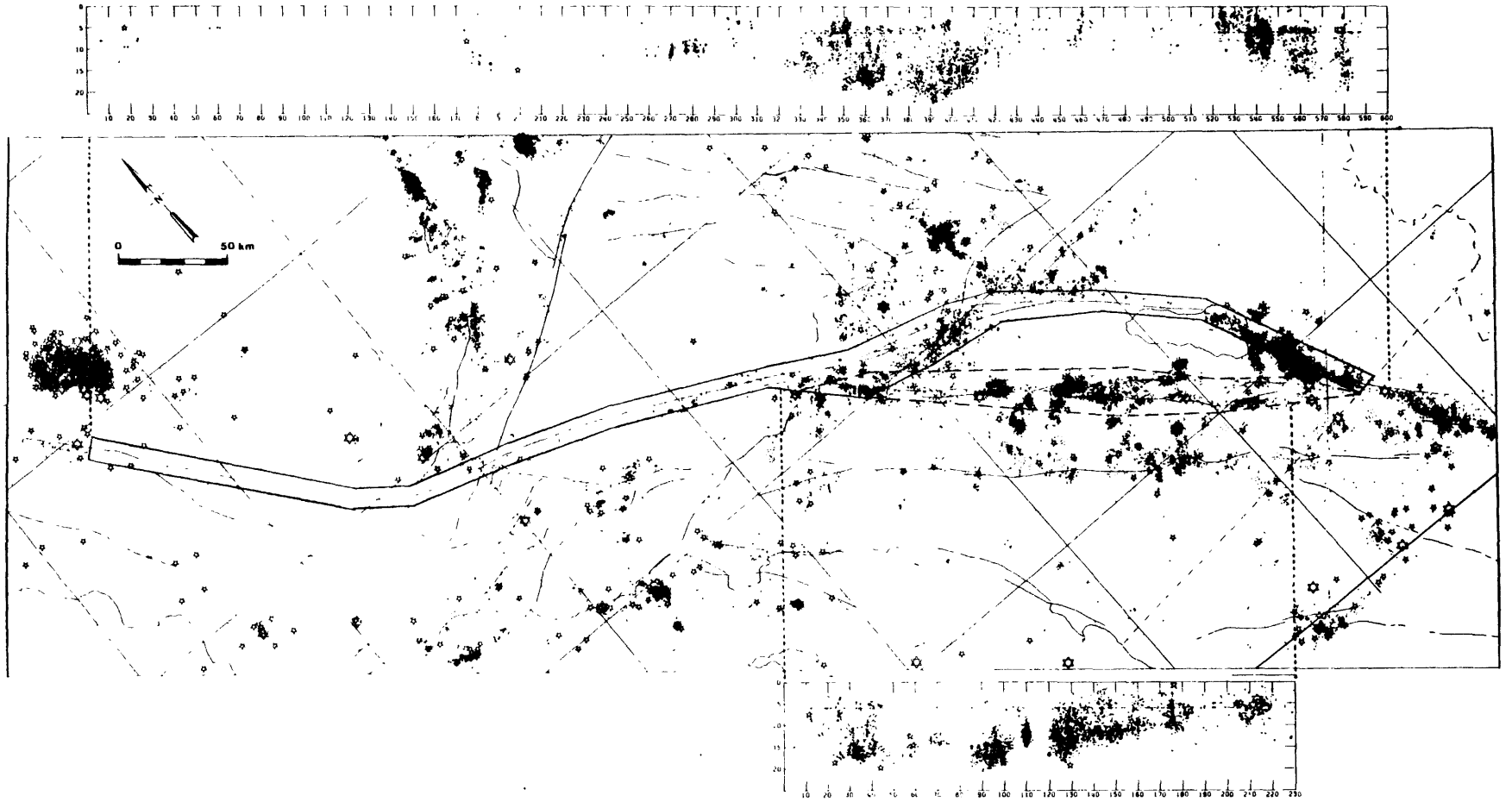

ALL CIT-USGS CATALOG EVENTS 1979-1984
(APPROX. 65,000 EVENTS)

Abstract

Recent fractures of the southern San Andreas fault in the Coachella Valley form a sawtooth geometry consisting of five 7-14Km long segments that alternate in trend from N40W to N48W. The relationship between this simple geometry and the inferred plate slip vector (N40W) is responsible for the topographic features of the fault zone, for the spatial distribution of triggered slip in 1968 and 1979 and for active uplift near the fault zone. The study of strainfields surrounding the oblique slipping N48W segments may provide clues concerning the rupture of the southern San Andreas in a future major earthquake.

The southern San Andreas Fault from the Cajon Pass to the Salton Sea is a seismic gap. It has not experienced a major earthquake in historic time (>240 years) and adjoins the rupture zones of major historic earthquakes to the north (1857 Fort Tejon), and to the south (1915, 1940 and 1979 Imperial Valley earthquakes). It is characterized by an almost total absence of microseismicity. A possible magnitude for a future earthquake on this segment of the fault has been estimated to be $7.6<Mw<7.8$ with a recurrence interval of between 160 and 360 years. [1] Holocene fault activity has resulted in clear topographic expression of the fault in numerous locations. [2-5] Trilateration in the last decade[6,7] and triangulation since 1931 [8] reveal 25mm/a of dextral displacement across the Coachella Valley. Prehistoric movements of the fault are evident in trench studies across the fault at Indio and at Cajon Pass [9]. Ongoing aseismic slip on the fault[18] may be responsible for the pronounced topographic features of the mapped fault, especially where Lake Cahuilla sediments should have obliterated transient features in the last several hundred years.[5,10,11]

On most fault maps of California the Coachella Valley section of the San Andreas fault south of the Banning Fault is shown as an approximately straight line. Careful mapping of recent fault features[5] reveals three N48W linear segments separated by N43W and N40W segments (Figure 1). Recent fault features are found within 50m of these linear trending segments except for the northern end of the central N48W segment and the southern end of the south N48W segment, where the deviation from straightness locally exceeds 100m. The 7-14Km dimensions of the fault segments form significant structural elements extending perhaps to the seismogenic zone as proposed by Wallace[12] in central California. The North-American/Pacific plate slip vector is estimated[13] to be locally parallel to N40W which would result in

approximately pure shear along the N43W and N40W segments of the fault and oblique slip on the N48W segments. The oblique slip gives rise to transpressive folding[3] on segments forming the Indio Hills[4], Mecca Hills[3] and Durmid Anticline.[2]

Part of the southern San Andreas fault slipped soon after the Borrego Mountain and Imperial Valley earthquakes in 1968 and 1979. The process was described[11] as "triggered-slip" because aseismic dextral movements of the fault occurred at the time of, and shortly after, nearby seismic events. Puzzling features of this aseismic triggered-slip were the small amplitudes (1-20mm) of dextral displacements (Figure 2) that occurred along a 40Km long section of the fault, the much reduced slip in the central 13Km of the triggered section and the evident increase in slip from south to north that terminated abruptly without apparent cause.[11,14,15] The fault geometry reported in this article provides additional insight into the mechanism of triggered slip. The triggered section embraces the three southern segments defining the saw-tooth geometry of the fault. Major bends in the fault zone occur within 2Km of the ends of the northern triggered-slip section and within 4Km of the southern triggered section in 1979. The N40W segment corresponds to the zone where no slip was observed 1979 and where 6-8mm of slip was observed on a 500m long surface break in 1968.[15]

An apparent paradox exists. Triggered-slip is confined to the oblique slip segments of the fault where normal forces inhibiting slip are large[15] and is insignificant on the pure shear segments where slip may be anticipated to occur more readily. A possible mechanism is that the N40W segments are creeping uniformly with time and that the N48W segments are "pinned". A similar scheme has been invoked[17] to describe the nature of seismic slip on the San Andreas in central California. Data from leveling surveys in 1974 and 1978 confirm that part of the Durmid Anticline segment is actively deforming[2] and that the observed bulge coincides approximately with the 1979 southern triggered segment. Evidence for continuous creep in the N40W and N43W segments is more elusive since most of the data for fault creep have been acquired on the N48W fault segments where the fault is well-expressed. A creep rate of 2mm/a is present at Dillon Road close to the bend between the northern N48W and the N43W segment[18].

Indirect evidence for creep in the N40W segment near North Shore exists as damage to a 36 year old, 5Km long, North-South concrete drain known as Wasteway No.1 that extends from the Coachella Canal to the northermost shore of the Salton Sea (Figure 1). Compressional cracks in the concrete and deformed reinforcing bars are found in two clusters; a pair of northern fractures within 500m of the interpolated intersection of the fault with the wasteway and a sequence of five southern fractures 2Km SW of the fault induced by hydraulic forces[19]. An apparent shortening by

50±10mm in the northern two fractures appears to be the result of tectonic movements in the last 36 years. The southern of the two northernmost fractures exhibits greater damage to the eastern lip of the structure consistent with clockwise rotation of the wasteway to the north by right lateral shear. If the fractures are the result of dextral slip on the fault, a value of 1.8±0.4mm/a is indicated, a creep rate that is intermediate between slip monitored on adjacent N48W segments[18].

A subsurface survey using an impulse radar profiling system was conducted along the west side of the wasteway and in a number of nearby locations to determine the precise intersection of the fault with the wasteway. These data reveal an abundance of possible fractures that appear to have disturbed the 1-2m deep Cahuilla Lake beds (Figure 2). The disturbances evident in the sediments occur over a 1Km wide zone and are not restricted to where thrust joints in the wasteway are located. They diminish in frequency and complexity in the southern half of the wasteway. The fault zone is perhaps wider in this segment than in adjacent segments and it is therefore possible that distributed slip could occur without causing ground cracks. The absence of recorded creep on the North Shore creepmeter (within the N40W segment) and the approximately 1mm/a measured on the nearby geodetic array[18] suggest that creep may be occurring either on a fault strand other than one on which cracks occurred in 1968 or that creep is distributed over a wide shear zone.

We note that the mean of the maximum values of triggered-slip measured in each kilometer section of the fault in 1968 (14.5mm) is roughly twice that observed in 1979 (6.5mm). Earthquakes capable of generating comparable accelerations to those that triggered the fault in 1968 and 1979 occurred in 1940 (El Centro), 1942 (San Jacinto) and 1948 (Desert Hot Springs). The period of time between the most recent of these and 1968 is twice as long as the interval between 1968 and 1979. A slip-predictable model for triggered-slip may be applicable in which the magnitude of triggered slip is proportional to the time since previous triggered slip occurred. No slip was recorded on the southern San Andreas in the 1940's nor was evidence for it sought. Aperiodic creep on the fault in the Coachella Valley and triggered-slip appear to be manifestations of the same phenomenon. The creep rate following triggered-slip in these segments is typically lower than at other times[18]. Similar accelerated creep (0.1-8.7mm) was triggered on the San Andreas fault in central California at the time of the Coalinga earthquake.[22]

Leveling data from the NW end of the southern N48W segment indicate a tilt rate up to the east of the order of 1 microradian/a in the period 1980-83 [20], followed in April 1984 by an 8mmm creep event at Mecca Beach.[18] NGS Leveling data reveal a similar tilt rate to have occurred in 1974-78 (Figure 1) close to part of the triggered slip segment of 1979. If this uplift (≈3mm/a) were entirely due to vertical strains

induced by horizontal compressional confinement of a 15Km thick crust, we calculate a horizontal strain rate of -0.6 microstrain/a, assuming a Poisson's ratio of 0.25 in the elastic zone centered on the fault. The width of the zone of folding near the fault is of the order of 5Km which suggests that the observed uplift requires convergence of the order of 3mm/a outside the zone of folding. This figure is consistent with the observed long term creep rate and confirms that elastic strain must be accumulating away from the fault, since this represents less than 20% of the dextral displacement observed geodetically across the Coachella Valley. USGS trilateration at Bat Caves Buttes mostly to the north of the fault and 3Km from the SE termination of triggered-slip (outside the uplift zone) indicates that no deformation has occurred (±1 microstrain) in the last decade [21].

The association of N48W trending segments of the fault with high ground, well-developed fault features, thrusting and folding is in marked contrast to the poor surface expression, subdued topography and low elevation of the fault to be found in the N40W and N43W segments. The absence of topographic relief in direct line with the southernmost expression of the San Andreas Fault SE of the Salton Sea supports the hypothesis that the trend of the active southern continuation of the San Andreas is less than N48W, perhaps passing through Bombay Beach [10]. The swarm of seismic activity on the Brawley fault zone [24] preceeding the Imperial Valley 1979 event trends at N22±2W and may represent the effective continuation of the San Andreas Fault southward. The observed elevation changes near the Salton Sea in 1974-8 were presumably related to the Brawley earthquake swarm.

Angular relationships between adjacent linear segments of the San Andreas fault have recently been discussed in terms of their influence in the control of strain release during late stages of the earthquake cycle.[16,17] King and Nabelek[23] demonstrate the generality of such observations and provide a kinematic mechanism for the nucleation and termination of slip at bends in faults. The possibility exists that each of the N48W segments on the San Andreas, or the Banning fault, could act as a nucleus for rupture of the southern San Andreas. The geometry and slip vector associated with this 90Km segment of the fault are well determined. Strainfields will be most intense at the ends of the mapped straight segments[16], generally requiring networks with baselines of less than a few kilometers, extending tens of kilometers from the fault. Existing trilateration and leveling networks are inappropriately scaled and poorly distributed to monitor these strainfields. It is of great importance to establish a few key networks in strategically placed locations if we are to learn more about the rupture process in the Coachella Valley.

Roger Bilham
Lamont Doherty Geological Observatory, Palisades, N.Y. 10964: Current address, Joint Institute for Laboratory Astrophysics, University of Colorado, Boulder, CO, 80309

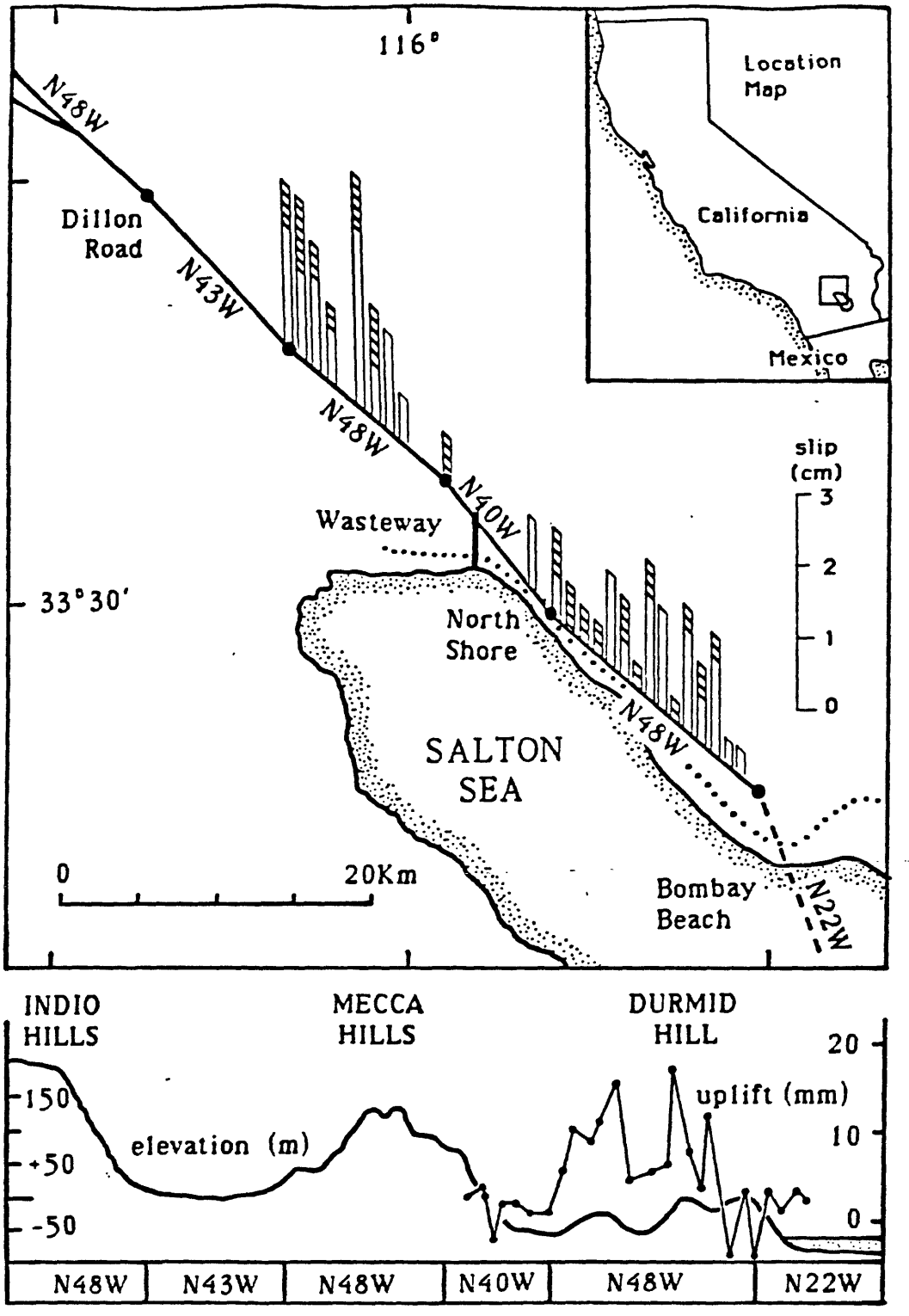

Figure 1 Coachella Valley section of the San Andreas fault from the intersection of the Banning Fault to the Brawley seismic swarm (dashed line). Recent fault features follow a series of 7-18Km long segments that are linear to ±50m but differ in trend by 3-8°. The cumulative, mean, maximum triggered-slip observed on the fault is shown for each kilometer of the fault (open bars=1968, striped bars=1979). Uplift observed on a leveling line near the fault (dotted line) between 1974 and 1978 is plotted on the lower figure which also shows the relationship between fault trend and fault-trace elevation. A North-South trend believed to be due to a magnetic bias in one of the surveys has been removed from the NGS leveling data.

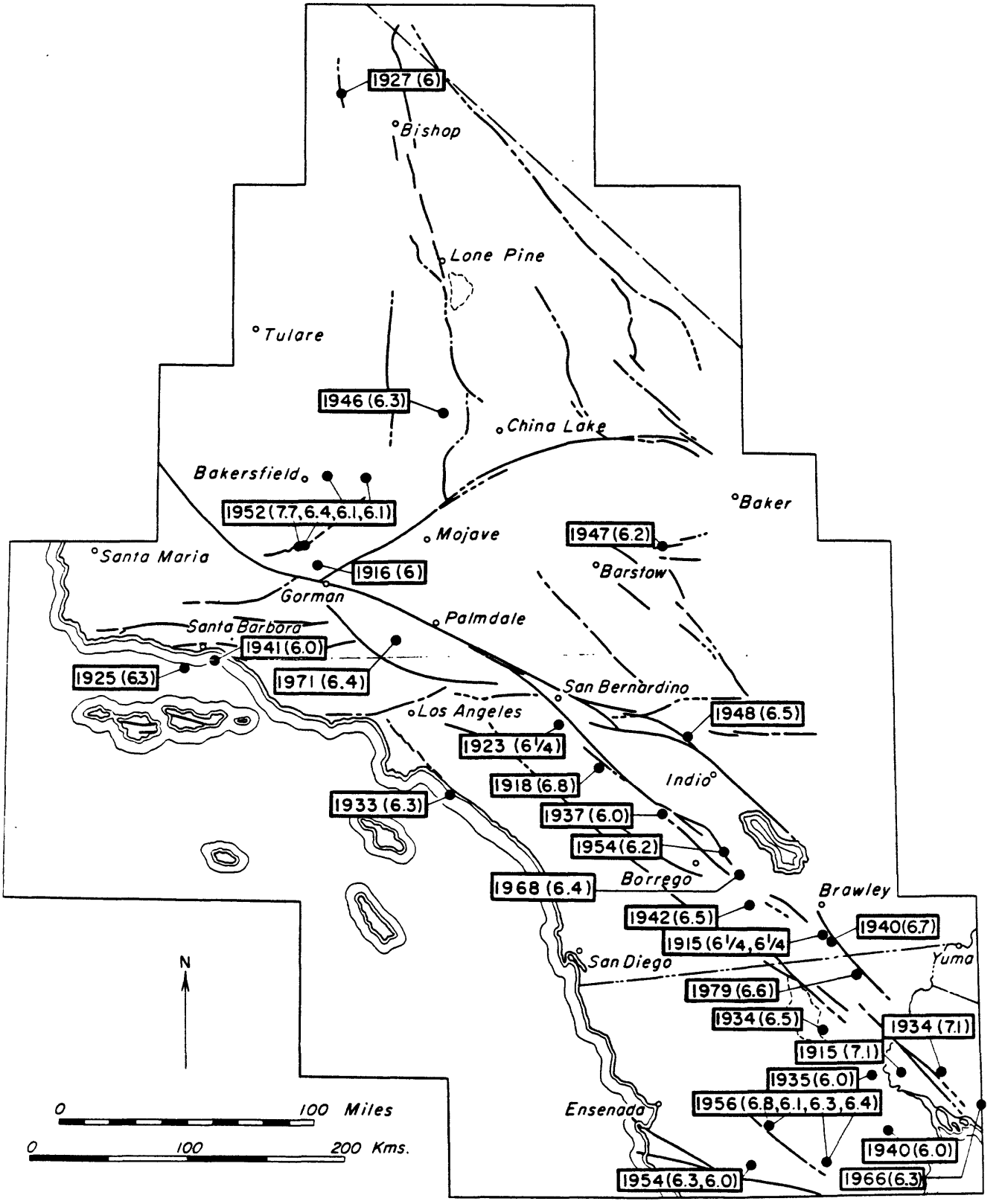
1927 (6)
Bishop
Lone Pine
Tulare
1946 (6.3)
China Lake
Bakersfield
1952 (7.7, 6.4, 6.1, 6.1)
Baker
Mojave
1947 (6.2)
Santa Maria
1916 (6)
Barstow
Gorman
Palmdale
Santa Barbara
1941 (6.0)
1925 (6.3)
1971 (6.4)
San Bernardino
1948 (6.5)
Los Angeles
1923 (6¼)
1918 (6.8)
Indio
1933 (6.3)
1937 (6.0)
1954 (6.2)
Borrego
1968 (6.4)
Brawley
1942 (6.5)
1940 (6.7)
1915 (6¼, 6¼)
San Diego
Yuma
1979 (6.6)
1934 (6.5)
1934 (7.1)
1915 (7.1)
1935 (6.0)
1956 (6.8, 6.1, 6.3, 6.4)
Ensenada
1940 (6.0)
1954 (6.3, 6.0)
1966 (6.3)
N
0 100 Miles
0 100 200 Kms.

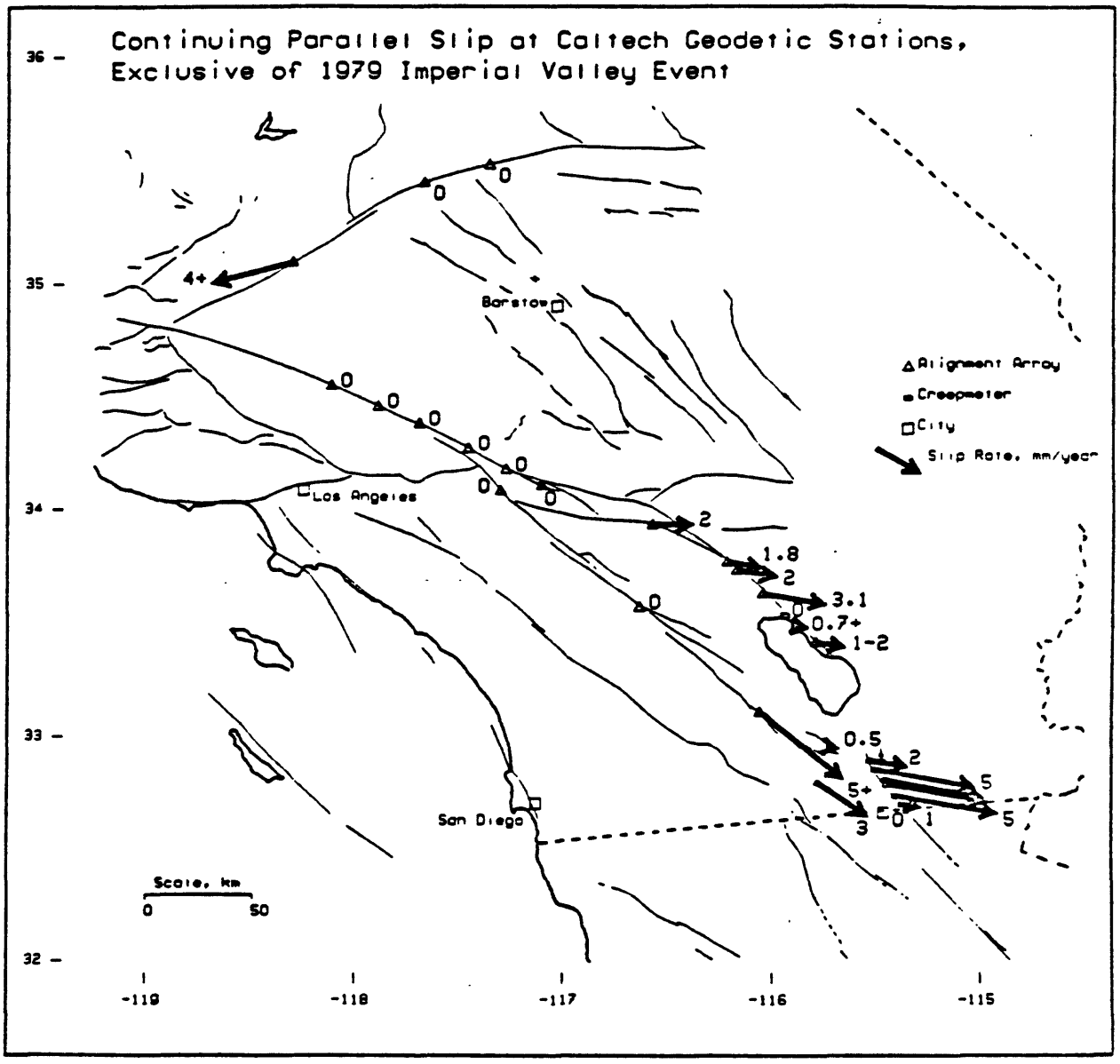

Figure 5.—Map summarizing observations in southern California of fault slip rates not associated with individual earthquakes showing surface rupture. All motion is assumed to be parallel to the fault traces; the arrows have lengths proportional to slip rates but are oriented only for pictorial purposes. Note the faults on which no slip has been measured.

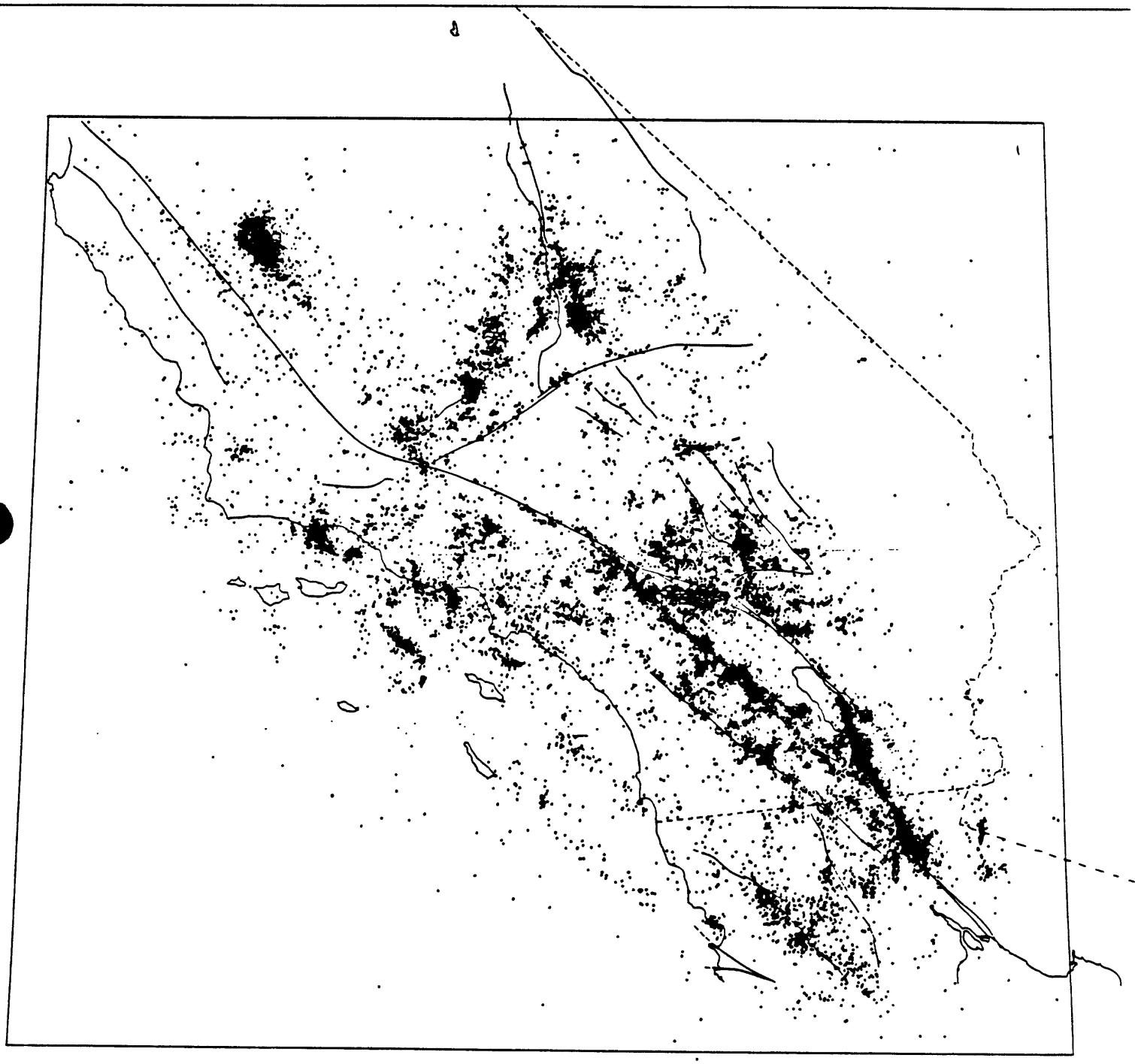


50 KM

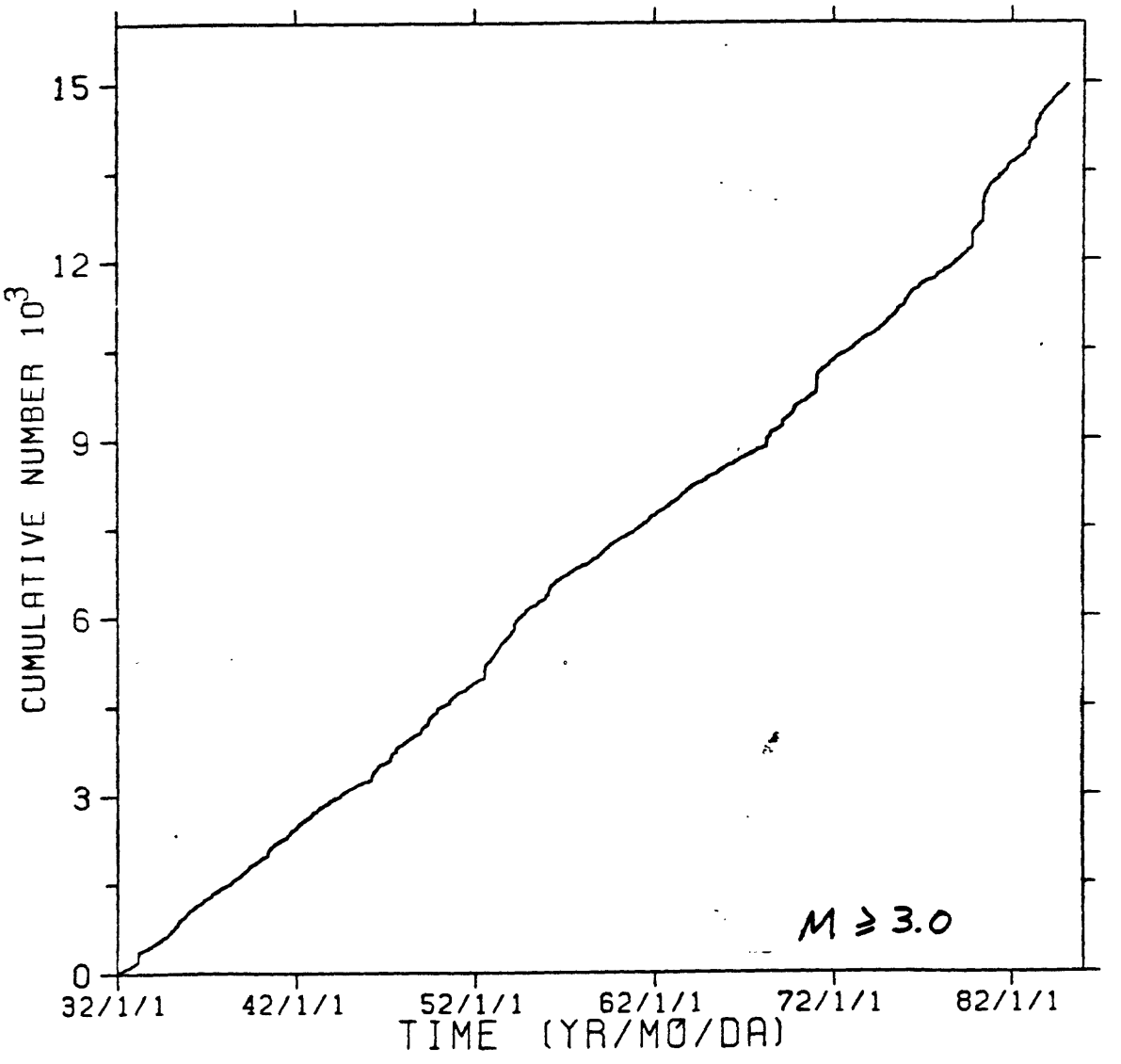
15
12
9
6
3
0
CUMULATIVE NUMBER 10^3
32/1/1
42/1/1
52/1/1
62/1/1
72/1/1
82/1/1
TIME (YR/MO/DA)
M ≥ 3.0

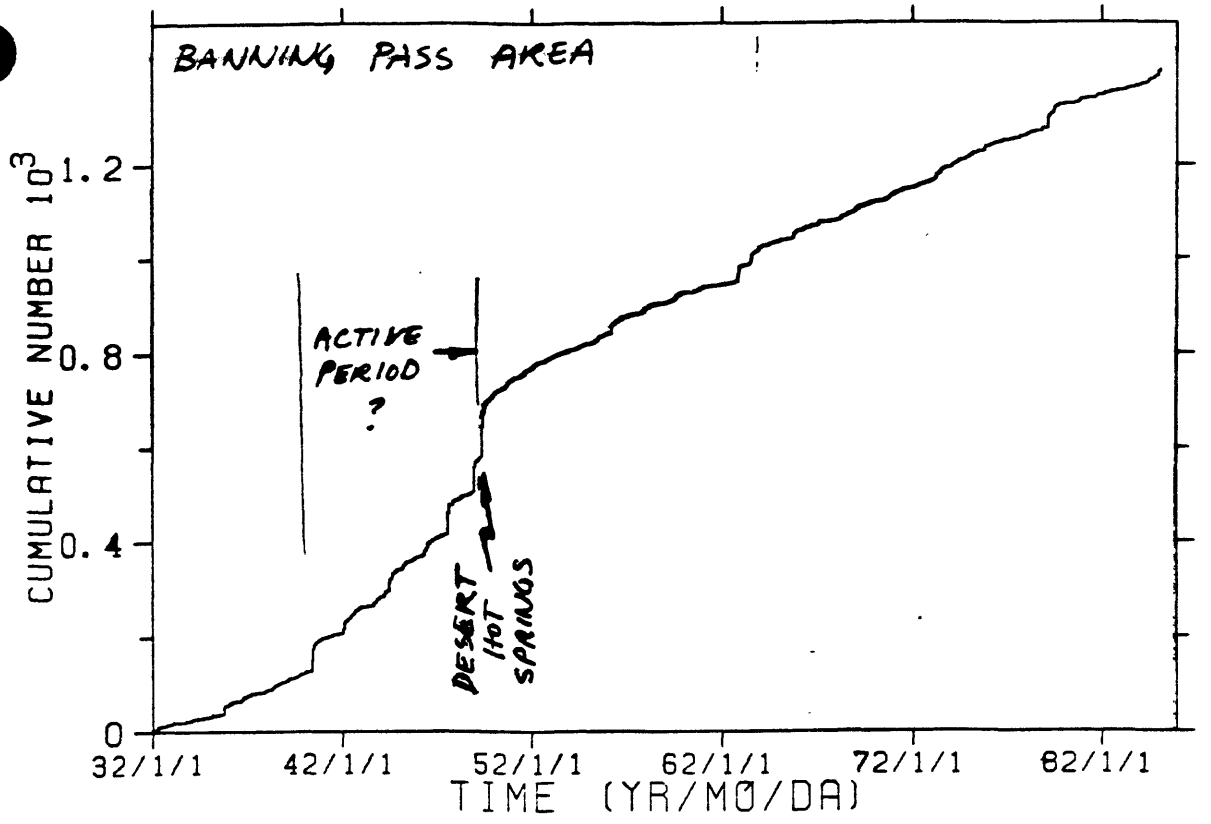
BANNING PASS AREA
CUMULATIVE NUMBER 10^3
1.2
0.8
0.4
0
ACTIVE PERIOD ?
DESERT HOT SPRINGS
32/1/1
42/1/1
52/1/1
62/1/1
72/1/1
82/1/1
TIME (YR/MO/DA)

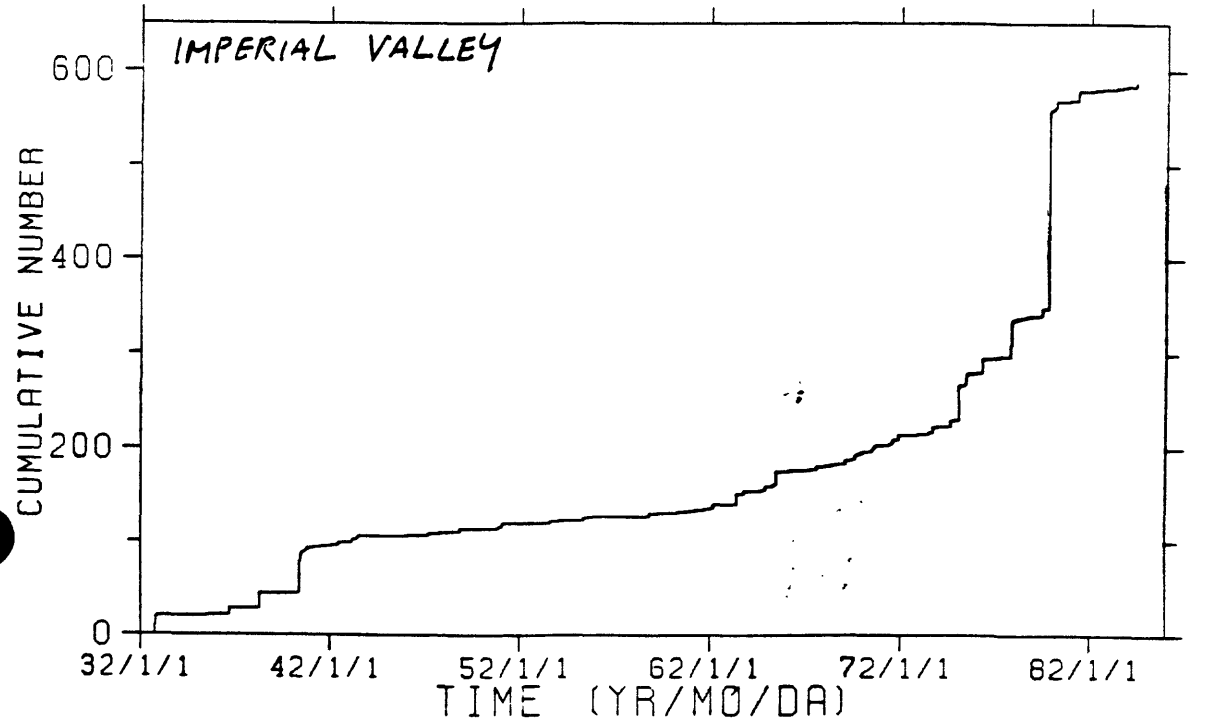
IMPERIAL VALLEY
CUMULATIVE NUMBER
600
400
200
0
32/1/1
42/1/1
52/1/1
62/1/1
72/1/1
82/1/1
TIME (YR/MO/DA)

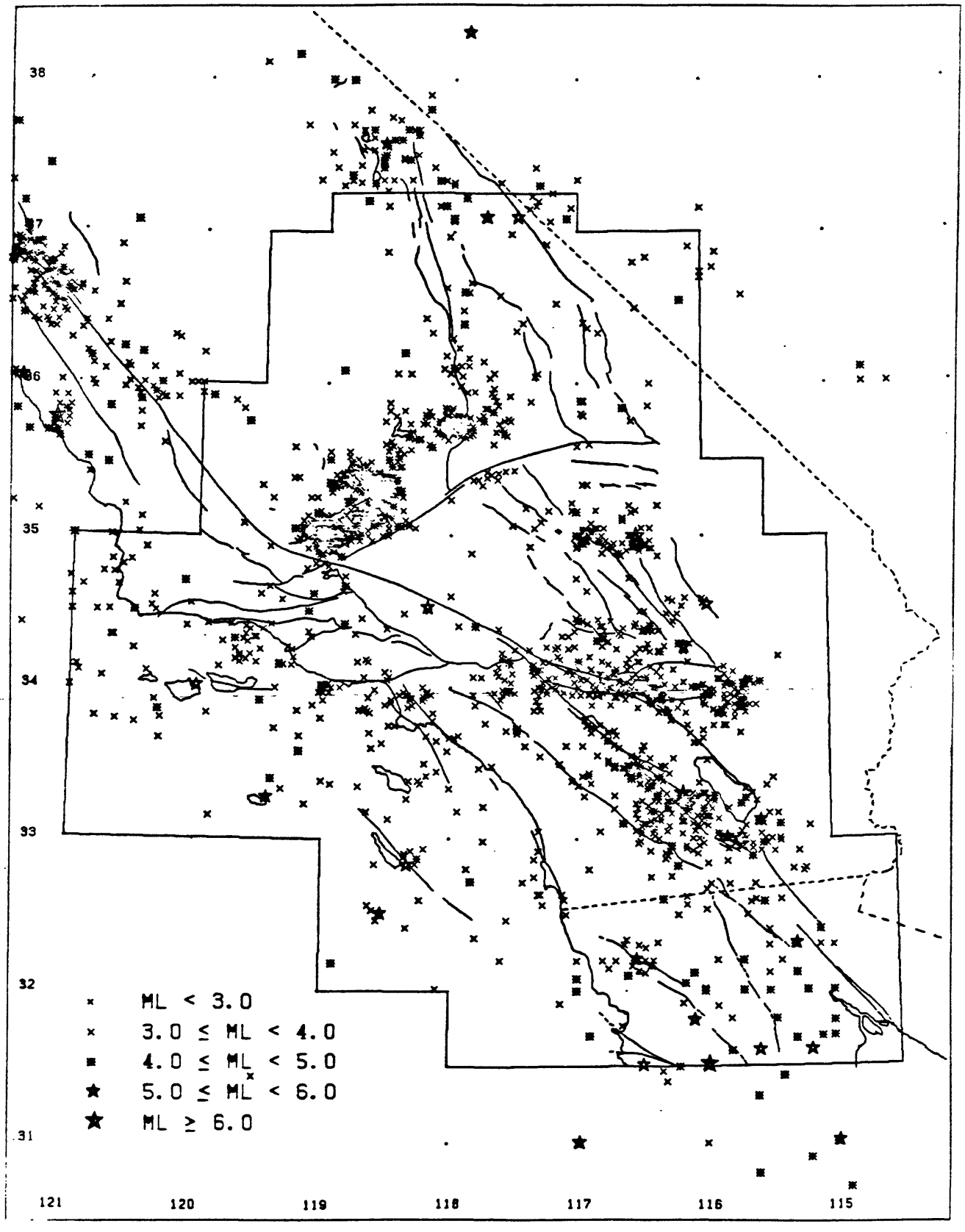
38
37
36
35
34
33
32
31
121
120
119
118
117
116
115
ML < 3.0
3.0 ≤ ML < 4.0
4.0 ≤ ML < 5.0
5.0 ≤ ML < 6.0
ML ≥ 6.0

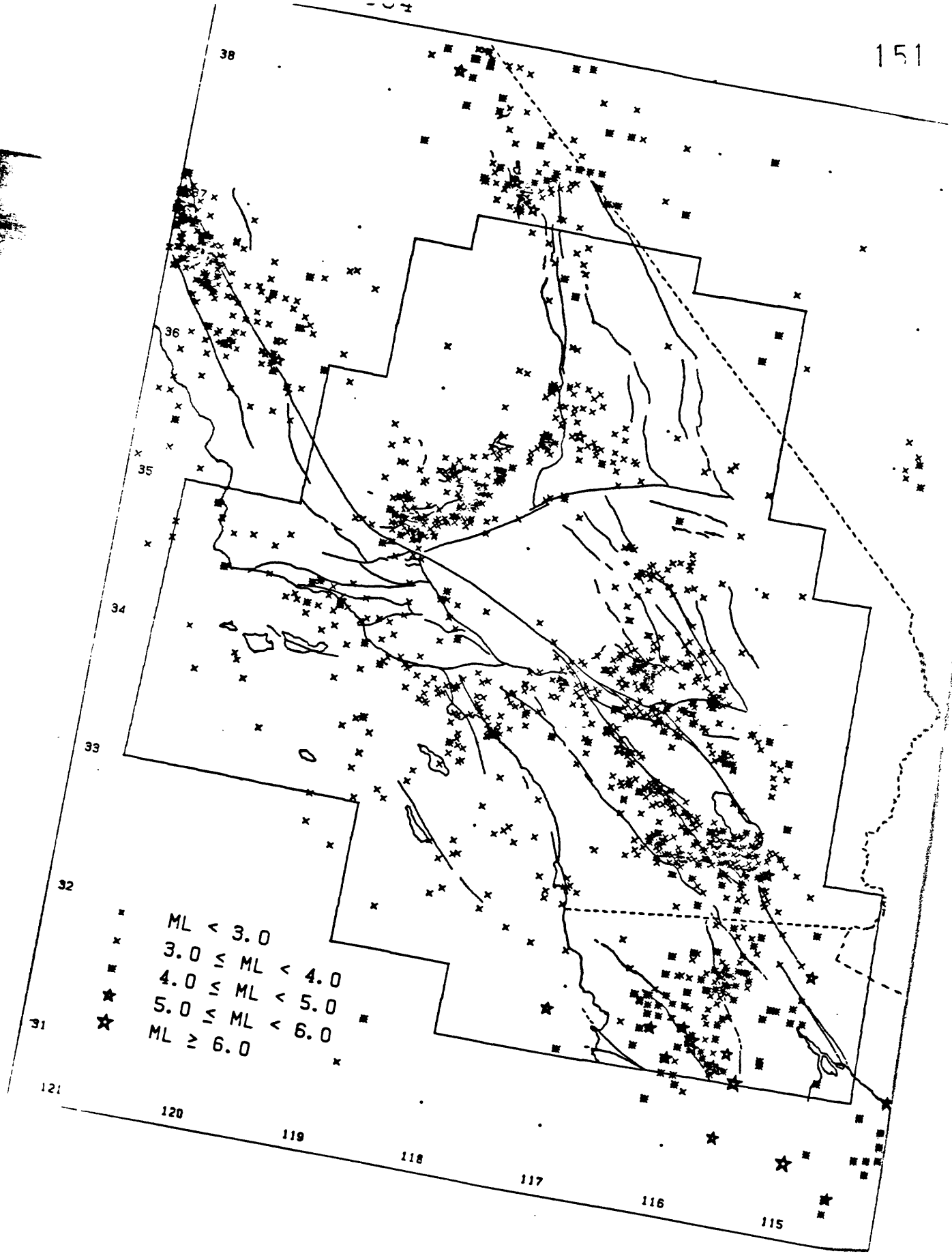
38
37
36
35
34
33
32
31
121
120
119
118
117
116
115
ML < 3.0
3.0 ≤ ML < 4.0
4.0 ≤ ML < 5.0
5.0 ≤ ML < 6.0
ML ≥ 6.0

1965 - 1974

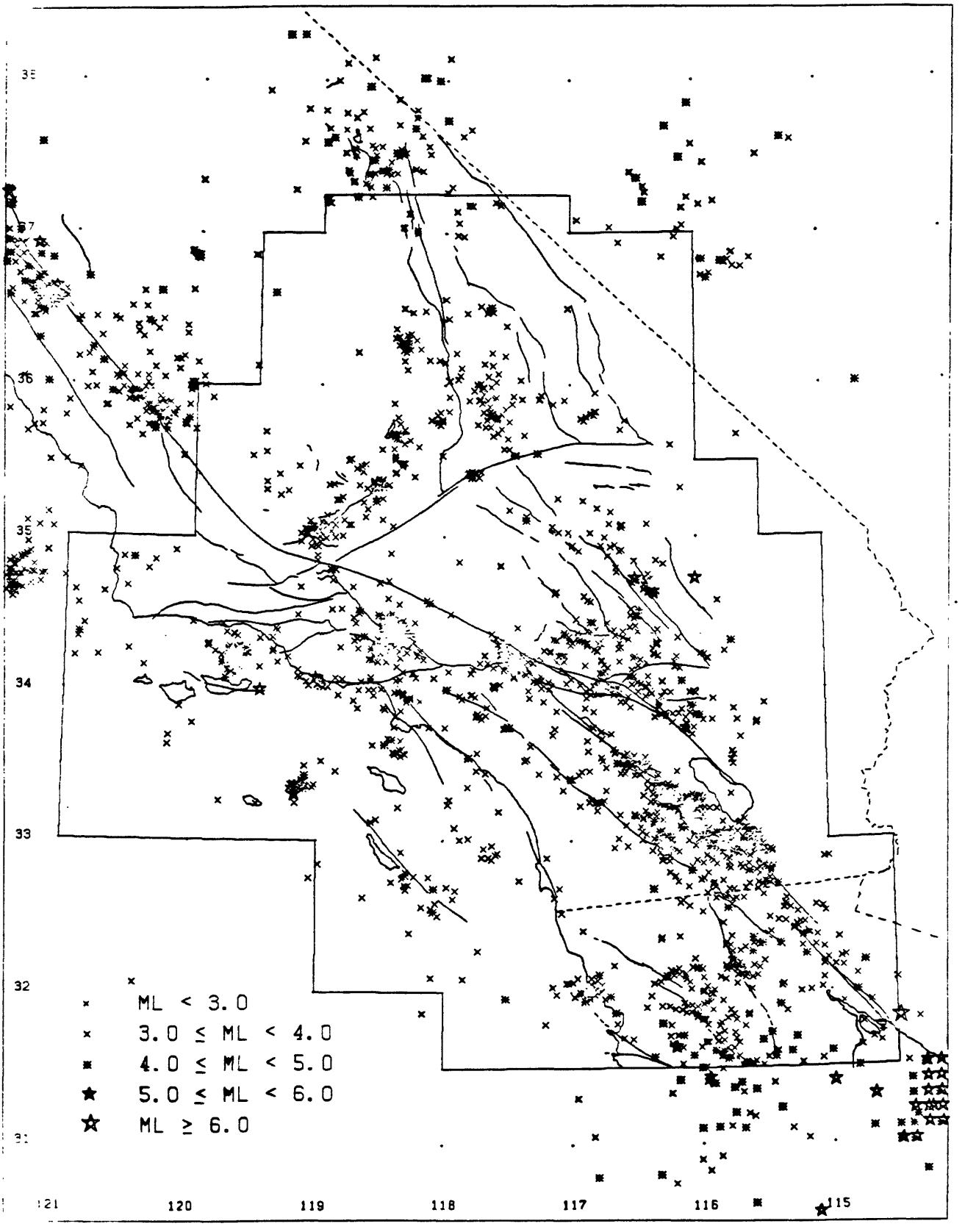
ML < 3.0
3.0 ≤ ML < 4.0
4.0 ≤ ML < 5.0
5.0 ≤ ML < 6.0
ML ≥ 6.0
121
120
119
118
117
116
115
34
33
32

February 28, 1985

Kerry Sieh

MATERIALS TO FACILITATE DISCUSSION

Based upon the historical and prehistoric record, three segments of the San Andreas fault in southern California appear to be the most likely to generate a large (M>7) earthquake within the next 50 years. These are labelled 2, 5 and 6 in Figure 1. Figures 2 through 16 and 20 illustrate some of the data upon which these forecasts are based.

Figures 17 through 19 depict evidence for historic slippage on the southern most 100 kilometers of the San Andreas fault. Figure 21 is Stuart's suggestion for future activity on the San Andreas fault.

Clearly, the southern San Andreas and the San Jacinto faults can be divided into segments of differing behavior and perceived risk. Is our understanding adequate, however, for selecting one or more sites for expensive and intensive monitoring?

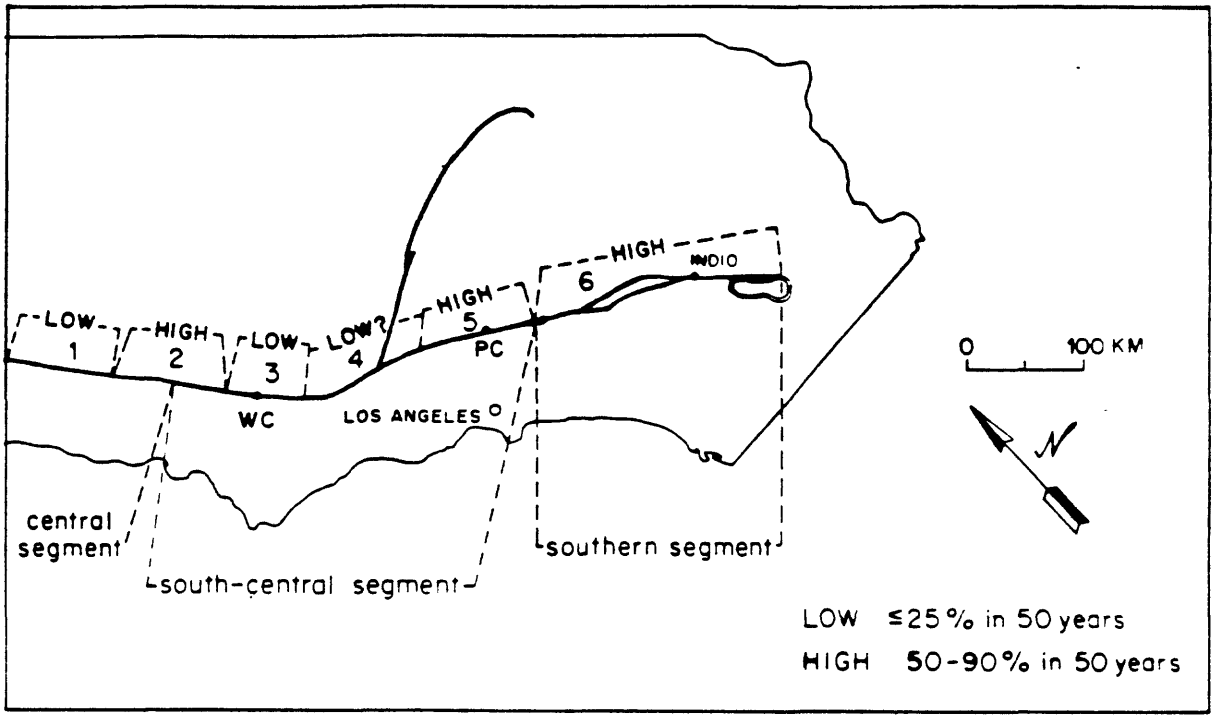

Figure 2. Probabilistic forecasts of large earthquakes along the San Andreas fault in southern California can now be made on the basis of the fault's prehistoric and historic behavior.

Segments labelled 2, 5 and 6 possess the greatest likelihood of rupture within the next 50 years. We plan to concentrate our efforts in 1986 along segments 2 and 6.

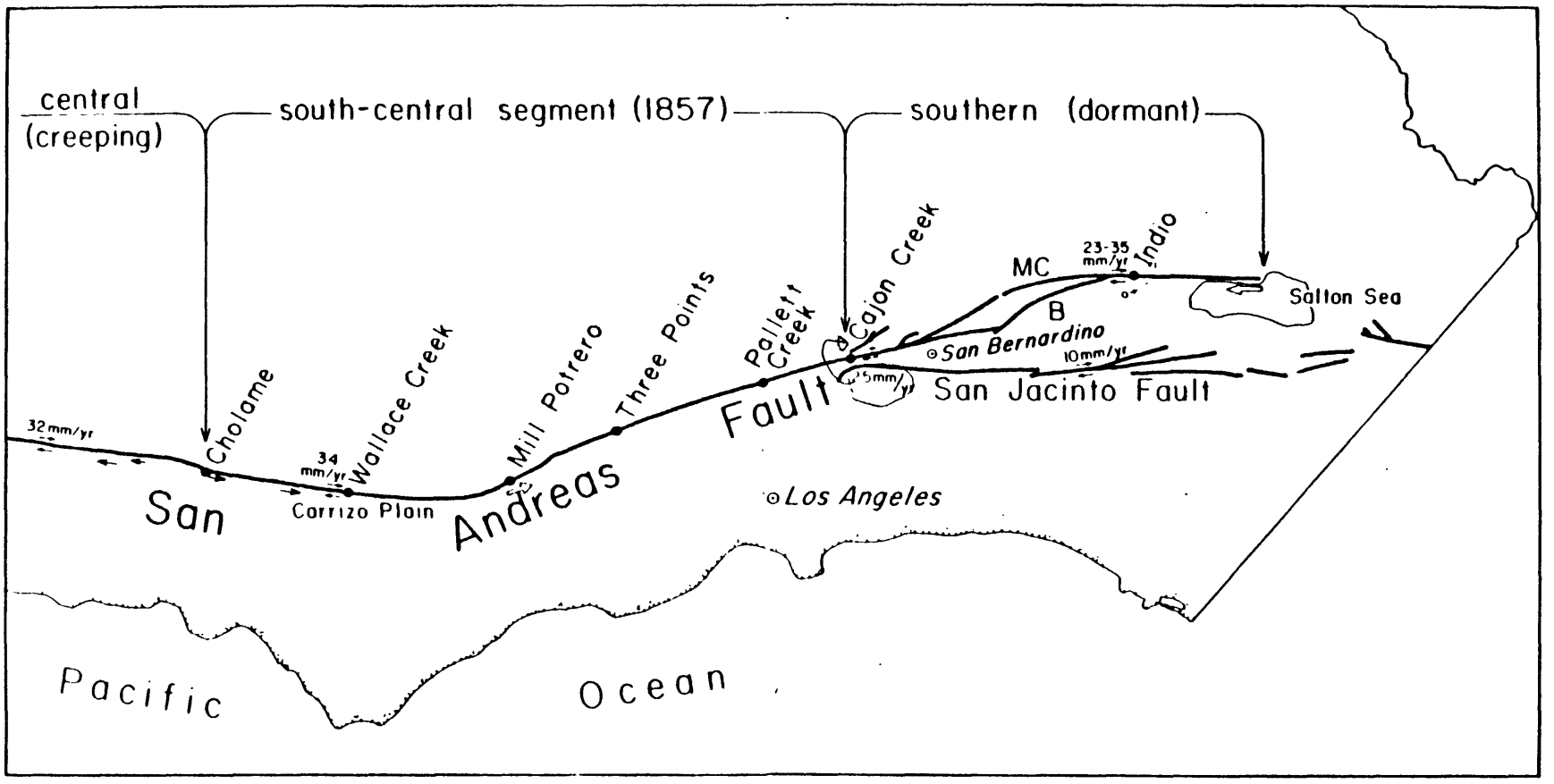

Figure 1. Map of the San Andreas fault in southern California with localities and slip rate values discussed in the proposal. B=Banning fault; MC=Mission Creek fault.

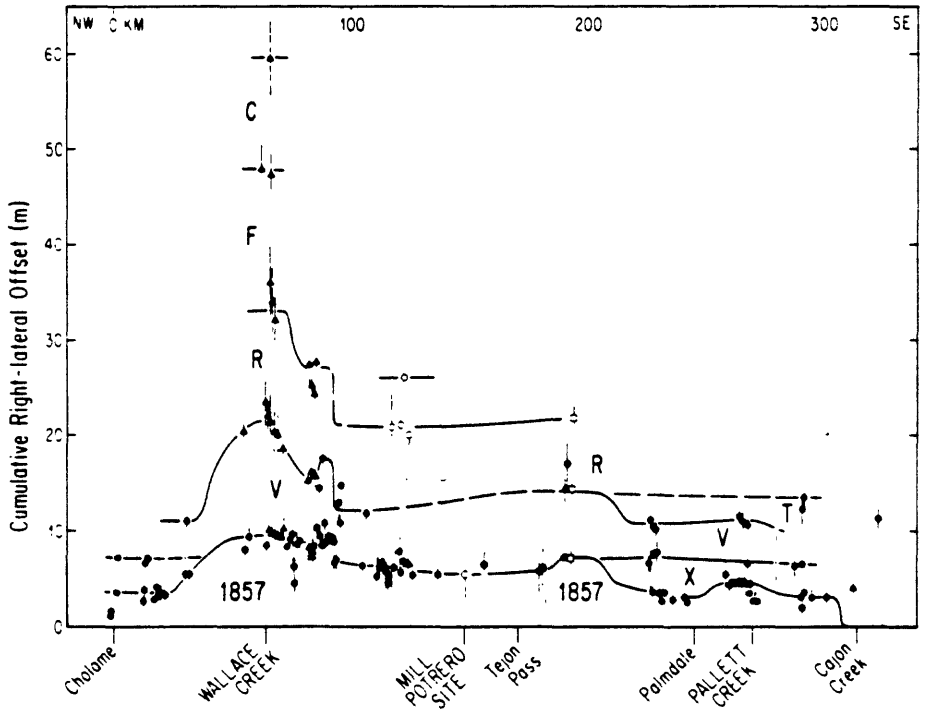

Figure 10. Right-lateral offsets measured along the south-central (1857) segment of the San Andreas fault suggest that slip at each locality is characterized by a particular value. Solid circles are data from Sieh (1978c), with poor-quality data deleted. Open circles are data from Davis (1983). Triangles are new data and remeasurements at sites reported by Sieh (1978c). Open squares are new data. Vertical bars indicate magnitude of imprecision in measurement.

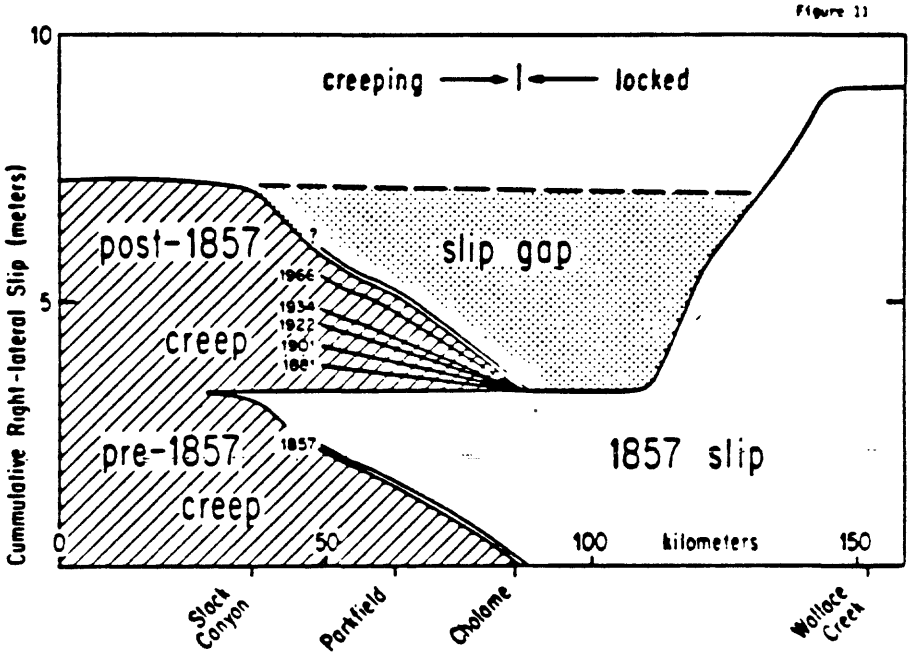

Figure BV-1. A plot of distance along the fault versus cumulative right-lateral slip reveals a historical "slip gap" over a 90-km stretch of the San Andreas fault centered on Cholame. Slip in 1857 amounted to about $3\frac{1}{2}$ m within the gap, whereas at Wallace Creek it was about $9\frac{1}{2}$ m. Assuming strain has been accumulating at 34 mm/yr since 1857, the period between local 1857-size slip events ought to be 240 to 450 years at Wallace Creek, but only 100 years in the "slip gap." Post-1857 creep inferred from modern measurements of creep rate is equal to the accumulated strain to the left (northwest) of Slack Canyon, but is lower between Slack Canyon and Cholame – hence the "slip gap" includes this segment. Pre-1857 slip is assumed to be like post-1857 creep. Location of 1966 rupture is plotted for reference. The slip-gap could generate an M_s = 7 to $7\frac{1}{2}$ earthquake. Figure is from Sieh and Jahns, 1984.

TABLE 2 SMALLEST STREAM OFFSETS NEAR WALLACE CREEK AND PROPOSED INTERVALS BETWEEN GREAT EARTHQUAKES

(1) Stream offsets (m)	(2) Remarks	(3) Produced by	(4) Slip associated with earthquake (m)	(5) Proposed interval between events (yr)
9.5 ± 0.5 (1σ)	Average of 5 measurements	1857 event	9.5 ± 0.5 (1σ)	
21.8 ± 1.1	Average of 4 measurements**	1857 plus last prehistoric event	12.3 ± 1.2*	240 to 320†
32.8 or 33.5 ± 1.9	Average of 3 measurements**	1857 plus latest 2 prehistoric events	11.0 or 11.7 ± 2.2*	300 to 440‡ 240 to 450‡

*$32.8 - 9.5 = (0.5^2 + 1.1^2)^{1/2}$

†$32.8 - 21.8 = (1.1^2 + 1.9^2)^{1/2}$ or $33.5 - 21.8 = (1.1^2 + 1.9^2)^{1/2}$

‡Slip during following earthquake in column 4 divided by average late Holocene slip rate (33.9 ± 2.9 mm/yr)

**Offset values are all between Wallace Creek and Gully D in Figure 1

TABLE 3 SMALLEST STREAM OFFSETS NEAR WALLACE CREEK AND PROPOSED DATES AND CORRELATION OF LATEST FOUR GREAT EARTHQUAKES

(1) Stream offsets (m)	(2) Time required to accumulate offset as elastic strain using average late Holocene slip rate (years)	(3) Proposed dates for latest earthquakes (A.D.)	(4) Possible correlations with events recognized at Pallett Creek	(5) Possible correlations with events recognized at Mill Potrero by Davis (1983)
		1857	Z(1857)	Z(1857)
9.5 ± 0.5 (1σ)	240 to 320			
		1540 to 1630*	V(1550 ± 70)	V(1584 ± 70)
21.8 ± 1.1	560 to 740			
		1120 to 1300†	R(1080 ± 65)	
32.8 or 33.5 ± 1.9	840 to 1140			
		720 to 1020‡	F(845 ± 75)	

*1857 − (240 to 320 yr)

†1857 − (560 to 740 yr)

‡1857 − (840 to 1140 yr)

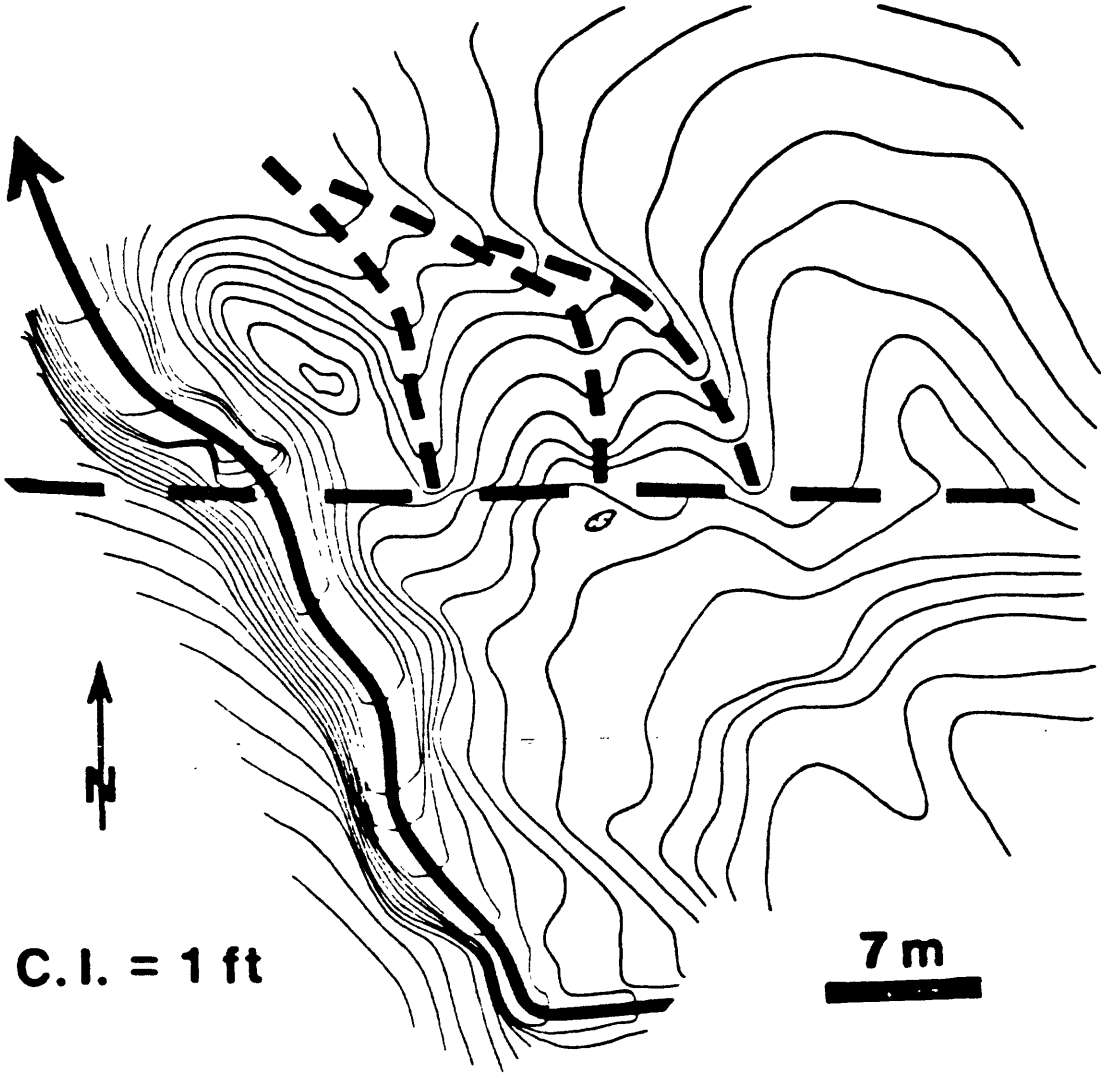

Figure 7. This topographic map shows three offset segments of Cow Spring Creek, From this and related data it appears that right-lateral offsets at the tunnel crossing are characteristically about 7 meters.

TABLE 2. Estimated Dates of Latest 12 Earthquakes at Pallett Creek

Event	Date,[a] A.D.	Remarks
Z	1857	Historically documented.
X	1720 ± 50	Unit 81 date is within period from 140 to 305 years B.P.[b] (i.e., 1730 ± 80 A.D.); event occurs at top of unit, so ~20 years must be added to unit 81 date[c], thus 1750 ± 80 A.D.; historical record precludes event after 1769, thus 1720 ± 50 A.D.
V	1550 ± 70	Weighted average of upper unit 68 (1405–1630 = 1518 ± 112 A.D.) and unit 72 (1485–1660 = 1573 ± 88 A.D.), which bracket the earthquake horizon.
T	1350 ± 50	Unit 61 date is within period from 1280 to 1380 (i.e., 1330 ± 50 A.D.), event occurs at top of unit, so ~20 years must be added to unit 61 date, thus 1350 ± 50 A.D.
R	1080 ± 65	Weighted average of samples PC-223a, PC-28, and PC-207c, which bracket the earthquake horizon.

TABLE 3. Estimated Dates of Earthquakes A Through N, Using Alternate Method

Event	Date, A.D
N	1015 ± 100
I	935 ± 85
F	845 ± 75
D	735 ± 60
C	590 ± 55
B	350 ± 80
A	260 ± 90

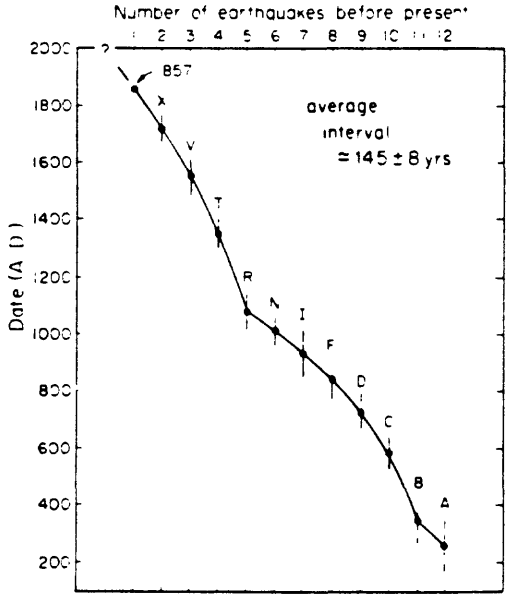

Fig. 16. Revised dates of each earthquake at Pallett Creek

SLIP RATE ON THE SAN ANDREAS FAULT AT CAJON CREEK

FIGURE 7. Slip rate on the San Andreas fault at Cajon Creek. The points represent our best estimates of the offsets and ages and the boxes represent 95% confidence limits. Each box represents independent offset features, radiocarbon dates and geologic assumptions. The points are not in the center of the boxes due to the asymmetric limits on some of the ages and measurements. The heavy line represents our best estimate of the slip rate at Cajon Creek and the lighter lines are the limits on the rate, constrained to touch each box. The starting point for each line is 170 years ago. This is our best estimate for one-half recurrence intervals after the last earthquake (see text for details).

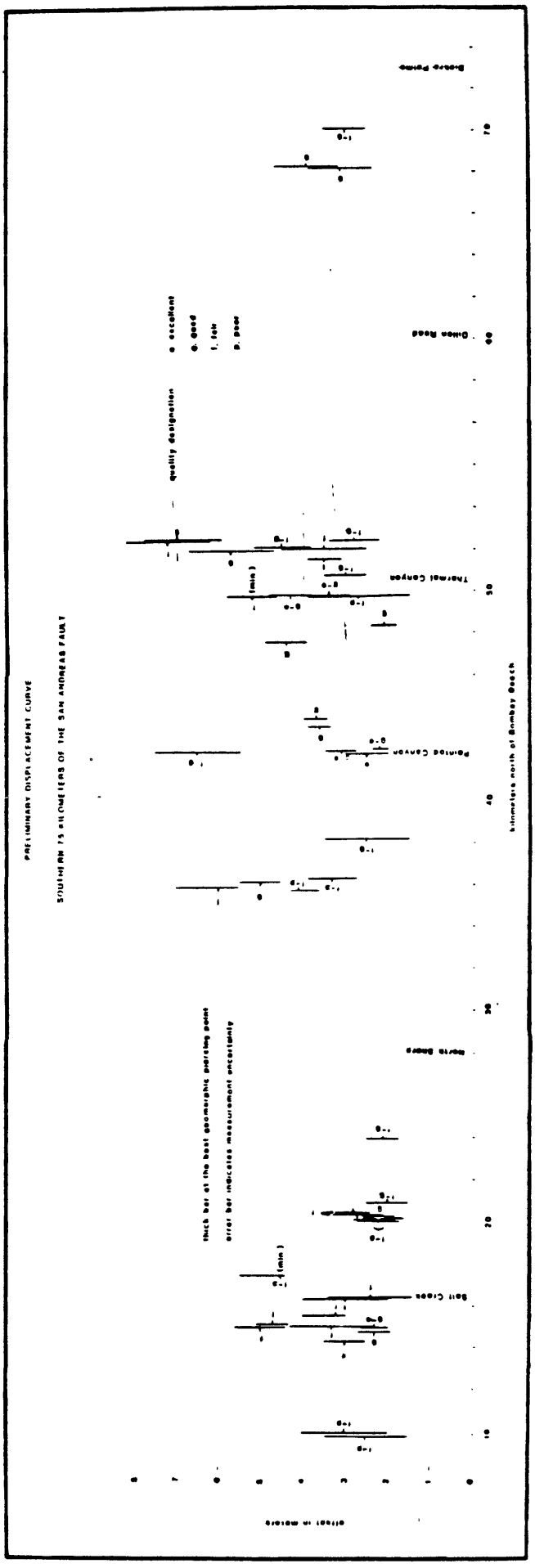
PRELIMINARY DISPLACEMENT CURVE
SOUTHERN 75 KILOMETERS OF THE SAN ANDREAS FAULT
quality designation
e. excellent
g. good
f. fair
p. poor
Bodega Point
Dillon Road
Tomales Canyon
Pointed Canyon
kilometers north of Bombay Beach
Point Reyes
Bolinas
thick bar at the best geometric parting point
error bar indicates measurement uncertainty
offset in meters

Figure 3.

SAN ANDREAS FAULT AT LAKE CAHUILLA SHORELINE.

EXPLANATION

- 4 — FAULT; DASHED WHERE INFERRED; NUMBERED AS IN TEXT
- FOLD AXES
- MAPPABLE BEDS IN PLEISTOCENE UNIT
- CONTACTS
- TRENCHES (13-1)

LATE HOLOCENE

- POST-LAKE
  - CANAL EMBANKMENTS
  - ALLUVIUM AND AEOLIAN DEPOSITS
- —1700 A.D.—
- LATEST FIVE LAKES
  - SILT, CLAY, AND FINE SAND (EMBAYMENT FACIES)
  - COARSE SAND AND GRAVEL (BAR FACIES)
- ~5000 YRS B.P.

PLEISTOCENE(?)

- FLUVIAL SANDS AND GRAVELS (PALM SPRING FORMATION?)
- RED CLAY (FAULT GOUGE?)

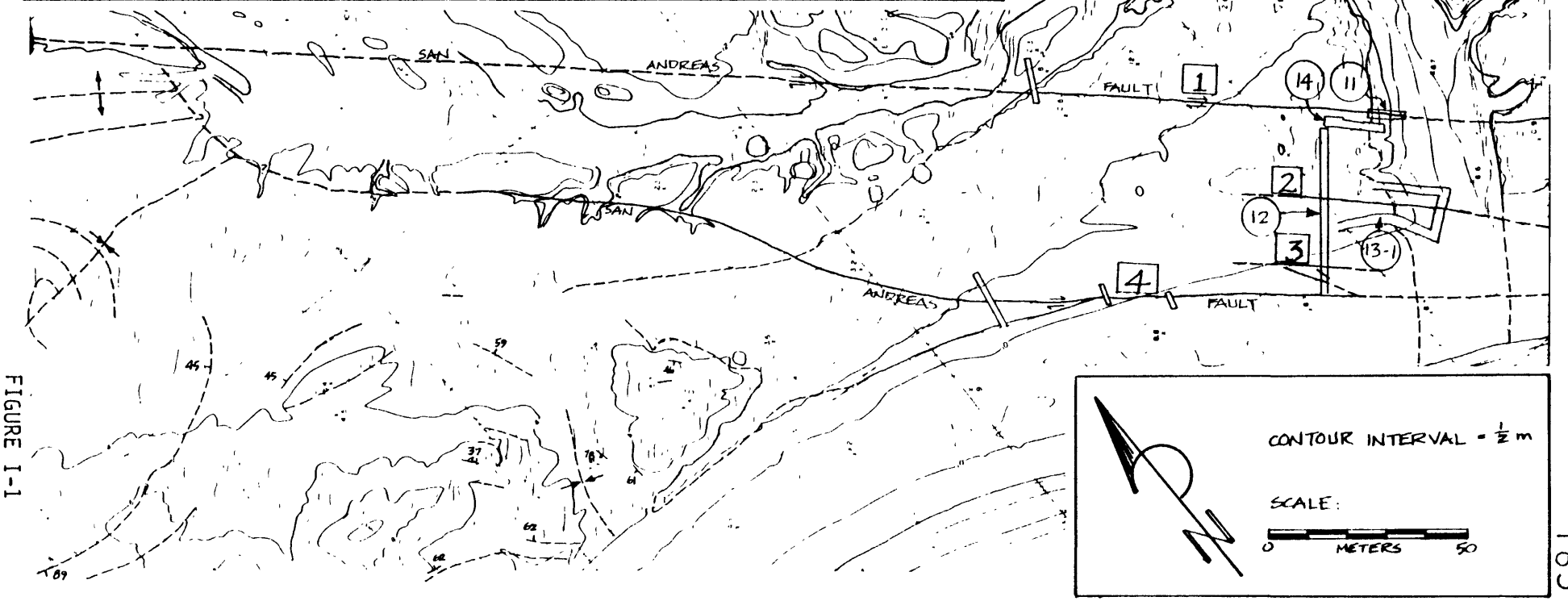

FIGURE I-1

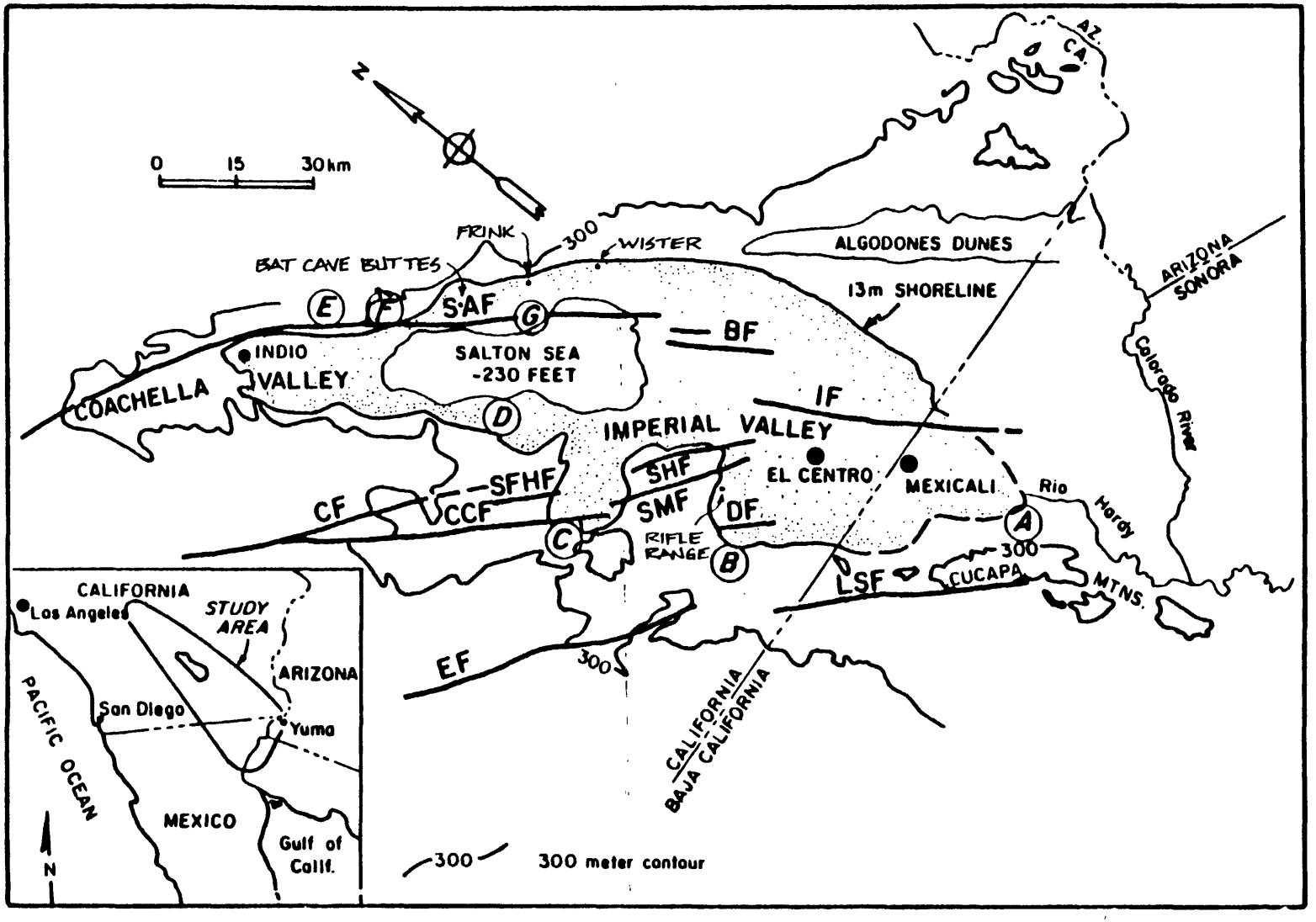

Figure IV-1. Index map of the Imperial and Coachella Valleys showing the major faults and localities mentioned in the text. The faults are named as follows: IF=Imperial fault; BF=Brawley fault; LSF=Laguna Salada fault; SHF=Superstition Hills fault; SMF=Superstition Mountain fault; EF=Elsinore fault; CCF=Coyote Creek fault; CF=Clark fault; SFHF=San Filipe Hills fault; SAF=San Andreas fault. Stipple shows the extent of ancient Lake Cahuilla. The capital letters A through G (clockwise around trough with A at Cerro Prieto) indicate localities mentioned in the text.

Table I–2. Best Estimates for Timing of Lake Cahuilla Activity

Event	Date
Desiccation of latest lake[1]	before 1720
Filling of latest lake[2]	between 1630 and 1700
Penultimate lake full[2]	between 1435 and 1539
Filling of penultimate lake[2]	between 1390 and 1455
Dessication of 3rd lake back[1]	between 1280 and 1420
3rd lake full[2]	between 1210 and 1320 or 1370 and 1385
4th lake full[2]	about 600
Dessication of 5th lake back	before 2550 B.C.

[1] Lake surface below level of Indio Site

[2] Lake surface above level of Indio Site

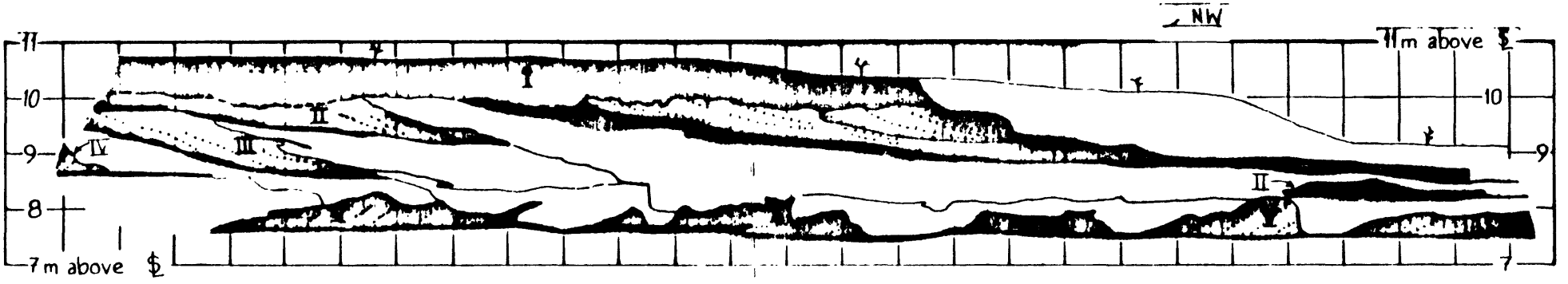

Figure I-2. Highly simplified cartoon of exposed sediments in excavation #13-1 (see Fig. I-1 for location) within and parallel to San Andreas fault zone east of Indio. Lake deposits are shaded (black: bottomset beds; gray: foreset and topset beds) and labelled I to V (from youngest to oldest). Lake I filled between 1630 and 1700 A.D. Lake II filled between 1390 and 1455 A.D. Lake III filled between 1210 and 1320 A.D. Lake IV filled in about 600 A.D. and Lake V filled prior to 2550 B.C. Unshaded beds are fluvial and aeolian deposits laid down during periods of lake dessication.

TRENCH 11, EXPOSURE 6.37

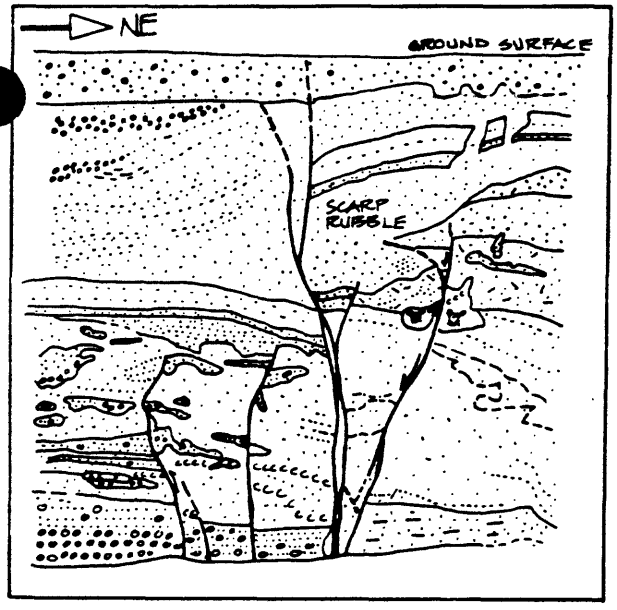

Figure I-4. Various exposures of faulted lake and channel beds at the Indio site.

A. Major disruption of penultimate lake beds in lower left quadrant is buried by unfaulted bottomset beds of latest lake. Fault in center postdates latest lake.

B. Major disruption of channel deposits in lower left quadrant is capped by unfaulted bottomset beds of latest lake. In upper right quadrant, movement on dipping fault resulted in collapse of penultimate lake sands and formation of scarp rubble, which is buried by bottomsets of latest lake. Central fault postdates latest lake beds.

C. Cut parallel and immediately southwest of fault 2 of Figure I-1 displays penultimate and latest lake sediments and superjacent and subjacent channel deposits. See text for discussion.

TRENCH 11, EXPOSURE 8.66

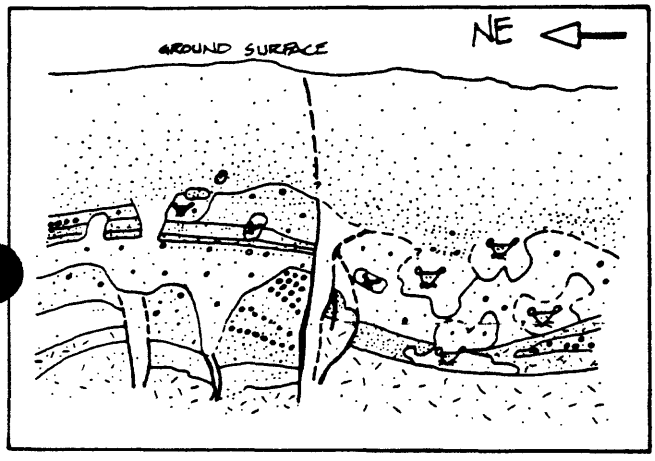

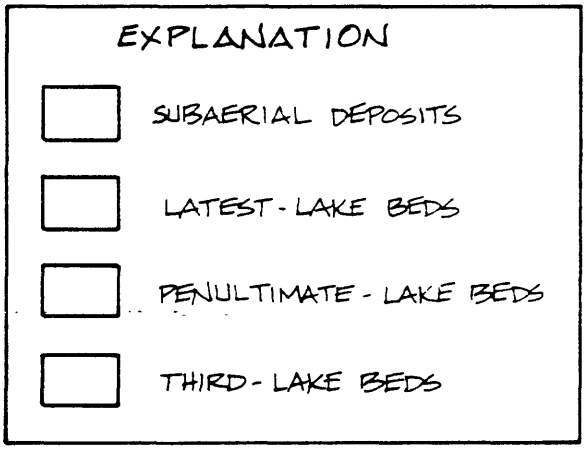

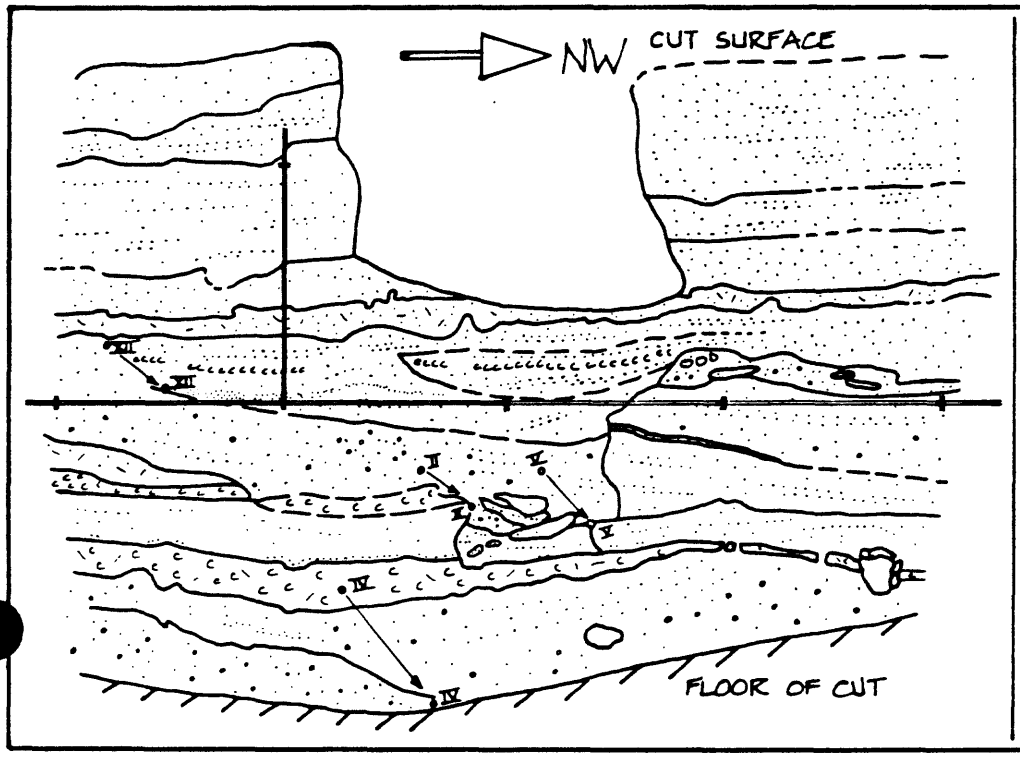

PIERCING POINT	HORIZ. SLIP	VERT. SLIP
XII	12 cm	10 cm
II	11 cm	10 cm
V	13 cm	11 cm
IV	21.5 cm	29 cm

TRENCH 13, EXPOSURE 3v

15

NW

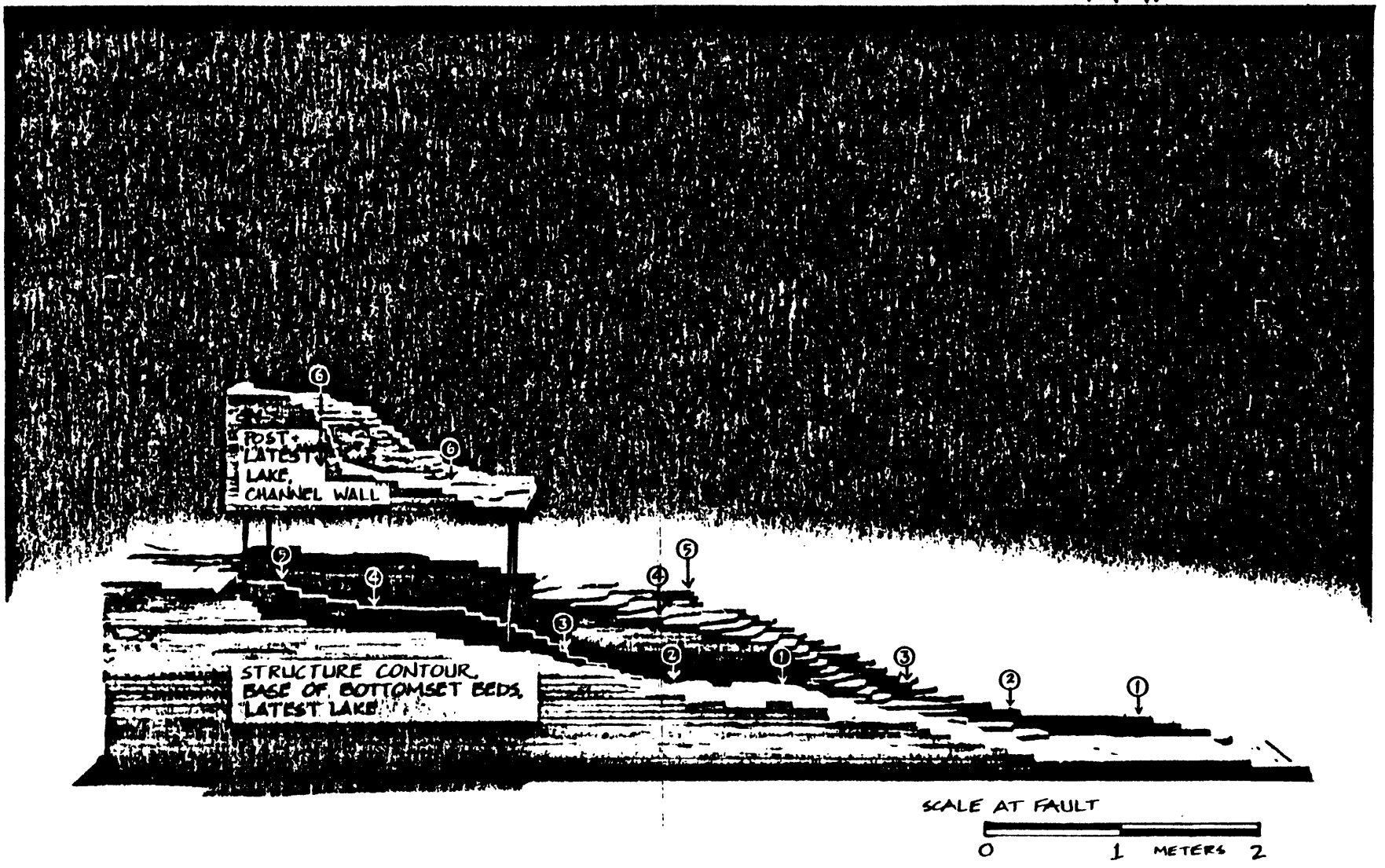

Figure I-5. Balsa models of structure contours drawn on two surfaces offset by fault 1 at site 11 at Indio. Bottomset beds of latest lake are offset about 2.7m, about 1.7m of which occurred during an earthquake in about 1680 A.D. Channel wall of latest lake has been offset about 1 meter since dessication of latest lake. Actual piercing points are not visible in upper model on block nearest viewer because of viewing angle. Circled numbers and arrows indicate offsets.

Table I–3. Offsets Recorded at the Indio Site

FAULT TRACE	1		2		3	4
EVENT	H	V	H	V		
post–1700 A.D.	1 m	0.10 m	0.03 m	0	**	**
~1680 A.D.	1.7 m	0.15	0.10	0.12	**	**
~1550 A.D.	yes*	*	0.10	0.18	**	**
~1250 A.D.	*	*	*	*	**	**
~600 A.D.	*	*	*	*	yes**	**

H = horizontal offsets

V = vertical offsets

* indicates data I expect to collect in 1985.

**indicates data I expect to collect in 1986.

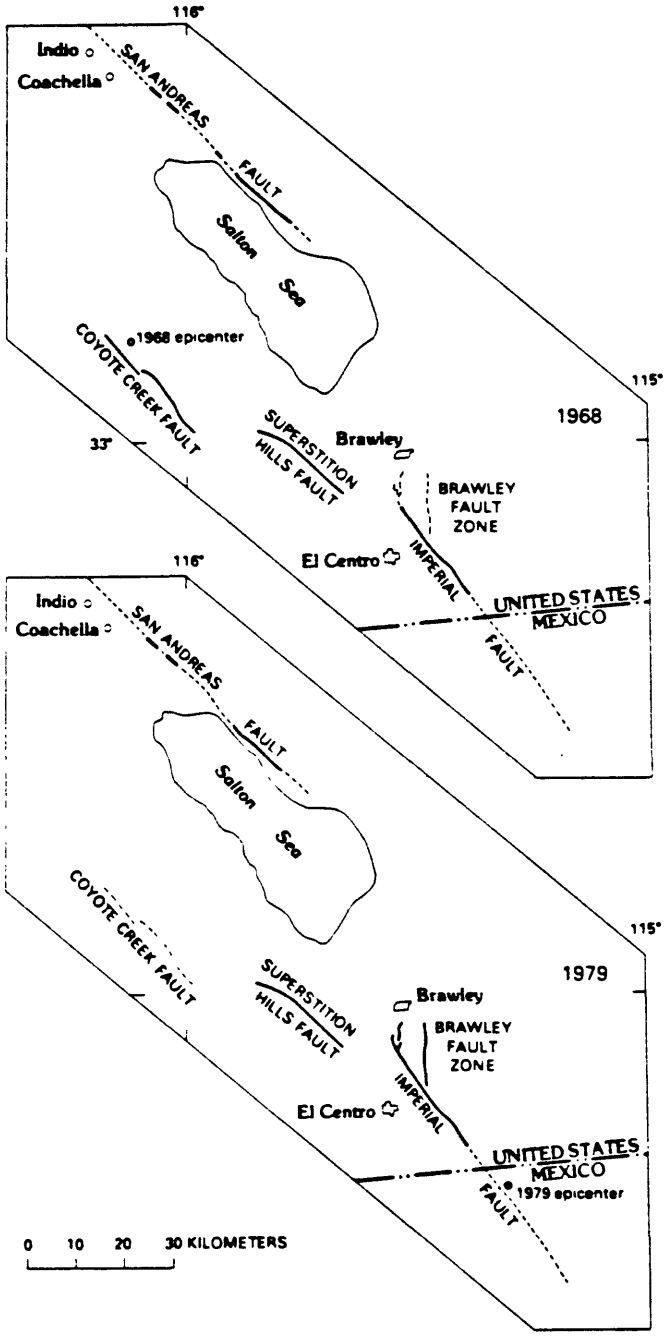

FIGURE 117.—Comparison of slip triggered in 1968 and 1979. In 1968, seismic movement along Coyote Creek fault triggered slip along parts of San Andreas, Superstition Hills, and Imperial faults (heavy lines). In 1979, triggered slip on heavy-lined sections of Superstition Hills and San Andreas faults was associated with seismic rupture on Imperial fault and in Brawley fault zone.

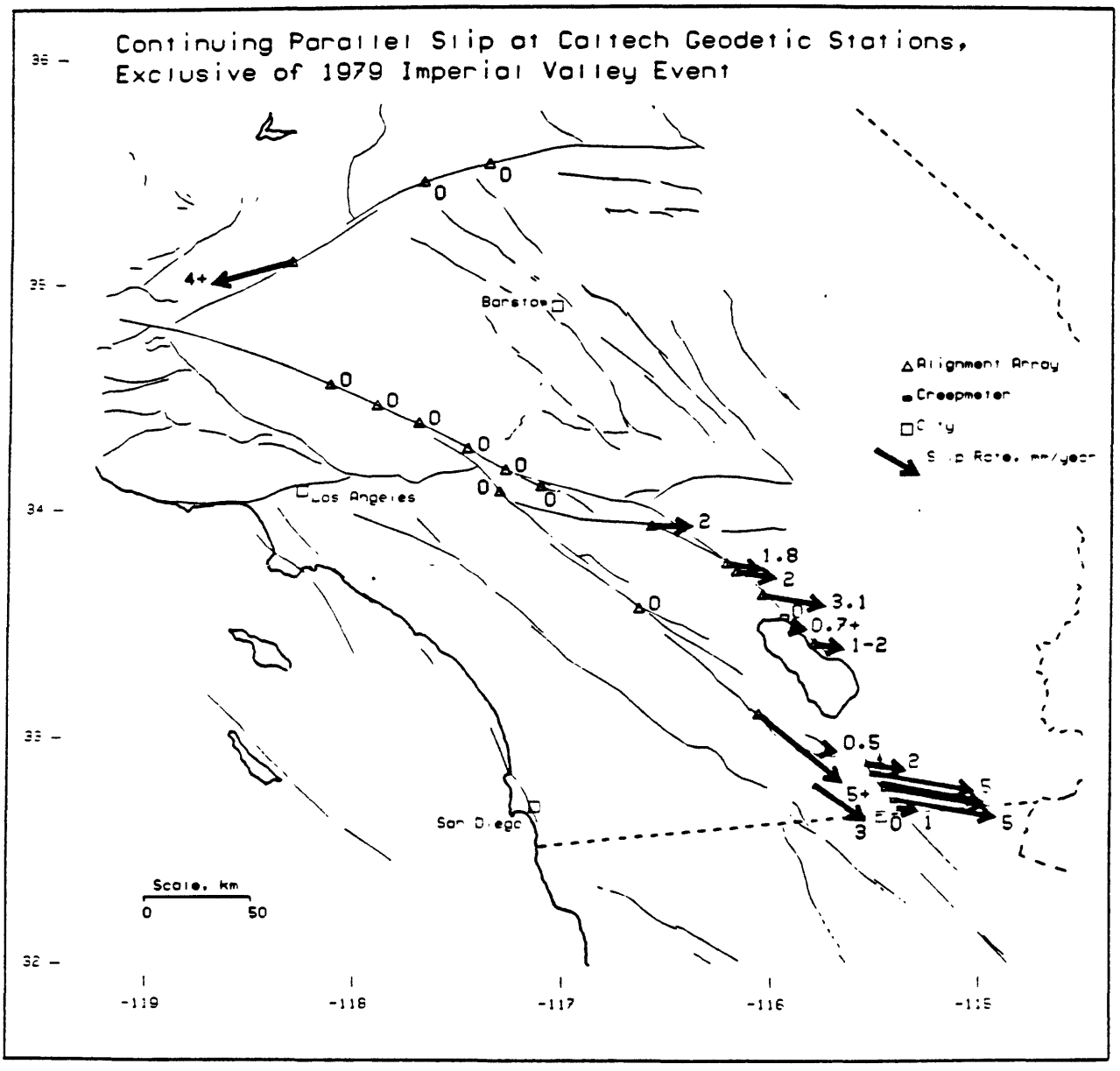
Continuing Parallel Slip at Caltech Geodetic Stations,
Exclusive of 1979 Imperial Valley Event
36 –
35 –
34 –
33 –
32 –
-119
-118
-117
-116
-115
Barstow
Los Angeles
San Diego
Alignment Array
Creepmeter
City
Slip Rate, mm/year
Scale, km
0
50
4+
0
2
1.8
3.1
0.7+
1-2
0.5
5+
3
1
5

Fig 9

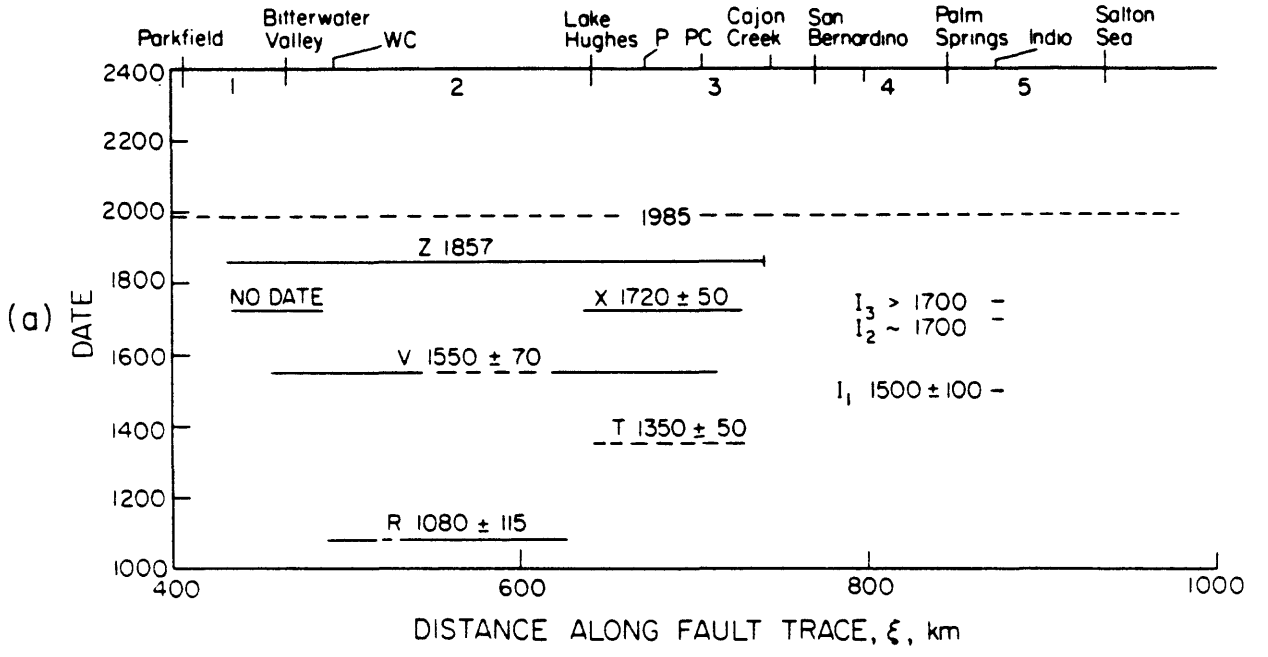
Parkfield
Bitterwater Valley
WC
Lake Hughes
P
PC
Cajon Creek
San Bernardino
Palm Springs
Indio
Salton Sea
1
2
3
4
5
2400
2200
2000
1800
1600
1400
1200
1000
1985
Z 1857
NO DATE
X 1720 ± 50
V 1550 ± 70
T 1350 ± 50
R 1080 ± 115
I_3 > 1700
I_2 ~ 1700
I_1 1500 ± 100
(a)
DATE
400
600
800
1000
DISTANCE ALONG FAULT TRACE, ξ, km

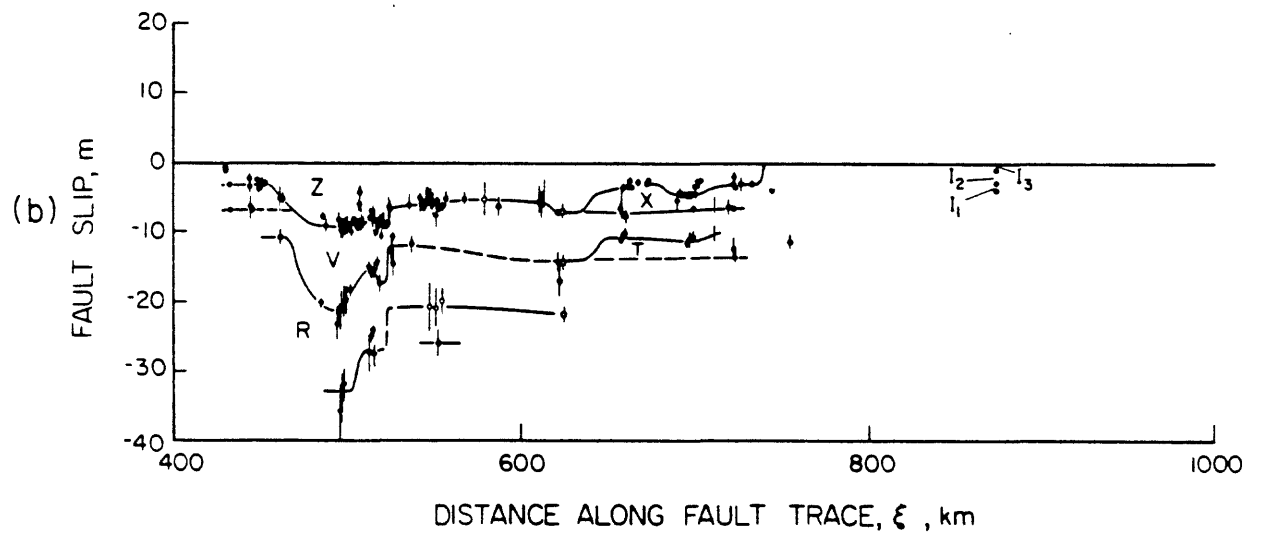
(b)
FAULT SLIP, m
20
10
0
-10
-20
-30
-40
Z
X
V
T
R
I_2
I_3
I_1
400
600
800
1000
DISTANCE ALONG FAULT TRACE, ξ , km

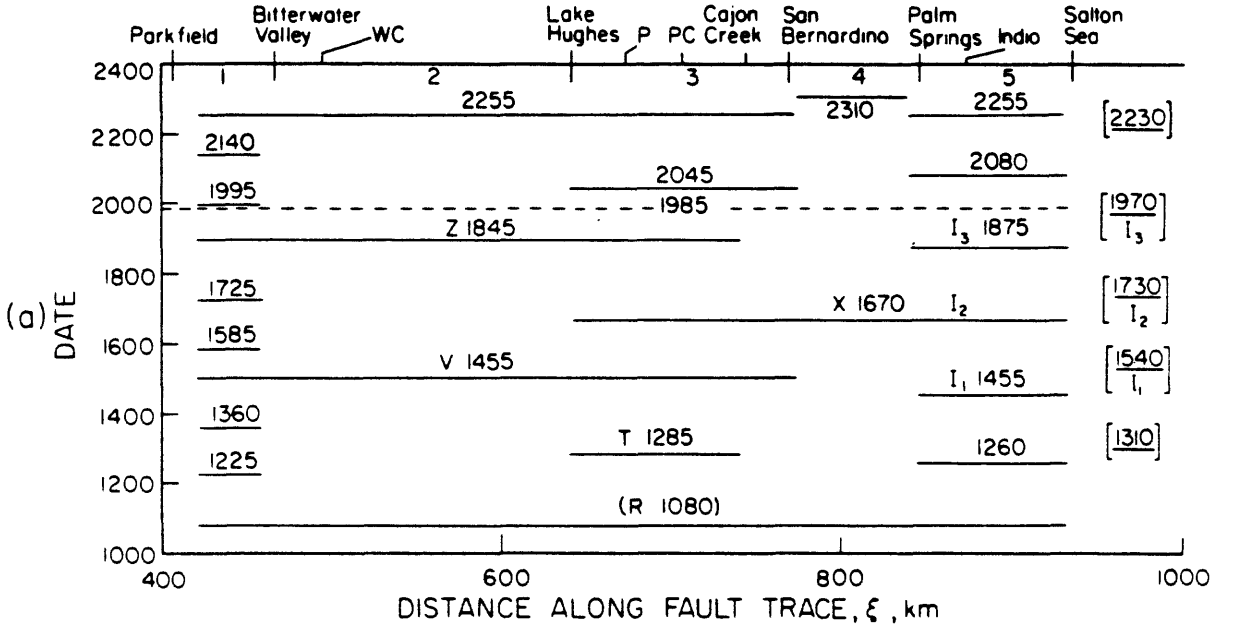
Parkfield
Bitterwater Valley
WC
Lake Hughes
P
PC
Cajon Creek
San Bernardino
Palm Springs
Indio
Salton Sea
1
2
3
4
5
2255
2310
2255
[2230]
2140
2045
2080
1995
1985
[1970/I3]
Z 1845
I3 1875
1725
X 1670
I2
[1730/I2]
1585
V 1455
[1540/I1]
I1 1455
1360
T 1285
1260
[1310]
1225
(R 1080)
(a)
DATE
2400
2200
2000
1800
1600
1400
1200
1000
400
600
800
1000
DISTANCE ALONG FAULT TRACE, ξ, km

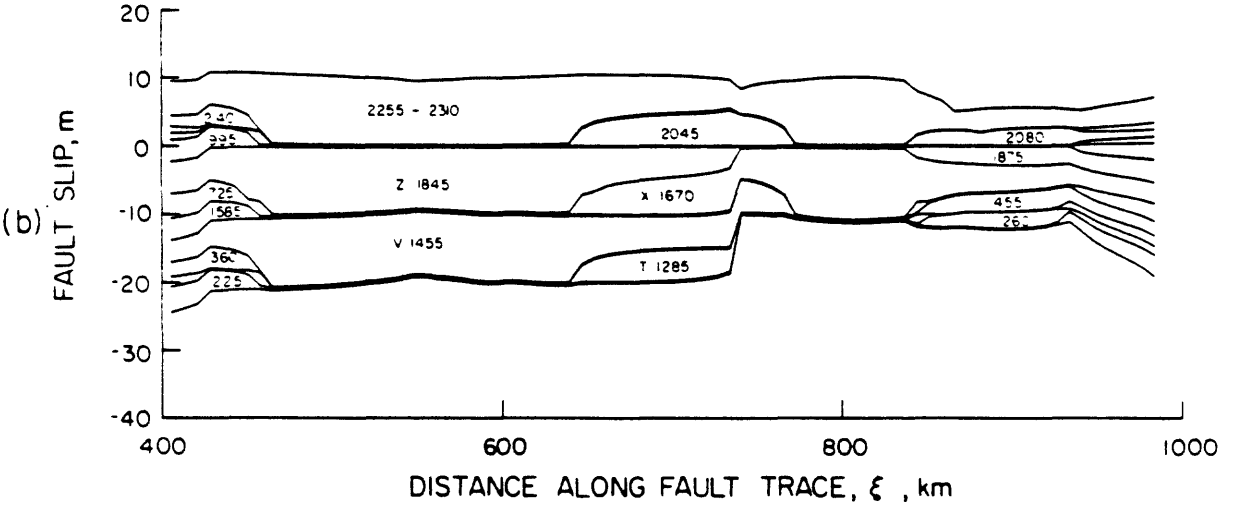
(b)
FAULT SLIP, m
20
10
0
-10
-20
-30
-40
2255 - 2310
2045
2080
Z 1845
X 1670
V 1455
T 1285
400
600
800
1000
DISTANCE ALONG FAULT TRACE, ξ, km

Fig. 6

SEISMIC DEFORMATION ALONG THE SOUTHERN SAN ANDREAS FAULT:

Implications for Rotational Block Tectonics.

Craig Nicholson, Leonardo Seeber, Pat Williams,

and *Lynn Sykes*

Lamont-Doherty Geological Observatory

Abstract

The pattern of microseismicity in southern California indicates that much of the activity is presently occurring on secondary fault structures. Near the intersection of the San Jacinto and San Andreas faults, these secondary structures exhibit predominantly left-lateral strike-slip motion, and, in conjunction with both normal and reverse faulting earthquakes, suggests a series of small crustal blocks undergoing contemporary clockwise rotation as a result of regional right-lateral shear. Other left-lateral faults have been identified in adjacent areas from geologic and seismologic data. Many of these structures predate the modern San Andreas system and may control the pattern of strain accumulation in southern California. Thus, although the total slip along these secondary structures is small, they may affect where large earthquakes nucleate and the characteristic length of large earthquake ruptures. A complete description of what these structures are, and how they interact, may prove critical to any fundamental understanding of the earthquake process and any realistic assessment of the regional seismic hazard.

Introduction

One of the more enigmatic features of southern California seismicity is the lack of correlation between present activity and the major through-going faults [Allen *et al.*, 1965; Allen, 1981]. This is particularly true for those segments responsible for the largest earthquakes (*e.g.*, the 1857 fault rupture), as well as for the southern San Andreas fault; even though these faults are known to be accumulating strain at the rate of centimeters per year. Only the San Jacinto fault, Brawley fault, and the creeping section of the San Andreas are well defined on the basis of present seismicity. There do appear, however, to be many earthquakes on secondary structures, many of which are oriented orthogonal to the strikes of the major faults [Nicholson *et al.*, 1984]. Considering the abundance of this secondary activity, a framework is needed in order to understand the structures at depth responsible for the earthquakes and to determine what relation the present pattern has to the seismic behavior of the major fault strands.

We therefore began a systematic examination of the geologic and geophysical evidence in an attempt to resolve the exact nature of some of these active secondary structures. The procedure was to invert arrival-time data from microearthquakes for local velocity structure and accurate earthquake hypocenters. Focal mechanism solutions were then analyzed for internal consistency with the orientation of the resulting structural elements defined on the basis of the hypocenter alignments. This permitted a qualitative description of the overall kinematic pattern controlling fault interaction and the discrimination between various tectonic models for the contemporary deformation of southern California [*e.g.*, Bird and Rosenstock, 1984; Luyendyk *et al.*, 1985; Weldon and

Humphreys, 1985].

Our initial study involved only a small segment of the San Andreas, where the fault begins to make its "big bend". This segment lies between the San Bernardino Mountains and the San Jacinto Mountains, and includes San Gorgonio Pass (SGP) and the intersection of the San Andreas with the San Jacinto fault (Fig. 1). It is an area characterized by a complex surface geology, intersecting right- and left-lateral faults, high topography as a result of recent uplift, and one of the highest levels of deep seismicity (>20 km) anywhere along the entire San Andreas [Allen, 1957; Meisling, 1984; Corbett and Hearn, 1981]. Microearthquakes show a wide range of focal mechanism solutions [Green, 1983], and waveforms on seismograms suggest high stress drops [Frankel and Kanamori, 1983]. These indicators imply a region of high strength under unusually high stress [*e.g.*, Sibson, 1984], and as a consequence, one of the highest potentials for initiating a large earthquake rupture. Failure of this segment could then result in an earthquake that would not stop until it stretched from as far north as Palmdale to as far south as the Salton Sea (Fig. 1, C-D).

Summary of Results

Using data supplied by the southern California seismic network, we found that although this area is unusually seismogenic, very few earthquakes were occurring in the upper 5 km, or could be directly associated with any of the major through-going faults. Instead, an active system of relatively short left-lateral faults striking north-east to east-west was identified for earthquakes between focal depths of 5 and 10-12 km. This pattern of deformation, in conjunction with an unusual set of both normal and reverse faulting earthquakes, suggested a series of small rigid blocks undergoing clockwise rotation as a result of regional right-lateral shear (Fig. 2). The normal and reverse faulting earthquakes represent the corners of the blocks rotating into or away from the sides of the major bounding faults. If valid, this is the first study to identify blocks undergoing contemporary rotations - rotations that are more commonly identified on the basis of paleomagnetic work and only for much longer time scales.

Other earthquakes that show left-lateral slip on north-east trending structures include several events along sub-parallel features located west of the San Jacinto fault and first identified by Hadley and Combs [1974] (focal mechanism A in Fig. 2). Each of these structures, as well as the northeast trend of earthquakes located under the town of San Bernardino (focal mechanism H in Fig. 2), corresponds to a known vertical aquiclude affecting ground-water migration in the sediments of the San Bernardino valley [Dutcher and Garrett, 1963]. Where these structures intersect the San Jacinto and San Andreas faults, hot springs and thermal wells are evident that are relatively rare for other sections of the San Andreas system [Jennings, 1975]. Thus, motion along these presumed fault structures must have been sufficient to generate a clay fault gouge capable of acting as an effective water barrier. This implies that although these fault segments are relatively short, they may still constitute a significant seismic hazard to the local population. In fact, intensity data suggests that the 1923 magnitude 6¼ earthquake may have actually occurred along the fault segment that parallels the Santa Ana river (focal mechanism G in Fig. 2) rather than along the San Jacinto fault where it is presumed to be located [Laughlin *et al.*, 1923; Toppozada *et al.*, 1982]. If this earthquake did in fact occur along one of these secondary structures, then the northern section of the San Jacinto fault has not experienced a large earthquake since 1899, and so is more highly susceptible to an earthquake rupture in the near future.

Further east, between the Banning and Mission Creek faults, another set of earthquakes occur that also appear to exhibit left-lateral slip on north-east trending features (Fig. 3). These events align along sub-parallel trends that dip steeply to the south and agree quite well with the orientation of the north-east striking nodal plane seen in the composite focal mechanism solution. Slip along the *en echelon* northeast planes would be left-lateral, but with a larger component of reverse faulting. This type of deformation matches the long-term history of the Pinto Mountain and Morrango Valley faults with which these events align, and may indicate that slip along these features may have at one time extended across the Mission Creek fault. Such high-angle reverse faulting has been previously observed in the shallow surface sediments of San Gorgonio Pass [Allen, 1957], although most of the deformation more closely corresponds to slip along right-lateral strike-slip and shallow-angle thrust faults [Matti and Morton, 1983].

An interesting feature of all this seismicity is that those earthquakes exhibiting left-lateral slip on northeast trends all occur at depths less than ≈10 km (see cross section Fig. 3); suggesting that what ever mechanism is controlling this behavior, it is primarily restricted to shallow depths. Furthermore, if these left-lateral faults are the result of small crustal blocks that are currently rotating then this presupposes a detachment surface at depth, decoupling the blocks, and allowing rotational movement. Regional mid-crustal detachments or ductile shear zones have been suggested based on the occurrence of large earthquakes at depth with shallow-angle nodal planes [Webb and Kanamori, 1985], by the regional pattern of teleseismic travel-time residuals [Hadley and Kanamori, 1977], and by the finite elastic thickness of the upper crust [Turcott *et al.*, 1984]. If a detachment is present, then the possibility exists that the geology and/or the deformation observed at the surface is different from the deformation at depth.

In fact the microearthquakes below 10-12 km are distinctly different from those above. At greater depths, regional north-south shortening resulting from the collision of the San Jacinto Mountains with the San Bernardino Mountains, was found to be accommodated by a combination of strike-slip faults interbedded between a series of subparallel shallow-angle thrust faults dipping to the north (Fig. 4). Determinations of velocity structure from the earthquake arrival times also indicate a possible low-velocity layer at about 10 km depth under the San Bernardino Mountains but not under the San Jacinto Mountains [Nicholson and Simpson, 1985]. This is about the same depth as the transition between the block rotations and the deeper deformation, and suggests the overthrust San Bernardino Mountains are allochthonous. Regional gravity data and the distribution of P_g velocities also support this interpretation [Hearn and Clayton, 1984].

Discussion and Conclusions

If these results have applications elsewhere along the San Andreas system, it provides several new concepts for understanding the kinematic behavior and fault tectonics for southern California. Shallow-angle structures like detachments need to be examined, and in the analysis of regional strain data rotations must be considered. The elastc behavior of the crust may thus strongly dependent on the nature of any pre-existing fabric and the depth to either a decollment or ductile shear zone. More important, the pattern of deformation presently observed during the interseismic period differs from the type of deformation expected to take place during a large earthquake. Current seismicity cannot then be used to extrapolate the effects of a large event on various segments of the San Andreas, since large earthquakes are the result of right-lateral slip along major faults, whereas much of the present activity is on secondary

faults, some of which are accommodating left-lateral motion as a result of block rotation.

As blocks rotate, the level of normal stress may increase or decrease along strike as block corners rotate into or away from the sides of the major bounding faults. This increased or decreased level of normal stress may account for the alternating pattern of high and low levels of earthquake activity seen along strike of some of the major fault strands (*e.g.*, the San Jacinto fault). Block dimensions may also control the characteristic size of earthquake ruptures. An example would be the northeast trend of left-lateral earthquakes located near the Mission Creek branch of the southern San Andreas and just south of the Pinto Mountain fault [Williams *et al.*, 1984]. These events defined a series of *en echelon* faults and separate the aftershocks of the 1947 Morrango Valley earthquake from those of the 1948 Desert Hot Springs event. Where large earthquakes nucleate may also be controlled by where blocks come together, and faults intersect [*e.g.*, Jones, 1984]. The result is often a cross-pattern of either foreshocks or aftershocks, as in the case of the Borrego Mountain earthquake of 1968, the Homestead sequence of 1979, or the Manix earthquake of 1947. The regional pattern of strains and tilts is also likely to reflect the block nature of the crust [Bilham and Beavan, 1979].

Detailed mapping of the geologic structures in southern California reveal a number of shallow-angle thrust surfaces and left-lateral faults much like those suggested by the seismicity [Engel and Schultejann, 1984]. Many of these structures pre-date the development of the modern San Andreas system. If these older structures are effectively segmenting southern California into discrete crustal blocks, then efforts must be made to determine the extent to which these blocks are involved in the overall seismic deformation of southern California.

The seismic data examined so far require neither large rotations nor large left-lateral displacements, but if rotations persist and eventually accumulate with time, then large deflections from the paleomagnetic pole would be expected. Luyendyk *et al.* [1985] summarize most of the available paleomagnetic data for southern California. They show that for large parts of southern California large clockwise deflections are in fact observed in deposits of Neogene and Quarternary age (Fig. 5). Previous models used to explain these observations typically invoke large rotations of large rigid blocks. If however these measurements are the result of simple shear involving only small crustal blocks, wedges, or slices, then both the paleomagnetic data are satisfied, and many of the geologic contradictions caused by large rigid block rotation are avoided. These data thus imply that large rotations induced by tectonic shear do occur and are closely coupled to the wrench fault environment of the San Andreas system.

How long this particular pattern of kinematic behavior will persist in time is uncertain. The present pattern may only characterize the interseismic period and may change as this region prepares to accommodate large earthquake ruptures. Should this change be systematic, then there is a higher probability of identifying the precursory change and thereby predicting the impending large earthquake and the occurrence of large right-lateral displacements.

References.

Allen, C.R., San Andreas fault zone in San Gorgonio Pass, southern California, *Geol. Soc. Am. Bull.*, 68, 315-350, 1957.

Allen, C.R. The modern San Andreas fault, in *The Geotectonic Development of California*, W.G. Ernst, ed., Prentice-Hall, Inc., Englewood Cliffs, NJ, 511-534

(1981).

Allen, C.R., P. St. Armand, C.F. Richter, and J.M. Nordquist, Relationship between seismicity and geologic structure in the southern California region, *Bull. Seismol. Soc. Am.*, 55, 753-797, 1965.

Bilham, R.G. and R.J. Beavan, Strains and tilts on crustal blocks, *Tectonophysics*, 52, 121-138, 1979.

Bird, P. and R.W. Rosenstock. Kinematics of present crust and mantle flow in southern California, *Geol. Soc. Am. Bull.*, 95, 946-957 (1984).

Corbett, E.J. and T.M. Hearn, The depth of the seismic zone in the Transverse Ranges of southern California, *presented* at The John Muir Geophysical Society Meeting, 1981.

Dutcher, L.C. and A.A. Garrett. Geologic and hydrologic features of the San Bernardino area, California, *U.S. Geol. Surv. Water-Supply Paper 1419*, 111 pp. (1963).

Engel, A.E.J. and P.A. Schultejann. Late Mesozoic and Cenozoic tectonic history of south central California, *Tectonics*, 3, 659-676 (1984).

Frankel, A. and H. Kanamori. Determination of rupture duration and stress drop for earthquakes in southern California, *Bull. Seism. Soc. Am.*, 73, 1527-1554 (1983).

Green, S.M. Seismotectonic study of the San Andreas, Mission Creek, and Banning fault system, *Master's Thesis*, University of California Los Angeles, 52 pp. (1983).

Hadley, D. and J. Combs. Microearthquake distribution and mechanisms of faulting in the Fontana-San Bernardino area of southern California, *Bull. Seism. Soc. Am.*, 64, 1477-1499 (1974).

Hadley, D. and H. Kanamori. Seismic structure of the Transverse Ranges, California, *Geol. Soc. Am. Bull.*, 88, 1469-1478 (1977).

Hearn, T.M. and R.W. Clayton. Crustal structure and tectonics in southern California (abstract), *EOS Trans. A.G.U.*, 65, 992 (1984).

Jennings, C.W., *Fault Map of California*, Calif. Div. Mines and Geology, 1975.

Jones, L.M. Foreshocks (1966-1980) in the San Andreas System, California, *Bull. Seism. Soc. Am.*, 74, 1361-1380 (1984).

Laughlin, H., R. Arnold and W.S.W. Kew. Southern California earthquake of July 22, 1923, *Bull. Seism. Soc. Am.*, 13, 104-106 (1923).

Luyendyk, B.P., M.J. Kamerling, R.R. Terres and J.S. Hornafius. Simple shear of southern California during the Neogene, *Am. Assoc. Petrol. Geol.*, in press (1985).

Matti, J.C. and D.M. Morton, Earthquake hazard studies, Upper Santa Ana Valley and adjacent areas, southern California, *U.S. Geol. Surv. Open-file Report 83-918*, 17, 24-28, 1983

Meisling, K.E. Neotectonics of the north frontal fault system of the San Bernardino Mountains, southern California: Cajon Pass to Lucerne Valley, *PH.D. Thesis*, California Institute of Technology, 394 pp. (1984).

Nicholson, C., L. Seeber, P. Williams and L.R. Sykes. A new paradigm for understanding southern San Andreas fault tectonics (abstract), *EOS Trans. A.G.U.*, 65, 996 (1984).

Nicholson, C. and D.W. Simpson. Changes in V_p/V_s with depth: implications for appropriate velocity models, improved earthquake locations, and material properties of the upper crust, *Bull. Seism. Soc. Am.*, in press (1985).

Sibson, R.H. Roughness at the base of the seismogenic zone: contributing factors, *J. Geohys. Res.*, **89**, 5791-5800 (1984).

Toppozada, T.R., D.L. Parke, L. Jensen and G. Campbell. Areas damaged by California earthquakes, 1900-1949, *Calif. Div. Mines and Geol. Open-file Report 82-17 SAC*, 65 pp. (1982).

Turcott, D.L., J.Y. Liu and F.H. Kulhawy. The role of an intercrustal asthenosphere on the behavior of major strike-slip faults, *J. Geophys. Res.*, **89**, 5801-5816 (1984).

Webb, T.H. and H. Kanamori. Earthquake focal mechanisms in the Eastern Transverse Ranges and San Emigdio Mountains, southern California, and evidence for a regional decollment, *J. Geophys. Res*, in press (1985).

Weldon, R. and G. Humphreys. A kinematic model of southern California, *Tectonics*, submitted for publication (1985).

Williams, P., C. Nicholson, L. Seeber and L.R. Sykes. Seismicity of the southern San Andreas fault, California (abstract), *EOS Trans. A.G.U.*, **65**, 996 (1984).

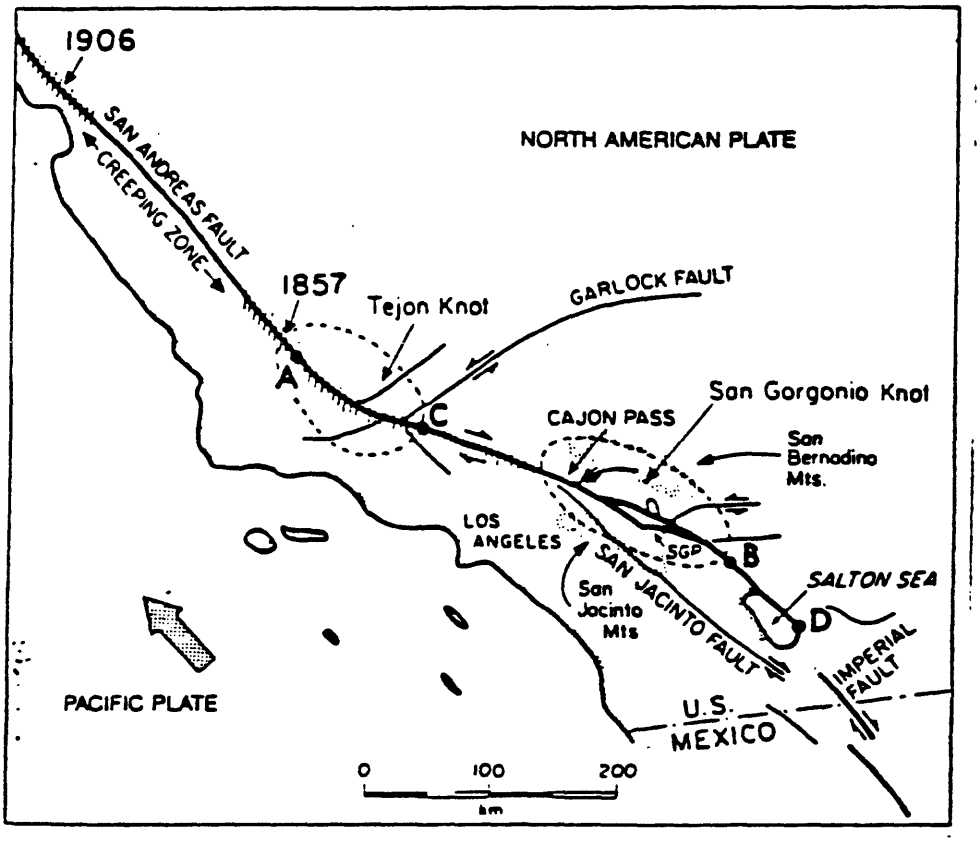

Figure 1. Major faults and earthquake ruptures in Southern California. A-B represents the "big bend" section of the San Andreas fault. The western end (Tejon Knot) broke in 1857 and ruptured as far south as Cajon Pass. The eastern end (San Gorgonio Knot) has not broken since the early 1700's and has a probable repeat time of 300 years. Should this section fail all at once, the potential rupture length of the resulting great earthquake could extend from C to D.

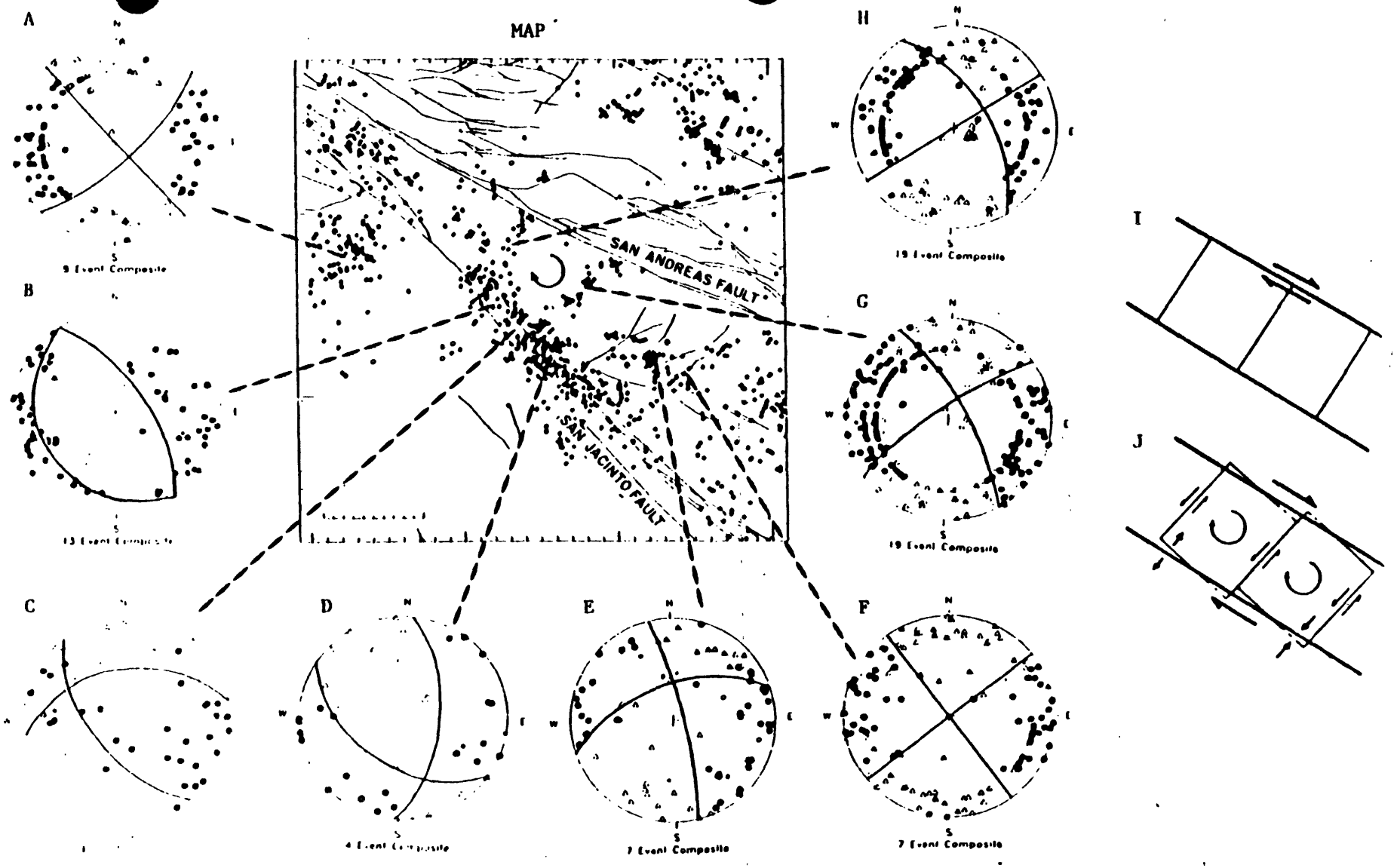

Figure 2. Shallow seismicity used to define rotating blocks near the intersection of the San Andreas and San Jacinto faults - see map. During a large earthquake right-lateral strike-slip motion (I) occurs on one of the major bounding faults; however, during the inter-seismic period, the major faults become locked causing small blocks in between to rotate (J). This produces a pattern of northeast striking left-lateral faults (E-H), between which alternating groups of normal (B&D), and reverse (C) faulting earthquakes occur that match the particular pattern predicted by the model (compare J with map). Focal mechanism diagrams (A-H) are composite upper hemisphere projections; solid symbols are compressions, open symbols are dilatations. Composite A (upper left) represents a set of sub-parallel left-lateral faults previously identified by Hadley and Combs (1974).

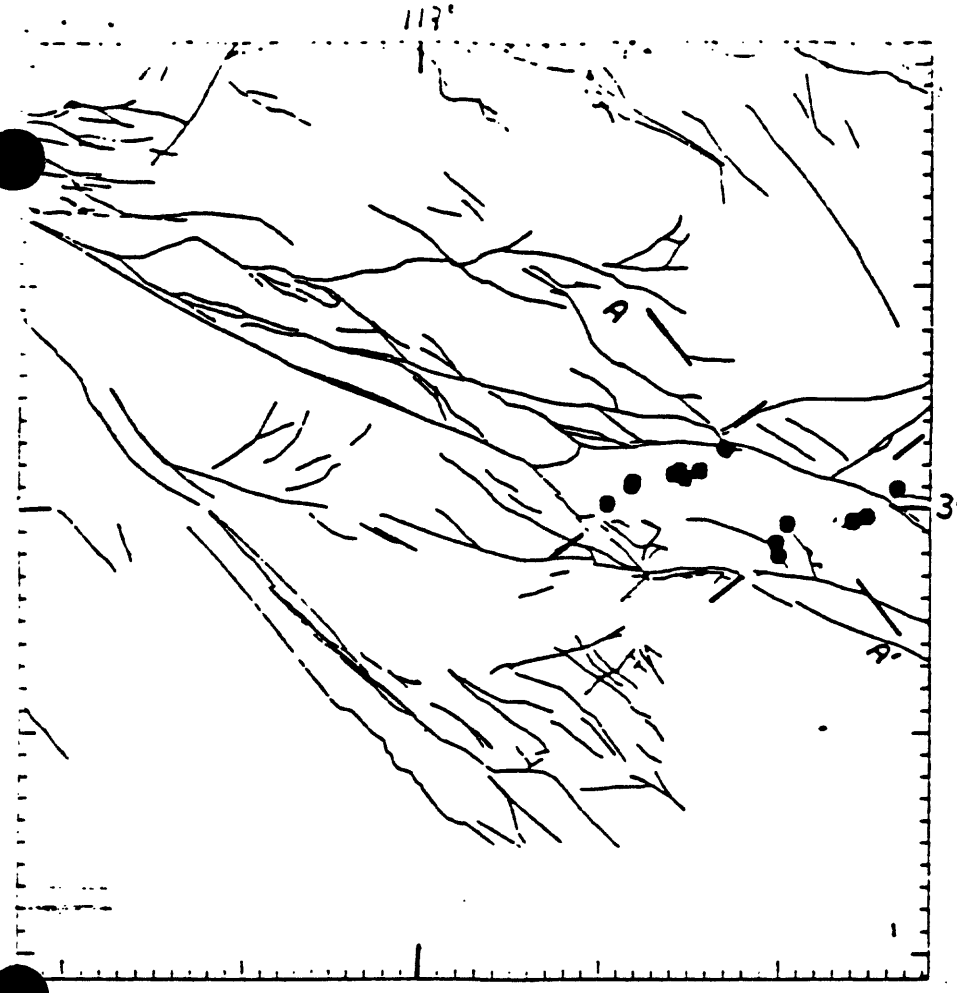

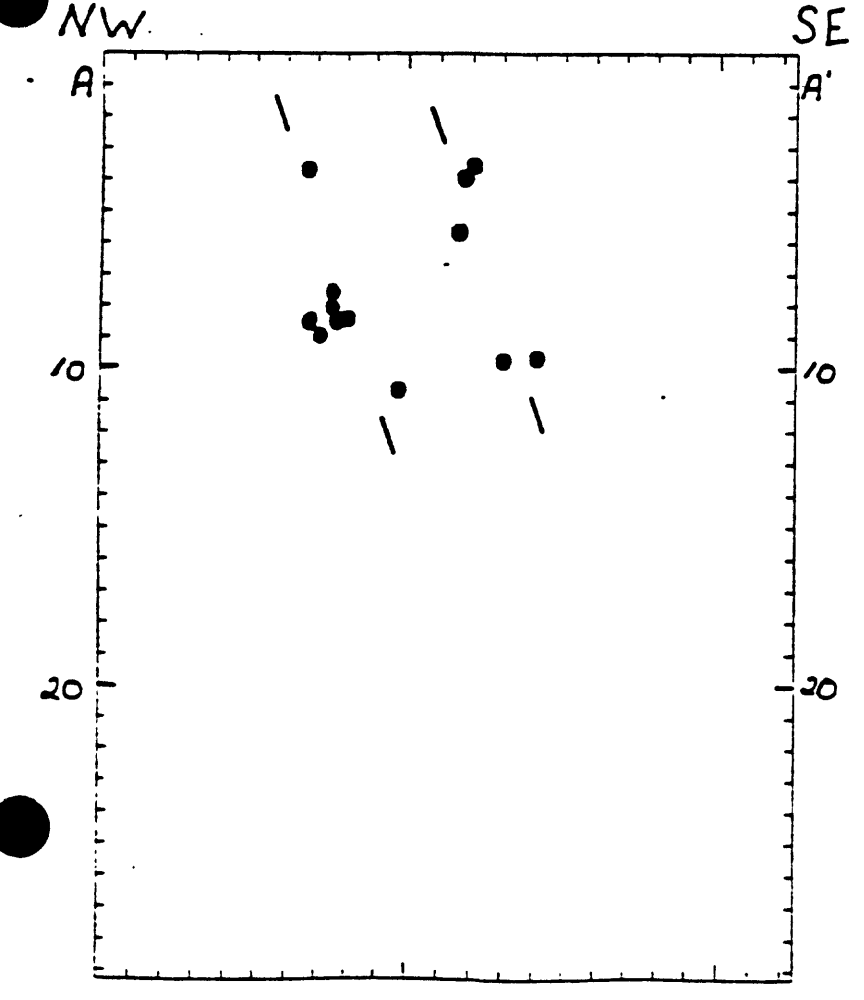

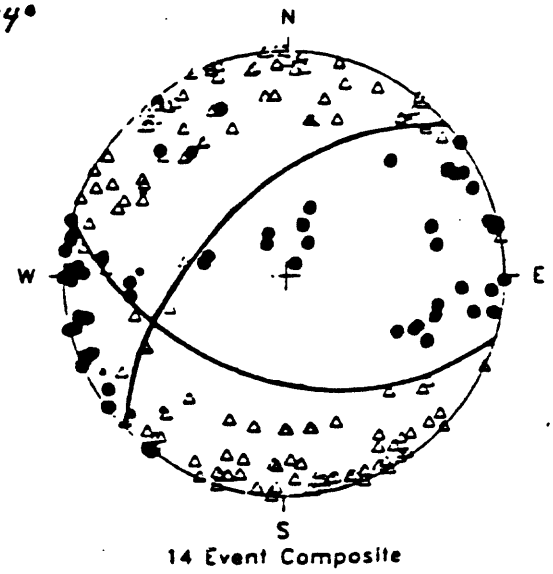

Fig. 3. Map and cross section of events between the Mission Creek and Banning Faults. These earthquakes align along planes that dip steeply to the south and exhibit compressional left-lateral strike-slip motion along northeast oriented nodal planes.

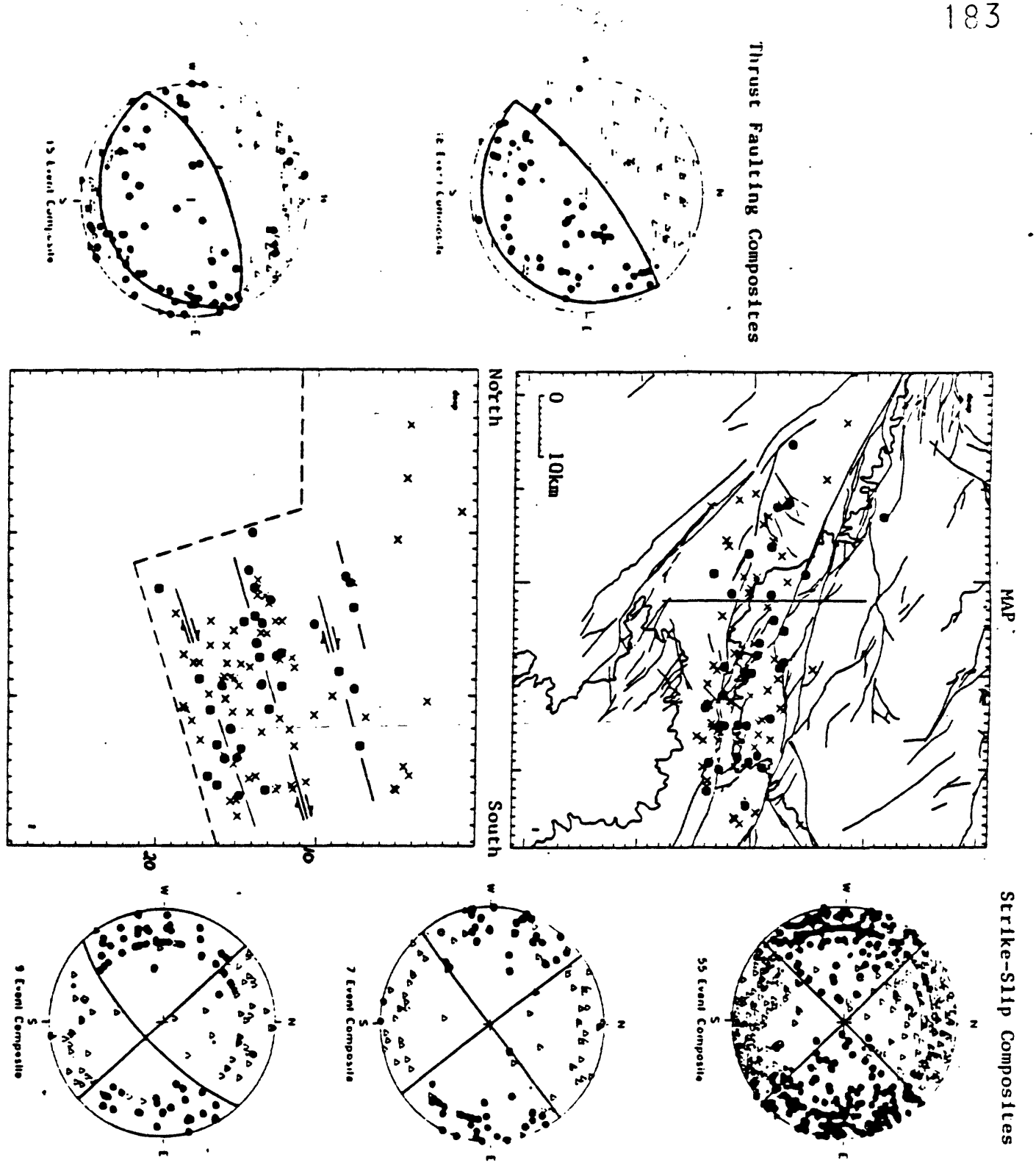

Figure 4. Map and cross section of the predominately deeper strike-slip (X's) and shallow-angle thrust events (solid circles) near San Gorgonio Pass. The thrust earthquakes define a series of planes that dip to the north and parallel the shallow-dipping interface that defines the base of the seismogenic zone (dashed line) and match the shallow-angle nodal plane seen in the composite focal mechanisms shown at left. The seismicity shows a wedge-shaped volume internally deforming as a result of north-south shortening between the San Bernardino Mts to the north and the San Jacinto Mts to the south. Contours are elevations above 3,000 feet.

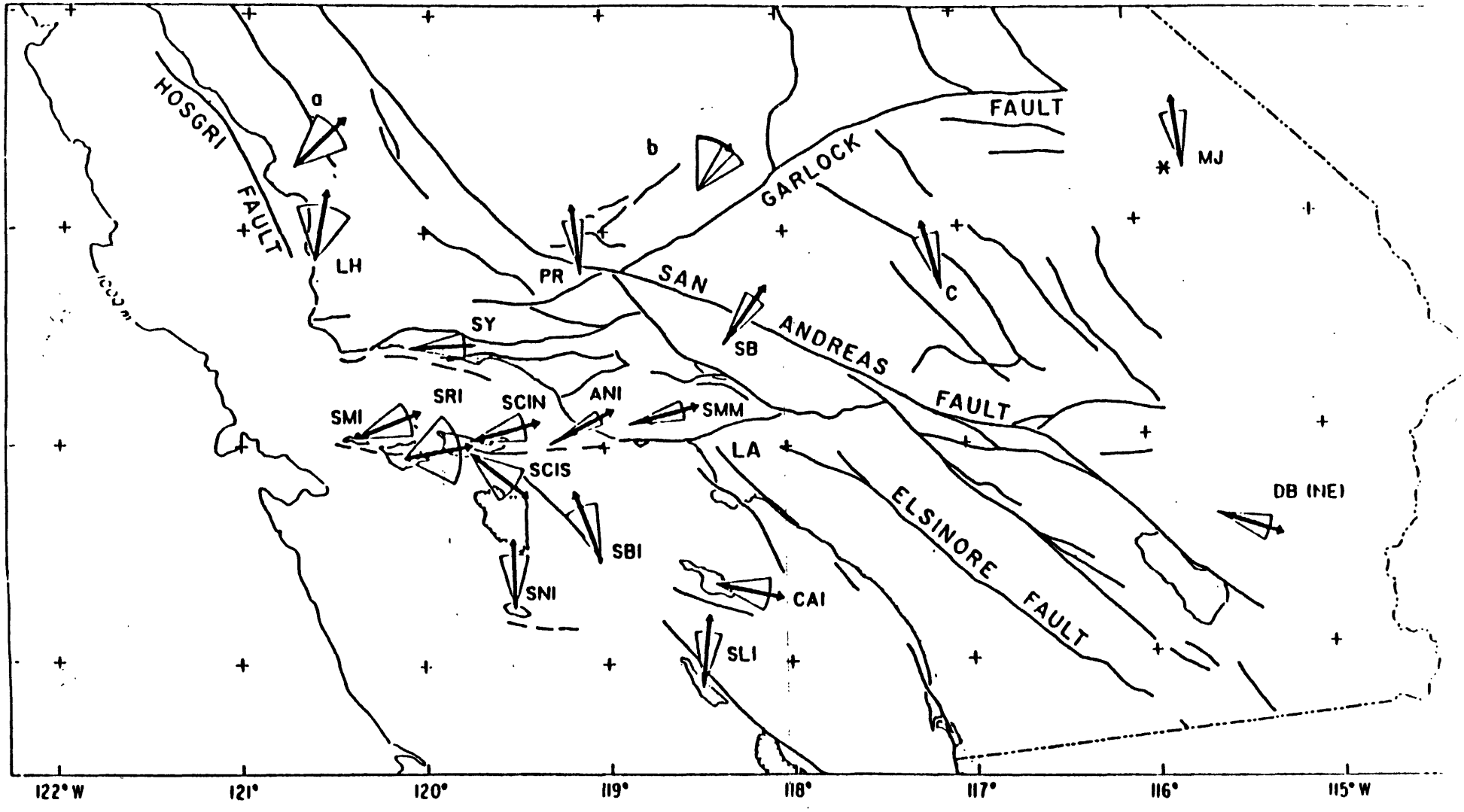

Figure 5. Paleomagnetic declinations measured in Neogene age rocks (about 13 m.y.) at sites throughout southern California. The mean declination at the site is shown along with the 95% confidence limit. Faults are from Jennings (1975). See Luyendyk et al. (1985) for more specific information and site keys.

1st Draft

BLOCK/FAULT ROTATION IN GEOLOGIC AND INTERSEISMIC DEFORMATION

by L. Seeber and C. Nicholson
Lamont-Doherty Geological Observatory of Columbia University
Palisades, NY 10964

ABSTRACT

Systems of rotating blocks and fault may play an important role in the interseismic deformation between great earthquakes on master right lateral faults in Southern California. We have now evidence for block rotation from geologic and from earthquake data. Qualitative models suggest that block rotation adjacent to a major fault strand may generate time dependent asperities that lock this fault for a time that depends on the size of the blocks and on the thickness and mechanical properties of the fractured zone along this fault.

INTRODUCTION

The work discussed in this paper stems from a number of key observations. Two of these have been in the literature for some time. Freund (1970) in the Dead sea rift/transform zone, followed by Garfunkel (1974) in the Mohave region of southern California, focused their attention on sets of regularly spaced, subparallel faults with similar displacements. These fault sets are contained within simply shaped domains often bounded by major faults. They proposed a model where regional shear is accomplished by rotation of the blocks and the faults within the domains preserving their linear boundaries, akin to a set of books tilting on a bookshelf. Simple geometry relates the overall shear to the angle of block/fault rotation and the slip on each of the faults within the domain.

The second key observation was by Luyendyk et al. (1980) on the rotation of Neogene magnetic pole directions. He found that Miocene poles in the western Transverse Ranges had rotated clockwise by large angles, often approaching 90 degrees. Luyendyk et al. (1980) and Luyendyk et al. (1985) proposed a block rotation model similar to Garfunkel's (1974), but with different specific predictions about the kinematic evolution of southern California. The blocks in this model are large, implying for example that much of the western Transverse Ranges rotated by 90 degrees as a whole, raising some problems with geologic constraints.

The third fundamental observation involves seismicity. In a study of the San Bernardino-San Gorgonio Pass region, currently one of the most active areas in southern California (Fig. 1), we could resolve many detailed features of the pattern of faulting (Nicholson et al., 1984). The results were more ore less directly suggestive of a rotating block model. In general, we found the San Andreas and other major right lateral faults to be mostly aseismic. Wherever active faulting could be resolved by fault-plane solutions and hypocenter distribution, we tended to find either left-lateral northeast trending faults, or reverse faults. Crustal deformation during the interseismic period may be dominated by slip on secondary faults

rather than diffuse elastic strain. Moreover, block rotations may play a particularly important role and may offer a key to the pattern of deformation leading to a great earthquake.

Geologic versus Interseismic Deformation

The rotating block/fault model can be applied to two families of deformations, to interseismic deformation that occurs during the period between great earthquakes, and to geologic deformation that accumulates over much longer geologic time. Geologic deformation results from the superposition of deformation during many earthquake cycles, including both the deformation during great earthquake sequences and the nonelastic component of interseismic deformation. Our results for southern California suggest that interseismic deformation differs systematically from the great earthquake deformation, and we would generally expect geologic deformation to differ from interseismic deformation as well.

At an ideal plate boundary interseismic deformation is purely elastic, is recovered in great earthquakes and contributes nothing to geologic deformation. In the real world, interseismic deformation is probably a combination of elastic and nonrecoverable deformation. A very important task is to compare the long term kinematics deduced from structural and paleomagnetic data, with short term deformation deduced from seismicity and geodesy. What portion of the interseismic deformation is recovered during the major earthquakes? Once the relationship between geologic and interseismic rotation is better understood, geologic data may be found to have information on the short term interseismic behavior.

The Coyote Ridge, San Jacinto Fault Zone

At the southeastern end of the Anza gap on the San Jacinto fault zone, the Coyote ridge is a prominent topographic/structural feature associated with a right step of the main strand (Figure 2). The San Jacinto fault proper is the active strand through the Anza gap to the Coyote ridge. At this point the Coyote Creek fault, which is displaced to the right from the San Jacinto fault by about 4 km, continues to the SE as the main active strand of the fault zone (Sharp, 1967). The Borrego Mtn/Coyote Mtn sequence of 1968-69 was asssociated with surface rupture along about 40 km of this fault.

In the classical interpretation, the right step between the San Jacinto and the Coyote Creek faults would require a pull-apart basin. This basin would have to account for about 3 km of extension along strike of the fault zone, according to the displacement on the Coyote Creek fault (Figure 2). Structural features do include transverse faults with a dip slip component, but instead of a basin, there is evidence of recent rapid upflit (Sharp, 1967). We propose a model where 3 km of right-lateral displacement along the fault zone is accomplished by a system of blocks and faults rotating clockwise by 50° (Figure 3). This model predicts 1.7 km of left slip on the rotational faults and can account for the prominent thrusting that characterizes the edges of the blocks on the main fault strands.

The radial pattern of the cross faults on Coyote ridge and the gradually decreasing displacement towards the northwest on the Coyote

Creek fault (Sharp, 1967), can be accounted for by a system of rotating blocks that propagates to the northwest. In this model new cross faults would be generated as extension fractures by advancing the northwestern end of the system. The newly generated blocks would begin to rotate in response to right-lateral shear stress. This rotation would increase normal stress across the San Jacinto fault and lock it. As the rotation progresses beyond perpendicularity with the fault zone, normal stress across this zone would decrease and the Coyote Creek fault would begin to accumulate right-lateral slip. Thus, the Coyote Creek fault would propagate to the northwest at the expense of the San Jacinto fault. Total accumulated displacement along the Coyote ridge should decrease northwestward on the Coyote Creek fault and increase in the same direction on the San Jacinto fault. The along strike extension required by the right step of the master strand of the San Jacinto fault zone at Coyote ridge can be accomplished not only by a component of normal displacement on the cross faults, but also by block rotation if the initial angle between cross faults and the master fault is larger than the first angle (Figure 4).

The block/fault rotation model for the Coyote ridge can be tested by further structural mapping, by a survey of paleomagnetic pole directions, and by detailed analysis of earthquake data on Coyote ridge. Specific predictions that can be tested are whether the cross faults have left-lateral components of displacement increasing to the southeast, whether clockwise rotations similarly increasing to the southest have occurred during the last 1/2 my, and whether the pattern of current interseismic deformation reflects block rotation. In general, earthquake epicenters along the San Jacinto fault zone and other fault zones in southern California (Figure 1) often do not trace individual strands, rather they cluster in areas bounded by the major fault strands. This suggests that current seismicity is primarily generated by left-lateral cross faults founding rotating blocks. Block/fault rotations are more directly indicated by earthquake data from the 1979 Coyote Lake sequence (see below) and our results from the San Bernardino and Eastern Transverse Ranges (Nicholson et al., 1984).

Paleomagnetic data are often thought to give the strongest evidence in favor of block rotation (e.g., Luyendyk et al., 1985) The detailed control on the timing of uplift and rotation that Johnson et al. (1983) obtained for the Fish Creek basin places further constraints on the kinematics. The basin began filling about 4 my ago; 0.9 my ago it was suddenly uplifted and rotated by 30°. Clearly, the short time and large rotation require that the area involved be small, much smaller than the rotating blocks in the model proposed by Luyendyk et al. (1985). The amount and timing for the uplift of the Fish Creek basin is similar to the value predicted by our model for the Coyote ridge. In both areas uplift accompanied the rotation. The same type of model may be applicable in both areas.

Available data on fault arrays in southern California (Figure 1) are suggestive of numerous rotational block/fault systems. Although the pattern characteristic of rotating fault systems, series of subparallel faults terminating at common boundaries, is often recognized, data on the sense and amount of block rotation, are not available in most cases. Structural mapping should be addressed to further explore the kinematic properties of rotating systems. In a preliminary survey

of the Borrego Badland area of the San Jacinto fault zone southeast of Coyote ridge, Bogen and Seeber (in preparation) found evidence of left-lateral Quaternary displacement on northeast cross faults.

The 1979 Coyote Lake Aftershock Sequence

Reasenberg and Ellsworth (1982) relocated the aftershocks of the August 6, 1979 Coyote Lake earthquake that ruptured the Calaveras fault in central California. These data provide excellent time-space constraints on the evolution of this sequence. The aftershocks delineate a complex 3-4 km wide fault zone bounded by two narrow rupture planes in en echelon configuration stepping to the right by the width of the fault zone and including a more diffuse zone of seismicity between these master faults and their extensions. Very little, if any, seismicity occurred outside this zone (Figure 5). Fault plane solutions are consistent with right-lateral slip on the main faults. In between these faults, fault plane solutions are also primarily strike-slip, but the right-lateral plane is rotated ≈14° clockwise relative to the strike of the fault zone.

Reasenberg and Ellsworth (1982) proposed a model where right slip along the Calaveras fault zone is bridged across the right step between the main strands by a zone of diffuse deformation where scattered earthquakes reflect a stress field locally altered by the interaction between the ends of the en echelon strands. We propose a different model where right-lateral displacement along the fault zone is accounted for either by slip over the major strands or by rotation of blocks, straddling the fault zone (Figure 6). These blocks are bounded by left-lateral cross faults that rotate with the blocks and are the source of seismicity in the volume between the major strands and their extenstions.

The block fault rotation model seems to fit the data in greater detail (Figures 7 and 8). The complex pattern of right-lateral slip and clockwise rotation through the 1979 aftershock sequence accounts for right-lateral displacement on a 20 km long portion of the Calaveras fault zone. During the aftershock sequence these two patterns of deformation do not overlap. Either the one or the other is active on any one portion of the fault zone. Prior to the main shock, however, the portion of the fault zone that was about to experience the main right-lateral rupture was affected by block rotation (Figure 9). This suggests that interactions between block rotation and slip on the major strands in a fault zone follow a complex space-time pattern in which the two modes of deformation alternate in any one portion of the fault. The coupling between these two modes of deformation may be a key to understanding phenomena precursory to a large rupture on a master fault and to develop efficient monitoring programs for earthquake prediction.

Ancient and Deeply Eroded Block Rotation Systems

If block rotation is an important mechanism in the San Andreas fault zone, block rotation systems must be active in other regions, different tectonic regimes and older geologic times. Figure 10 illustrates a rotational event in the Devonian Appalachians. The age of the structures and sense of movement deduced from the geometry is

consistent with results obtained from paleomagnetic pole directions (Kent, 1982). This deeply eroded rotational system may reveal the type of deformation associated with block rotation at mid crustal depths.

Geometric Properties of Rotating Block Systems and the Cycle of Great Earthquakes

The roles played by block rotations in the interseismic period and in the sequences of great earthquakes may be very pertinent to a earthquake prediction effort. The block/fault rotation model applied to interseismic deformation leads to the concept of time-dependent asperities and to repeat times for rupture that depend on the geometry of adjacent block systems.

Figure 11 illustrates a mechanism by which block rotation can play a direct role in determining the timing of failure on an adjacent master fault. The sketch at the top depicts a system of blocks in a fault zone just after the area has been destressed by major slip on the master fault. The regional faults bounding the blocks are characterized by a thick layer of highly fractured rock markedly weaker than the surrounding rocks (e.g., Feng and McEvilly, 1983; Stierman, 1984). In the interseismic period strike-slip displacement is primarily accomplished by block rotation. The secondary deformation caused by block rotation is concentrated in the weak fault zones bounding the blocks (middle sketch). The rotation raises stress across the fault zone increasing its strength (time-dependent asperities). When the main fault-strand ruptures (bottom sketch) the blocks rotate back and partially recover the interseismic rotation, the rachet is disengaged and the system is ready to start the next cycle.

Figure 12 shows the possible evolution of stress and strength on the master fault during the cycle depicted in Figure 11. Shear stress and strength are low after the great eartquake. For some time thereafter blocks can easily rotate because the gouge zone they are impinging upon is weak. How rapidly shear stress and strength raise along the master fault probably depends on the mechanical properties of the gouge zone and on the geometry of the system. For the system to operate by stick-slip, strength has to raise faster than stress and remain higher for the interseismic period. Eventually the gouge zone will be compressed at the corners of the rotating blocks to the point where its resistence to further compression will drastically increase (i.e., when all the cracks are closed). Further strike-slip displacement will require the stress to increase rapidly and to rupture the master fault. A model for the interaction between block rotation and rupture on the master fault along the lines suggested in Figures 11 and 12 can be constructed incorporating constraints on the mechanical properties of fault zones and on the kinematics of rotating block systems.

SUMMARY

Block rotations in southern California can be detected both from data that integrate deformation over geologic time and from data that detect short term deformation during the interseismic period

between great earthquakes. While most of the deformation during a large earthquake on a master right-lateral fault is directly related to the slip on that fault, during the interseismic period much of the deformation seems to be related to slip on left lateral cross faults defining systems of rotating blocks. Some of this deformation may be permanent and contribute to the geologically detected rotations, some of it may be elastic and recovered during the large earthquakes on right lateral master faults. Active systems of rotating blocks typically occur between major strands of a fault zone where current seismicity is often concentrated. Right steps of the active master fault from one strand to another seems to be accommodated by rotating blocks between these strands in a structurally well documented case on the San Jacinto fault at the Coyote ridge and on a seismically well documented case on the Calveras fault for the Coyote Lake earthquake (1979). Block rotation may account for continuity in right lateral displacement across the step and for the required along-strike extension. These rotating block systems are predicted to achieve large rotatings in short geologic times and to propagate along a fault zone increasing the length of an active strand at the expenses of another.

Rotating blocks are expected to interact with the adjacent active major strand by increasing normal stress across portions of this fault and locking it. These rotating blocks would generate time-dependent asperities. Elements such as the size of the blocks and the width and mechanical properties of the weak fractured zone along this fault may contribute to determine how long it will take for the shear stress along the fault to overide the ratchet effect of the blocks and to determine the repeat time for failure. Block rotation may play a critical role in the unstable (stick-slip) nature of fault slip.

REFERENCES

Feng, R., and T. V. McEvilly, Interpretation of seismic reflection profiling data for the structure of the San Andreas fault zone, Bull. Seismol. Soc. Am., 73, 1701-1720, 1983.

Freund, R., Rotation of strike-slip faults in Sistan, southeast Iran, J. Geol., 78, 188-200, 1970.

Garfunkel, Z., Model for the late Cenozoic tectonic history of the Mojave Desert, California, and its relation to adjacent regions, Geol. Soc. Am. Bull., 85, 1931-1944, 1974.

Johnson, N. M., C. B. Officer, N. D. Opdyke, G. D. Woodard, P. K. Zeitler, and E. H. Lindsay, Rates of late Cenozoic tectonism in the Vallecito-Fish Creek basin, western Imperial Valley, California, Geology, 11, 664-667, 1983.

Kent, D. V., Paleomagnetic evidence for post-Devonian displacement of the Avalon platform (Newfoundland), J. Geophys. Res., 8709-8716, 1982.

Luyendyk, B. P., M. J. Kamerling, and R. Terres, Geometric model for Neogene crustal rotations in southern California, Geol. Soc. Am. Bull., 91, 211-217, 1980.

Luyendyk, B. P., M. J. Kamerling, R. R. Terres, and J. S. Hornafius, Simple shear of southern California during the Neogene, Am. Assoc. Petrol. Geol., in press, 1985.

Nicholson, C., L. Seeber, P. Williams, and L. R. Sykes, A new paradigm for understanding southern San Andreas fault tectonics (abstract), EOS, Trans. AGU, 65, 996, 1984.

Reasenberg, P., and W.L. Ellsworth, Aftershocks of the Coyote Lake, California, earthquake of August 6, 1979: A detailed study, J. Geophys. Res., 87, 10637-10655, 1982.

Sharp, R. V., San Jacinto fault zone in the Peninsula Ranges of southern California, Geol. Soc. Am. Bull., 78, 705-729, 1967.

Stierman, D. J., Geophysical and geological evidence for fracturing, water circulation and chemical alteration in granitic rocks adjacent to major strike-slip faults, J. Geophys. Res., 89, 5849-5857, 1984.

Wetmiller, R.J., J. Adams, F.M. Anglin, H.S. Hasegawa and A.E. Stevens, Aftershock sequences of the 1982 Miramichi, New Brunswick, Earthquakes, Bull. Seismol. Soc. Am., 74, 621-653, 1984.

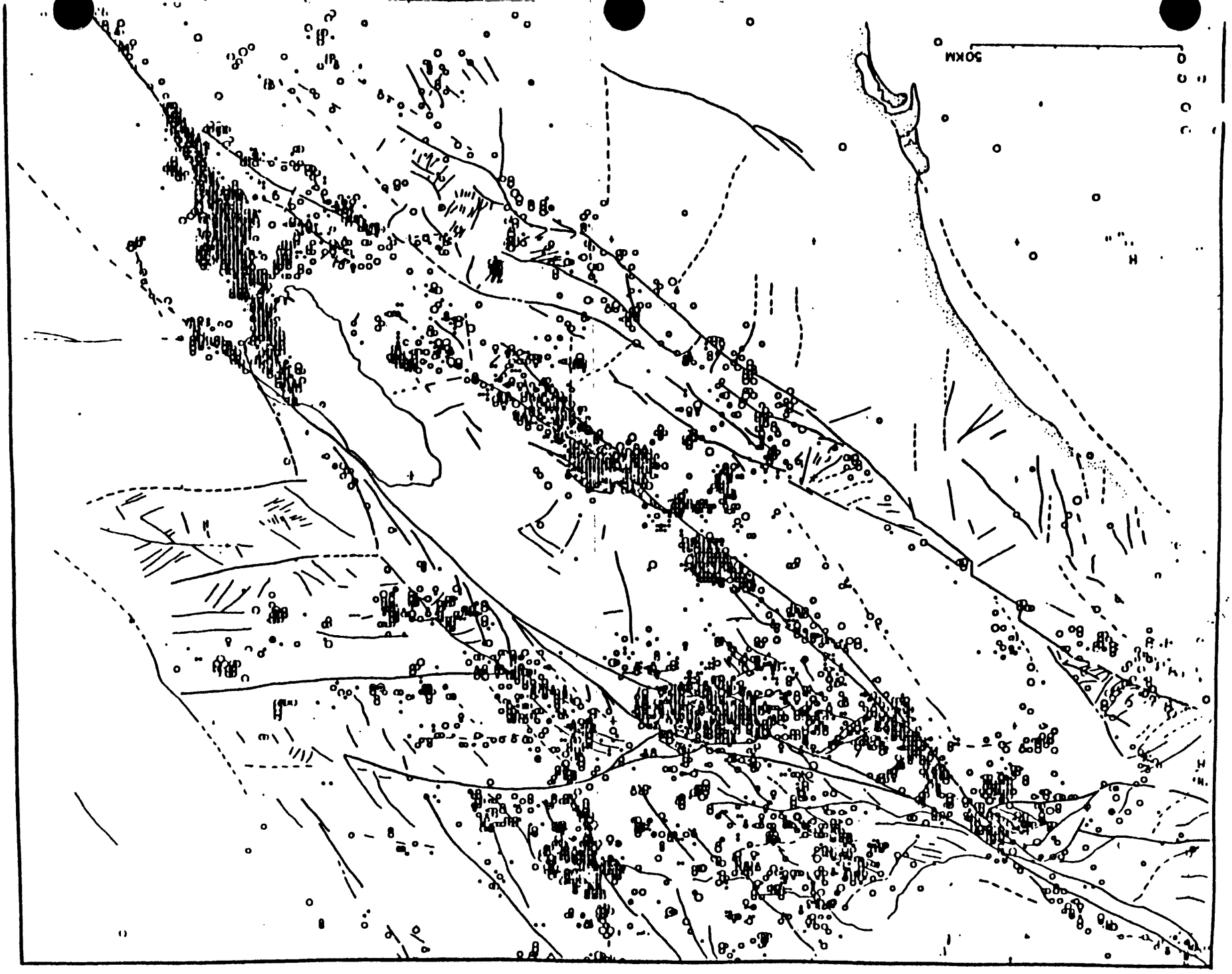

Fig. 1. Well-located 1975-83 hypocenters from the USGS/Caltech network and

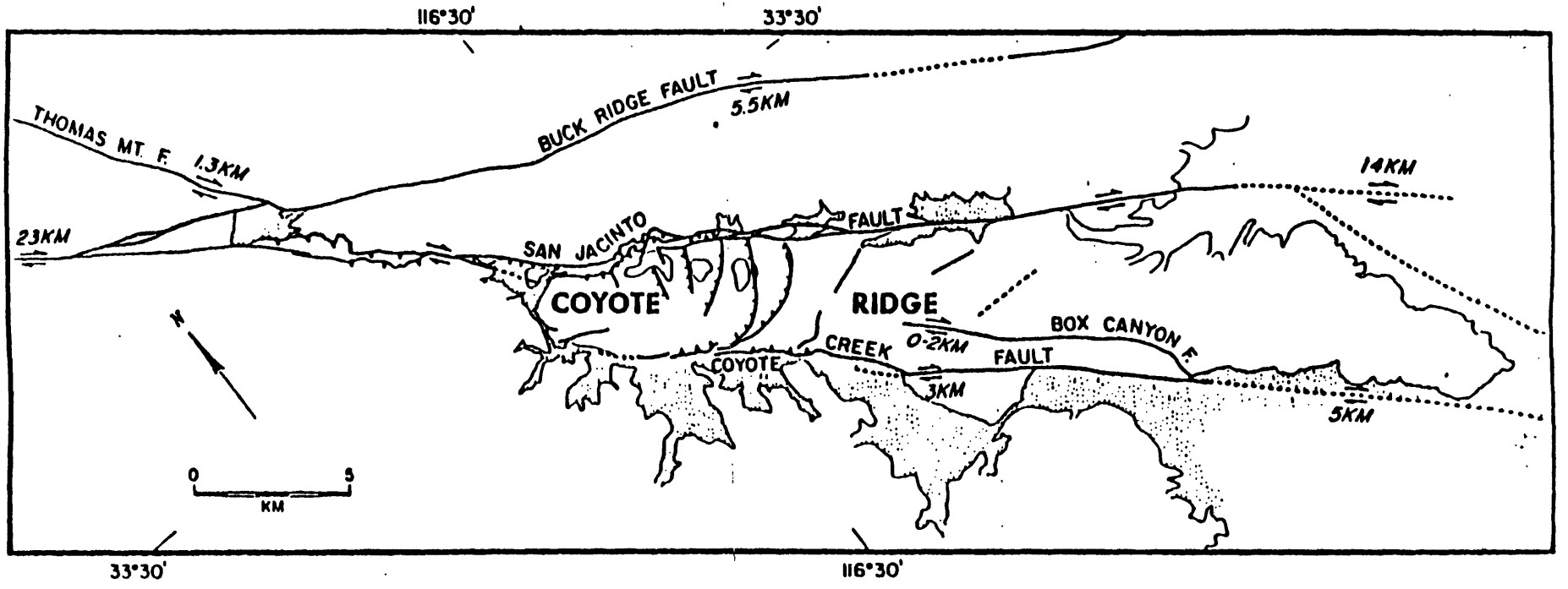

Figure 2. Fault array in the Coyote Ridge region of the San Jacinto fault zone (from Sharp, 1967). Numbers and arrows indicate sense and amount of displacement. The current main active strand of the fault zone is the San Jacinto fault proper southeastward to the Coyote ridge where it takes a right step to the Coyote Creek fault. Note the radial pattern of cross faults along the Coyote ridge and the reverse faults flanking the ridge.

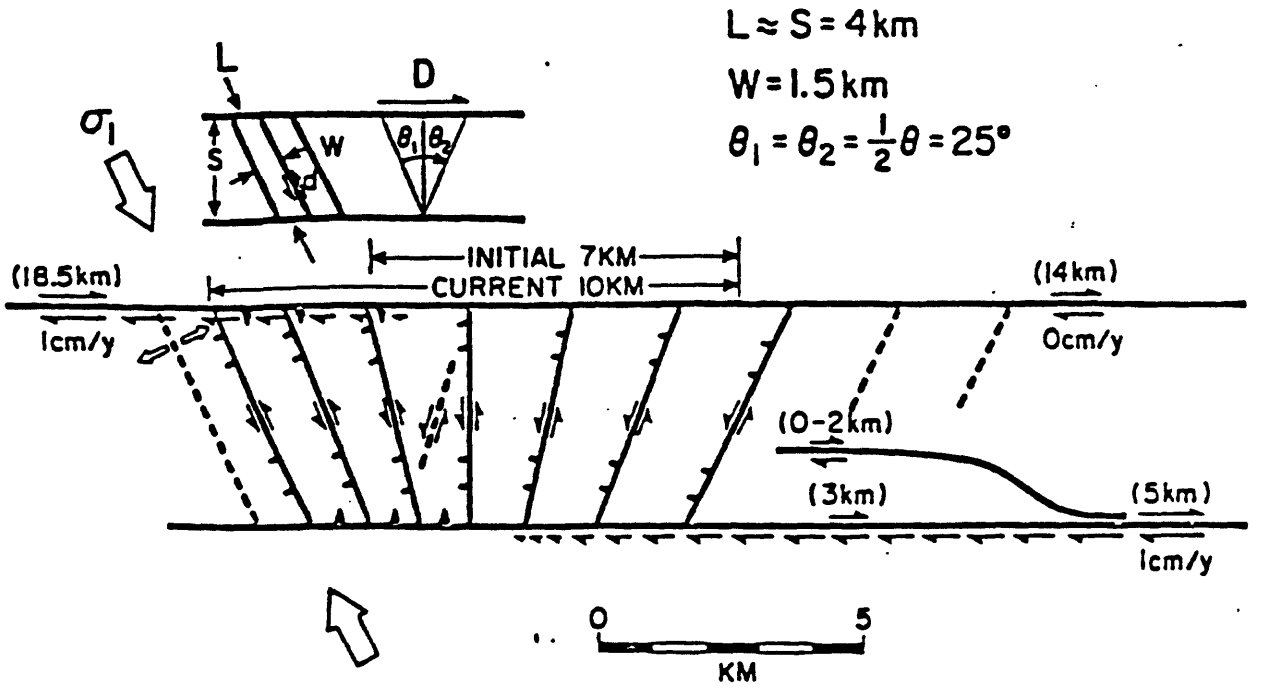

$D = L(\sin\theta_2 - \sin\theta_1) \approx 3\text{km}$

$d = W(\tan\theta_2 - \tan\theta_1) \approx 1.7\text{km}$

in 400,000 years

Figure 3. Block rotation model that can account for bridging the right-lateral displacement across the right step of the main strand of the San Jacinto fault zone at Coyote ridge. From the structural constraints provided by Sharp (1967), the model predicts 50° of block rotation and 1.7 km of left-lateral offset on the cross faults in 400,000 years. This rotating block system advances to the northwest as new faults and rotating blocks are generated (see text).

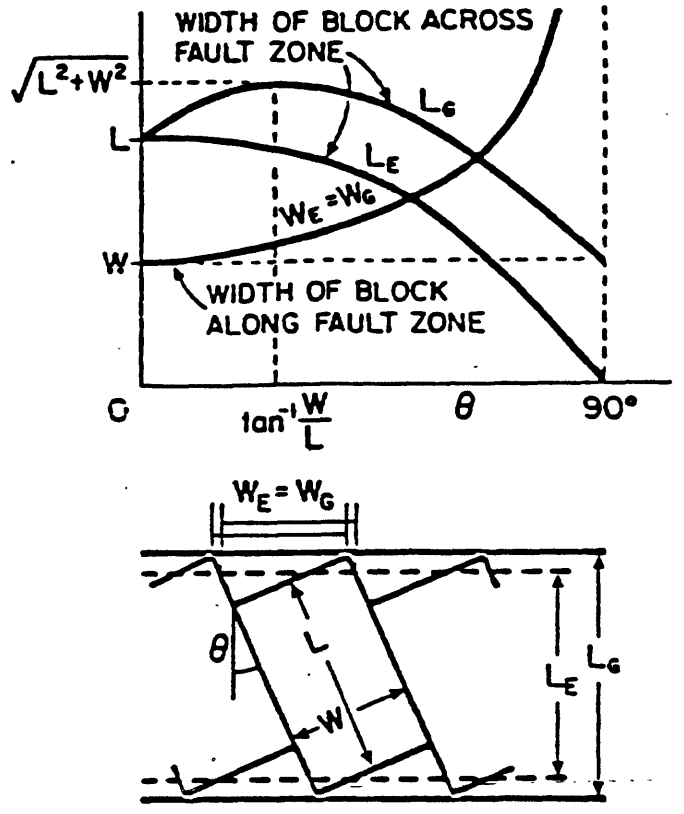

$$W_E = W_G = W/\cos\theta$$

$$L_E = L\cos\theta$$

$$L_G = (L^2+W^2)^{1/2}\cos(\theta - \tan^{-1}\frac{W}{L})$$

Figure 4. Some geometric properties of rotating block systems. In a strike-slip regime the primary reason for block rotation is to accommodate shear strain. Deformation along (W-direction) and across (L-direction) the shear plane are secondary deformations, a consequence of the geometry. Some of the along-strike extension required by the right step on the San Jacinto zone at Coyote ridge can be accounted for by block rotation (see text).

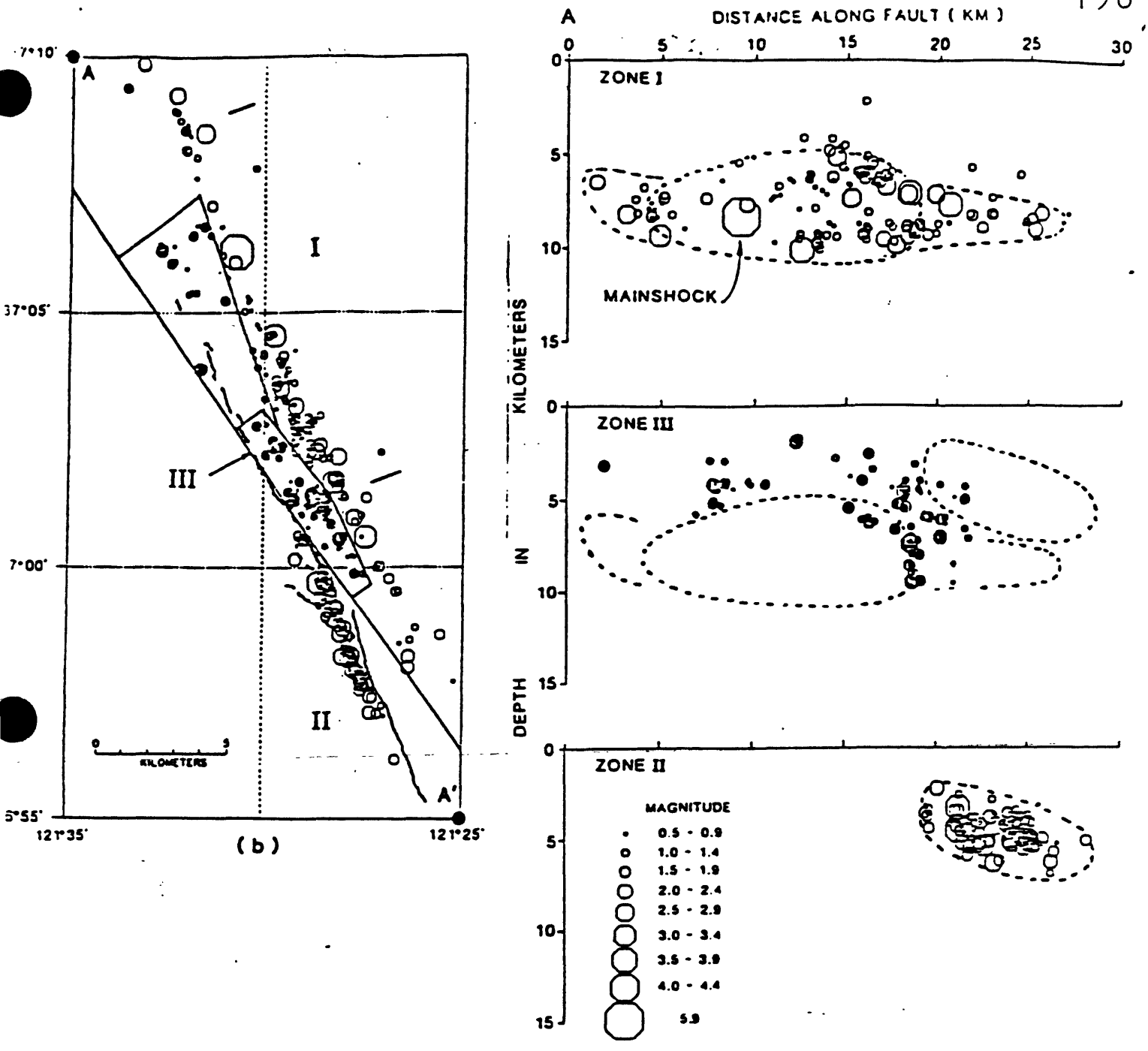

Figure 5. Hypocenters for the aftershocks of the August 6, 1979 Coyote Lake earthquake relocated by Reasenberg and Ellsworth (1982). This aftershock zone reveals a right step of the Calaveras fault. Reasenberg and Ellsworth (1982) proposed a zone of diffuse deformation and distorted stress field (zone III) between the "overlapping" en echelon main strands (zones I and II) to account for the seismicity and for clockwise rotation of fault-plane solution axes in this gap. We offer a reinterpretation of these data based on the block/fault rotation concept. We extend zone III to include all hypocenters that do not fall on the main right-lateral strands (filled symbols). When viewed in section (from the southwest) the three zones of distinct kinematic behavior do not seem to overlap. The central elliptical area in zone I includes all the aftershocks in the first three hours and probably delineates the main rupture. This initial phase terminated with the largest aftershock that initiated the activity in zone II. All of zone III became active at this time.

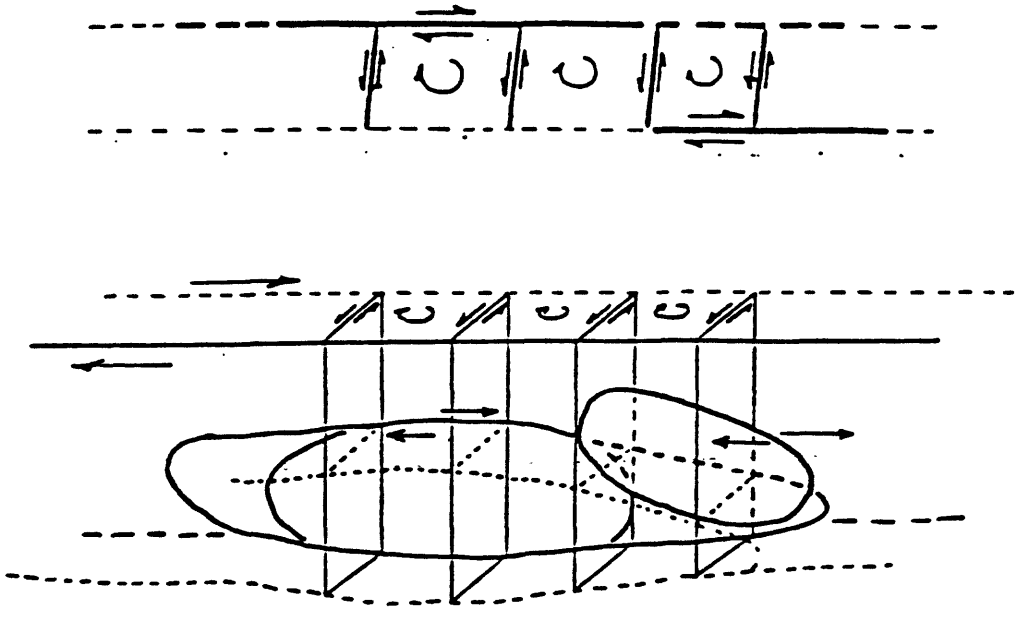

Fig. 6.. Interpretative sketch of the kinematics in the Coyote Lake, 1979 sequence. Map view above and oblique view from the SSW below. A 25-30 kilometer section of the Calaveras fault zone moved right laterally in this sequence. Part of this movement was accomplished by right lateral slip on one of the two main strands and the rest by clockwise rotation of blocks between these strands. From the time of the main shock onward, either one or the other of these two mechanisms were active on any portion of the fault zone without overlap. Before the mainshock, however, the portion of the fault zone corresponding to the main rupture was active with block rotation. Along a wide fault zone such as this one, the time-space distribution of block rotations and slip events on the main strands may follow a complex but prescribed sequence during the earthquake cycle.

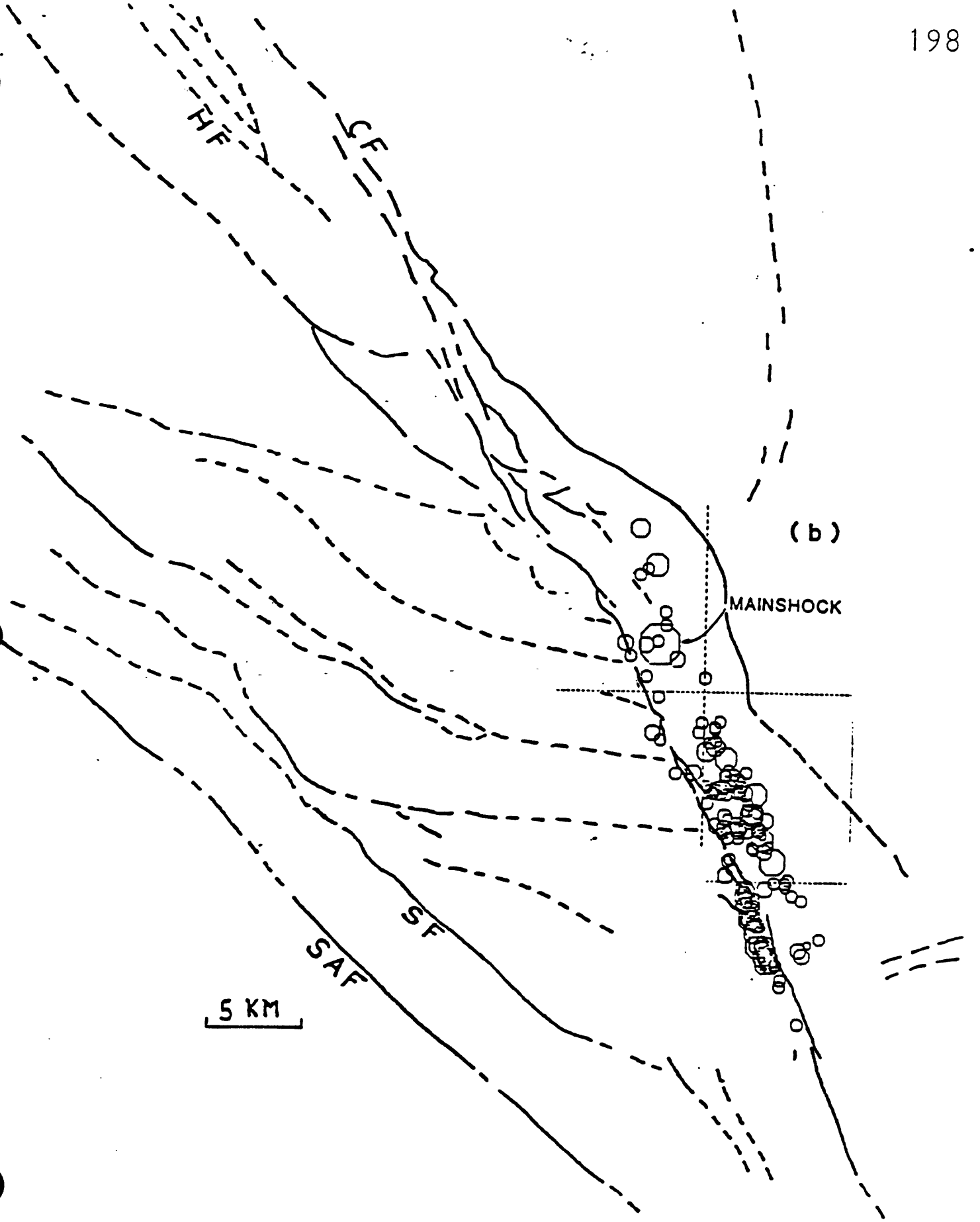

Fig. 7. Faults from the 1:250,000 California Atlas and 1979 Coyote Lake aftershocks (USGS catalog). The epicenters between the main northwesterly strands of the aftershock zone cluster on tight bends that strike east and are parallel to inferred faults that intersect the Calaveras fault zone at a high angle.

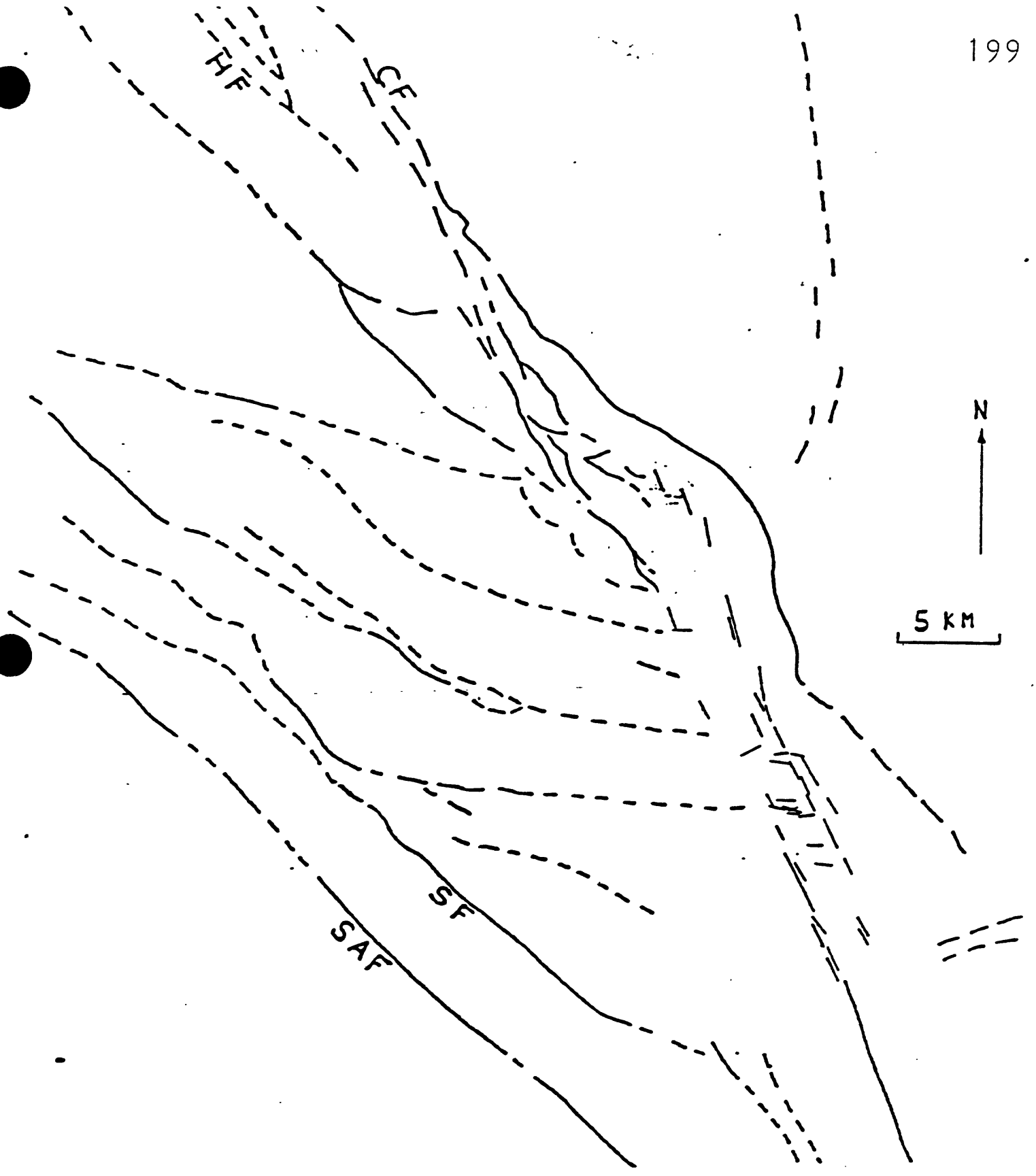

Fig 8. Faults from the 1:250,000 California Atlas and fault-plane solution data for the Coyote Lake 1979 sequence (Reasenberg and Ellsworth, 1982). Rather than choosing the right lateral northwesterly plane for all the solutions, we select the easterly left lateral plane for most of the solutions in the volume between the main strands (zone III). This choice seems justified because the planar features delineated by the hypocenters in this zone are parallel to the left lateral fault planes. we infer that zone III seismicity represents slip on left lateral cross faults separating a set blocks that rotate clockwise.

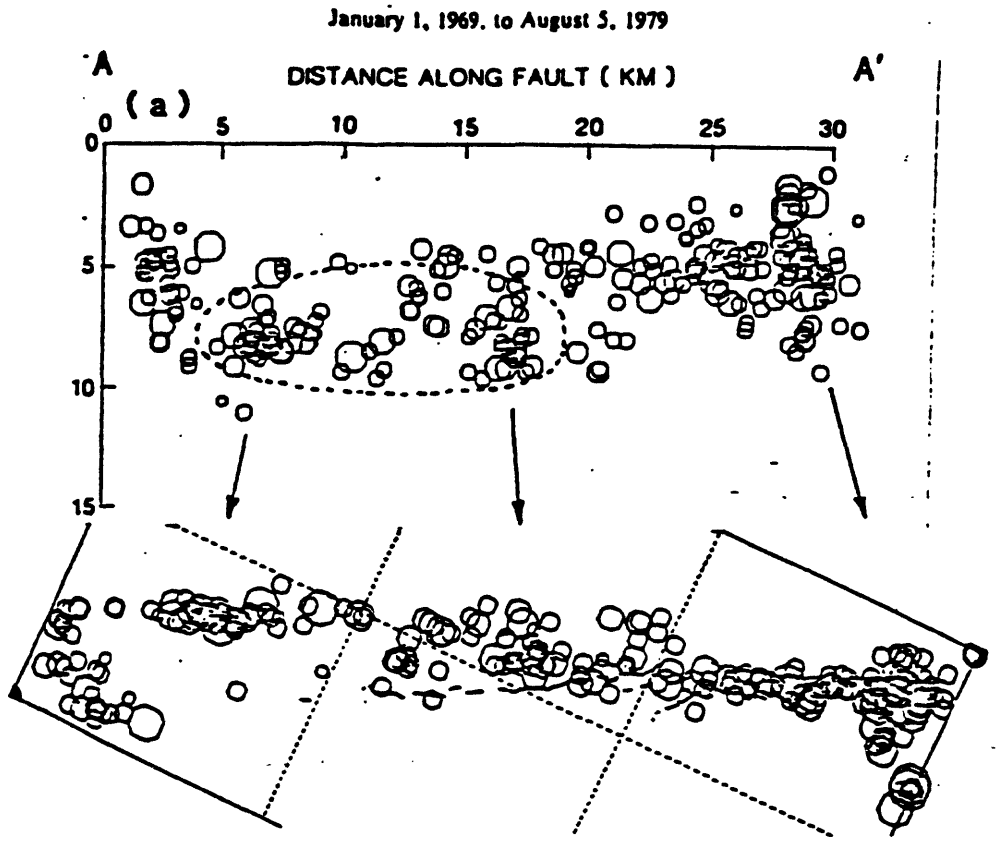

Figure 9. Hypocenters along the Coyote Lake aftershock zone for the six months preceeding the main shock. The map view clearly shows the right stepping main strands of the Calaveras fault. The section is viewed from the southwest and shows the inferred main shock rupture (dashed line). In this period zone III activity between the main strands overlaps the future rupture. After the main shock, activity in zone III is only adjacent to the rupture.

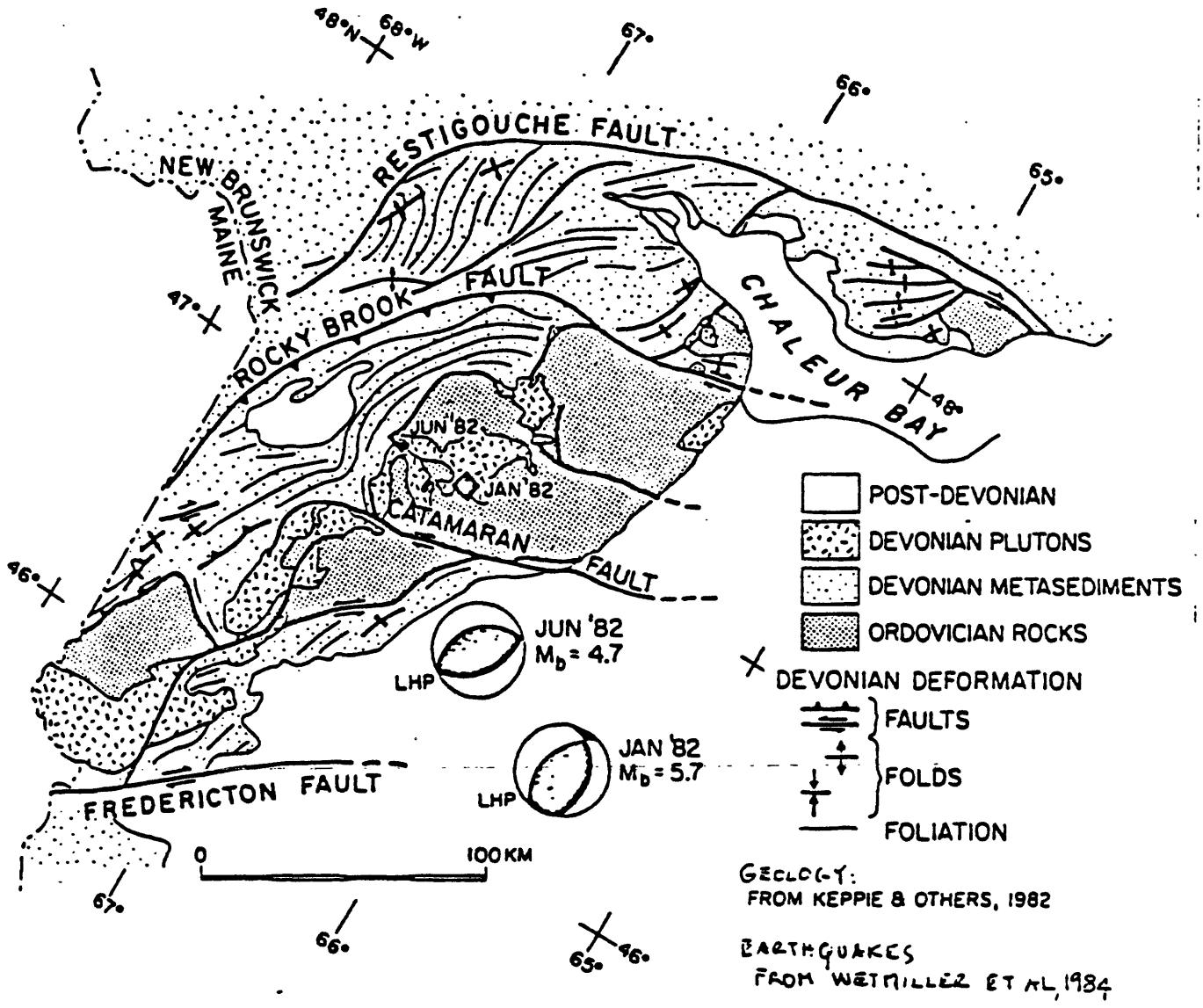

Figure 10. The configuration of Devonian faulting in New Brunswick suggests a rotational system where right-lateral displacement on the faults separating the blocks, such as the Catamaran fault, implies counter-clockwise block/fault rotation. Thus, most of the Devonian deformation in this area can fit into a single tectonic phase. Note that granitic bodies seem to occur preferentially where block rotation would tend to cause extrusion. This rotation is consistent with a regional left-lateral shear system along the Devonian Appalachians. Large left-lateral displacements along the northern Appalachians during the Devonian have been postulated by Kent (1982) on the basis of paleomagnetic data. Ancient and deeply eroded rotational systems such as this may yield geologic information on the modus operandi of these systems at seismogenic depths.

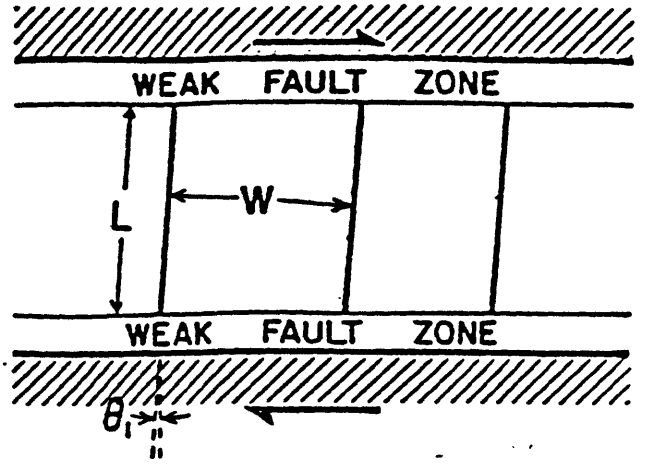

PREEXISTING BLOCKS
OR
FORMED NEOTECTONICALLY

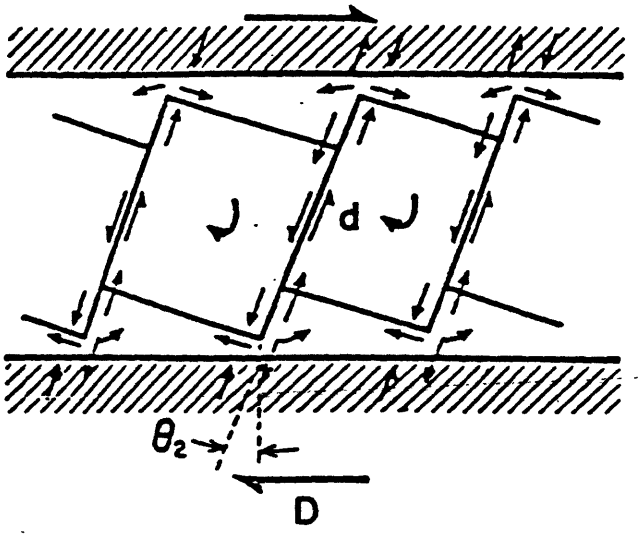

$d = W(\tan\theta_2 - \tan\theta_1)$

$D = L(\sin\theta_2 - \sin\theta_1)$

SMALL $(\theta_1 - \theta_2)$,

$\frac{D}{d} = \frac{L}{W}\cos^3\theta$

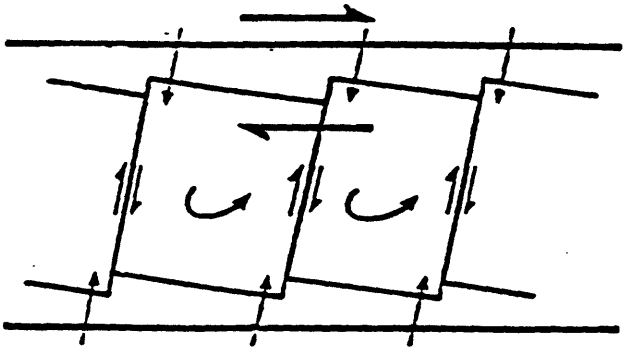

BACK-SLIP ON
ROTATING FAULTS
DURING AFTERSHOCK
SEQUENCE PARTIALLY
RECOVERS SLIP DURING
INTERSEISMIC PERIOD

Figure 11. Interaction of block rotation and rupture on the adjacent main strand of a major fault zone (see text).

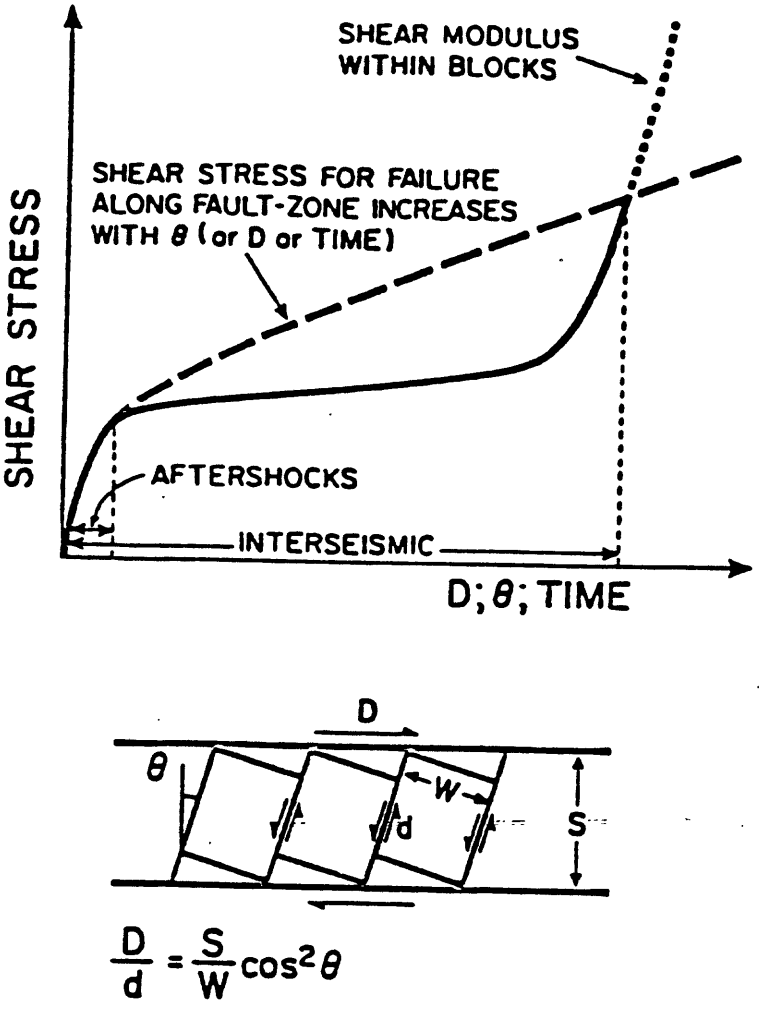

Figure 12. Possible evolution of stress and strength on the main strand of a fault zone adjacent to a system of rotating blocks (see text).

POST MEETING COMMENTS

United States Department of the Interior

GEOLOGICAL SURVEY
RESTON, VA. 22092

15 March 1985

In Reply Refer To:
Mail Stop 922

Memorandum

To: Wayne Thatcher
Bill Ellsworth

From: Rob Wesson Rob

Subject: Followup to Southern California Workshop

Thank you very much for inviting me to the workshop. I found it very stimulating. Please find enclosed a summary of the discussion on the San Jacinto fault zone.

It seems to me that the time is ripe to begin a carefully thought-out, methodical process culminating in a few years time with the installation of instrumentation for a second Parkfield-style experiment. It seems to me that initiating such an effort could focus and build on the enthusiasm apparent at the workshop in a very positive way.

For your consideration, my thoughts on how such an effort might be organized -- with times depending of course on budget -- are as follows:

1985 Based on the views expressed at the workshop identify three or four sites as "candidate special study zones." My impression was that two of the zones should be 1) Northern San Jacinto and 2) San Andreas fault/Indio-Bombay Beach. Charter "working groups": one working group for each "candidate zone" plus one for "seismic instrumentation" and one for "strain and other instrumentation". Each "candidate zone" group should be charged with outlining (and carrying out?) a set of preliminary studies to be carried out in the zone with the aim of determining whether it is the appropriate site for more intensive instrumentation. The instrumentation groups should be charged to outline the kinds of instrumentation to be considered for the final site and the surrounding region, as well as the process of development or testing, as required. Instrumentation could

be considered as "nearfield" and "farfield." The "nearfield," of course will be in the immediate vicinity of the site, but the "farfield" would be of a more regional character.

1986 Begin preliminary investigations at candidate sites.
Begin deployment of "farfield" or regional instrumentation.
Begin testing or development of instruments as required.

1987 Complete preliminary studies.
Choose site
Complete "farfield" network
Reform working groups to shift emphasis onto installation, analysis, modeling, selection of second site, etc.

1988 Begin "nearfield" instrumentation at selected site.

1989 Concentrate efforts on data analysis and modelling, improving instrumentation as appropriate.

I myself am quite enthusiastic about this effort, and would be delighted to work on one of the working groups. My first choice would be San Andreas/Indio-Bombay Beach.

Enclosure

United States Department of the Interior

GEOLOGICAL SURVEY
OFFICE OF EARTHQUAKES, VOLCANOES AND ENGINEERING
345 Middlefield Road, MS 977
Menlo Park, California 94025

MEMORANDUM

TO: Wayne Thatcher, Bill Ellsworth, Tom Hanks March 6, 1985

FROM: Bob Wallace

SUBJ: My vote on clusters

Some basic premises:

1. We are being permitted--being compelled?--to deploy new clusters in order to try to predict the next great southern California earthquake. To not try to predict that earthquake would be negligent.

2. To do the above we must understand the basic physics through a series of well conceived experiments.

3. Given any significant earthquake on the San Andreas fault, we must be prepared to say there were or were not short-term precursors, and what transpired before an event.

4. We must not miss critical coseismic physical phenomena.

5. Clusters help focus experiments so redundancy and coherence of observations are possible. Some experiments need not be clustered.

High priority clusters

1. Parkfield to Cajon Pass or 1857 revisited

   - o Parkfield cluster is both a critical experiment in itself, and may be a nucleation point for a repeat of 1857.
   - o Parkfield-extended cluster: For study of strain redistribution from Parkfield 1988 event, and to evaluate a Parkfield-extended event add modest instrument about 30 km southeast of Cholame.
   - o Cajon Pass - Punchbowl cluster: Add new cluster at northwest end of Cajon Pass structural knot where San Andreas and San Jacinto faults bifurcate. This will also capture data on a possible southern San Andreas event.

- o Tejon Pass cluster: Add new cluster in mid section of 1857 break, at either Tejon Pass or possibly elsewhere - Palmdale, Carrizo Plain?- to analyze a "simple" reach of fault, and to have a midpoint and 2 or 3 starting and stopping sites covered in the next big earthquake.

2. Cajon Pass to Salton Sea

- o Bombay Beach cluster: Needs further instrumentation regardless.
- o Northern Coachella Valley cluster: Add new cluster on southeast edge of Cajon Pass structural knot; from Whitewater Canyon to vicinity of Palm Springs.
- o These two clusters will cover both starting and stopping sites. The northern Coachella Valley cluster will capture data for either a southern or a northern event prediction, as well as coseismic data.

3. Anza Gap

This is a good prediction experiment in itself, but does not constitute a direct attempt to predict the next great earthquake, thus has a slightly lower priority and more selected set of experiments.

4. Long Beach 1933 revisited and other LA Basin events

Don't forget that this type of event in densely populated LA is the most ominous in terms of dollars and lives. I don't know even how to begin a cluster approach to this. Regional seismicity and regional geological studies must be continued to build the needed background.

5. Additional thoughts

Our studies should be considered an evolutionary process. We should think in terms of adding new and better experiments as we learn. I can't see success coming from an assumption of a static program or a long-term decrease in budgets, but only with an increase in areal coverage with constantly improving experiments.

PROPOSED CLUSTERS

R.E. WALLACE
3/85

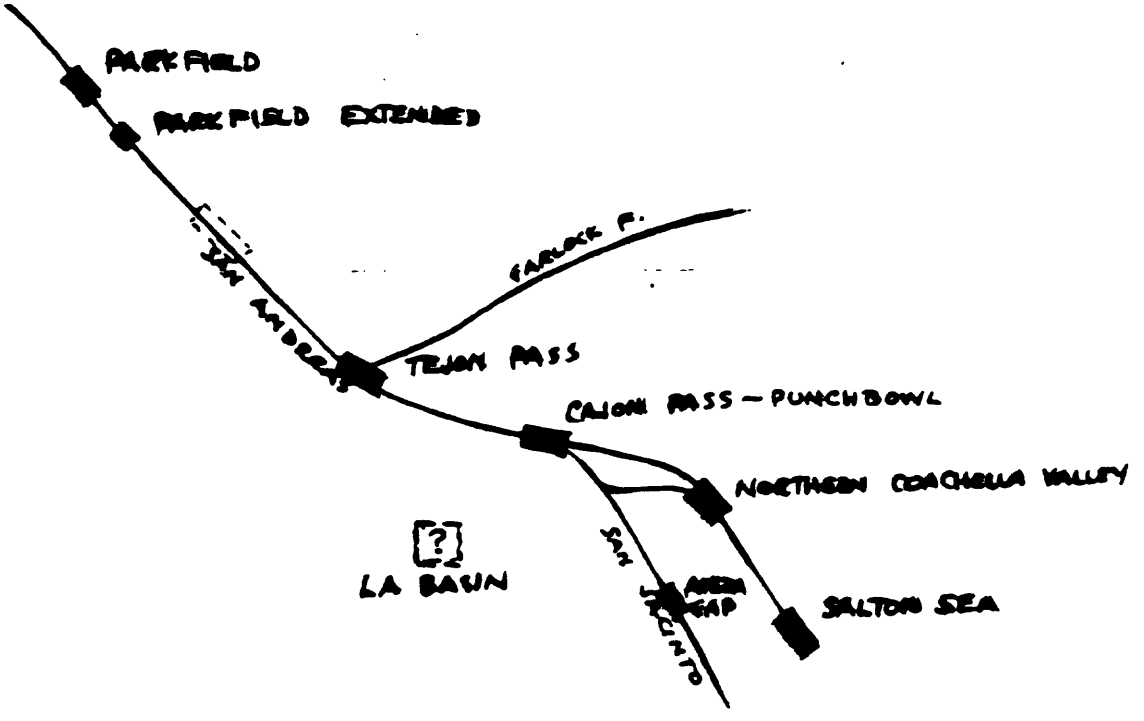

DEEP-SHAFT EXPERIMENTAL SITE ON SAN ANDREAS FAULT

We should continue to think of exciting new, major experiments. Consider, for example, a 2 km deep shaft with crosscuts for really meaningful studies at hypocentral sites. Mining companies long ago learned that drill holes are "point samples" and can readily miss the ore bodies, even very large ones. Companies explore by sinking shafts and driving drifts and crosscuts.

Deep Shaft Experiment		(Millions $)
2 shafts each 2 km deep @ $4000/m	=	$16
10 km of cross cuts and drifts @ $600/m	=	6
Drilling below 2 km deep platform		2
Pumping and ventilation equipment	=	2
Capital outlay for geophysical experiments	=	10
Total		$36
Operating expense per year	=	$15

DEEP-SHAFT EXPERIMENT

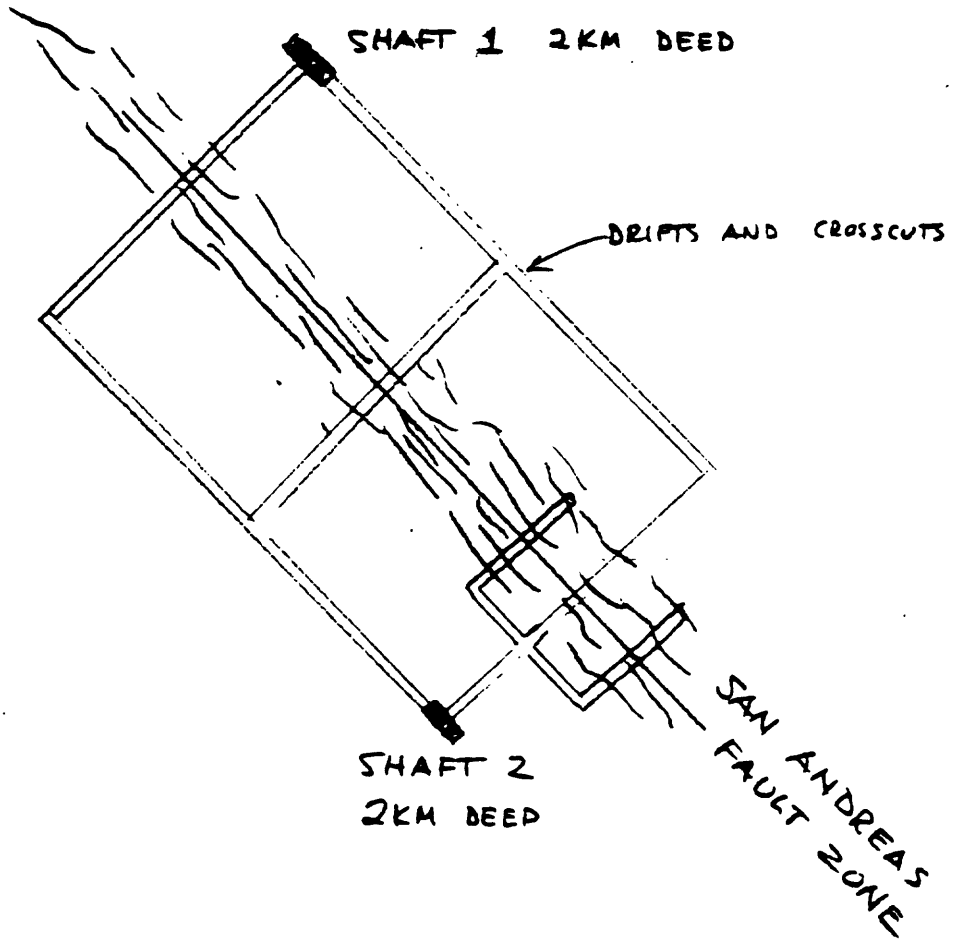

United States Department of the Interior

GEOLOGICAL SURVEY

Geologic Division
Branch of Western Regional Geology
345 Middlefield Road MS 975
Menlo Park, California 94025

March 6, 1985

Memorandum

To: Wayne R. Thatcher, William L. Ellsworth
Office of Earthquakes, Volcanoes, and Engineering

Through: Desiree Stuart-Alexander, Chief, Branch of Western Regional Geology

From: Jonathan C. Matti, Chief, Earthquake Hazards Project, Southern California JCM

Subject: Earthquake Prediction Workshop, San Diego, California
February 28 - March 2, 1985

Thank you for a stimulating workshop on prediction possibilities in southern California. I think the mix of people was a good one, and I learned a good deal from the experience.

I would like to take this opportunity to summarize my thoughts on the stated goal of siting a Parkfield-type prediction experiment within the San Andreas or San Jacinto fault zones in southern California.

Where to site.--I suspect that the Department is more interested in predicting an earthquake that would severely impact large population centers than predicting an earthquake that would impact sparsely populated regions. Thus, the politics of the matter presumably require siting an experiment either (a) along a fault segment proximal to populated regions or (b) along a fault segment where an earthquake could nucleate and propagate toward populated areas. If valid and relevant, this rationale must be balanced against (c) fault segments for which we have the most information about their modern and paleoseismic behavior, and (d) fault segments that appear to be about ready to go. I don't envy your responsiblity.

Anza probably is the best suited for a thoughtful fault-physics experiment. However, I don't think it satisfies either (a) or (b) above, nor is their much information about paleoseismicity (c) or imminent potential (d).

On the accompanying geologic map and Appendix, I explore several alternative sites.

How to site.--The goal of siting a single Parkfield-type experiment in southern California carries the implicit assumption that a Parkfield-type

fault configuration exists in southern California. In my view, this assumption is not valid: the geologic framework of the subject region is significantly different from that of the Parkfield region, with the result that experimental conditions are significantly different. Should we then employ the same experiment?

My answer is no (at the present time). I vote against deploying a dense cluster of instruments along a single 30-kilometer-long fault segment. I don't think we have enough information to objectively and validly single out one segment as a more likely target than some other segment. If we are given the opportunity to purchase and install a package of expensive instruments, we better have justifiable reasons for putting them on a particular narrow patch of ground.

My recommendation for "how to site": either go for the whole package (i.e., six to ten Parkfields), or spread yourself out over the map with smaller-scale experiments by choosing the best suite of instruments for particular sites on the basis of their site-specific geologic makeup and their uniqueness within compressional, extensional, or purely strike-slip frameworks. Either choice sends a strong signal to the Department and Congress: (1) go for "star wars" because basically that is the only justifiable and appropriate means of getting the job done, or (2) go for a reasonable compromise, because basically (in my opinion) we don't know enough about any particular fault segment in southern California to legitimize its choice for one single experiment. For example, to capture a devasting earthquake I could as legitimately recommend either the Newport-Inglewood fault or the Whittier fault as I could the San Andreas or San Jacinto faults: the paleoseismicity (slip-rates and faulting recurrence) of the first two is poorly understood, and yet each has generated a bad shock in this Century that could be worse in today's urban setting. Thus, why not either of these two? If the Department wants to focus on particular targets in the near future, then they will have to pay for more data acquisition to permit us to separate high-priority targets from low-priority targets.

Granted, you can't cover every bet, and granted you have to be responsive to the Department. However, I am down on selecting a specific 30-km segment and up on choosing particular points on specific fault zones. At each point, the strain behavior and seismicity can be compared and contrasted with other points on the same fault. Such a strategy seems to make sense given the assumption that local departures from "normal" geophysical and seismological signatures can be recognized as premonitory signals only if there is a baseline for "normalcy" along the entire reach of the fault segment. Using this rationale, I have identified several prospective local sectors of the San Andreas and San Jacinto fault zones that conceivably would lend themselves to useful comparison with adjacent sectors. (See accompanying map). The identified sectors include points where the pattern of surface faulting is anomalous or is markedly different from adjacent sectors, as well as sectors where the seismological and geophysical signatures could be viewed as "routine".

Need for Geologic Framework.--In contrast to Parkfield, in southern California it is clear that the historical seismicity and geology of one fault may be related intimately to the seismicity and geology of one or more adjacent fault zones. Therefore, I believe it is essential to work out (a) the earthquake history of each fault zone along several reaches and (b) the structural role and geometric relationship of each fault relative to adjacent faults. It seems to me that we would be better prepared to make the decision facing us if we had better information on late Quaternary slip rates and faulting-recurrence intervals as well as better control on the actual distribution and structure of neotectonic fault zones. We have a good start on these fronts. However, I recommend that the operational plan include an appropriate element devoted to continued paleoseismicity studies and geologic framework studies, both regional as well as site-specific to the monitoring sectors.

Conclusion.--I suppose you have heard most of what I have said many times, and I probably haven't helped you very much. However, I think the accompanying geologic map conveys a clear message: the geology and seismicity of faults in this part of southern California are complex and regionally inter-related, and the faults may not easily be amenable to a Parkfield approach.

Accordingly: I recommend a gradual phased-in program covering a 3-to 5-year period during which we learn more about the geophysics and neotectonic geology of the study region. I recommend that this phase-in include upgrading geophysical and seismological monitoring of the sectors identified on the accompanying map, accompanied by detailed studies of paleoseismicity and neotectonic framework of each sector. The expanded data base generated by this build-up will allow us to focus on sectors potentially suitable for a Parkfield-type experiment. At the present time, I don't think we are ready to commit dollars and resources to a quick fix.

If I can be of assistance to you as you work your way through this difficult decision, please do not hesitate to call upon me.

Good hunting!

Attachments

Appendix
Recommended sites for Scaled-Down Monitoring

Site 1 (Southern Cajon Pass sector)

Targets: San Bernardino strand, San Andreas fault zone
Glen Helen strand, San Jacinto fault zone (± other strands?)
Normal (extensional?) faults in Devore area

Rationale: Includes coverage for both San Jacinto and San Andreas faults in a region that includes the north end of the San Bernardino seismic gap for the SJF as well as the southern terminus (±) of the 1857 rupture on the SAF. Detailed mapping exists (Weldon, Morton, Matti). Paleoseismicity beginning to be understood (Weldon and Sieh to the NW at Lost Lake).

Site 2 (Reche Canyon sector of San Jacinto fault)

Targets: San Jacinto fault
Claremont strand, San Jacinto fault

Rationale: Includes coverage of San Jacinto fault at the south end of the San Bernardino seismic gap. Detailed mapping exists (Morton and Matti, San Bernardino South 7.5' quad, in press). Paleoseismicity in preliminary form (Sieh, unpubl.; Morton, in progress). Clot of seismicity here is distinctive, and could be significant (see C. Johnson seismicity map; Nichelson also). Site of change in regional strike for SJF.

Site 3 (San Jacinto Valley sector)

Target: Multiple strands of San Jacinto fault in right-stepping zone

Rationale: Site of two large earthquakes. Detailed mapping (Morton, Matti). Site of historically subsiding extensional graben with deep sediment fill. Possible site where slip steps left from SAF to SJF system. Directly north of Anza seismic gap.

Site 4 (Mill Creek sector)

Target: San Bernardino strand, San Andreas fault
Normal (extensional) faults of Crafton Hills-Yucaipa Valley region
Compressional deformation adjacent to SAF

Rationale: Includes coverage of San Andreas fault where its clean, well defined tectonic geomorphology falls apart and the zone is complicated by extensional and compressional faulting, left steps, and multiple active traces. Detailed map coverage (Matti, Morton). Slip-rate studies ongoing (Harden, Matti).

Could an earthquake nucleate near here because it is the south terminus of the San Bernardino strand? Could a burst of extensional seismicity be a premonitory signal?

Site 5 (San Gorgonio Pass sector)

Target: Reverse, thrust, and tear faults of San Gorgonio Pass fault system

Rationale: Detailed mapping (Matti, Morton). Possible site of left step in San Andreas fault system. Site of convergence due to right-lateral slip on Coachella Valley segment, Banning fault and Garnet Hill fault(?). Could loading be taking place on SGP fault system due to 2 mm annual creep on BF (Allen)? Could release of strain here unzip the Coachella Valley segment of BF? or the San Bernardino strand, in combination with extensional faulting at site 4?

Overall rationale for northern San Andreas (sites, 1, 4, 5): Monitoring of strain, geodesy, creep, and local seismicity at selected sectors along this reach could yield premonitory signals leading to several possible earthquake scenarios:

(1) Strain buildup and release at site 5, leading to relaxation at site 4 and nucleation of ground rupture that propagates northward to site 1 and beyond.
(2) Relaxation at site 4, leading to nucleation of ground rupture that propagates northward to site 1 and beyond.
(3) Relaxation at site 4 leads to strain release at site 5, which in time causes failure on the southern San Andreas (see overall rationale for that segment).
(4) Nucleation at site 1 propagates southeastward to site 4, with unknown consequences.

Site 6 (Devers Hill sector)

Target: Coachella Valley segment, Banning fault

Rationale: Site of 2 mm annual creep (Allen). Site of late Quaternary slip, probably Holocene (paleoseismicity needs to be studied). Detailed mapping in progress (Matti). Would this trace be the site of ground rupture on the San Andreas fault in the Coachella Valley?

Site 7 (Indio Hills sector)

Target: Coachella Valley segment, San Andreas fault

Rationale: Is this sector neotectonic? Does slip step left onto the Coachella Valley segment of the Banning fault? Is the fault creeping here?

Site 8 (Indio Sector)

Target: San Andreas fault

Rationale: Paleoseismicity studies in progress (Sieh). Does slip propagate from here to the Coachella Valley segment of the San Andreas fault or to the Coachella Valley segment of the Banning fault?

Site 9 (Bombay Beach sector)

Target: Junction between San Andreas fault and Brawley seismic zone

Rationale: Change in recent seismicity here suggests that an earthquake on the San Andreas could nucleate in this region (C. Johnson). Also, proximity to 1979, 1980 events that occurred in similar positions (ends of spreading segments at junction with transforms).

Overall rationale for southern San Andreas (sites 5 through 9): Monitoring of strain, geodesy, creep, and local seismicity of selected sectors along this reach could yield premonitory signals leading to several possible earthquake scenarios:

(1) nucleation at Bombay Beach, and subsequent propagation through sites 8, 7, and 6, terminating at site 5.

(2) strain buildup and release at site 5, leading to nucleation at Devers Hill and unzipping south through sites 7, 8, 9.

(3) strain buildup and release at site 5, leading to nucleation at site 9 and northward propagation through sites 8, 7 and 6.

Tectonic Elements, Greater San Gorgonio Pass Region
J. C. Matti and D. M. Morton

San Gorgonio Pass fault system

(a) East-oriented reverse and thrust faults;

(b) NW-oriented right-lateral wrench faults;

(c) Quaternary (late Pleistocene through Holocene);

(d) = zone of compression and convergence;

San Andreas fault system

(a) NW-oriented, with local departures from this trend;

(b) Multiple strands, from oldest to youngest:

1) Banning fault (10-5 m.y.B.P.)

2) San Andreas fault zone (5 m.y.B.P. to Recent)

a) Wilson Creek strand (5 m.y.B.P. to 3.5? m.y.B.P.)

b) Mission Creek Strand (3.5? to 2? m.y. B.P.) = (Counterpart of Punchbowl fault)

c) Mill Creek strand (? to late Pleistocene)

d) San Bernardino strand (150,000? to Recent) = Counterpart of Coachella Valley segment of Banning fault

(i) were these two strands ever connected to form a through-going fault?

(ii) Relations between these two strands (S.B. strand, C. V. strand of B.F.) = origin of modern SGP knot?

Crafton Hills horst-and-graben complex

a) NE-oriented normal faults in region where San Bernardino strand has several left steps and other complications

b) = zone of extension?

Comments and Questions

(1) The San Gorgonio Pass region has been a problem for the San Andreas fault system throughout its history:

a) Wilson Creek strand was deformed in this region;

b) Mission Creek strand was deformed in this region;

c) Mill Creek strand was deformed in this region;

d) San Bernardino strand has a complicated relationship with Coachella Valley segment of Banning fault in this region;

(2) Throughout Quaternary time, the San Gorgonio Pass system appears to have been the site of a giant left step in the San Andreas fault zone.

(3) What role does the Pinto Mountain fault play in this left step?

(4) What role does the San Jacinto fault play in this left step?
Does short-term and long-term behavior on the San Jacinto fault reflict events in the San Gorgonio Pass region? (accelerated versus decelerated slip and seismicity through time?)

(5) Is the San Jacinto fault segmented as a result of complications in San Gorgonio Pass? (origin of quiet and noisy segments)

(6) Given that the Mill Creek strand does not appear to have Holocene activity, how is right-lateral slip on the Coachella Valley segment of the San Andreas fault carried through the San Bernardino Mountains? Does activity step left onto the Coachella Valley segment of the Banning fault, and thence left across the San Gorgonio Pass fault system and onto the San Jacinto fault?

(7) How far south on the San Bernardino strand does the Weldon-Sieh 25 mm slip rate carry? To the vicinity of the Crafton Hills horst-and-graben complex? Does the 25 mm rate fall off to 0 in this vicinity?

(8) Is the past a key to the present in the SGP region? Is the modern San Andreas system behaving according to rules established earlier during the Quaternary?

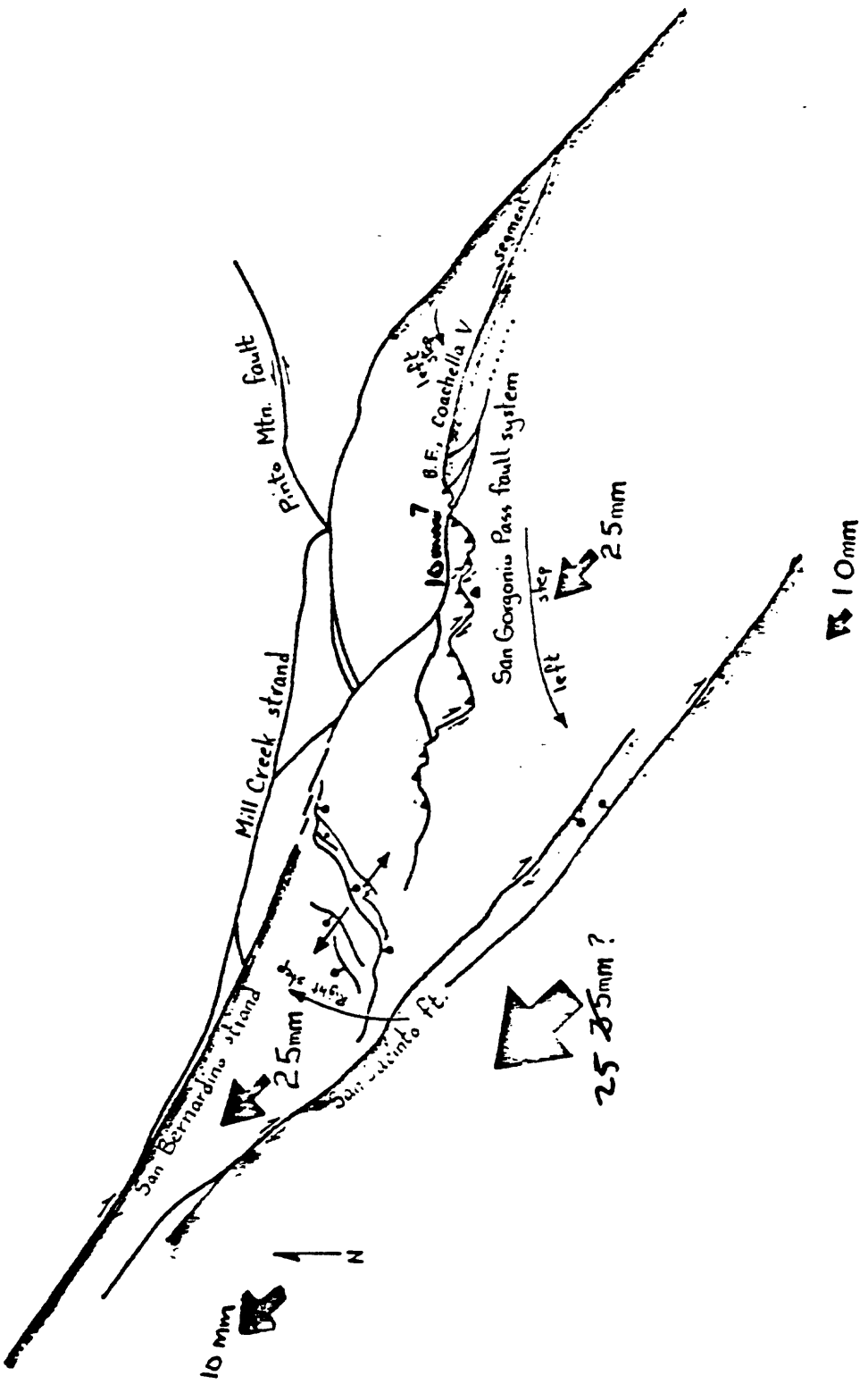
Pinto Mtn. fault
Mill Creek strand
San Bernardino strand
San Jacinto Ft.
B.F. Coachella V segment
San Gorgonio Pass fault system
10mm
25mm
left
step
25mm
25-35mm?
10mm
N

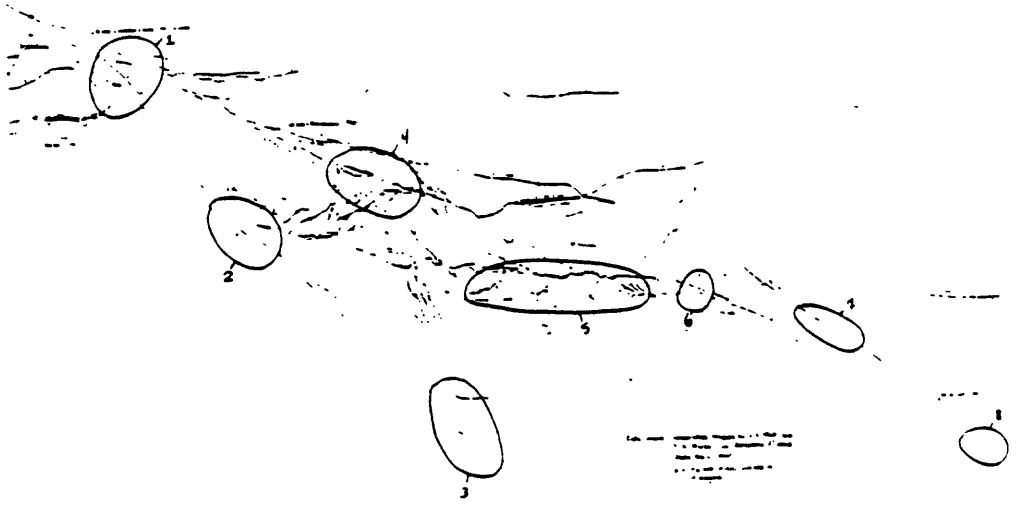

Distribution of Recommended Monitoring Sites in Southern California

1. So. Cajon Pass
2. Reche Canyon
3. San Jacinto Valley
4. Mill Creek
5. San Gorgonio Pass
6. Devers Hill
7. Indio Hills
8. Indio
9. Bombay Beach

CALIFORNIA INSTITUTE OF TECHNOLOGY

SEISMOLOGICAL LABORATORY 252-21

3 March 1985

Drs. Wayne Thatcher and William Ellsworth
Office of Earthquakes, Volcanoes, and Engineering
U. S. Geological Survey
345 Middlefield Road
Menlo Park, California 94025

Dear Wayne and Bill:

I appreciate the opportunity to participate yesterday and the day before in the conference on the opportunities for Parkfield-like clusters in southern California. Although the following comments are roughly similar to those that I gave during our wrap-up session, I've had the chance to think a bit more about the problem, and I've also added some explanatory thoughts. Hopefully these may be of some use to you and your colleagues.

I am impressed--increasingly so--that every new earthquake in California seems to involve many "surprises." For example, if we had stood here in 1856, even knowing all that we now know about the geology of California, my guess is that we would have "called" only one of the four sites of magnitude 7+ earthquakes in the following 100 years. (i.e., I think we would have "hit" on the 1857 break, but we would have "missed" on the 1872, 1927, and 1952 localities.) In this light, and on the basis of even more recent experience (e.g., Coalinga), I unhappily predict that the next two or three magnitude 6-7 earthquakes in southern California will probably occur in places that are <u>not</u> near the top of our present list of likely epicentral sites. And this seems to be true even more in southern California than in central and northern California, where we can be somewhat more confident of our eventual success at Parkfield. Thus, we must be careful not to put too much of our effort into a few localized sites in southern California, if we are to gain the maximum research potential. In particular, if it is important to the prediction effort to understand better the physics of earthquakes, and I believe this is so, then perhaps the most important thing we could do in southern California is to make sure that there are a few wide-band, high-dynamic-range, digitally recording seismometers scattered <u>throughout</u> the USGS-Caltech network, recognizing that such instruments located even well outside of the near-field will yield critical and important scientific data in the next earthquake.

Having said this, however, I think that we must be responsive to the Department of Interior's request to attempt to identify one or more areas in southern California for an intensified instrumental effort--

although not necessarily as a replicate of Parkfield. The Department is apparently sincere in its request, and we simply can't afford to thumb our noses at it. Furthermore, I think there is something to be said--on a purely scientific basis--for a well-coordinated group effort aimed at trying to understand one area exceedingly well, rather than scattering our individual efforts too widely. Almost certainly, we will learn alot about earthquake prediction, even if we don't in fact predict one! And having now listened to the various proposals, I feel that the following two areas (not necessarily in order of priority) offer the greatest promise for relatively dense instrumental concentrations:

(1) The Anza gap should, in my opinion, be instrumented and studied even more fully than at present, for the following reasons:

(a) A fair amount of sophisticated instrumentation is already in place here, and we should build strength on strength. The proximity of the Pinon Flat Observatory is an added bonus.

(b) This seems to be the most impressive seismicity gap anywhere along the fault systems of southern California, except for the very large--and thus more debatable--ones, and we should give one such area our best shot.

(c) The surficial fault trace, and perhaps the fault at depth, are simpler here than is typical elsewhere along the San Jacinto fault and as compared to many other southern California faults.

(d) The fault is in crystalline bedrock at the surface throughout most of this segment, so some types of observations may be simpler here, and more capable of reasonable interpretation, than in areas (such as #2 below) with thick sedimentary cover.

(e) The Anza area is an easy one in which to operate from a logistical point of view.

I am somewhat more confident of the southeast termination of the Anza gap than that to the northwest, where one could argue that the gap extends all the way to San Bernardino. But I think we must simply take the risk and assume that the gap is in fact relatively short and limited to the Anza area itself, recognizing that we could be dead wrong but would still stand a good chance of trapping the initiation of rupture. An argument was made by Jim Dieterich that the local population density was too low for effective political support, but I would argue just the contrary: I suspect that our initial successes with "prototype operational earthquake-prediction networks" are going to be so limited that the less public exposure, the better! And the socio-political problems of predicting a significant earthquake would be far easier solved in Anza than in (e.g.) San Bernardino. Also, of course, higher population densities go hand-in-hand with greater permitting and instrumentation problems.

(2) The southernmost San Andreas fault, say from Bombay Beach south to the northern end of the Brawley seismic zone, seems to be a particularly promising area for the following reasons:

(a) Even if the minor seismic activity now located northeast of the fault trace in this area turns our instead to be squarely on the fault, a major 100-km-long seismic gap seems to exist along this trend--and has existed for at least 50 years--from San Gorgonio Pass to the southern Salton Sea. And the adjacent Coachella Valley is almost uniquely devoid of earthquakes.

(b) Kerry Sieh's ongoing field work at Indio, although not complete, certainly suggests that this fault segment could be a temporal seismic gap that is close to being "due."

(c) This is one of the very few fault segments in California where fault creep (or at least episodic slip) is taking place along a trend of low to nil microseismicity. Although we have no firm reason to say that the unusual creep is necessarily premonitory to a large event, this is certainly as possible scenario.

(d) Carl Johnson has pointed out that the activity at the north end of the Brawley seismic zone has expanded and changed within the past 5-10 years, with much higher and more focused activity at the southern termination of the "Coachella Valley seismic gap" than in earlier years. Few large areas in southern California have experienced temporal changes since the start of the catalog in 1932, aside from activity related to specific larger events, but this is certainly one.

(e) This area is, from a logistical point of view, also an easy one in which to work. Much of the actual fault trace is within the State Park, whose people have been very cooperative in our instrumentation thus far. The proximity of the Salton Sea does admittedly pose some special problems, but some kinds of instrumentation--such as seismometers--could probably be placed on the lake floor without too much effort.

Even if no special initiatives are funded at this time, I hope that consideration can be given to placing a couple of seismic stations on the floor of the Salton Sea, in order to bring the station density in this area up to that of the overall region, and to help resolve the important question of the exact location of the minor seismicity in the Bombay Beach area.

In addition to the above two areas of very concentrated effort, I would like to see expanded instrumentation, at a somewhat lower "grade" of clustering, in the Cajon Pass region. This is a large area, with a number of candidate faults, so we simply can't focus our efforts with the same degree of concentration as at Anza or the southernmost San Andreas ("Bombay Beach"). But there are several reasons for worrying about Cajon Pass: (a) It represents the area of southern termination of the 1857 earthquake and is thus a likely place for the "next" earthquake to initiate (or end). (b) It encompasses the northern end of the San Jacinto fault, which may well represent a current seismic gap in itself. (c) From a simple geometric point of view, the junction of the various faults here seems to constitute a major asperity in the overall fault system.

Two of the areas that were discussed at some length at the meeting that I would tend not to favor are the San Gorgonio Pass and northern Carrizo Plain areas. Much as I love San Gorgonio Pass (having spent 3 years of my life there!), I see it as simply too large and too complicated to make a reasonable area for clustering of instruments. It's not clear to me exactly what we would be looking for or how we would interpret various anomalies even if we spotted them. San Gorgonio Pass represents a fascinating area for further geological and geophysical work in the attempt to understand this major "knot," but I simply don't see it as an appropriate area for a prototype prediction network.

I fully agree with Kerry Sieh that the northern Carrizo Plain area is intriguing, in that the projected M = 7+ Parkfield event would presumably terminate or initiate here. But we already have a very major effort at Parkfield, and I think that to put too many of our eggs in one basket would be unwise; instrumenting the northern Carrizo Plain would in fact represent part of the same overall experiment. Furthermore, such an effort would not really be responsive to the Department's request to establish a prototype prediction network in southern California, presumably in addition to the ongoing experiment at Parkfield.

One final comment: At our meeting, we really did not discuss the Garlock fault, nor did we have all of the appropriate people there to do so. Nevertheless, I hope that we are not dismissing it. With a slip rate as high or higher than that of the San Jacinto fault, but with no historic large earthquakes, what could be a more likely target? And a promising area on which to concentrate would be the junction of the creeping and "locked" segments--if we could identify it; perhaps it is coincident with the major en-echelon offset at Koehn Lake (Fremont Valley). I doubt that at this moment we can identify specific target sites on the Garlock fault with the same degree of confidence that we can along the San Andreas and San Jacinto faults, but certainly part of our overall "game plan" during the next couple of years should be to attempt to do so. In the long run, my hunch is that the Garlock will be just as promising as the faults farther south in terms of prediction research.

Thanks again for the opportunity to participate in the conference.

Sincerely,

Clarence R. Allen
Professor of Geology
and Geophysics

UNIVERSITY OF CALIFORNIA, SAN DIEGO

BERKELEY • DAVIS • IRVINE • LOS ANGELES • RIVERSIDE • SAN DIEGO • SAN FRANCISCO SANTA BARBARA • SANTA CRUZ

INSTITUTE OF GEOPHYSICS AND
PLANETARY PHYSICS, A-025
SCRIPPS INSTITUTION OF OCEANOGRAPHY

LA JOLLA, CALIFORNIA 92093

March 12, 1985

Dr. Wayne Thatcher
and Dr. William Ellsworth
Via Ms. Thelma Rodriguez
Office of Earthquake Studies
U.S. Geological Survey
345 Middlefield Road, MS 977
Menlo Park, CA 94025

Dear Wayne and Bill:

First of all let me once again congratulate you on having organized such a successful and informative meeting; it was high on light and low on heat. I certainly learned a lot and came out of it with a clearer understanding of the problems and some new ideas. The purpose of this letter is as you suggested, to pass on some of the latter after having had time for reflection. I have thought of enough additional sites that they would make a good Option 2½ or even 3; after discussing sites I will offer a few thoughts on some specific techniques.

First of all, for completeness I will offer some opinions on where not to cluster (i.e., only monitor seismicity, put out alignment arrays, and maybe do large-scale geodetic strain). I can think of two categories:

1) Places where there is no clear evidence for a lot of activity. Some good current examples would be the Elsinore, Raymond Hill, and Rose Canyon faults. Unfortunately any earlier list might have included the White Wolf, the Newport-Inglewood, and the San Fernando zone. This class of faults will be where Clarence Allen's "surprises" come from, a situation we simply have to live with (short of Option 4).

2) Places where we do not understand where to look. My type area would be the southernmost San Jacinto, from Borrego to the border. Kerry Sieh may be right in believing this to be a probable place, but for much of it we don't even know where the faults really are. This might be a good place for more mapping and alignment arrays, but not one to focus on.

Now for the positive suggestions. I think Jim Brune's distinction between studying fault physics versus trying to predict is a useful one (though there is plenty of overlap), and will say which category I think each site falls into. My preference is for understanding the physics, but I can accept both sorts of sites if they are well chosen. The following list is roughly in order of preference; you could certainly reverse the order of any pair, but not put #5 first.

1) Anza (physics; prediction). Obviously, I have all sorts of vested interest here, but it still is the first place to point to as a gap (slip or seismic), and is certainly displaying interesting seismicity patterns (e.g., the Cahuilla swarm). There is also the sizable monitoring effort already in place. Given this, is more needed? My feeling is that the most appropriate additions would be paleoseismicity (if possible), and deformation monitoring to the tune of two borehole strainmeters SE of the fault and some 2-color nets (I would of course like to see a laser-strainmeter/two-color comparison).

2) Bombay Beach (physics). While I am worried about how fast many of us (myself included) climbed on this bandwagon without kicking the tires, I still think this looks interesting. The seismicity shows clearly that some sort of transition is taking place there, and also that things appear to be pretty simple. Understanding this transition would have to be good for the program. Better seismic measurements would be good (indeed this holds at all the sites from here on). More spatially detailed geodesy would be appropriate (a 2-color net done occasionally) to understand the details. Better monitoring of fault creep really goes along with this, and could include shallow strain and tilt to set bounds on creep events. This area has one big advantage for such measurements: it almost never rains.

3) The San Bernardino triangle (prediction). More specifically, the area delineated by a Wrightwood-Riverside-Yucaipa triangle (+10 km strips on the edges). This is the one populated area with highly active faults. It is probably too complex to understand, and partly for this reason might be the most appropriate place for a "Chinese" approach; if you can't model the measurements you do understand, the less the gap between them and the ones you don't (e.g., groundwater geochemistry). Because it is populous and relatively small it is also cheaper and easier to do anything, long-shot or otherwise. More geodesy seems to be the first need, including leveling over some of Jon Matti's thrusts and normal faults.

4) Palmdale (physics). When you're hot you're hot but when you're not you're not. I certainly got the impression that no one found this area interesting; does not that, by Murphy's Law, make it a good place to go? More seriously, this is a simple place and hence a good one to study fault physics, and the geodetic basis is there for further monitoring. Surely the gravity-strain correlation is worth trying to understand.

5) San Andreas, Whitewater to Indio (prediction). This is more of a long-shot, for a possible event heading south out of San Gorgonio Pass, but the area is again economically of relatively high value. Certainly the location of earthquakes (on or off the fault) needs to be cleared up, and since creep is occurring it needs to be monitored.

Now, as to techniques that could be used in the clusters. A popular wish seems to be for "broad-band, high-dynamic-range" seismometers. I share the belief that this is the direction we ought to be moving, but have to note that since so little of this type of data has been available, much of the interest in it seems to come from a conviction that it is bound to be useful, rather than experience with it. It therefore seems to me important that data from the Anza network be widely disseminated and experimented on, before a commitment is made to redo large parts of the existing network.

On strain and tilt (non-geodetic) you already know my opinions, which can be summed up as if you are going to do them at all, do them well; unfortunately it is not yet clear what doing them well will demand. The borehole strainmeters look pretty good, and other things being equal I would prefer three components to one. On the geodetic side, I hope the rush to get more 2-color EDM's will not override the need for thorough tests in a tectonically dull area (such as Boulder); especially if Larry is building more than one, this is a great opportunity to do some really thorough comparisons and sort out just how big the noise terms are.

A technology that seems to me in even worse shape is the monitoring of fault creep, not necessarily creep events but simply whether or not there is aseismic surface slip. Caltech has done a meritorious job of collecting data on this, and certainly the results are exciting, but they are a lot thinner than they ought to be. I don't have any brilliant ideas on this; the best solution would seem to be lots of small arrays, which means lots of manpower. I am also willing to accept the plausibility of Roger Bilham's argument (in his preprint) that no current measurement covers "wide slip zones," though measuring them would not be easy because of monument motions. In this connection, a set of relevant measurements might be the Mekometer net in the Imperial Valley, which I believe covers just the scale of interest. Has this been resurveyed enough to compare it with the post-1979 alignment array data?

Just for completeness I will close by stating the obvious, which is that we need more trenching and paleoseismicity studies everywhere possible because the historical record is so thin.

I seem to have been typically long-winded, I trust somewhat usefully. I look forward to hearing further deliberations on where the focus might next go.

Yours faithfully,

Duncan Carr Agnew

Duncan Carr Agnew

DCA:kb

Meeting on Earthquake Prediction in Southern California

organized by W. Ellsworth and W. Thatcher, USGS Menlo Park

March 1-2, San Diego

Afterthoughts by L. Seeber; March 13, 1985.

I thought the meeting was successful on several grounds. It served as a forum where information and ideas were effectively transferred. Small size, informal environment and intelligent guidance of the discussion were factors. Sociopolitical aspects of the prediction program, and the impact they will probably have on the program were brought home to some of the participants in the external program. I, for one, left the meeting determined to shift emphasis in my work from generally trying to decifer neotectonics in southern California to specifically addressing earthquake prediction strategies for that area.

Even strictly within the context of prediction, however, we still do not have the material for an intelligent choice of a single 30-km segment of the San Jacinto fault or of the San Andreas fault south of Cholame for an intensive multidisciplinary investigation and monitoring effort. We are still too unaware of what to expect and when to expect it to put all our eggs in one basket. A prediction experiment like the one in Parkfield would be much more risky in southern California at this point. This is not surprising considering the relatively little research effort dedicated so far to the major active faults in that area. Additional resources dedicated to this area can be expected to bring important new results soon. Until then, new effort should be distributed among a number of critical ares. Detailed data should be obtained to test hypotheses that are particularly promising for prediction and methods should be applied where they have the best chance for success.

Jack Healy's suggestion of a pre prediction-experiment phase where several sites will be studied seems the correct approach. A regional approach may also be desirable at the prediction phase in southern California in view of the possible large ruptures.

Specifically, I would advise the following:

1. Intersection between the San Andreas fault and Brawley zone of seismicity:
   a. detailed geodetic monitoring by trilateration and releveling;
   b. detailed study of seismicity from existing data and possibly adding some new stations;
   c. historic data should be systematically searched for evidence for a M ≈ 7 event on the southernmost San Andreas near the Brawley zone;
   d. intensify paleoseismicity program to identify characteristic earthquakes on the southern San Andreas.
2. San Jacinto/San Andreas fault intersection:
   a. continuing joint analysis of seismicity and surface structural featurs of both the basin and the uplifted San Bernardino region. The high seismicity in this region allows for a very detailed view in space and time;
   b. Intensify geodetic control of the area southwest of the San Andreas/San Jacingo fault intersection to resolve whether interseismic deformation is controlled by rotating blocks (seismicity) or by pull-apart at a right step (geology), or by both;
   c. available and possible new data on the hydrolics of the San Bernardino basin should be examined for possible clues to the structural features and for chages in underground water circula-

tion, temperature and chemistry that may be related to the deformation of the fault zones in the interseismic period.

3. The Anza region of the San Jacinto fault is an obvious gap in the current seismicity, may be a gap in historical seismicity, and has the advantage of good exposure of the brittle structure in pre Tertiary rocks. Conteracting the characteristics that suggest the opportunity of intense monitoring, the Pineon Flat data show no detectible strain 15 km from the San Jacinto fault in the gap. The gap in the seismicity may reflect the absence of secondary branches of the fault zone in the Anza region and be a permanent characteristic controlled by the structure rather than being a symptom of near rupture conditions. Most of the seismicity on either side of the gap is occurring between subparallel strands. The Anza region seems particularly adept for a detailed structural study directed at understanding fault behavior at side steps and the structural role of cross fault and blocks. Given the good exposure, the high seismicity and the god network coverage, this area is optimal for a detailed correlation between seismicity and structure.

4. The Carizo Plain portion of the San Andreas south of Cholame is also a candidate for the next big ruptue (e.g., K. Sieh). If this portion of the fault will rupture with the next Parkfield event, the rupture may start at the Cholame right step/asperity. Thus, particular attention should be given to the interseismic behavior at Cholame (e.g., seismicity, strain, long-term geologic deformation near the fault).

Rec'd from Craig Nicholson, LDG. 3-14-85 TR

Recommendations for an expanded earthquake prediction research program in southern California.

It is unquestionable that southern California has a high seismic risk for a major earthquake in the next few decades. This is because part of the San Andreas fault that ruptured in the great earthquake of 1857 (Lake Hughes to Cajon Pass) has been estimated to have a repeat time of about 150 years. Another segment extending from San Bernardino to the Salton Sea appears to have last broken about 1680, and may have a repeat time of about 250 to 400 years. Thus, a great earthquake along the southern San Andreas could involve rupture from near Fort Tejon to the Salton Sea and could involve damage in excess of several billion dollars. An earthquake of magnitude near 7 along the northern part of the San Jacinto fault also appears likely, and could be equally costly in terms of damage and loss of lives.

Irregardless of whether an "operational earthquake prediction program" is established within these potential rupture zones, we are likely to be held responsible should such a damaging earthquake occur and no immediate warning given. This is because a large public is aware of the current commitment to predict an earthquake in California and many would fail to make the distinction between specific fault segments that are currently instrumented (i.e., Parkfield and Anza) and the entire San Andreas system. Thus, we need to begin to develope monitoring programs for those fault segments that are likely to fail in the near future and that are likely to cause the most damage. By the time such systems are in place, we may be in a position to identify and understand various forerunning effects in these areas that the failure to instrument would preclude. Furthermore, because of the large potential rupture lengths involved, the particular research program required would necessarily have to be more of a regional nature than the present "cluster concept" would permit.

A regional approach allows for a greater chance of identifying unusual activity on secondary structures that may signal forerunning effects to large earthquakes on or off the major wrench faults of the San Andreas system. The keystone of a regional monitoring program would be an upgraded seismic network with 3-component broadband digital stations. This would permit greater depth control and greater discrimination between earthquakes of different seismic character. Other monitoring programs would need to be tailored to specific areas under investigation.

For example, detailed instrumentation of the southern San Andreas for seismicity studies would not be particularly appropriate at the present time since much of this segment is currently quiescent. However, one could begin geodetic work to measure the elastic strain fields associated with various bends in the fault (where large earthquakes are likely to originate) and to augment existing research on paleoseismicity and the monitoring of creep. This work would help to establish a better understanding of repeat times for large slip events; the partition of elastic and non-elastic strain during the interseismic period; the variation in creep along strike; and whether creep is a recent phenomenon or something more typical of the long-term fault behavior in this area. On the other hand, geodetic work through San Gorgonio Pass and San Bernardino Valley would be difficult because of the extreme variations in elevations and the presence of large secondary signals of non-tectonic origin (e.g., subsidence from ground water pumping). But because of the high seismicity and expected uplift rates in this area, both a microgravity survey and a detailed seismicity study could be instituted. Paleoseismic work also needs to be begun to determine whether the northern San Jacinto fault fails in characteristically

large events of 3-4 meters slip (as suggested by some preliminary evidence), or more often in smaller events with less slip.

Since each fault segment is sufficiently unique in terms of its seismic behavior, ultimate shear strength and accumulated strain energy, a duplication of the Parkfield experiment along other fault segments would be premature until it has been determined how much information is gained by such a concentrated effort, and how likely the knowledge acquired at Parkfield is transportable to other sections of the fault in southern California. The fault geometry near Parkfield is not as complicated as other sections of the San Andreas system. More complex areas, like Bombay Beach and San Gorgonio Pass, are more likely to exhibit precursory phenomenon then the simplier fault segments. As these areas are also likely to control where large earthquakes nucleate or how slip is distributed, they should be given equal consideration as sites where an expanded earthquake prediction program should be instituted.

CALIFORNIA INSTITUTE OF TECHNOLOGY

SEISMOLOGICAL LABORATORY 252-21

March 21, 1985

Dr. Wayne Thatcher and Dr. Bill Ellsworth
U.S. Geological Survey, MS 977
345 Middlefield Road
Menlo Park, CA 94025

Dear Wayne and Bill,

I was glad to be a part of the recent meeting in San Diego about earthquake prediction experiments along the southern San Andreas and San Jacinto fault zones, and I thank you for the invitation. Before the meeting my general feeling was that an important first effort should be the upgrading of much of the array in that area. This priority has not changed and was rather strengthened by one of the conclusions of the meeting that many places along the entire length of the San Jacinto fault zone and the San Andreas fault zone southeast of San Gorgonio Pass could, as far as we know, be sites for large earthquakes in the near future. We should be sure and not lose important seismic and geodetic information from any of these locations. State-of-the-art three-component seismometers are needed throughout this area so that meaningful waveform studies can be carried out.

After listening to the final discussions and then reflecting on the data I would cast my vote for the San Jacinto fault zone near Anza as a place to concentrate effort if that is desired. There are several reasons to chose this area:

1. Many of the "classic" precursory phenomenon are seen here, such as historic seismic slip gap, modern seismicity gap, clustering of seismicity, and extended earthquake swarms.

2. Parts of the prediction experiment are already in existence, i.e. Pinyon Flat strain observatory and the telemetered, digital seismograph network.

3. Many interesting seismic phenomenon are occurring in the area including some of the deepest and some of the shallowest earthquakes in southern California.

4. Bedrock is at the surface throughout most of the area and is fairly uniform crystalline terrain. Thus seismograms are less affected by the strong attenuation through sedimentary basins.

For these reasons I feel that any intensification of effort in the Anza area, including geodetic, will be rewarded with new and interesting data about fault zone processes and the earthquake source.

I hope that your efforts will be fruitful in securing support for quality earthquake studies in the southern San Andreas and San Jacinto regions. I will continue my use of the existing data and know that new insights await discovery.

Sincerely,

Chris Sanders

PASADENA CALIFORNIA 91125 TELEPHONE (818) 356-6911

NATIONAL EARTHQUAKE PREDICTION EVALUATION COUNCIL MEMBERS

NATIONAL EARTHQUAKE PREDICTION EVALUATION COUNCIL

Dr. Lynn R. Sykes CHAIRMAN	Higgins Professor of Geological Sciences Lamont-Doherty Geological Observatory of Columbia University Palisades, New York 10964 Office: 914/359-2900 Home: 914/359-7428
Dr. John R. Filson VICE CHAIRMAN	Chief, Office of Earthquakes, Volcanoes, and Engineering U.S. Geological Survey National Center, MS 905 Reston, Virginia 22092 Office: 703/648-6714 Home: 703/648-2807
Dr. Clement F. Shearer EXECUTIVE SECRETARY	Hazards Information Coordinator Office of the Director U.S. Geological Survey National Center, MS 106 Reston, Virginia 22092 Office: 703/648-4425 Home: 703/620-9422
Dr. Keiiti Aki	Department of Geological Sciences University of Southern California Los Angeles, California 90007 Office: 213/743/3510 Home: 213/559-1350
Dr. John N. Davies	State Seismologist, Alaska Department of Natural Resources, Division of Geological and Geophysical Surveys, and, Adjunct Associate Professor, Geophysical Institute, University of Alaska 794 University Avenue, Basement Fairbanks, Alaska 99701 Office: 907/474-7190 Home: 907/455/6311
Dr. James F. Davis	State Geologist, California Department of Conservation California Division of Mines and Geology 1416 Ninth Street, Room 1341 Sacramento, California 95814 Office: 916/445-1923 Home: 916/487-6125

Dr. James H. Dieterich
Research Geophysicist
Branch of Tectonophysics
U.S. Geological Survey
345 Middlefield Road, MS 977
Menlo Park, California 94025
Office: 415/323-8111, ext. 2573
Home: 415/856-2025

Dr. William L. Ellsworth
Chief, Branch of Seismology
U.S. Geological Survey
345 Middlefield Road, MS 977
Menlo Park, California 94025
Office: 415/323-8111, ext. 2782
Home: 415/322-9452

Dr. Hiroo Kanamori
Division of Geological & Planetary Science
California Institute of Technology
Pasadena, California 91125
Office: 818/356-6914
Home: 818/796-8452

Dr. Thomas V. McEvilly
Department of Geology and Geophysics
University of California, Berkeley
Berkeley, California 94720
Office: 415/642-4494
Home: 415/549-0967

Dr. I. Selwyn Sacks
Department of Terrestrial Magnetism
Carnegie Institution of Washington
5241 Broad Branch Road, N.W.
Washington, D.C. 20015
Office: 202/966-0863
Home: 301/657-3271

Dr. Wayne Thatcher
Chief, Branch of Tectonophysics
U.S. Geological Survey
345 Middlefield Road, MS 977
Menlo Park, California 94025
Office: 415/323-8111, ext. 2120
Home: 415/326-4680

Dr. Robert E. Wallace
Chief Scientist, Office of Earthquakes, Volcanoes, and Engineering
U.S. Geological Survey
345 Middlefield Road, MS 977
Menlo Park, California 94025
Office: 415/323-8111, ext. 2751
Home: 415/851-0249

Dr. Robert L. Wesson

Research Geophysicist
Branch of Seismology
U.S. Geological Survey
National Center, MS 922
Reston, Virginia 22092
Office: 703/648-6785
Home: 703/476-8815

Dr. Mark D. Zoback

Professor of Geophysics
Department of Geophysics
Stanford University
Stanford, California 94305
Office: 415/497-9438
Home: 415/322-9570